

## Table of Contents

6.0	Engineered Safety Features
6.1	General
6.1.1	Containment System
6.1.2	Emergency Core Cooling System
6.1.3	Containment Spray System
6.1.4	Containment Air Return and Hydrogen Skimmer System
6.1.5	Ice Condenser System
6.1.6	Containment Isolation System
6.1.7	Hydrogen Control System
6.1.8	Annulus Ventilation System
6.2	Containment Systems
6.2.1	Containment Functional Design
6.2.1.1	Containment Structure
6.2.1.1.1	Design Bases
6.2.1.1.2	Design Features
6.2.1.1.3	Design Evaluation
6.2.1.2	Containment Subcompartments
6.2.1.2.1	Design Basis
6.2.1.2.2	Design Features
6.2.1.2.3	Design Evaluation
6.2.1.3	Mass and Energy Release Analysis for Postulated Loss-of-Coolant Accidents
6.2.1.3.1	Short Term Mass and Energy Release Data
6.2.1.3.2	Long-Term Mass and Energy Release Data
6.2.1.4	Mass and Energy Release Analysis for Postulated Secondary System Pipe Ruptures Inside Containment
6.2.1.4.1	Pipe Break Blowdowns Spectra and Assumptions
6.2.1.4.2	Break Flow Calculations
6.2.1.4.3	Single Failure Effects
6.2.1.5	Minimum Containment Pressure Analysis for Performance Capability Studies of Emergency Core Cooling System
6.2.1.5.1	Mass and Energy Release Data
6.2.1.5.2	Initial Containment Internal Conditions
6.2.1.5.3	Containment Volume
6.2.1.5.4	Active Heat Sinks
6.2.1.5.5	Steam-Water Mixing
6.2.1.5.6	Passive Heat Sinks
6.2.1.5.7	Heat Transfer to Passive Heat Sinks
6.2.1.5.8	Other Parameters
6.2.1.6	Testing and Inspection
6.2.1.6.1	Preoperational Testing
6.2.1.6.2	Periodic Inservice Surveillance
6.2.1.7	Instrumentation Requirements
6.2.1.8	Materials
6.2.2	Ice Condenser System
6.2.2.1	Floor Structure and Cooling System
6.2.2.1.1	Design Bases
6.2.2.1.2	System Design
6.2.2.1.3	Design Evaluation
6.2.2.2	Wall Panels
6.2.2.2.1	Design Basis

- 6.2.2.2.2 System Design
- 6.2.2.2.3 Design Evaluation
- 6.2.2.3 Lattice Frames and Support Columns
  - 6.2.2.3.1 Design Basis
  - 6.2.2.3.2 System Design
  - 6.2.2.3.3 Design Evaluation
- 6.2.2.4 Ice Baskets
  - 6.2.2.4.1 Design Basis
  - 6.2.2.4.2 System Design
  - 6.2.2.4.3 Design Evaluation
- 6.2.2.5 Crane and Rail Assembly
  - 6.2.2.5.1 Design Basis
  - 6.2.2.5.2 System Design
  - 6.2.2.5.3 Design Evaluation
- 6.2.2.6 Refrigeration System
  - 6.2.2.6.1 Design Basis
  - 6.2.2.6.2 System Design
  - 6.2.2.6.3 Design Evaluation
- 6.2.2.7 Air Handling Units
  - 6.2.2.7.1 Design Basis
  - 6.2.2.7.2 System Design
  - 6.2.2.7.3 Design Evaluation
- 6.2.2.8 Lower Inlet Doors
  - 6.2.2.8.1 Design Basis
  - 6.2.2.8.2 System Design
  - 6.2.2.8.3 Design Evaluation
- 6.2.2.9 Lower Support Structure
  - 6.2.2.9.1 Design Basis
  - 6.2.2.9.2 System Design
  - 6.2.2.9.3 Design Evaluation
- 6.2.2.10 Top Deck and Doors
  - 6.2.2.10.1 Design Basis
  - 6.2.2.10.2 System Design
  - 6.2.2.10.3 Design Evaluation
- 6.2.2.11 Intermediate Deck and Doors
  - 6.2.2.11.1 Design Basis
  - 6.2.2.11.2 System Design
  - 6.2.2.11.3 Design Evaluation
- 6.2.2.12 Air Distribution Ducts
  - 6.2.2.12.1 Design Basis
  - 6.2.2.12.2 System Design
  - 6.2.2.12.3 Design Evaluation
- 6.2.2.13 Equipment Access Door
  - 6.2.2.13.1 Design Basis
  - 6.2.2.13.2 System Design
  - 6.2.2.13.3 Design Evaluation
- 6.2.2.14 Ice Technology, Ice Performance and Ice Chemistry
  - 6.2.2.14.1 Design Basis
  - 6.2.2.14.2 System Design
  - 6.2.2.14.3 Design Evaluation
- 6.2.2.15 Ice Condenser Instrumentation
  - 6.2.2.15.1 Design Basis
  - 6.2.2.15.2 Design Description
  - 6.2.2.15.3 Design Evaluation
- 6.2.2.16 Ice Condenser Structural Design
  - 6.2.2.16.1 Applicable Codes, Standards, and Specifications

- 6.2.2.16.2 Loads and Loading Combinations
  - 6.2.2.16.3 Design and Analytical Procedures
  - 6.2.2.16.4 Structural Acceptance Criteria
  - 6.2.2.17 Seismic Analysis
    - 6.2.2.17.1 Seismic Analysis Methods
    - 6.2.2.17.2 Seismic Load Development
    - 6.2.2.17.3 Vertical Seismic Response
  - 6.2.2.18 Materials
    - 6.2.2.18.1 Design Criteria
    - 6.2.2.18.2 Environmental Effects
    - 6.2.2.18.3 Compliance with 10CFR 50, Appendix B
    - 6.2.2.18.4 Materials Specifications
  - 6.2.2.19 Tests and Inspections
  - 6.2.3 Annulus Ventilation System
    - 6.2.3.1 Design Bases
    - 6.2.3.2 System Design
    - 6.2.3.3 Safety Evaluation
    - 6.2.3.4 Tests and Inspections
    - 6.2.3.5 Instrumentation Application
      - 6.2.3.5.1 Containment Pressure
      - 6.2.3.5.2 Annulus Pressure
      - 6.2.3.5.3 Filter Train Differential Pressure
      - 6.2.3.5.4 Annulus Ventilation Fans Inlet Header Flow
      - 6.2.3.5.5 Carbon Filter Temperature
    - 6.2.3.6 Materials
  - 6.2.4 Containment Isolation Systems
    - 6.2.4.1 Design Basis
    - 6.2.4.2 System Design
    - 6.2.4.3 Safety Evaluation
    - 6.2.4.4 Tests and Inspections
    - 6.2.4.5 Instrumentation Application
    - 6.2.4.6 Materials
  - 6.2.5 Combustible Gas Control in Containment
    - 6.2.5.1 Design Bases
    - 6.2.5.2 Deleted Per 2008 Update
    - 6.2.5.3 Design Evaluation
    - 6.2.5.4 Deleted Per 2008 Update
    - 6.2.5.5 Deleted Per 2008 Update
    - 6.2.5.6 Deleted Per 2008 Update
  - 6.2.6 Hydrogen Production and Accumulation
    - 6.2.6.1 Method of Analysis
    - 6.2.6.2 Typical Assumptions
      - 6.2.6.2.1 Zirconium-Water Reaction
      - 6.2.6.2.2 Primary Coolant Hydrogen
      - 6.2.6.2.3 Corrosion of Plant Materials
      - 6.2.6.2.4 Radiolysis of Core and Sump Water
    - 6.2.6.3 Core Solution Radiolysis
    - 6.2.6.4 Sump Solution Radiolysis
  - 6.2.7 Supplemental Hydrogen Control System/Hydrogen Mitigation System
  - 6.2.8 References
- 
- 6.3 Emergency Core Cooling System
    - 6.3.1 Design Basis
      - 6.3.1.1 Range Of Coolant Ruptures And Leaks
      - 6.3.1.2 Fission Product Decay Heat
      - 6.3.1.3 Reactivity Required For Cold Shutdown

- 6.3.1.4 Capability To Meet Functional Requirements
- 6.3.2 SYSTEM DESIGN
  - 6.3.2.1 Schematic Piping And Instrumentation Diagrams
  - 6.3.2.2 Equipment and Component Design
    - 6.3.2.2.1 Components Description
    - 6.3.2.2.2 System Operation
  - 6.3.2.3 Applicable Codes and Classifications
  - 6.3.2.4 Materials Specifications and Compatibility
  - 6.3.2.5 Design Pressures and Temperatures
  - 6.3.2.6 Coolant Quantity
  - 6.3.2.7 Pump Characteristics
  - 6.3.2.8 Heat Exchanger Characteristics
  - 6.3.2.9 ECCS Flow Diagrams
  - 6.3.2.10 Relief Valves
  - 6.3.2.11 System Reliability
  - 6.3.2.12 Protection Provisions
  - 6.3.2.13 Provisions for Performance Testing
  - 6.3.2.14 Net Positive Suction Head
  - 6.3.2.15 Control of Motor-Operated Isolation Valves
  - 6.3.2.16 Motor Operated Valves and Controls
  - 6.3.2.17 Manual Actions
  - 6.3.2.18 Process Instrumentation
  - 6.3.2.19 Materials
    - 6.3.2.20 General Letter 2004-02
- 6.3.3 Performance Evaluation
  - 6.3.3.1 Evaluation Model
  - 6.3.3.2 ECCS Performance
  - 6.3.3.3 Fuel Rod Perforations
  - 6.3.3.4 Effects of ECCS Operation on the Core
  - 6.3.3.5 Use Of Dual Function Components
  - 6.3.3.6 Lag Times
  - 6.3.3.7 Thermal Shock Considerations
  - 6.3.3.8 Limits on System Parameters
  - 6.3.3.9 Use of RHR Spray
  - 6.3.3.10 Boron Precipitation Evaluation
- 6.3.4 Tests and Inspections
- 6.3.5 INSTRUMENTATION APPLICATION
  - 6.3.5.1 Temperature Indication
  - 6.3.5.2 Pressure Indication
  - 6.3.5.3 Flow Indication
  - 6.3.5.4 Level Indication
  - 6.3.5.5 Valve Position Indication
  - 6.3.5.6 ECCS Leakage Detection
- 6.3.6 References
  
- 6.4 Control Area (Habitability) Ventilation System
  - 6.4.1 Design Bases
  - 6.4.2 System Description
  - 6.4.3 Safety Evaluation
  - 6.4.4 Tests and Inspections
  - 6.4.5 Instrument Application
  
- 6.5 Containment Spray System
  - 6.5.1 Design Bases
  - 6.5.2 System Design
  - 6.5.3 Safety Evaluation

- 6.5.4 Tests and Inspections
- 6.5.5 Instrumentation Application
- 6.5.6 References

## List of Tables

Table 6-1. Containment Subcompartment Pressures

Table 6-2. Containment Subcompartment Differential Pressures. (Table 6-2 and Table 6-3 were originally one table)

Table 6-3. Containment Subcompartment Differential Pressures. (Table 6-2 and Table 6-3 were originally one table.)

Table 6-4. TMD Element Input Data

Table 6-5. TMD Flow Path Input Data - Ventilation Duct Intact

Table 6-6. TMD Flow Path Input Data - Ventilation Duct Intact

Table 6-7. Mass And Energy Release Rates For Peak Reverse Differential Pressure

Table 6-8. Compartment Volume and Initial Condition Data For Peak Reverse Differential Pressure

Table 6-9. Active Heat Sink Data For Peak Reverse Differential Pressure

Table 6-10. Upper Compartment Passive Heat Sink Data For Peak Reverse Differential Pressure

Table 6-11. Lower and Dead Ended Compartments Passive Heat Sink Data For Peak Reverse Differential Pressure

Table 6-12. Sensitivity Studies For D.C. Cook Plant

Table 6-13. McGuire Ice Condenser Design Parameters

Table 6-14. Deleted Per 1998 Update

Table 6-15. Containment Sump Volume Vs. Time Peak Containment Pressure Transient

Table 6-16. Containment Sump Volume Vs. Elevation(1)

Table 6-17. ECCS Flow Rates1

Table 6-18. Structural Heat Sink Data

Table 6-19. Comparison of Design Parameters - McGuire and D. C. Cook

Table 6-20. Allowable Leakage Area For Various Reactor Coolant System Break Sizes

Table 6-21. Summary Of Heat Transfer Correlations Used To Calculate Steam Generator Heat Flow In The SATAN Code

Table 6-22. Deleted Per 2009 Update.

Table 6-23. Deleted Per 2009 Update.

Table 6-24. Deleted Per 2009 Update.

Table 6-25. Deleted Per 2009 Update.

Table 6-26. Deleted Per 2009 Update.

Table 6-27. Deleted Per 2009 Update.

Table 6-28. Deleted Per 1998 Update

Table 6-29. Deleted Per 1998 Update

Table 6-30. Deleted Per 1998 Update

Table 6-31. Deleted Per 1998 Update

Table 6-32. Deleted Per 1998 Update

Table 6-33. Deleted Per 1998 Update

Table 6-34. Deleted Per 1998 Update

Table 6-35. Deleted Per 1998 Update

Table 6-36. Deleted Per 1998 Update

Table 6-37. Deleted Per 1998 Update

Table 6-38. Deleted Per 1998 Update

Table 6-39. Deleted Per 1998 Update

Table 6-40. Deleted Per 1998 Update

Table 6-41. Deleted Per 1998 Update

Table 6-40. Deleted Per 1998 Update.

Table 6-41. Deleted Per 1998 Update

Table 6-42. TMD Input Data - 2 Node Steam Generator Enclosure

Table 6-43. TMD Input Data - 9 Node Steam Generator Enclosure

Table 6-44. Peak Differential Pressures - 2 Node Steam Generator Enclosure

Table 6-45. Peak Differential Pressure - Steam Generator Enclosure - 9 Node

Table 6-46. TMD Input Data - 2 Node Pressurizer Enclosure

Table 6-47. TMD Input Data - 4 Node Pressurizer Enclosure

Table 6-48. Mass and Energy Releases into Steam Generator Enclosure

Table 6-49. Mass and Energy Release Rates Into Pressurizer Enclosure

Table 6-50. Reactor Cavity Analysis Volumes - Cold Leg Break

Table 6-51. Reactor Cavity Analysis Flow Paths - Cold Leg Break Flow

Table 6-52. Mass and Energy Release Rates Into Reactor Cavity

Table 6-53. Reactor Cavity Design Pressures

Table 6-54. Mass and Energy Release Rates for Steam Line Rupture. 2.4 ft2 Double Ended Break at 3479 MWt (rated thermal power plus measurement uncertainty)

Table 6-55. Deleted Per 1998 Update

Table 6-56. Deleted Per 1998 Update

Table 6-57. Deleted Per 1998 Update

Table 6-58. Deleted Per 1998 Update

Table 5-59. Deleted Per 1998 Update

Table 6-60. Deleted Per 1998 Update

Table 6-61. Deleted Per 1998 Update

Table 6-62. Mass and Energy Release Rates for Minimum Post-LOCA Containment Pressure

Table 6-63. Deleted Per 1998 Update.

Table 6-64. Volume and Temperature Data For Minimum Post-LOCA Containment Pressure McGuire and Catawba

Table 6-65. Active Heat Sink Data For Minimum Post-LOCA Containment Pressure

Table 6-66. Structural Heat Sink Data For Minimum Post-LOCA Containment Pressure

Table 6-67. Deleted Per 1998 Update.

Table 6-68. Air Return Fans and Hydrogen Skimmer Fans Failure Analysis

Table 6-69. Wall Panel Design Loads<sup>1</sup>

Table 6-70. Lattice Frame Loads Horizontal 1/2 Safe Shutdown Earthquake<sup>2</sup>

Table 6-71. Local Seismic Loads on Lattice Frames Due to Single Ice Basket

Table 6-72. Ice Condenser Lattice Frame Loads<sup>1</sup> Blowdown Pressure Loads for Design Basis Earthquake (SSE) And Design Basis Accident (DBA)

Table 6-73. Vertical DBA Loads On Lattice Frames

Table 6-74. Vertical Friction Loads On Lattice Frames

Table 6-75. Lattice Frames Summary of Maximum Stresses

Table 6-76. Summary of Fatigue Analysis<sup>1</sup> For Lattice Frames

Table 6-77. Ice Basket Load Summary - Minimum Test Loads

Table 6-78. Ice Basket Load Summary - Basic Design Loads

Table 6-79. Summary of Stresses in Basket Due to Design Loads

Table 6-80. Ice Basket Material Minimum Yield Stress

Table 6-81. Allowable Stress Limits (D + 1/2 SSE) For Ice Basket Materials

Table 6-82. Allowable Stress Limits (D + SSE), (D + DBA) For Ice Basket Materials

Table 6-83. Allowable Stress Limits (D + SSE + DBA) For Ice Basket Materials

Table 6-84. Ice Basket Clevis Pin Stress Summary

Table 6-85. Ice Basket Mounting Bracket Assembly Stress Summary

Table 6-86. Ice Basket Plate Stress Summary

Table 6-87. Ice Basket U-Bolt Stress Summary

Table 6-88. Ice Basket - Basket End Stress Summary

Table 6-89. Ice Bucket Coupling Screw Stress Summary 3 Inch Elevation<sup>1</sup>

Table 6-90. Ice Bucket Coupling Screw Stress Summary 12 Foot Elevation<sup>1</sup>

Table 6-91. Ice Bucket Coupling Screw Stress Summary 24 Foot Elevation<sup>1</sup>

Table 6-92. Ice Bucket Coupling Screw Stress Summary 36 Foot Elevation<sup>1</sup>

Table 6-93. Crane and Rail Assembly Design Loads

Table 6-94. Refrigeration System Parameters

Table 6-95. Lower Inlet Door Design Parameters and Loads

Table 6-96. Design Loads Three Pier Lower Support Structure. (See Figure 6-142)

Table 6-97. Design Loads and Parameters Top Deck

Table 6-98. Summary of Results Upper Blanket Door Structural Analysis - LOCA

Table 6-99. Design Loads and Parameters Intermediate Deck

Table 6-100. Summary of Waltz Mill Tests

Table 6-101. Ice Condenser Allowable Limits<sup>(1)</sup>

Table 6-102. Summary of Duke-McGuire Loads-Tangential Case Obtained Using the Two-Mass Dynamic Model

Table 6-103. Summary of Duke-McGuire Loads-Radial Case Obtained Using the Two-Mass Dynamic Model

Table 6-104. Summary of Load Results of Five Non-Linear Dynamic Models (Loads Are For East-West SSE Earthquake)

Table 6-105. Summary of Parameters Used in the Seismic Analysis

Table 6-106. Selection of Steels in Relation to Prevention of Non-Ductile Fracture of Ice Condenser Components

Table 6-107. Deleted Per 1999 Update

Table 6-108. Annulus Ventilation System Malfunction Analysis

Table 6-109. Annulus Ventilation Discharge. (Pressure setpoint range -4.2 inwg to -1.2 inwg)

Table 6-110. Comparison of Engineered Safety Feature Ventilation Systems With Regulatory Guide 1.52 (Rev. 0)

Table 6-111. Containment Piping Penetration Data. (See Table 6-114 for description of notes.)

Table 6-112. Containment Isolation Valve Test Data. (See Table 6-114 for description of notes.)

Table 6-113. Containment Isolation Valve Data. (See Table 6-114 for description of notes.)

Table 6-114. Containment Piping Penetrations and Isolation Valve Data. (Notes to Table 6-111, Table 6-112 and Table 6-113.)

Table 6-115. Bi directional Leakage Test Results for Typical Diaphragm Value

Table 6-116. Deleted Per 2008 Update

Table 6-117. Parameters Used to Determine Hydrogen Generation

Table 6-118. Total Hydrogen Generation 2. (TID-14844 Release Model - 5.0 Percent Zirconium-Water Reaction)

Table 6-119. Deleted Per 1991 Update

Table 6-120. Fission Product Decay Deposition in Sump Solution 1

Table 6-121. Total Hydrogen Generation - Westinghouse Basis (TID Release Model - Noble Gas in Core; 0.5 Percent Zirconium-Water Reaction 2)

Table 6-122. Total Hydrogen Generation - NRC Basis (TID-14844 Release Model - 1.5% Zirconium-Water Reaction 2)

Table 6-123. Emergency Core Cooling System Component Parameters

Table 6-124. Normal Operating Status of Emergency Core Cooling System Components for Core Cooling

Table 6-125. Sequence of Operations: Injection to Cold Leg Recirculation

Table 6-126. Deleted Per 2009 Update

Table 6-127. Failure Analysis for Switchover to Cold Leg Recirculation

Table 6-128. Sequence of Operations: Cold Leg Recirculation to Residual Containment Spray

Table 6-129. Sequence of Operations: Cold Leg Recirculation to Hot Leg Recirculation

Table 6-130. Maximum Potential Recirculation Loop Leakage External to Containment

Table 6-131. Materials Employed for Emergency Core Cooling System Components

Table 6-132. ECCS Relief Valve Data

Table 6-133. Single Active Failure Analysis for Emergency Core Cooling System Components

Table 6-134. Emergency Core Cooling System Recirculation Piping Passive Failure Analysis - Long Term Phase

Table 6-135. Valves Required to Ensure Safe Shutdown of the Reactor

Table 6-136. Emergency Core Cooling System Shared Functions Evaluation

Table 6-137. Parameters for Boron Precipitation Analysis

Table 6-138. Control Area Ventilation System Failure Analysis

Table 6-139. Containment Spray System Component Parameters CSS Pump Data

Table 6-140. Types and Location of Insulation Used in the Containment

Table 6-141. Single Failure Analysis-Containment Spray System

Table 6-142. Swivel Bracket Stress Summary. (Ref. 80, Section 6.2.8) Load Case IV

Table 6-143. Containment Coatings

Table 6-144. Deleted Per 1999 Update

Table 6-145. McGuire Cold Leg Pump Discharge Break - Sequence of Events

## List of Figures

Figure 6-1. Symbols for Flow Diagrams

Figure 6-2. Symbols and System Abbreviations for Flow Diagrams

Figure 6-3. Index for Flow Diagrams

Figure 6-4. Sensitivity of Pressure to Air Compression Ratio

Figure 6-5. Steam Concentration in a Vertical Distribution Channel

Figure 6-6. Peak Compression Pressure Versus Compression Ratio

Figure 6-7. Upper Compartment Compression Pressure Versus Energy Release for Tests at 100% and 200% of Initial DBA Blowdown Rate

Figure 6-8. Peak Containment Pressure Transient - Pressure

Figure 6-9. Peak Containment Pressure Transient - Upper Containment Temperature

Figure 6-10. Peak Containment Pressure Transient - Lower Containment Temperature

Figure 6-11. Peak Containment Pressure Transient - Sump Temperature

Figure 6-12. Peak Containment Pressure Transient - Ice Melted

Figure 6-13. Containment Spray Return Drains From Air Return Fan Pits

Figure 6-14. Containment Spray Return Drains From Refueling Canal

Figure 6-15. Containment Spray Return Drains From Refueling Canal

Figure 6-16. Ice Melted Versus Energy Release for Tests at Different Blowdown Rates

Figure 6-17. Upper Compartment Peak Compression Pressure Versus Blowdown Rate for Tests With .75% Energy Release

Figure 6-18. Peak Reverse Differential Pressure Transient

Figure 6-19. Peak Reverse Differential Pressure Transient

Figure 6-20. Peak Reverse Differential Pressure Transient Assuming Enhanced Lower Compartment Heat Transfer

Figure 6-21. Peak Reverse Differential Pressure Transient Assuming Enhanced Lower Compartment Heat Transfer

Figure 6-22. Pressure Increase Versus Deck Area From Deck Leakage Tests

Figure 6-23. Energy Release at Time of Compression Peak Pressure From Full-Scale Section Tests With 1-Foot Diameter Baskets

Figure 6-24. Peak Containment Temperature Transient - Lower Containment Temperature

Figure 6-25. Peak Containment Temperature Transient - Break Compartment Temperature

Figure 6-26. Deleted Per 1998 Update.

Figure 6-27. Upper and Lower Compartment Pressure Transient for Worst Case, Break Compartment (Element 1) Having a DEHL Break

Figure 6-28. Upper and Lower Compartment Pressure Transient for Worst Case Break Compartment (Element 1) Having A DECL Break

Figure 6-29. Plan at Equipment Rooms Elevation

Figure 6-30. Containment Section View

Figure 6-31. Plan View at Ice Condenser Elevation - Ice Condenser Compartments

Figure 6-32. Layout of Containment Shell

Figure 6-33. TMD Code Network

Figure 6-34. Nine Volume Nodalization of the Steam Generator Enclosure

Figure 6-35. Illustration of Choked Flow Characteristics

Figure 6-36. Double Ended Steam Line Break in Steam Generator Enclosure

Figure 6-37. Double Ended Steam Line Break in Steam Generator Enclosure

Figure 6-38. Double Ended Steam Line Break in Steam Generator Enclosure

Figure 6-39. Double Ended Steam Line Break in Steam Generator Enclosure

Figure 6-40. Double Ended Steam Line Break in Steam Generator Enclosure

Figure 6-41. Two Volume Nodalization of the Steam Generator Enclosure

Figure 6-42. Two Volume Nodalization of the Pressurizer Enclosure

Figure 6-43. Four Volume Nodalization of the Pressurizer Enclosure

Figure 6-44. Developed View of the TMD Code Network for the Reactor Cavity Analysis

Figure 6-45. Flow Path Connections for the Reactor Cavity Analysis

Figure 6-46. Containment Model for the Reactor Cavity Analysis

Figure 6-47. Reactor Vessel Nozzle Break Supports

Figure 6-48. Reactor Cavity Analysis Element 1

Figure 6-49. Reactor Cavity Analysis Element 2

Figure 6-50. Reactor Cavity Analysis Element 3

Figure 6-51. Reactor Cavity Analysis Element 4

- Figure 6-52. Reactor Cavity Analysis Element 5
- Figure 6-53. Reactor Cavity Analysis Element 6
- Figure 6-54. Reactor Cavity Analysis Element 7
- Figure 6-55. Reactor Cavity Analysis Element 8
- Figure 6-56. Reactor Cavity Analysis Element 9
- Figure 6-57. Reactor Cavity Analysis Element 10
- Figure 6-58. Reactor Cavity Analysis Element 11
- Figure 6-59. Reactor Cavity Analysis Element 12
- Figure 6-60. Reactor Cavity Analysis Element 13
- Figure 6-61. Reactor Cavity Analysis Element 14
- Figure 6-62. Reactor Cavity Analysis Element 15
- Figure 6-63. Reactor Cavity Analysis Element 16
- Figure 6-64. Reactor Cavity Analysis Element 17
- Figure 6-65. Reactor Cavity Analysis Element 18
- Figure 6-66. Reactor Cavity Analysis Element 19
- Figure 6-67. Reactor Cavity Analysis Element 20
- Figure 6-68. Reactor Cavity Analysis Element 21
- Figure 6-69. Reactor Cavity Analysis Element 22
- Figure 6-70. Reactor Cavity Analysis Element 23
- Figure 6-71. Reactor Cavity Analysis Element 24
- Figure 6-72. Reactor Cavity Analysis Element 25
- Figure 6-73. Reactor Cavity Analysis Element 26
- Figure 6-74. Reactor Cavity Analysis Element 27
- Figure 6-75. Reactor Cavity Analysis Element 28
- Figure 6-76. Reactor Cavity Analysis Element 29
- Figure 6-77. Reactor Cavity Analysis Element 30
- Figure 6-78. Reactor Cavity Analysis Element 31
- Figure 6-79. Reactor Cavity Analysis Element 32

Figure 6-80. Reactor Cavity Analysis Element 33

Figure 6-81. Reactor Cavity Analysis Element 45

Figure 6-82. Reactor Cavity Analysis Element 46

Figure 6-83. Reactor Cavity Analysis Element 47

Figure 6-84. Reactor Cavity Analysis Element 53

Figure 6-85. Reactor Cavity Analysis Element 54

Figure 6-86. Hot Leg Double Ended Guillotine Break

Figure 6-87. Hot Leg Double Ended Guillotine Break

Figure 6-88. Cold Leg Double Ended Guillotine Break

Figure 6-89. Cold Leg Double Ended Guillotine Break

Figure 6-90. Hot Leg Single Ended Split Break

Figure 6-91. Hot Leg Single Ended Split Break

Figure 6-92. Cold Leg Single Ended Split Break

Figure 6-93. Cold Leg Single Ended Split Break

Figure 6-94. Comparison of Satan to Henry-Fauske

Figure 6-95. Comparison of Satan to Moody Subcooled

Figure 6-96. Zaloudek Measured Data Versus Modified Zaloudek Correlation

Figure 6-97. Zaloudek Short Tube Data

Figure 6-98. Exit Plane Quality as a Function of Upstream Pressure for Saturated Liquid

Figure 6-99. Henry Anl 7740 Data

Figure 6-100. Loft Tests 809 and 813 Gate P-1

Figure 6-101. Deleted Per 2001 Update

Figure 6-102. Deleted Per 2001 Update

Figure 6-103. Deleted Per 2001 Update

Figure 6-104. Deleted Per 2001 Update

Figure 6-105. Deleted Per 2001 Update

Figure 6-106. Deleted Per 2001 Update

Figure 6-107. Flow Diagram of Containment Air Return Exchange and Hydrogen Skimmer System

Figure 6-108. Reactor Building Heating-Ventilation-Air Conditioning

Figure 6-109. Containment Air Return Fan Performance Curve

Figure 6-110. Hydrogen Skimmer System

Figure 6-111. Hydrogen Skimmer Fan Performance Curve

Figure 6-112. Potential Areas of Hydrogen Pocketing and Minimum Flows

Figure 6-113. Isometric of Ice Condenser

Figure 6-114. Floor Structure

Figure 6-115. Wear Slab Top Surface Area Showing Typical Coolant Piping Layout

Figure 6-116. Lattice Frame Orientation

Figure 6-117. Load Distribution for Tangential Seismic and Blowdown Loads in Analytical Model

Figure 6-118. Lattice Frame

Figure 6-119. Lattice Frame Analysis Model

Figure 6-120. Typical Bottom Ice Basket Assembly

Figure 6-121. Combination of Concentric Axial Load and Distribution Load That Will Cause Failure of a Perforated Metal Ice Condenser Basket Material Layout

Figure 6-122. Crane Assembly

Figure 6-123. Crane Rail Assembly

Figure 6-124. Refrigerant Cycle Diagram

Figure 6-125. Glycol Cycle to Each Containment

Figure 6-126. Schematic Flow Diagrams of Air Cooling Cycle

Figure 6-127. Air Handling Unit Support Structure

Figure 6-128. Deleted Per 2011 Update

Figure 6-129. Lower Inlet Door Assembly

Figure 6-130. Details of Lower Inlet Door Showing Hinge, Proportioning Mechanism Limit Switches and Seals

Figure 6-131. Inlet Door Frame Assembly

Figure 6-132. Inlet Door Panel Assembly

Figure 6-133. Lower Inlet Door Shock Absorber Assembly

Figure 6-134. Four Loop Ice Condenser Lower Support Structure Conceptual Plan and Sections

Figure 6-135. Four Loop Ice Condenser Lower Support Structure General Assembly

Figure 6-136. ANSYS Model Assembly

Figure 6-137. Finite Element Model of Portal Frame

Figure 6-138. Schematic Diagram of Forces Applied to Three Pier Lower Support Structure

Figure 6-139. Force Transient Hot Leg Break

Figure 6-140. DLF Spectra Hot Leg Break Force Transient

Figure 6-141. Top Deck Test Assembly

Figure 6-142. Details of Top Deck Door Assembly

Figure 6-143. Intermediate Deck Door Assembly

Figure 6-144. Air Distribution Duct

Figure 6-145. Phase Diagram for NA2 B4 O7 .10 H/Water System at One Atmosphere

Figure 6-146. Ice Bed Compaction Versus Time

Figure 6-147. Test Ice Bed Compaction Versus Ice Bed Height

Figure 6-148. Model of Horizontal Lattice Frame Structure

Figure 6-149. Group Six Interconnected Lattice Frames

Figure 6-150. Lattice Frame Ice Basket Gap

Figure 6-151. Typical Displacement Time Histories for 12 Foot Basket With End Supports - Pluck Test

Figure 6-152. Non Linear Dynamic Model

Figure 6-153. 3 Mass Tangential Ice Basket Model

Figure 6-154. 9 Mass Radial Ice Basket Model

Figure 6-155. 48 Foot Beam Model

Figure 6-156. Phasing Mass Model of Adjacent Lattice Frame Bays

Figure 6-157. Phasing Study Model, 1 Level Lattice Frame 300 Degrees NonLinear Model

Figure 6-158. Typical Crane Wall Acceleration

Figure 6-159. Typical Crane Wall Velocity

Figure 6-160. Typical Crane Wall Displacement

Figure 6-161. Typical Ice Basket Displacement Response

Figure 6-162. Typical Ice Basket Impact Face Response

Figure 6-163. Typical Crane Wall Panel Load Response

Figure 6-164. Wall Panel Load Distribution Obtained Using the 48-Foot Beam Model Tangential Case

Figure 6-165. Wall Panel Load Distribution Obtained Using the 48-Foot Beam Model Radial Case

Figure 6-166. Ice Basket Impact Load Distribution Obtained Using the 48-Foot Beam Model Tangential Case

Figure 6-167. Ice Basket Impact Load Distribution Obtained Using the 48-Foot Beam Model Radial Case

Figure 6-168. Lower Inlet Door Differential Pressure - Time History

Figure 6-169. Flow Diagram of Annulus Ventilation System

Figure 6-170. Reactor Building Annulus - Developed Elevation From 270° to 90°

Figure 6-171. Reactor Building Annulus - Developed Elevation From 90° to 270°

Figure 6-172. Containment Piping Penetration Classification

Figure 6-173. Butterfly Valve Details

Figure 6-174. Aluminum Corrosion in DBA Environment 1

Figure 6-175. Results of Westinghouse Capsule Irradiation Tests

Figure 6-176. Flow Diagram of Safety Injection (NI) System

Figure 6-177. Flow Diagram of Safety Injection System

Figure 6-178. Deleted Per 1993 Update

Figure 6-179. NPSH and Head Capacity Curves for RHR Pumps

Figure 6-180. NPSH and Head Capacity Curves for Safety Injection Pumps

Figure 6-181. NPSH and Head Capacity Curves for Charging Pumps

Figure 6-182. ECCS Piping Layout

Figure 6-183. ECCS Process Flow Diagram

Figure 6-184. UHI Water Accumulator

Figure 6-185. Leak Rates for Bushing

Figure 6-186. Bushing Leak Rate After Severe Operation

Figure 6-187. Cutaway View of Motor Operated Valve Actuator

Figure 6-188. Flow Diagram of Control Area Chilled Water System

Figure 6-189. Flow Diagram of Control Area Chilled Water System

Figure 6-190. Flow Diagram of Control Area Chilled Water System

Figure 6-191. Flow Diagram of Control Area Ventilation System

Figure 6-192. Deleted Per 1993 Update

Figure 6-193. Deleted Per 1993 Update

Figure 6-194. Flow Diagram of Containment Spray (NS) System

Figure 6-195. Spray Nozzle Mass Distribution

Figure 6-196. Containment Sump - Units 1 & 2

Figure 6-197. Intermediate Deck Differential Pressure - Time History

Figure 6-198. Zinc Corrosion in DBA Environment

Figure 6-199. Flow From Intact And Broken Loops

Figure 6-200. Ice Basket Swivel Bracket Assembly

Figure 6-201. Double-Ended LBLOCA Mass and Energy Release Analysis

Figure 6-202. Double-Ended LBLOCA Mass and Energy Release Analysis

Figure 6-203. Double-Ended LBLOCA Mass and Energy Release Analysis

Figure 6-204. Double-Ended LBLOCA Mass and Energy Release Analysis

Figure 6-205. Upper and Lower Compartment Pressure, Min. Pressure Analysis

Figure 6-206. Upper Compartment Heat Removal Rate, Min. Pressure Analysis

Figure 6-207. Lower Compartment Heat Removal Rate, Min. Pressure Analysis

Figure 6-208 Upper and Lower Compartment Temperature, Min. Pressure Analysis

Figure 6-209. Ice Bed Heat Removal Rate, Min. Pressure Analysis

Figure 6-210. Heat Removal Rate by Lower Compartment Drain, Min. Pressure Analysis

Figure 6-211. Heat Removal Rate by Sump and Spray, Min. Pressure Analysis

## 6.0 Engineered Safety Features

The central safety objective in reactor design and operation is the control of fission products. The methods used to assure this objective are:

1. Core design to preclude release of fission products from the fuel [Chapter 4](#).
2. Retention in the reactor coolant of any fission products which may leak from the fuel [Chapter 5](#).
3. Retention of fission products by the Containment for operational and accidental releases beyond the reactor coolant boundary ([Chapter 6](#)).
4. Analyzing fission product dispersal to assure minimum population exposure for an accidental release beyond the Containment ([Chapter 2](#) and [Chapter 15](#)).
5. Provide adequate cooling of the core under all circumstances ([Chapter 5](#) and [Chapter 6](#)).

The Engineered Safety Features are the provisions in the Station which embody methods 2, 3 and 5 above to prevent the occurrence or to minimize the effects of any serious accident.

Separate and independent Engineered Safety Features are provided for each of the two units. Operability of Engineered Safety Features equipment is assured. Some of the equipment serves a function during normal reactor operation. In cases where equipment is used for emergency functions only, such as the Containment Spray System, provisions for meaningful periodic testing have been incorporated into the design. Quality control and quality assurance procedures are imposed on Engineered Safety Features components. These procedures incorporate the use of accepted codes and standards as well as supplementary test and inspection requirements to assure that all components will perform their intended function under accident conditions. Classification and code criteria applying to Engineered Safety Features are presented in various table of this section and in Section [3.2](#), [Figure 6-1](#), [Figure 6-2](#) and [Figure 6-3](#), Flow Diagram Symbols, is provided to assist in analysis of system diagrams.

Other chapters of the safety analysis report contain information which is pertinent to the Engineered Safety Features. [Chapter 7](#) describes the Engineered Safety Features Actuation System. [Chapter 8](#) describes the emergency power provisions. [Chapter 15](#) describes the analysis of the Engineered Safety Features capability to provide adequate protection during accident conditions. [Chapter 9](#) discusses functions performed by some Engineered Safety Features components during normal operation and gives further design details and descriptive information concerning their operation.

The Technical Specifications for operation establish limiting conditions governing the maintenance of Engineered Safety Features components during unit operation with the core critical. Maintenance of a component is permitted if the remaining components meet the minimum conditions required for operation and the following conditions are also met:

1. The remaining equipment has been demonstrated to be in operable condition.
2. A suitable time limit is placed on the total time span of successful maintenance which returns the component to an operable condition, ready to function.

The design philosophy with respect to active components in the Engineered Safety Features is to provide redundant equipment so that maintenance is possible during service. Maintenance of equipment of this type would generally be scheduled for periods of refueling and maintenance outages.

THIS IS THE LAST PAGE OF THE TEXT SECTION 6.0.

**THIS PAGE LEFT BLANK INTENTIONALLY.**

## 6.1 General

The design, fabrication, testing and inspection of the core, reactor coolant pressure boundary and their protection systems gives assurance of safe and reliable operation under all anticipated normal, transient, and accident conditions. Redundant component systems have been provided as an Engineered Safety Feature for additional protection. These Engineered Safety Features have been designed to provide protection during:

1. Any size break up to and including the circumferential rupture of the largest pipe in the reactor coolant system.
2. Any steam or feedwater line break.

The release of fission products from the Containment is limited in two ways:

1. Blocking the potential leakage paths from the Containment. This is accomplished by:
  - a. A free standing steel Containment with an outer reinforced concrete Reactor Building, and an annular space that is maintained at a pressure below atmospheric following a loss-of-coolant with piping penetrations either anchored or utilizing testable expansion bellows which form a virtually leaktight barrier preventing the escape of fission should a loss-of-coolant accident occur.
  - b. Isolation of process lines not required following an accident by the Containment Isolation System which imposes double barriers for each line which penetrates the Containment.
2. Reducing the Containment temperature and pressure and thereby limiting the driving potential for fission product leakage. This is accomplished by the Containment Spray System, the Ice Condenser System and Containment Air Return Fans.

### 6.1.1 Containment System

The general purpose of the Containment System is to provide a barrier confining potential releases of radioactivity from severe accidents. This is accomplished by maintaining leaktightness within specified bounds. As a design feature, the Containment System is provided primarily for the protection of public health and safety. The free standing steel Containment has an outer reinforced concrete Reactor Building and an annular space which is maintained at a lower-than-atmospheric pressure following a loss-of-coolant accident. These structures form a double barrier to the escape of fission products should a loss-of-coolant accident occur. Refer to Section [6.2.1](#) for details of the Containment and Reactor Building.

### 6.1.2 Emergency Core Cooling System

The principal design basis for the Emergency Core Cooling System (ECCS), as described in the General Design Criteria 44, has been met. Protection for the entire spectrum of Reactor Coolant System break sizes is provided. Separate and independent flow paths are provided and redundancy in active components assures that the required functions are performed if a single failure occurs. Separate emergency power sources are supplied to the redundant active components and separate instrument channels are used to actuate the systems.

ECCS and related pumps which must operate following the Design Basis Accident (DBA) include the residual heat removal, safety injection, Containment spray, centrifugal charging, component cooling water, and nuclear service water pumps.

All active components of the ECCS are located outside the Containment and are not subject to Containment accident conditions.

Emergency Core Cooling System provides borated water to cool the core in the event of an accidental depressurization of the Reactor Coolant System. The combination of the control rods and the boron in the injected water provide the necessary control of reactivity required. Refer to details in Section [6.3](#).

### **6.1.3 Containment Spray System**

The Containment Spray System is designed to furnish building atmosphere cooling to reduce the postaccident building pressure to nearly atmospheric pressure. Particulate matter is also captured by the spray and held in suspension in the Containment sump.

The Containment Spray System, in conjunction with melting ice, provides long-term cooling of the Containment. Refer to details in Section [6.5](#).

### **6.1.4 Containment Air Return and Hydrogen Skimmer System**

The Containment air return fans are provided to limit postaccident Containment pressure to the design value. Under DBA conditions, both equal capacity air return fans are started. The system is also designed such that a single failure of an active component during the injection or recirculation phases will not degrade the system's ability to fulfill the design objectives.

Air return fans return air to the lower Containment compartment after loss-of-coolant blowdown. The hydrogen skimmer fans prevent hydrogen pocketing in dead ended Containment compartments. Refer to details in Section [6.2.1.1.3.1](#).

### **6.1.5 Ice Condenser System**

The ice condenser prevents high pressure in the Containment and thus reduces the potential for the escape of fission products from the Containment. This low temperature heat sink, located on the inside of the steel Containment, consists of a suitable quantity of borated ice in a cold storage compartment. Refer to details in Section [6.2.2](#).

### **6.1.6 Containment Isolation System**

The Containment Isolation System provides means of isolating the piping which penetrates the Containment to prevent the release of radioactivity to the outside environment. Refer to details in Section [6.2.4](#).

### **6.1.7 Hydrogen Control System**

The original licensing bases credited the Hydrogen Recombiners to maintain post-LOCA Hydrogen concentrations below combustible limits (Refer to Sections [6.2.5](#) and [6.2.6](#)). Regulatory Guide 1.7, Rev. 3 and 10CFR50.44 were later revised, to only require the analysis of Hydrogen generation for the beyond-design-basis degraded core event (Refer to Section [6.2.7](#)). The combustible gas generated by a beyond-design-basis accident was deemed to be the risk-significant threat to containment integrity, whereas that for the design basis LOCA was not deemed risk-significant.

### **6.1.8 Annulus Ventilation System**

The Annulus Ventilation System maintains the post-accident negative pressure in the annulus between the Containment and the Reactor building, and collects and filters gaseous leakage from the Containment during accident conditions. Refer to details in Section [6.2.3](#).

THIS IS THE LAST PAGE OF THE TEXT SECTION 6.1.

**THIS PAGE LEFT BLANK INTENTIONALLY.**

## 6.2 Containment Systems

### 6.2.1 Containment Functional Design

#### 6.2.1.1 Containment Structure

##### 6.2.1.1.1 Design Bases

The functional design of the Containment is based upon the following accident input source term assumptions and conditions:

1. The design basis blowdown energy of  $324.2 \times 10^6$  Btu and mass of 498,200 lb put into the Containment.
2. The hot metal energy is considered.
3. A reactor core power of 3479 MWt (rated thermal power plus measurement uncertainty) used for decay heat generation.
4. The minimum Engineered Safety Features performance (i.e., the single failure criterion applied to each safety system) comprised of the following:
  - a. The ice condenser which condenses steam generated during a LOCA thereby limiting the pressure peak inside the Containment (see Section [6.2.2](#)).
  - b. The Containment Isolation System which closes those fluid penetrations not serving accident consequence limiting purposes (see Section [6.2.4](#)).
  - c. The Containment Spray System which sprays cool water into the Containment atmosphere, thereby limiting the pressure peak (particularly in the long term - see Section [6.5](#)).
  - d. The Annulus Ventilation System which produces a slightly negative pressure within the annulus, thereby precluding outleakage and relieving the post-accident thermal expansion of air in the annulus (see Section [6.2.3](#)).
  - e. The air return fans which return air to the lower compartment (see Section [6.2.1.1.3.1](#)).

Refer to Section [6.2.1.1.3.1](#) for the peak Containment pressure transient analysis where the above assumptions are discussed and utilized.

The Containment is designed to ensure that an acceptable upper limit of leakage of radioactive material is not exceeded under design accident conditions. For purposes of integrity, the Containment may be considered as the Containment Vessel and the Containment Isolation System. This structure and system are directly relied upon to maintain Containment integrity. The Annulus Ventilation System and Reactor Building function to keep outleakage minimal (the Reactor Building also serves as a protective structure), but are not factors in determining the design leak rate.

Although the Containment System incorporates the Annulus Ventilation System to maintain a negative pressure in the annulus as described in Section [6.2.3](#), assurance of Containment leak-tightness does not depend upon this system at any time. The design leak rate is the same whether or not this system is in operation. This leak rate is a property of the Containment Vessel alone, as verified by tests described in Section [6.2.1.6](#). The effect of the Annulus Ventilation System may be considered a margin of conservatism built into the leak rate as the system collects, delays and filters gases leaking from the Containment Vessel. The design evaluation in Section [6.2.3.3](#) includes a failure analysis to show the capability of the Annulus Ventilation System to function reliably and accurately under conditions of operating interruptions. The Containment Isolation System serves to maintain Containment integrity in

the event of a fluid penetration leak. The design evaluation of this system is presented in Section [6.2.4.3](#), and testing and inspection of this system are discussed in Section [6.2.4.4](#) and in the Technical Specifications.

The Containment is specifically designed to meet the intent of the applicable General Design Criteria listed in [3.1](#). This Section ([6.2.1](#)), [Chapter 3](#), and other portions of [Chapter 6](#) present information showing conformance of design of the Containment and related systems to these criteria.

The ice condenser is designed to limit the Containment pressure below the design pressure for all reactor coolant pipe break sizes up to and including a double-ended severance. Characterizing the performance of the ice condenser requires consideration of the rate of addition of mass and energy to the Containment as well as the total amounts of mass and energy added. Analyses have shown that the accident which produces the highest blowdown rate into an Ice Condenser Containment results in the maximum Containment pressure rise. That accident is the double-ended severance of a reactor coolant pipe.

Post-blowdown energy releases can also be accommodated without exceeding Containment design pressure.

#### **6.2.1.1.2 Design Features**

Consideration is given to subcompartment differential pressure resulting from a design basis accident in Section [6.2.1.2](#). If a design basis accident were to occur due to a pipe rupture in one of these relatively small volumes, the pressure would build up at a faster rate than in the Containment, thus imposing a differential pressure across the wall of these structures.

Parameters affecting the assumed capability for post-accident pressure reduction are discussed in Section [6.2.1.1.3](#).

There are four conditions which have a potential for resulting in a net external pressure on the Containment:

1. Rupture of a hot or high pressure process pipe in the annulus.
2. Inadvertent Containment Spray System initiation during normal operation.
3. Inadvertent Containment air return fan initiation during normal operation.
4. Containment purge fan operation with Containment purge inlet valves closed.

The Containment design of 1.5 psig negative is not violated in the above listed cases due to either equipment limitations or design features. The maximum Containment purge fan differential pressure is 0.75 psig, which would produce a 0.75 psig negative pressure in the Containment with the purge inlet valves closed.

Design features (such as guards, energy absorbing restraints, etc) are provided to ensure the ability of Containment and the Containment Subcompartments to withstand the pressures, temperatures, and dynamic effects of a LOCA. Specific discussion of these designs can be found in relevant subsections of [6.2](#) and [6.5](#) according to the system being discussed and the protection being provided.

The guard pipe for hot penetrations is discussed in Section [3.9.2](#). This design feature provides a path to the Containment for the fluid from a rupture in the annulus region.

Inadvertent spray or air return fan operation is precluded by design features consisting of an additional set of Containment pressure sensors which prevent operation of either of these systems when the Containment pressure is below the Containment Pressure Control System (CPCS) permissive setpoint. The pressure sensors are set such that the CPCS will provide a smart permissive function and a termination function.

To avoid unnecessary starting cycles of the Containment Air Return Fans, the CPCS is designed with a dead band feature that automatically cycles the Containment Air Return Fans off below 0.35 psig and on again at 0.80 psig if a Sp signal is still present. The logic of these sensors is presented in Section [7.6.16](#).

Therefore, the Containment Vessel is designed to withstand the maximum expected net external pressure in accordance with ASME Boiler and Pressure Vessel Code Section III paragraph NE-7116.

The Containment consists of a Containment Vessel and a separate Reactor Building enclosing an annulus. The Containment Vessel is a freestanding welded steel structure with a vertical cylinder, hemispherical dome, and a flat circular base. The Reactor Building is a reinforced concrete structure similar in shape to the Containment Vessel. The design of these structures is described in Section [3.8.1.4](#) for the Reactor Building and Section [3.8.2.4](#) for the Containment Vessel.

The design internal pressure for the Containment is 15 psig, and the design temperature is 250°F. The environment qualification (EQ) limit for all equipment in containment is 340°F. (The Peak Containment Temperature Transient is discussed in Section [6.2.1.1.3.3](#).) The design basis accident leakage rate is 0.3 percent/24 hr for the first 24 hours of the accident and 0.15 percent/24 hr thereafter. The design methods to ensure integrity of the Containment internal structures and subcompartments with respect to accident pressure pulses are described in Section [3.8.3.4](#).

The type of Containment used for the McGuire Nuclear Station was selected for the following reasons:

1. The Ice Condenser Containment can accept large amounts of energy and mass inputs and maintain low internal pressures and leakage rates. A particular advantage of the ice condenser is its passive actuation not requiring an actuation system signal.
2. The Ice Condenser Containment combines the required integrity, compact size, and a carefully considered advanced design desirable for a nuclear station.
3. The double-enclosure concept affords minimal interaction between the Containment Vessel (leakage barrier) and the Reactor Building (protective structure), a margin of conservatism in leakage rate from the use of two structures plus the Annulus Ventilation System, and a reduction of gaseous and particulate radioactive release due to annulus mixing and holdup prior to filtering and release.

The Ice Condenser Containment incorporating forced circulation of the Containment atmosphere, together with the Containment Spray System, ensures the functional capability of Containment for as long as necessary following an accident. The peak internal design pressure (15.0 psig) of the Containment is greater than the peak compression pressure (7.8 psig) occurring as the result of the complete blowdown of the reactor coolant through any rupture of the Reactor Coolant System up to and including the hypothetical double-ended severance of the largest reactor coolant pipe. The design pressure is not exceeded during any subsequent long term pressure transient.

### **6.2.1.1.3 Design Evaluation**

#### **6.2.1.1.3.1 Loss of Coolant Accident**

The time history of conditions with an Ice Condenser Containment during a postulated loss of coolant accident can be divided into 2 periods for calculational purposes:

1. The initial reactor coolant blowdown, which for the largest assumed pipe break occurs in approximately 10 seconds, and
2. The post blowdown phase of the accident which begins following the blowdown and extends several hours after the start of the accident.

During the first few seconds of the blowdown period of the Reactor Coolant System, Containment conditions are characterized by a rapid pressure and temperature increase. It is during this period that the

peak differential pressures, and blowdown loads occur. To calculate these transients a detailed spatial and short time increment analysis is necessary. This analysis is performed with the TMD computer code with the calculation time of interest extending up to a few seconds following the accident initiation.

Physically, tests at the ice condenser Waltz Mill test facility have shown that the blowdown phase represents that period of time in which the lower compartment air and a portion of the ice condenser air are displaced and compressed into the upper compartment and the remainder of the ice condenser. The Containment pressure at or near the end of blowdown is governed by this air compression process.

Containment pressure during the post blowdown phase of the accident is calculated with the GOTHIC 4.0/DUKE code which models the Containment structural heat sinks and Containment safeguards systems.

#### Compression Ratio Analysis

As blowdown continues following the initial pressure peak from a double ended cold leg break, the pressure in the lower compartment again increases, reaching a peak at or before the end of blowdown. The pressure in the upper compartment continues to rise from beginning of blowdown and reaches a peak which is slightly lower than the lower compartment pressure. After blowdown is complete, the steam in the lower compartment continues to flow through the doors into the ice bed compartment and is condensed.

The primary factor in producing this upper compartment pressure peak and, therefore, in determining the design pressure, is the displacement of air from the lower compartment into the upper compartment. The ice condenser quite effectively performs its function of condensing virtually all the steam that enters the ice beds. Essentially, the only source of steam entering the upper Containment is from leakage through the drain holes and other leakage around crack openings in hatches in the operating deck separating the lower and upper portions of the Containment building.

A method of analysis of the compression peak pressure was developed based on the results of full-scale section tests. This method consists of the calculation of the air mass compression ratio, the polytropic exponent for the compression process, and the effect of steam bypass through the operating deck on this compression.

The compression peak pressure in the upper Containment for the McGuire design is calculated to be 7.8 psig (for an initial air pressure of 0.3 psig). This compression pressure includes the effect of a pressure increase of 0.4 psi from steam bypass and also for the effects of the dead-ended volumes. The nitrogen partial pressure from the accumulators is not included since this nitrogen is not added to the Containment until after the compression peak pressure has been reduced, which is after blowdown is completed. This nitrogen is considered in the analysis of pressure decay following blowdown as presented in the long term performance analysis. In the following sections, a discussion of the major parameters affecting the compression peak will be discussed. Specifically they are air compression, blowdown energy, blowdown rate and steam bypass.

#### Air Compression Process Description

The volumes of the various Containment compartments determine directly the air volume compression ratio. This is basically the ratio of the total active Containment air volume to the compressed air volume during blowdown. During blowdown air is displaced from the lower compartment and compressed into the ice condenser beds and into the upper Containment above the operating deck. It is this air compression process which primarily determines the peak in Containment pressure, following the initial blowdown release. A peak compression pressure of 7.8 psig is based on the McGuire design compartment volumes shown in [Table 6-13](#). [Figure 6-4](#) and [Figure 6-6](#) shows the sensitivity of the compression peak pressure with different air compression ratios.

The actual Waltz Mill test compression ratios were found by performing air mass balances before the blowdown and at the time of the compression peak pressure, using the results of three special full-scale section tests. These three tests were conducted with an energy input representative of the plant design.

In the calculation of the mass balance for the ice condenser, the compartment is divided into two sub-volumes; one volume representing the flow channels and one volume representing the ice baskets. The flow channel volume is further divided into four sub-volumes, and the partial air pressure and mass in each sub-volume is found from thermocouple readings that the air is saturated with steam at the measured temperature. From these results, the average temperature of the air in the ice condenser compartment is found, and the volume occupied by the air at the total ice condenser pressure is found from the equation of state as follows:

$$V_a = \frac{M_a R_a T_a}{P}$$

where

$V_a$  = Volume of ice condenser occupied by air (ft<sup>3</sup>)

$M_a$  = Mass of air in ice condenser compartment (lbm)

$T_a$  = Average temperature of air in ice condenser (°R)

$P$  = Total ice condenser pressure (lbf/ft<sup>2</sup>)

The partial pressure and mass of air in the lower compartment are found by averaging the temperatures indicated by the thermocouples located in that compartment and assuming saturation conditions. For these three tests, it was found that the partial pressure, and hence the mass of air in the lower compartment, was zero at the time of the compression peak pressure. The actual Waltz Mill test compression ratio is then found from the following:

$$C_r = \frac{V_1 + V_2 + V_3}{V_3 + V_a}$$

where

$V_1$  = Lower compartment volume (ft<sup>3</sup>)

$V_2$  = Ice condenser compartment volume (ft<sup>3</sup>)

$V_3$  = Upper compartment volume (ft<sup>3</sup>)

The polytropic exponent for these tests is then found from the measured compression pressure and the compression ratio calculated above. Also considered is the pressure increase that results from the leakage of steam through the deck into the upper compartment.

The compression peak pressure in the upper compartment for the tests or Containment design is then given by

$$P_3 = P_O (C_r)^n + \Delta P_{\text{deck}}$$

where

$P_3$  = Compression peak pressure (psia)

$C_r$  = Volume compression ratio

$P_o$  = Initial containment pressure, 15.0 psia

$n$  = Polytropic exponent

$\Delta P_{deck}$  = Pressure increase caused by deck leakage (psi)

Using the method of calculation described above, the compression ratio is calculated for the three full-scale section tests. From the results of the air mass balances, it was found that air occupied 0.645 of the ice condenser compartment volume at the time of peak compression, or,

$$V_a = 0.645 V_2$$

The final compression volume includes the volume of the upper compartment as well as part of the volume of air in the ice condenser. The results of the full-scale section tests ([Figure 6-5](#)) show a variation in steam partial pressure from 100 percent near the bottom of the ice condenser to essentially zero near the top. The thermocouples and pressure detectors confirm that at the time when the compression peak pressure is reached steam occupies less than half of the volume of the ice condenser. The analytical model used in defining the Containment pressure peak uses upper compartment volume plus 64.5 percent of the ice condenser air volume as the final volume. This 64.5 percent value was determined from appropriate test results.

The calculated volume compression ratios are shown in ([Figure 6-6](#), along with the compression peak pressures for these tests. The compression peak pressure is determined from the measured pressure, after accounting for the deck leakage contribution. From the results shown in [Figure 6-6](#), the polytropic exponent for these tests is found to be 1.13.

For the McGuire design, the volume compression ratio, not accounting for dead-ended volume effect, is calculated using the data in [Table 6-4](#) :

$V_1$  is the sum of elements 1-6, 27, 31, 33 and 51

$V_2$  is the sum of elements 7-24 and 40-45

$V_3$  is the sum of elements 25, 38, 39, and 46-49

$$C_r = \frac{282,668 + 110,521 + 717,101}{717,101 + 0.645 \times 110,521}$$

$$C_r = 1.41$$

The peak compression pressure, based on an initial containment pressure of 15.0 psia, is then given by Equation 3 as:

$$P_3 = 15.0(1.41)^{1.13} + 0.4$$

$$P_3 = 22.5 \text{ psia or } 7.8 \text{ psig}$$

This peak compression pressure includes a pressure increase of 0.4 psi from steam bypass through the deck. The effect of the dead-ended compartment volumes is to trap additional air and thus reduce the compression ratio and the above calculated peak pressure.

#### Sensitivity To Blowdown Energy

The sensitivity of the upper compartment compression pressure peak versus the amount of energy released is shown in [Figure 6-7](#). This figure shows the magnitude of the peak compression pressure versus the amount of energy released in terms of percentage of Reactor Coolant System energy release. These

data are based on test results in which each of the tests were run at 110 percent and 200 percent of the initial blowdown rate equivalent to the maximum coolant pipe break flow.

These test results indicate the very large capacity of the ice condenser for additional amounts of energy with only a small effect on compression peak pressure. For example, during testing, 100 percent energy release gave a pressure of about 6.8 psig, while an increase up to 220 percent energy release gave an increase in peak pressure of only about 2 psi. It is also important to note that maldistribution of steam into different sections of the ice condenser would not cause even the small increase in peak pressure that is shown in [Figure 6-7](#). For every section of the ice condenser which may receive more energy than that of the average section, there are other sections which receive less energy. Thus, the compression pressure in the upper compartment would be indicated by the test performance based on 100 percent energy release, rather than either the maximum energy release section or the minimum energy release section.

[Figure 6-16](#) gives some insight as to the very large capacity for energy absorption of the ice condenser, as obtained from test results. [Figure 6-16](#) is a plot of the amount of ice melted versus the amount of energy released, based on test results at different energies and blowdown rates. These test results indicate that a 200 percent energy release melts only about 74 percent of the ice, while 100 percent energy release melts only 37 percent of the ice. Thus, even for energy release considerably in excess of 200 percent, there would still be a substantial amount of ice remaining in the condenser.

#### Effect of Blowdown Rate

[Figure 6-17](#) shows the effect of blowdown rate upon the final compression pressure in the upper compartment as obtained from test results. [Figure 6-17](#) is based on a series of tests, all of which had the plant design ice condenser configuration, but with the important difference that all of these tests were run with 175 percent of the Reactor Coolant System energy release quantity. There are two important effects to note from [Figure 6-17](#). First, the magnitude of the compression peak pressure in the upper compartment is low (about 7.7 psig) for the reactor plant design blowdown rate. Second, even an increase in this rate up to 200 percent blowdown rate produces only a small increase in the magnitude of this peak pressure (about 1 psi).

#### Effect of Steam Bypass [HISTORICAL INFORMATION NOT REQUIRED TO BE REVISED]

*The mass of steam which leaks through the operating deck into the upper Containment is a function of the relative flow areas and loss coefficients of the deck and inlet doors to the ice condenser, the mass of steam input to the lower compartment at the time of peak compression pressure, and the mass of steam stored in the lower compartment at the time of peak compression pressure.*

*Following is a discussion of the results of four full-scale section tests, which were conducted at Waltz Mill to measure the effect of deck leakage on the final compression peak pressure, and the calculational technique used to obtain the maximum allowable deck leakage area.*

*The effect of deck leakage on upper Containment pressure has been verified by a series of four special, full-scale section tests. These tests were all identical except different size deck leakage areas were used.*

*The results of these tests are given in [Figure 6-22](#), which includes two curves of test results. The slope of the increase in pressure at the end of blowdown is approximately  $0.107 \text{ psi/ft}^2$  in the range of interest for deck leakage area. Each curve shows the difference in upper compartment pressure between one test and another resulting from a difference in deck leakage area. One curve shows the increase in upper compartment pressure at the end of the boiler blowdown (after the compression peak pressure, at about 50 seconds in these tests), and the second curve shows the increase in upper compartment peak pressure, (at about 10 seconds in these tests). It should be noted that the pressure at the end of the blowdown is less than the peak upper compartment pressure, which occurred at about 10 seconds for the reference blowdown test.*

The Containment pressure increase due to deck leakage is directly proportional to the total amount of steam leakage into the upper compartment. The amount of this steam leakage is, in turn, proportional to the amount of steam released from the boiler minus the inventory of steam remaining in the lower compartment. Notably, the increase in upper compartment compression peak pressure is substantially less than the increase in upper compartment pressure at the end of blowdown. This is because the peak compression pressure occurs before the boiler has released all of its energy, and the measured increase in peak compression pressure due to increased deck leakage, is proportionately reduced. For the case of the station design, the final peak compression pressure is conservatively assumed to occur when the Reactor Coolant System has released 75 percent of its total energy. This value is selected as a reference value, based on the results of a number of tests conducted with different blowdown rates and total energy releases, as shown in [Figure 6-23](#). The actual deck leakage coefficient is therefore,

$$\Delta P_{\text{deck}} / A_{\text{bypass}} = 0.107 \times 0.75 = 0.080 \text{ psi/ft}^2$$

The divider barrier, including the enclosures over the pressurizer, steam generators and reactor vessel, is designed to provide a reasonably tight seal against leakage. Holes are purposely provided in the bottom of the refueling cavity to allow water from sprays in the upper compartment to drain to the sump in the lower compartment. Potential leakage paths exist at all the joints between the operating deck and the pump access hatches and reactor vessel enclosure slabs. The total of all deck leakage flow areas is approximately 5 square feet. The effect of this potential leakage path is small and is found to be:

$$\Delta P_{\text{deck}} = 5 \times 0.080 = 0.4 \text{ PSI}$$

In the event that the Reactor Coolant System break flow is so small that it would leak through these flow paths without developing sufficient differential pressure (1 lbf/ft<sup>2</sup>) to open the ice condenser doors, steam from the break slowly pressurizes the Containment. The Containment Spray System has sufficient capacity to maintain pressure well below design for this case.

The method of analysis used to obtain the maximum allowable deck leakage capacity as a function of the primary system break size is as follows.

During the blowdown transient, steam and air flow through the ice condenser doors and also through the deck bypass area into the upper compartment. For the Containment, this bypass area is composed of two parts, a known leakage area of 2.2 ft.<sup>2</sup> with a geometric loss coefficient of 1.5 through the deck drainage holes located at the bottom of the refueling canal and an undefined deck leakage area with a conservatively small loss coefficient of 2.5. A resistance network similar to that used in TMD is used to represent 6 lower compartment volumes each with a representative portion of the deck leakage and the lower inlet door flow resistance. Flow area is calculated for small breaks that would only partially open these doors. The coolant blowdown rate as a function of time is used with this flow network to calculate the differential pressures on the lower inlet doors and across the operating deck. The resultant deck leakage rate and integrated steam leakage into the upper compartment is then calculated. The lower inlet doors are initially held shut by the cold head of air behind the doors (approximately one pound per square foot). The initial blowdown from a small break opens the doors and removes the cold head on the doors. With the door differential removed, the door position is slightly open. An additional pressure differential of one pound per square foot is then sufficient to fully open the doors. The nominal door opening characteristics are based on test results.

One analysis conservatively assumed that flow through the postulated leakage paths is pure steam. During the actual blowdown transient, steam and air representative of the lower compartment mixture leak through the holes, thus less steam would enter the upper compartment. If flow were considered to be a mixture of liquid and vapor, the total leakage mass would increase, but the steam flow rate would decrease. The analysis also assumed that no condensing of the flow occurs due to structural heat sinks. The peak air compression in the upper compartment for the various break sizes is assumed with steam

mass added to this value to obtain the total Containment pressure. Air compression for the various break sizes is obtained from previous full-scale section tests conducted at Waltz Mill.

The allowable leakage area for the following Reactor Coolant System (RCS) break sizes was determined: DE, 0.6 DE, 3 ft<sup>2</sup>, 0.5 ft<sup>2</sup>, 8 inch diameter, 6 inch diameter, 2.5 inch diameter and 0.5 inch diameter. For break sizes 3 ft<sup>2</sup> and above, a series of deck leakage sensitivity studies were made to establish the total steam leakage to the upper compartment during the blowdown transient. This steam was added to the peak compression air mass in the upper compartment to calculate a peak pressure. Air and steam were assumed to be in thermal equilibrium, with the air partial pressure increased over the air compression value to account for heating effects. For these breaks, sprays were neglected. Reduction in compression ratio by return of air to the lower compartment was conservatively neglected. The results of this analysis are shown in [Table 6-20](#). This analysis is confirmed by Waltz Mill tests conducted with various deck leaks equivalent to over 50 ft<sup>2</sup> feet of deck leakage for the double-ended blowdown rate and is shown in [Figure 6-22](#).

For breaks 0.5 ft<sup>2</sup> and smaller, the effect of Containment sprays was included. The method used is as follows: For each time step of the blowdown, the amount of steam leaking into the upper compartment was calculated to obtain the steam mass in the upper compartment. This steam was mixed with the air in the upper compartment, assuming thermal equilibrium with air. The air partial pressure was increased to account for air heating effects. After sprays were initiated, the pressure was calculated based on the rate of accumulation of steam in the upper compartment.

This analysis was conducted for the 0.5 ft<sup>2</sup>, 8 inch, 6 inch and 2.5 inch break sizes, assuming one spray pump operating (3400 gpm at 100°F). As shown in [Table 6-20](#), the 6 inch and the 8 inch breaks are the limiting cases for this range of break sizes.

A second, more realistic, method was used to analyze the 0.5 ft<sup>2</sup> and the 8 inch diameter breaks. This analysis assumed a 30 percent air-70 percent steam mixture flowing through the deck leakage area. This is conservative considering the amount of air in the lower compartment during this portion of the transient. Operation of the deck fan increases the air content of the lower compartment, thus increasing the allowable deck leakage area. Based on the LOTIC code (References [20](#) and [24](#)) analysis, a structural heat removal rate of over 6000 Btu/sec from the upper compartment is indicated. Therefore, a steam condensation rate of 6 lbm/sec was used for the upper compartment. The results indicate that with one spray pump operating and a deck leakage area of 50 ft<sup>2</sup>, the peak Containment pressure is below design pressure.

In this deck leakage sensitivity study, the 0.5 inch break is not sufficient to open the ice condenser inlet doors. For this break size, the upper containment spray is sufficient to condense the break steam flow. The deck leakage sensitivity study employs conservative assumptions to maximize the steam content in upper containment. As such, it should not be viewed as reflecting the actual plant behavior (with regard to ice condenser door behavior or containment pressurization) following Reactor Coolant System breaks.

In conclusion, it is apparent that there is a substantial margin between the design deck leakage area and that which can be tolerated without exceeding containment design pressure.

#### Long Term Containment Pressure Analysis

The GOTHIC 4.0/DUKE (Reference [83](#)) code is used to determine the containment response to high-energy line breaks. It solves the conservation equations for mass, energy, and momentum for multi-component two-phase flow. These equations are solved numerically on a finite-volume mesh made up of numerous computational cells. The code features a nodalization scheme in which lumped parameter, one-, two-, and three-dimensional analysis or any combination of these may be performed.

GOTHIC includes finite-difference conduction models for passive thermal conductors. Concrete walls and structural steel within the containment building are simulated with these models. The various

mechanical components in the emergency safeguards systems, such as valves, heat exchangers, spray nozzles, and air return fans are also modeled.

Ice condenser heat transfer is calculated explicitly in the GOTHIC code. It is assumed that the ice remains at its initial temperature until it melts. The ice mass and surface area in each node is adjusted to account for the melted ice in each time increment. It is assumed that the ice remains in cylindrical columns within each node.

There are four different regions in an ice condenser containment building. These are the lower containment, upper containment, ice condenser, and dead-ended compartments. Slightly different modeling approaches are utilized in each of these four regions in the GOTHIC ice condenser containment model to accurately and efficiently calculate the containment response. The validation of the GOTHIC ice condenser model is presented in Reference [61](#), along with a discussion of the overall methodology utilized.

#### Peak Containment Pressure Transient

The following are the major input assumptions used in the GOTHIC 4.0/DUKE analysis for the pump discharge pipe rupture case with the steam generators considered as an active heat source for the McGuire Nuclear Station Containment. Note the flow values used in the containment analyses have been reduced by approximately 2% to account for the frequency variation of  $\pm 2\%$  allowed by the Technical Specifications.

1. Minimum safeguards are employed in all calculations, i.e., one of two spray pumps and one of two spray heat exchangers, one of two RHR pumps and one of two RHR heat exchangers providing flow to the core, one of two safety injection pumps and one of two centrifugal charging pumps, and one of two air return fans.

There are no simulations performed for the scenario with two trains of NS spray in operation; this scenario is considered non-limiting, since two trains of NS would reduce containment pressures and preserve the ice inventory for a longer time into the transient. There would be no need for ND auxiliary spray flow for this scenario; the additional heat removal capabilities from having both trains of NS in service would more than compensate for the lack of ND auxiliary spray flow. It is expected that the peak containment pressure for a scenario with both NS trains in service and no ND auxiliary spray flow would be lower than the scenario documented above.

2.  $1.89 \times 10^6$  lbs. of ice initially in the ice condenser. This ice is distributed with  $1.577 \times 10^6$  lbs. in rows 1 through 7 (mean of 1043 lbs. per basket), and  $3.132 \times 10^5$  lbs. in rows 8 and 9 (mean of 725 lbs. per basket).
3. The blowdown, reflood, and post-reflood mass and energy releases described in Section [6.2.1.3.1](#) are used.
4. Nitrogen from the accumulators in the amount of 6459 lbm is included in the calculations.
5. Nuclear service water temperature of 82°F is used on the spray heat exchanger and the component cooling heat exchanger. The RWST water temperature was modeled at 105°F.
6. The air return fan is effective 10 minutes after the transient is initiated.
7. An ice condenser bypass area of 5.0 ft<sup>2</sup> is assumed. Of this area, 2.2 ft<sup>2</sup> is accounted for by the Containment Spray return drains. The remaining 2.8 ft<sup>2</sup> is unspecified.
8. The initial conditions in the Containment are a temperature of 95°F in the lower and dead-ended volumes and a temperature of 60°F in the upper volume. All volumes are at a pressure of 0.3 psig.
9. Pump flow rates versus time given in [Table 6-17](#) were used during the cold leg recirculation phase. Containment spray flow is not assumed during the injection phase from the RWST.

10. Containment structural heat sinks are assumed with conservatively low heat transfer rates. (See [Table 6-18](#).)
11. The operation of one Containment spray heat exchanger ( $UA = 1.70 \times 10^6$  Btu/hr-°F) for containment cooling and the operation of one RHR heat exchanger ( $UA = 1.64 \times 10^6$  Btu/hr-°F) for core cooling. The RHR flow is cooled by component cooling flow which is cooled, in turn, by its own heat exchanger ( $UA = 1.60 \times 10^6$  Btu/hr-°F).
12. The air return fan returns air at a rate of 29,400 cfm from the upper to lower compartment.
13. Containment spray flow from the RWST is not assumed. Containment spray is initiated taking suction from the building sump following RWST low level with an operator action time delay. A containment spray flow rate of 3325 gpm is assumed to initiate at 3988 seconds.
14. A power level of 3479 MWt (rated thermal power plus measurement uncertainty) is used in the calculations.
15. Subcooling of ECC water from RHR heat exchanger is assumed.
16. The nuclear service water flow rates assumed are 3724 gpm to the containment spray heat exchanger and 5390 gpm to the component cooling heat exchanger.
17. The component cooling water flow rate in the RHR heat exchanger and the component cooling heat exchanger is 4900 gpm.

The following plots are provided for the limiting case, the pump discharge:

- [Figure 6-8](#), Containment pressure transient
- [Figure 6-9](#), Upper compartment temperature transient
- [Figure 6-10](#), Lower compartment temperature transient
- [Figure 6-11](#), Sump temperature transients
- [Figure 6-12](#), Ice melt vs. time

[Table 6-15](#) gives total sump volume versus time. Comparing this table with [Table 6-16](#), which gives the total sump volume versus elevation, the sump elevation versus time can be determined. The calculated sequence of events for the accident is shown in [Table 6-145](#).

As can be seen from [Figure 6-8](#) the maximum calculated Containment pressure is 13.87 psig and occurring at approximately 5283 seconds. The value for the maximum pressure is calculated using NRC-approved methodology and is revised periodically to support plant operational activities. Thus, the UFSAR value for the maximum pressure may differ from the value contained in the plant Technical Specifications. However, the UFSAR value shall be less than or equal to the Technical Specifications value.

#### Structural Heat Removal

Provision is made in the Containment pressure analysis for heat storage in interior and exterior walls. Each wall is divided into a number of nodes. For each node, a conservation of energy equation expressed in finite difference form accounts for transient conduction into and out of the node and temperature increases within the node. [Table 6-18](#) is a summary of the Containment structural heat sink and material property data used in the analysis.

The heat transfer coefficient to the containment structure is based primarily on the work of Uchida. An explanation of the manner of application is given in Reference [83](#).

#### Comparison with D. C. Cook

The basic ice condenser annulus for McGuire is the same as that for D. C. Cook. The Containment inside diameters and the crane wall outside diameters are identical as well as the 300 degrees of the annulus. A

comparison of the design parameters is given in [Table 6-19](#). As this table shows, volumes and vent areas are very similar. However, the reactor power ratings differ and therefore the Reactor Coolant System blowdowns do also.

Because of the difference in blowdowns, the spray systems and peak internal design pressures differ. The peak internal design pressure for McGuire is 15 psig and that of D. C. Cook is 12 psig. Cook has sprays in the upper and lower compartments and McGuire has sprays only in the upper compartment. The spray pump flow rates for the two stations are given in [Table 6-19](#).

Ice bed design parameters are identical as are the lower, intermediate and top deck door parameters for the two stations. As a result of the similarity of the two stations, data and studies reported for one station generally hold for the other.

#### Containment Spray Return to Sump

Following a LOCA, containment spray water returns from the upper containment to the lower containment via several paths:

1. Spray which falls into the ice condenser drains out through the ten inch drains by which melted ice escapes.
2. Spray which falls into the air return fan pit (outside the crane wall between the ends of the ice condenser) drains out through one six inch pipe into lower containment. This line is illustrated in [Figure 6-13](#).
3. Spray which falls into the refueling canal drains out through six lines, each eight inches in diameter, from the refueling canal to the lower containment. These lines are illustrated in [Figure 6-14](#) and [Figure 6-15](#).
4. Spray which falls on the operating deck around the refueling canal could accumulate to a depth of three inches before spilling over the curb surrounding the refueling canal. This curb is to prevent material on the operating deck from accidentally entering the canal. This accumulated water is prevented from entering the air return fan pit by a pair of six inch high curbs on either side of the refueling canal. The three inch height difference between the fan pit curbs and the refueling canal curbs forces water to preferentially overflow into the refueling canal and also provides a margin to accommodate minor wave motion without spillover into the pit.

An analysis of the spray return drains has been made to show that they are adequately sized for maximum normal and auxiliary containment spray flow. Results indicate that the water head in the air return fan pit drain at the pit floor elevation is sufficient to establish a steady state drainage into the lower containment. It has also been shown that a water head of approximately 9 feet in the refueling canal is sufficient to establish a steady state drainage between the upper and lower compartments. This water head is well within the capacity of the refueling canal.

The administrative controls which ensure that the ice condenser floor drains and the refueling canal drains are open during normal operation are discussed in the Technical Specifications as described in [Section 6.2.1.6.2](#).

#### Air Return Fans

Air return fans, located in the upper compartment in pits at elevation 778' between the crane wall and the Containment vessel wall as shown in [Figure 6-107](#) and [Figure 6-108](#), are provided to return air from the upper compartment into the lower compartment after the initial high energy line break blowdown. Two full capacity fans, designed to criteria applicable to safeguards operation in the post-accident Containment environment, are provided for this purpose. All essential components of the Containment Air Return System are designed to withstand the Safe Shutdown Earthquake.

Test results (Reference [37](#)) indicate the air returns to the lower compartment by natural convection without the air return fan. The fans are provided to enhance ice condenser removal of heat and fission products by maintaining forced convection flow through it.

After the Containment pressure has been reduced, the ice condenser and Containment spray are capable of maintaining the pressure below the design pressure with the assumption of steam generation by residual energy until the ice bed is completely melted. If core steam generation is assumed after complete ice melt, the Containment Spray System maintains the pressure below design with the return fans circulating air through the Containment volume.

An air return system failure analysis is provided in [Table 6-68](#). Each fan has a capacity of 30,000 cfm. Although these fans were originally designed to meet 40,000 cfm, it was later determined that they might not achieve this value and that 30,000 cfm was more realistic. This flow rate is conservatively reduced to 29,400 cfm for use in the peak containment pressure calculation, where the fans play an important role due to the relatively long duration of the transient. For the peak containment temperature transient, the fans actuate after the times of the calculated peak pressure and temperature. Their impact in this transient is therefore minimal. Their only effect is a contribution to the rate of depressurization and temperature reduction after 10 minutes. Both fan motors are started  $9\pm 1$  minutes after Containment pressure reaches the high-high setpoint. The fans blow air from the upper compartment to the lower compartment, thereby returning the air which was displaced by the blowdown to the lower compartment. An isolation damper is provided on the discharge of each fan. The damper acts as a barrier between the upper and lower compartments to prevent reverse flow which would bypass the ice condenser. The damper is normally closed and remains closed throughout initial blowdown following a postulated high energy line break. The damper motor is actuated 10 seconds after the Containment high-high pressure setpoint is reached but the damper is prohibited from opening until such time as the pressure differential between the upper and lower compartments is less than 0.5 psi with the lower compartment positive to the upper compartment. The pressure differential permissive is accomplished through a differential pressure switch with normally closed contacts located in the damper motor start circuit. A back draft damper is also provided at the discharge of each fan to serve as a check valve. For conservative calculations, both the isolation damper and check damper are considered open when pressure equalization between lower and upper compartments has taken place. Fan discharge flow is past radial walls and into the fan rooms. Flow enters the lower compartment through ports in the fan room crane wall. These ports provide for equalization of pressure between the lower compartment and dead ended volumes. After discharge into the lower compartment, the air flows, together with steam leaving the break, through the lower inlet doors into the ice condenser compartment where the steam portion of the flow is condensed. The air flow returns to the upper compartment through the intermediate and upper doors of the ice condenser compartment. The fans operate continuously after actuation, circulating air through the Containment volume, provided that Containment pressure is above the Containment Pressure Control System termination permissive.

The air return fans have sufficient head to overcome the divider barrier differential pressure (a maximum of 7.17 psf) resulting from steam flow and fan air flow entering the ice condenser through the lower inlet doors. The fans are provided with both normal and emergency Class 1E power. Fan "A" of each unit is supplied power from emergency diesel generator "A" of that unit. Fan "B" of each unit is supplied emergency power from emergency diesel generator "B" of that unit. The isolation damper provided at each air return fan discharge is sized to withstand the maximum differential pressure across the divider barrier. Adequate design margin is used to ensure structural and operating integrity.

The performance curve for the air return fans is shown on [Figure 6-109](#). The air return fan safety class and code class requirements are given in [Table 3-4](#).

In response to NRC Bulletin 2003-01, "Potential Impact of Debris Blockage on Emergency Sump Recirculation at Pressurized Water Reactors," McGuire has the option of starting one air return fan at a containment pressure of 1 psig during certain small break LOCA (SBLOCA) transient events.

Although not required from a safety analysis perspective, non-safety related cooling to containment will be secured from SBLOCA scenarios when one air return fan is manually started. The shutdown or isolation of the non-safety related containment ventilation units is cued by procedure steps associated with the containment air return fans. This provides enhanced sump margin by melting additional ice and avoids sump dilution.

The containment SBLOCA analysis demonstrates that operation of one air return fan between 1 and 3 psig in containment will not result in a malfunction of the Air Return System. During a SBLOCA event, the differential pressure between upper and lower containment remains well below the isolation damper actuator and air return fan design limits. The manual start of one air return fan does not interfere with automatic operation as described above or impact the diesel generator load sequencing as described in the UFSAR section 8.3, "Onsite Power Systems."

#### Hydrogen Skimmer Fans

Hydrogen skimmer fans, located in the upper compartment between the crane wall and the Containment vessel at elevation 819' as shown in [Figure 6-107](#) and [Figure 6-110](#), are provided to prevent the accumulation of hydrogen in restricted areas within the Containment resulting from a loss-of-coolant accident, assuming no credit for the effects of LOCA-induced turbulence and natural convection. The potential areas of hydrogen pocketing are shown on [Figure 6-112](#). Hydrogen pocketing is prevented by continuously drawing air out of each of the above areas at such a rate as to limit the potential local hydrogen concentration to less than 4 percent by volume. Two full capacity fans, designed to criteria applicable to safeguards operation in the post-accident Containment environment, are provided for this purpose. Piping, rather than sheet metal duct, is utilized in the hydrogen skimmer system to eliminate a possible rupture of the air conduit that could provide a path for bypassing the ice condenser during a high energy line break blowdown.

A hydrogen skimmer system failure analysis is provided in [Table 6-68](#). Each hydrogen skimmer fan has a capability of 3000 cfm. This ensures that the minimum flow rates given in [Figure 6-107](#) can be met. There is a normally closed, motor-operated valve on the hydrogen skimmer header to prevent ice condenser bypass during initial blowdown. Since this valve is electric motor operated and is normally closed, it fails as-is or closed, should the unit experience a high-energy line break. It remains closed until the end of initial blowdown. After initial blowdown, a signal from the Control Room opens this valve coincident with air return fan startup. Once the motor operated valve has fully opened, the hydrogen skimmer fan will start. Thus ice condenser bypass through this path is not possible during the initial blowdown. Since only one of the two redundant hydrogen skimmer trains needs to operate, one of these valves may malfunction (stay closed after blowdown) with no loss to unit safety. The hydrogen skimmer fans operate continuously after actuation.

The performance curve for the hydrogen skimmer fans is shown on [Figure 6-111](#). The hydrogen skimmer fan safety class and code class requirements are given in [Table 3-4](#).

The hydrogen skimmer system has redundant piping and is powered from corresponding redundant Class 1E power supplies. Each train of the system is capable of exhausting the calculated amount of entrapped hydrogen from all compartments.

To study the possibility of hydrogen accumulation in confined volumes, the Containment was sectionalized into specific compartments as shown in [Figure 6-112](#). The free volume of air for each compartment was then determined. These geometric data, along with the assumptions discussed in Section [6.2.5](#), were used in a computer code to calculate hydrogen generation data. The assumptions used include those given in Regulatory Guide 1.7.

Hydrogen generated from the following sources was considered:

1. Zirconium - water reaction

2. Core radiolysis
3. Sump water radiolysis
4. Metal - water reactions
5. Hydrogen contained within the primary coolant system

The hydrogen accumulation in each compartment is determined considering:

1. that portion of sump radiolysis hydrogen which would go into the compartment
2. all of the core radiolysis hydrogen going into those confined compartments in which a break could occur, i.e., the reactor compartment or the pressurizer enclosure
3. hydrogen associated with corrosion of aluminum and zinc components within the compartment
4. hydrogen dissolved within the primary coolant is initially distributed throughout all upper and lower Containment compartments
5. hydrogen produced by the zirconium-steam reaction is initially distributed uniformly throughout all upper and lower Containment compartments.

For the analysis of those compartments in which a pipe break could not occur, the core radiolysis hydrogen source is initially distributed uniformly throughout all upper and lower Containment compartments. This method ensures the Hydrogen Skimmer System is sized to accommodate the hydrogen released from a reactor coolant pipe break in any one of the possible compartments. The air return fans and the hydrogen skimmer fans are assumed to start 10 minutes after initiation of the transient.

The steady state ventilation flow to keep each compartment below 4 volume percent was then calculated using the equation of continuity. Resulting flows required are listed in [Figure 6-110](#).

#### Peak Reverse Differential Pressure Transient

The LOTIC-2 computer code, described in Reference [24](#), is used to calculate the reverse differential pressure across the operating deck. The Containment Spray input assumptions for this analysis are bounding even with manual only actuation of Containment Spray. In order to calculate a maximum reverse differential pressure, the following assumptions were made:

1. The dead-ended compartment volumes adjacent to the lower compartment (accumulator rooms A and B, incore instrumentation room, etc.) were assumed to be swept of air during the initial blowdown. This is a conservative assumption, since this maximizes the air mass forced into the upper ice bed and upper compartment, thus raising the compression pressure. In addition, it minimizes the mass of the noncondensibles in the lower compartment. With this modeling the dead-ended volume is included with that of the lower compartment.
2. The minimum Containment temperatures are assumed in the various subcompartments. This maximizes the air mass forced into the upper containment. It also increases the heat removal capability of the cold lower compartment structures.
3. The maximum temperature, 100°F, is assumed in the RWST. This helps raise the upper Containment temperature and pressure higher for a longer period of time.
4. The upper Containment spray flowrates used are runout flows.
5. A summary of the Containment parameters is given in [Table 6-8](#) through [Table 6-11](#).
6. The Westinghouse ECCS model (Reference 7, Appendix A) is used for structural heat transfer.
7. The mass and energy release data is given in [Table 6-7](#).
8. Ice condenser doors are assumed to act as check valves, allowing flow only into the ice condenser.

9. It is conservatively assumed that the only available flow path for flow between the upper and lower compartments was through the air return fan system. The resistance ( $K/A^2$ ) for this path is calculated to be  $0.0168 \text{ ft}^4$ .

With these assumptions the maximum reverse pressure differential across the operating deck is calculated to be 0.95 psi. [Figure 6-18](#) and [Figure 6-19](#) present the upper and lower compartment pressure and temperature transients.

In addition to the above calculations an analysis was performed including the effect of other possible lower compartment heat sinks. This extremely conservative analysis models the ice condenser flow through the drains as a 100 percent thermally efficient spray and assumes heat transfer to the sump with the same coefficients as used for lower compartment structures. The peak reverse  $\Delta P$  calculated for this case is 1.3 psi. [Figure 6-20](#) and [Figure 6-21](#) present the upper and lower compartment pressure and temperature transients for this case.

Significant margin exists between the design reverse differential pressures, 15.0 psi and 8.6 psi across the operating deck and the ice condenser lower inlet doors respectively, and those calculated pressures.

#### 6.2.1.1.3.2 Loss of Coolant Accident at Low Power and Reduced Containment Temperature

The long term containment transient calculation was reevaluated using the LOTIC-1 (Reference [20](#)) computer code with initial containment temperature of  $60^\circ\text{F}$  and reduced power. This calculation was assuming postfroth core power was 5% of ESDR power (ESDR power is 3579 MWt, and is a value used for the original design of the plant) and the initial temperature in the upper, lower and dead ended compartments was  $60^\circ\text{F}$ . It should be noted that this calculation has the following conservatisms:

1. The blowdown, reflood, and froth mass and energy release were done at 100% of ESDR power. ESDR power is 3579 MWt, and is a value used for the original design of the plant.
2. All structural heat sinks were at temperatures consistent with the current analyses.

For this case the ice bed melted out at approximately 67,500 seconds. The peak pressure following ice bed meltout was less than 4.0 psig. Since design pressure is 15.0 psig, this transient results in insignificant consequences with respect to demonstration of containment structural integrity.

#### 6.2.1.1.3.3 Steam Line Break

Analyses are performed with the GOTHIC Version 4.0/DUKE code (Reference [83](#)) to determine the pressure and temperature response of the containment following a steam line break.

The purpose for calculating the containment response following a steam line break is to determine if the temperature in lower containment is higher than the environmental qualification requirements established for components in that area. Due to the extended release of superheated steam from the steam generators, it is expected that temperatures in lower containment will be higher for a steam line break than for any LOCA.

The steam line break containment response is calculated for 360 seconds in each case run. The long-term containment response is not calculated because once the affected steam generator is isolated, the release of steam to the containment is essentially finished.

#### Peak Containment Temperature Transient

The following input assumptions used in the GOTHIC analyses for the steamline breaks analyzed for the McGuire Nuclear Station Containment:

1. Minimum safeguards are employed.

2.  $2.132 \times 10^6$  lbs. of ice initially in the ice condenser. Since the peak containment temperature occurs well before ice meltout, this parameter has no effect on this transient.
3. The mass and energy releases described in Section [6.2.1.4](#) were used. Since these rates are considerably less severe than those of the Reactor Coolant System double-ended break, and their total integrated energy is not sufficient to cause ice bed melt out, the containment pressure transients generated for the Reactor Coolant System breaks will be limiting. However, since the steamline break blowdowns are superheated, the lower compartment temperature transients calculated in this analysis will be limiting.
4. The initial conditions in the Containment are a temperature of 135°F in the lower and dead-ended compartments, a temperature of 100°F in the upper compartment, and a temperature of 30°F in the ice condenser. All components are at a pressure of 0.3 psig .
5. Containment structural heat sinks and material property data are presented in [Table 6-18](#).
6. A series of cases were run to determine the limiting case break, as described in Section [6.2.1.4](#).
7. The heat transfer coefficients to the containment structures are based on the work of Uchida. This is based on guidelines given in Reference [84](#).

## Results

The lower containment volume-averaged temperature profiles for three different steam line break sizes are shown in [Figure 6-24](#). It is clear that the highest peak temperatures result from the largest break size. Once the ice condenser drain flow initiates, the temperatures in lower containment decrease to about 250°F. Since the largest break size (2.4 ft<sup>2</sup>) results in a larger, faster release of energy to containment, it is the limiting case. A peak lower containment volume-average temperature of 297°F is reached in this case. In [Figure 6-25](#), the peak temperature in the break compartment is shown for the 2.4 ft<sup>2</sup> break. The peak temperature reached in this compartment is 317°F.

### 6.2.1.1.3.4 Steam Line Break With Continued Auxiliary Feedwater Addition

Pursuant to a NRC request contained in I.E. Bulletin 80-04 the steam line break accident was reanalyzed to determine if the potential for Containment overpressure existed if runout flow from the Auxiliary Feedwater System and impact of other energy sources such as continued feedwater flow were included in the analysis. The ability to detect and isolate the damaged steam generator from these energy sources and the ability of the pumps to remain operable after extended operation at runout flow was considered in response to I.E. Bulletin 80-04.

Duke Power analysis for McGuire Units 1 and 2 demonstrated that the worst case MSLB double-ended guillotine rupture at zero power and no AFW runout protection resulted in considerably less severe mass and energy release rates than those predicted for the reactor coolant double ended break. In addition, the MSLB total integrated energy release during first 30 minutes is not sufficient to cause ice bed meltout, so that MSLB accident is mitigated sufficiently to prevent the potential for Containment overpressurization. Operator action is not required for first 30 minutes of the accident. This ensures that the operator has sufficient time to analyze the accident and take proper actions to isolate the faulted steam generator. The AFW pumps have adequate flow resistance protection to ensure that pumps do not incur damage during operation at runout conditions. The NRC Technical evaluation of the Duke analysis concluded that the concerns of the I.E. Bulletin 80-04 have been adequately addressed (Reference [26](#)).

## 6.2.1.2 Containment Subcompartments

### 6.2.1.2.1 Design Basis

Consideration is given in the design of the Containment internal structures to localized pressure pulses that could occur following a loss-of-coolant accident. If a loss-of-coolant accident were to occur due to a pipe rupture in these relatively small volumes, the pressure would build up at a rate faster than in the overall Containment, thus imposing a differential pressure across the walls of the structures.

These subcompartments include the steam generator enclosure, pressurizer enclosure, and the reactor cavity. Each compartment is designed for the largest blowdown flow resulting from the severance of the largest connecting pipe within the enclosure or the blowdown flow into the enclosure from a break in an adjacent region.

The basic performance of the Ice Condenser Reactor Containment System has been demonstrated for a wide range of conditions by the Waltz Mill Ice Condenser Test Program. These results have clearly shown the capability and reliability of the ice condenser concept to limit the Containment pressure rise subsequent to a hypothetical loss-of-coolant accident.

To supplement this experimental proof of performance, a mathematical model has been developed to simulate the ice condenser pressure transients. This model, encoded as computer program TMD (Reference [1](#)), provides a means for computing pressures, temperatures, heat transfer rates, and mass flow rates as a function of time and location through the Containment. This model is used to compute pressure differences on various structures within the Containment as well as the distribution of steam flow as the air is displaced from the lower compartment. Although the TMD code can calculate the entire blowdown transient, the peak pressure differences on various structures occur within the first few seconds of the transient.

### 6.2.1.2.2 Design Features

Subcompartment free volumes were calculated based on the actual net volume available for each subcompartment. When calculating the input data all flow obstructions were subtracted to obtain the net flow area, except for the ventilation ducting in the flow paths between elements 3, 4 and 33. This ducting is designed to blow away under a pressure difference of 2 psi, which should be negligible. If this ducting were considered, the flow path data given in [Table 6-6](#) would replace the comparable data in [Table 6-5](#). The TMD calculations with this new data give nearly identical results.

Design features (such as guards, energy absorbing restraints, etc) are provided to ensure the ability of Containment and the Containment Subcompartments to withstand the pressures, temperatures, and dynamic effects of a LOCA. Specific discussion of these designs can be found in relevant subsections of [6.2](#) and [6.5](#) according to the system being discussed and the protection being provided.

### 6.2.1.2.3 Design Evaluation

The mathematical modeling in TMD is similar to that of the SATAN blowdown code in that the analytical solution is developed by considering the conservation equations of mass, momentum and energy and the equation of state, together with the control volume technique for simulating spatial variation. The governing equations for TMD are given in Reference [1](#).

The moisture entrainment modifications to the TMD code are discussed, in detail, in Reference [1](#). These modifications consist of incorporating the additional entrainment effects into the momentum and energy equations.

As part of the review of the TMD code, additional effects are considered. Changes to the analytical model required for these studies are described in Reference [1](#).

These studies consist of:

1. Spatial acceleration effects in ice bed,
2. Liquid entrainment in ice beds,
3. Upper limit on sonic velocity,
4. Variable ice bed loss coefficient,
5. Variable door response,
6. Wave propagation effects.

Additionally the TMD code has been modified to account for fluid compressibility effects in the high Mach number subsonic flow regime.

#### Experimental Verification

The performance of the TMD code was verified against the 1/24 scale air tests and the 1968 Waltz Mill tests. For the 1/24 scale model the TMD code was utilized to calculate flow rates to compare against experimental results. The effect of increased nodalization was also evaluated. The Waltz Mill test comparisons involved a reexamination of test data. In conducting the reanalyses, representation of the 1968 Waltz Mill test was reviewed with regard to parameters such as loss coefficients and blowdown time history. The details of this information are given in Reference [1](#).

The Waltz Mill Ice Condenser Blowdown Test Facility was reactivated in 1973 to verify the ice condenser performance with the following redesigned plant hardware scaled to the test configuration:

1. Perforated metal ice baskets and new design couplings.
2. Lattice frames sized to provide the correct loss coefficient relative to plant design.
3. Lower support beamed structure and turning vanes sized to provide the correct turning loss relative to the plant design.
4. No ice baskets in the lower ice condenser plenum opposite the inlet doors.

The result of these tests was to confirm that conclusions derived from previous Waltz Mill tests have not been significantly changed by the redesign of plant hardware. The TMD code has, as a result of the 1973 test series, been modified to match ice bed heat transfer performance. Detailed information on the 1973 Waltz Mill test series is found in Reference [22](#).

#### Application to Station Design (General Description)

As described in Reference [1](#), the control volume technique is used to spatially represent the Containment. The Containment is divided into 53 elements to give a detailed representation of the local pressure transient on the Containment shell and internal concrete structures. This division of the Containment is similar for all ice condenser units.

The McGuire Containment has been divided into elements as shown in [Figure 6-29](#) through [Figure 6-32](#). The interconnection between Containment elements in the TMD code is shown schematically in [Figure 6-33](#). Flow resistance and inertia are lumped together in the flow paths connecting the elements shown. The division of the lower compartment into 6 volumes occurs at the points of greatest flow resistance, i.e., the four steam generators, pressurizer and refueling cavity.

Each of these lower compartment sections delivers flow through doors into a section behind the doors and below the ice bed. Each vertical section of the ice bed is, in turn, divided into three elements. The upper plenum between the top of the ice bed and the upper doors is represented by an element. Thus, a total of thirty elements (elements 7 through 24 and 38 through 49) are used to simulate the ice condenser. The six elements at the top of the ice bed between bed and upper doors deliver to element number 25, the upper compartment. Note that cross flow in the ice bed is not accounted for in the analysis; this yields the most conservative results for the particular calculations described herein. The upper reactor cavity (element 33)

is connected to the lower compartment volumes and provides cross flow for pressure equalization of the lower compartments. The less active compartments, called dead-ended compartments (elements 26 through 32, 34 through 37, and 50 through 53) outside the crane wall are pressurized by ventilation openings through the crane wall into the fan compartments.

For each element in the TMD network the volume, initial pressure, and initial temperature conditions are specified. The ice condenser elements have additional inputs of mass of ice, heat transfer area and condensate layer length. For each flow path between elements flow resistance is specified as a loss coefficient “K” or a friction loss “ $f \frac{L}{D}$ ” or a combination of the two based on the flow area specified between elements. Friction factor, equivalent length and hydraulic diameter are specified for the friction loss. Additionally, input for each flow path includes the area ratio (minimum area/maximum area) which is used to account for compressibility effects across flow path contractions. The code input for each flow path is the flow path length used in the momentum equation. The ice condenser loss coefficients have been based on the 1/4 scale tests representative of the current ice condenser geometry. The test loss coefficient was increased to include basket roughness effects and to include intermediate and top deck pressure losses. The loss coefficient is based on removal of door port flow restrictors. To better represent short term transients effects, the opening characteristics of the lower, intermediate and top deck ice condenser doors have been modeled in the TMD code. The Containment geometric data for the elements and flow paths used in the TMD code is confirmed to agree with the actual design by Duke and Westinghouse. An initial Containment pressure of 0.3 psig was assumed in the analysis. Initial containment pressure variation about the assumed 0.3 psig value has only a slight effect on the initial pressure peak and the compression ratio pressure peak. TMD input data is given in [Table 6-4](#) and [Table 6-5](#).

The reactor coolant blowdown rates used in these cases are based on the SATAN analysis of a double-ended rupture of either a hot or a cold leg reactor coolant pipe utilizing a discharge coefficient of 1.0. The blowdown analysis is presented in Section [6.2.1.3](#).

A number of analyses have been performed to determine the various pressure transients resulting from hot and cold leg reactor coolant pipe breaks in any one of the six lower compartment elements. The analyses were performed using the following assumptions and correlations:

1. Flow was limited by the unaugmented critical flow correlation.
2. The TMD variable volume door model, which accounts for changes in the volumes of TMD elements as the door opens, was implemented.
3. The heat transfer calculation used was based on performance during the 1973-1974 Waltz Mill test series. A higher value of the ELJAC parameter has been used and an upper bound on calculated heat transfer coefficients has been imposed. (See Reference [22](#).)
4. One hundred percent moisture entrainment was assumed.
5. Compressibility effects due to flow area contractions were modeled.
6. The 1/4 scale loss coefficients were used.
7. No inlet door port rounding was assumed.

[Figure 6-27](#) and [Figure 6-28](#) are representative of the typical upper and lower compartment pressure transients that result from a hypothetical double-ended rupture of a reactor coolant pipe for the worst possible location in the lower compartment of the Containment, i.e., hot leg and cold leg breaks in element 1.

#### Initial Pressures

Results of the analysis for McGuire are presented in [Table 6-1](#), [Table 6-2](#) and [Table 6-3](#). The peak pressures and peak differential pressures resulting from hot and cold leg reactor coolant pipe breaks in each of the 6 lower compartment control volumes were calculated.

[Table 6-2](#) and [Table 6-3](#) presents the maximum calculated differential pressures between the various elements in the TMD network. [Table 3-37](#) contains a comparison of the calculated differential pressure with those actually used for design of the compartments. The TMD network shown in [Figure 6-33](#) was used with the data given in [Table 6-4](#) and [Table 6-5](#) to calculate these results.

[Table 6-1](#) presents the maximum calculated pressure peaks resulting from hot and cold leg double ended pipe breaks. Generally, the maximum peak pressure within a lower compartment element results when the pipe break occurs in that element. A cold leg break in element 1 creates the highest pressure peak, also in element 1, of 15.9 psig. The maximum peak pressure in each of the ice condenser sections is found in the lower plenum element of the section. The peak pressure was calculated to be 10.7 psig in element 40.

#### Sensitivity Studies

A series of TMD runs for D. C. Cook investigated the sensitivity of peak pressures to variations in individual input parameters for the design basis blowdown rate and 100 percent entrainment. This analysis used a DEHL break in element 6 of D. C. Cook. [Table 6-12](#) presents the results of this sensitivity study.

As part of the short-term Containment pressure analysis of ice condenser units, the pressure response to both DEHL and DECL breaks are routinely considered for each of the loop compartments. Differences in blowdown parameters such as initial Containment conditions, compartment geometry, unit rated power, etc., can have different relative effects on the Containment pressure response to a break in each location. Differences in blowdown mass/energy release and release rates are of major importance to the Containment pressure response.

For D. C. Cook, the peak differential pressure occurs in loop compartment 6 and is associated with the DEHL break whereas, for McGuire, the peak differential pressure occurs in loop compartment 1 and is associated with the DECL break. These results can, to a large extent, be attributed to the relative differences in DEHL and DECL blowdowns for the two stations as discussed in the response to Question 12 of the D. C. Cook FSAR Amendment 45. In particular, the DECL blowdown is directly influenced by the initial core outlet temperature. The higher core outlet temperature for McGuire results in earlier flashing of the hot leg and upper plenum fluid at a higher system pressure thereby resulting in a greater subcooled blowdown from the vessel side of the DECL break.

The humidity level in the McGuire Containment at the time of a design basis accident, a double-ended hot leg break in compartment 1, has no significant effect on the initial pressure transient. The difference between peak operating deck pressure differentials calculated by TMD for 100 percent initial relative humidity and zero initial humidity is less than 0.5 percent.

#### Ice Condenser Flow Channel Blockage

Proper operation of the ice condenser requires the ice to be distributed throughout the ice condenser and for open flow paths to exist around the ice baskets consistent with DBA assumptions. This is especially important during the initial blowdown so that (1) the steam and water mixture entering the lower compartment do not pass through only part of the ice condenser depleting the ice there while bypassing the ice in other portions of the ice condenser, and (2) to ensure there is sufficient air and steam flow (i.e., no significant obstruction to flow) through the ice condenser to prevent lower compartment overpressurization, as this could result in structural failure of the subcompartment walls or containment vessel. Analysis has shown that overpressurization of the lower compartment will not occur provided the overall blockage does not exceed the 15 percent section blockage assumed in the TMD code analysis. This analysis is not a detailed flow channel analysis. Instead, it lumps the ice condenser bays into six

sections of 2.75, 3.25, 6.50, 4.50, 3.50, and 3.50 bays, as shown in [Fig 6-31](#). Sensitivity analyses performed in the 1970's showed that up to 15 percent of the flow area can be blocked. According to Westinghouse, an acceptable level of blockage is one that meets the 15 percent criterion based upon the TMD lumping method. That is, there can be individual bays with blockage of greater than 15 percent, or even individual channels blocked, provided the highest calculated percent blockage in any of the TMD lumped sections does not exceed 15 percent.

#### Choked Flow Characteristics

The data in [Figure 6-35](#) illustrate the behavior of mass flow rate as a function of upstream and downstream pressures, including the effects of flow choking. The upper plot shows mass flow rate as a function of upstream pressure for various assumed values of downstream pressure. For zero back pressure ( $P_d = 0$ ), the entire curve represents choked flow conditions with the flow rate approximately proportional to upstream pressure,  $P_u$ . For higher back pressure, the flow rates are lower until the upstream pressure is high enough to provide choked flow. After the increase in upstream pressure is sufficient to provide flow choking, further increases in upstream pressure cause increases in mass flow rate along the curve for  $P_d = 0$ . The key point in this illustration is that flow rate continues to increase with increasing upstream pressure, even after flow choking conditions have been reached. Thus choking does not represent a threshold beyond which dramatically sharper increases in compartment pressures could be expected because of limitations on flow relief to adjacent compartment.

The phenomenon of flow choking is more frequently explained by assuming a fixed upstream pressure and examining the dependence of flow rate with respect to decreasing downstream pressure. The approach is illustrated for an assumed upstream pressure of 30 psia as shown in the upper plot with the results plotted vs. downstream pressure in the lower plot. For fixed upstream conditions, flow choking represents an upper limit flow rate beyond which further decreases in back pressure do not produce any increase in mass flow rate.

The augmented choked flow relationship utilized in TMD is based on experimental data obtained for choked two-phase flow through long tubes, short tubes, and nozzles, as presented in Figure 1-8 of Reference [1](#). The short tube data was cited by Henry and Fauske in Reference [2](#). In that article, they report that the compressible discharge coefficient representing actual measured critical flow rates for single-phase flow through sharp-edged orifices is also representative of single-phase flow through short tubes. Henry and Fauske conclude that an identical discharge coefficient may be applied to two-phase flow through these geometries, which defines the actual critical flow rates through the two geometries to be the same. On this basis, since the augmented choked flow correlation has been based on short-tube data, it should be applicable to sharp-edged orifices as well. The similarity of critical mass flows through sharp-edged orifices and short tubes is also noted in Reference [3](#).

Carafano and McManus, Reference [4](#), have published data for the two-phase flow of air-water and steam-water mixtures. Actually, water vapor was present in the gas phase of the so-called air-water test, making it, in fact, an air-steam-water test. The data presented in Reference [3](#) demonstrates that the ratio of experimental air-steam-water critical flow values to homogeneous equilibrium model predictions is greater than the ratio of steam-water experimental critical flow values to homogeneous equilibrium model predictions. Therefore, augmentation factors derived by comparing steam-water data to the homogeneous equilibrium model may be used in air-steam-water calculations.

#### Steam Generator

The most severe break possible in the upper cavity of the steam generator enclosure is a double-ended break of the steam line pipe at no-load conditions. The worst break location is considered to be at the steam generator nozzle-to-piping junction which is downstream of the flow-limiting nozzle. A full guillotine break is assumed at this location. However, full flow area is not developed because pipe rupture restraints and guides are used to restrict the movement of the ruptured pipe after rupture. An

energy absorbing restraint system involving the process pipe, the guard pipe, internal pads between the process pipe and the guard pipe, a load transfer structure on the guard pipe, an energy absorber, and a load transfer structure on the building is designed to limit the pipe movement and thereby restrict the break opening area. The break remains covered by the guard pipe. The process pipe is limited in its upward travel by the structural system described above and the flow area is thus restricted to less than 3.85 sq. ft. The flow area used in TMD calculation was 3.05 ft<sup>2</sup>. A subsequent calculation showed that an area of 3.85 ft<sup>2</sup> is acceptable. The blowdown for the break above is given in [Table 6-48](#). Insulation is assumed to remain intact during blowdown. The TMD code using the compressibility factor and assuming unaugmented critical flow is used to calculate the pressure transients. The configuration of the steam generator enclosures is shown in [Figure 1-13](#) through [Figure 1-16](#). The nodalization of the steam generator enclosure where the break occurs is shown in [Figure 6-41](#). The adjacent steam generator enclosure is similarly divided into two nodes. The input data for the enclosures is given in [Table 6-42](#). Loss coefficients are calculated based on methods outlined in Reference [21](#) in topic 6.2.8. The peak differential pressures across the steam generator vessels and the enclosure are given in [Table 6-44](#).

A nodalization study was also performed. The number of nodes in the break enclosure and the adjacent enclosure was increased from two to nine. The nodalization used in each of the enclosures is shown in [Figure 6-34](#). The input data is given in [Table 6-43](#). The peak differentials across the steam generator vessel and the enclosure are given in [Table 6-45](#).

The major pressure differentials in the asymmetric direction occur when the blowdown rate changes. This is illustrated in [Figure 6-36](#) through [Figure 6-39](#). The pressure differential across the roof of the enclosure is shown in [Figure 6-40](#).

As is shown in [Table 6-48](#), step changes in blowdown rate were used in this analysis. This is unrealistic (but conservative), since it would take some time to accelerate the break flow. Because of this conservatism, there is a tendency to magnify the inertial peaks.

Comparing the results between the two node and the nine node steam generator models, it can be seen that a decrease in pressure occurs when the number of nodes is increased. Thus is due to the reduced flow resistance into the adjacent steam generator enclosure. (The flow resistance around the steam generator need not be considered for all nodes.)

As [Figure 6-36](#) through [Figure 6-39](#) show, the steady state peaks are fairly low and should not significantly affect the design.

The peak positive values of the differential pressures would cause a loading on the steam generator support that would tend to oppose the loads calculated in the dynamic analysis. The peak negative values of the differential pressures would cause a loading on the supports that would tend to increase the loads calculated in the dynamic analysis. However, the small value of this negative differential pressure (less than 1 psid) and the short duration of the peaks (less than .1 seconds) should not significantly influence the support loadings. All subsequent peaks in differential pressure are less than initial peaks and occur after the maximum loading conditions on the steam generator supports.

Any further nodalization of this enclosure would introduce node boundaries which are fictitious with respect to real geometric boundaries and is therefore not necessary.

Main steam mechanical piping design utilizes a continuous, straight guard pipe between the Reactor Building and the crane wall inside the Containment such that a postulated main steam line break is fully accommodated for in the design, i.e.,

1. Postulated break flows would be forced through the ice condenser.
2. Other interior compartments, volumes, pipe chases, etc., cannot be pressurized by a postulated main steam line break.

#### Pressurizer

The largest break possible in the pressurizer enclosure is a double ended break of the 6 inch spray line from the reactor coolant pump outlet. The break location is assumed to be at the top of the enclosure, based on an investigation of postulated break locations for the spray line. The blowdown is given in [Table 6-49](#). Insulation is assumed to remain intact during blowdown. The TMD code, using the compressibility factor and assuming unaugmented critical flow, is used to calculate the pressure transients. The configuration of the pressurizer enclosure is shown on [Figure 1-13](#) through [Figure 1-15](#). The nodalization of the pressurizer enclosure is shown in [Figure 6-42](#). The input data for the enclosure is given in [Table 6-46](#). Loss coefficients are calculated based on methods outlined in Reference [21](#). The peak differential pressure for node 1 is 18.3 psi at 0.35 sec. and the peak differential pressure for node 2 is 18.0 psi at 0.35 sec. A nodalization sensitivity study was also performed. The number of nodes in the enclosure were increased from 2 to 4. This nodalization is shown in [Figure 6-43](#). The input data is given in [Table 6-47](#). The peak differential for node 1, across the roof of the enclosure, was 18.4 psi at 0.35 sec. The peak differential between nodes 2 to 4 and the upper compartment was 17.6 psi at 0.35 sec. The peak differentials between the nodes around the enclosure, nodes 2 to 4, were always less than 0.2 psi. The pressurizer enclosure was originally designed for a uniformly applied differential pressure of 14.0 psi, using working stress design method as outlined in Section [3.8.3](#). The adequacy of the pressurizer enclosure has been checked using the ultimate strength design method as outlined in the Standard Review Plan Section [3.8.4](#), November 1975, for the load combination  $\mu = D + 1 + Ta + Ra + 1.5Pa$ , where Pa is equal to 18.4 psig.

#### Reactor Cavity

The TMD computer code with the unaugmented homogeneous critical flow correlation and the previously described compressible subsonic flow correlation was used to calculate pressure transients in the reactor cavity region.

The critical mass flow rate correlation utilized assumes a homogeneous mixture of air, steam and water. Data which show comparisons between measured critical mass flow rates and predictions using the homogeneous critical flow model at low pressures have been analyzed. Specifically, an equation which augments the homogeneous model critical mass flow rates has been developed which provides a conservative lower bound on experimental critical mass flow rates. The factor applied to homogeneous model flow rates is  $(1.2 - .2X)$ , where X is the quality of the upstream compartment. Although critical mass flow rates obtained using the augmentation factor are conservative with respect to experimental data, the results presented herein are based on unaugmented homogeneous model critical flow.

Nodalization sensitivity studies were performed before the analysis was begun. The total number of nodes used varied from 6 to 54. In the 6-element model, no detail of the reactor vessel annulus was involved, and for that reason the model was discarded. Subsequent model changes primarily involved greater detail in the reactor vessel annulus. First, the annulus was divided into two vertical and eight circumferential regions. Next, some additional detail was added in the nozzle region, resulting in a 32-element model. A change to a 44 element model was made by increasing to three vertical and eight circumferential regions. The total integrated pressure in the reactor cavity changed only slightly because of the change from 32 to 44 elements. The next change, to 54 elements, produced the model shown, with detailed modeling around the broken nozzle. This increase caused virtually no change in the integrated pressure. The additional elements from 48 to 52 are external to the reactor cavity (ice condenser). Additional elements were added to account for all real area changes in the immediate vicinity of the break (i.e., elements 53 and 54 were added to model the broken loop inspection port volume and the broken loop pipe annulus respectively).

Any further nodalization in the region near the break would introduce fictitious boundaries between elements.

The nodal scheme around the reactor vessel produces a very accurate post-accident pressure profile because of its design. Element 3 is a small element inside the primary shield and it can receive all of the

flow from the break element. If it were made any larger, it would contain internal flow losses due to turning and would thus contain a pressure gradient. If it were made any smaller, it could not receive all of the flow from the break element. The four elements numbered 33, 34, 45, and 46 are made small to minimize internal pressure variation, and the elements farther from the break are made larger because pressure gradients are low in those regions.

[Figure 6-44](#) shows the general configuration of the reactor vessel annulus nodalization. [Figure 6-45](#) shows the flow path connections for the 54 element model of the unit. [Figure 6-46](#) illustrates the positions of some of the compartments (21-24). The upper containment is represented by compartment 32. The ice condenser is modeled as five elements (48-52), neglecting any flow distribution effects. The break occurs in compartment 1, immediately around a nozzle. The corresponding pipe annulus is represented by compartment 54. The upper reactor cavity is compartment 47, the lower reactor cavity is compartment 2, and the remainder of the elements, as shown on [Figure 6-46](#), are in the reactor vessel annulus. Compartments 15, 42, and 16 are really adjoining compartments 17, 43, and 18 respectively. Thus, compartment 13 is on the opposite side of the vessel from the assumed break. Element 53 represents the inspection port volume above the break. Elements 5, 36, 38, 39, 40, 41, 42, 43, and 44 represent the neutron detector shafts. [Figure 1-9](#) through [Figure 1-16](#) show the general arrangement of equipment and structures in the reactor cavity area.

The break opening area calculation for reactor vessel nozzle breaks is performed in two stages. First, conservative estimates of reactor vessel motion and loop displacements based on past analytical experience are chosen and used to calculate an estimated break area. Second, an analysis is performed using that area to verify that the assumptions used in the estimate are conservative.

The break opening area of 85 square inches used in the analysis was determined using conservatively estimated displacements. The reactor coolant loop analysis and reactor vessel dynamic analysis were then performed using specific McGuire parameters. Details of the pipe restraints located in the pipe annulus are shown in [Figure 6-47](#). The reactor vessel pipe rupture analysis includes the transient forcing functions resulting from loop hydraulic forces, reacting at the vessel nozzles, reactor pressure vessel internals hydraulic loadings, asymmetric reactor cavity pressure forces, and dead weight. The loop analysis is described in Section [5.2.1.10](#).

The reactor vessel supports have been evaluated considering the above defined loads and it has been confirmed that the reactor vessel support design meets the requirements specified in Section [5.5.14](#).

The detailed LOCA analyses indicate the following peak displacements:

1. The reactor vessel displaces horizontally 0.074 inches directly away from the break location.
2. The reactor vessel vertical and rotational displacements cause an upward vertical displacement of 0.037 inches at the nozzle.
3. The broken end of the pipe displaces 0.34 inches axially away from the nozzle, 0.65 inches laterally and 0.47 inches vertically downward.

These peak displacements are combined to confirm the break opening area. Since all of the peak displacements would not occur simultaneously, this combination produces a conservative estimate of break opening area. The break area calculated for a reactor vessel inlet nozzle break is 37 square inches. A similar LOCA analysis of a reactor vessel outlet nozzle break indicates a break area of 32 square inches. These calculations of break area verify the adequacy of the original break area assumption and demonstrate conservatism in the calculated response of the system.

The mass and energy release rates are presented in [Table 6-52](#).

Pressurization of the reactor cavity can occur for a postulated pipe break either at the inlet or outlet vessel nozzle terminal ends. The cavity is analyzed based on a limited area circumferential rupture at these locations. The break types and locations are consistent with the analysis discussed in Section [3.6.2.1.1](#).

The break locations and types are chosen on the basis of detailed fatigue and stress analyses and do not include hot leg and cold leg breaks within the cavity wall penetration.

[Table 6-50](#) and [Table 6-51](#) provide the volumes, flow paths, lengths, diameters, flow areas, resistance factors and the area ratio information for the elements and their connections. Loss coefficients are calculated using the methods outlined in Reference [21](#).

The inspection port covers are either removed or unrestrained during normal unit operation. The analysis assumes that the covers are not present at the start of the accident. Unrestrained covers are displaced very early in an event and the impact on the peak pressure results is insignificant. (Reference [88](#)) All insulation is assumed in place and uncrushed during the entire transient. All obstructions to vent areas such as ventilation ducting and electrical cables are conservatively assumed to be in place during the entire transient.

[Figure 6-48](#) through [Figure 6-85](#) show representative pressure transients for the break compartment, the upper and lower reactor cavities, the inspection port volume and pipe annulus near the break, the upper containment and the reactor vessel annulus. These plots demonstrate that the pressure gradient is steep near the break location and is very gradual farther away from the break. This indicates that the model must be very detailed close to the break location, but less detail is required with increasing distance.

Design pressures and calculated peak pressures for the reactor cavity volumes are presented in [Table 6-53](#).

#### Nitrogen Break

Nitrogen is supplied to the accumulators at a maximum pressure of 700 psig through a supply line one inch in diameter. If the supply line should break, a double-ended blowdown through the ruptured pipe would release the nitrogen present at 700 psig in the accumulators and in the nitrogen supply system. Because a 1 inch pipe is involved, the effective break area is only 0.01 ft<sup>2</sup> for a double-ended break. As a result, the blowdown rate is limited to a peak value of 22.8 lb/sec immediately following the break. As the blowdown proceeds the nitrogen pressure in the accumulators decreases, reducing the blowdown rate. A compartment pressure response analysis using the TMD code has shown that the blowdown rate is slow enough that no significant pressure differentials are developed between compartments.

Overall, 10,000 lbm of nitrogen are released from the accumulators and the nitrogen supply system during the blowdown. This results in a pressure increase of 1.75 psi in the Containment.

### **6.2.1.3 Mass and Energy Release Analysis for Postulated Loss-of-Coolant Accidents**

#### **6.2.1.3.1 Short Term Mass and Energy Release Data**

From the hot and cold leg studies, the design basis mass and energy release rates have been finalized. The mass and energy release rate transients for all the design cases are given in [Figure 6-86](#) through [Figure 6-93](#). All cases are generated from the SATAN-V break model consisting of Moody-Modified Zaloudek critical flow correlations applied at the break element. Since no mechanistic constraints have been established for full guillotine pipe rupture, an instantaneous pipe severance and disconnection is assumed for all transients. Assumptions specific to the presented transients are as follows:

For the hot leg mass and energy release rate transient to loop compartments:

[Figure 6-86](#) and [Figure 6-87](#)

1. A double ended guillotine type break.
2. A break located just outside the biological shield.
3. A break located in the worst loop.
4. A six node upper plenum model.

5. A 16 node broken hot leg pipe model.
6. A discharge coefficient ( $C_D$ ) equal to 1.0
7. A power condition of 3479 MWt (rated thermal power plus uncertainty) with  $T_{hot} = 623.9^\circ\text{F}$  and  $T_{cold} = 561.3^\circ\text{F}$ .

For the cold leg mass and energy release rate transient to loop compartments:

[Figure 6-88](#) and [Figure 6-89](#)

1. A double ended guillotine type break.
2. A break located just outside the biological shield.
3. A break located in the worst loop.
4. A six node upper plenum model.
5. A 16 node broken hot leg pipe model.
6. A discharge coefficient ( $C_D$ ) equal to 1.0
7. A power condition of 3479 MWt (rated thermal power plus uncertainty) with  $T_{hot} = 623.9^\circ\text{F}$  and  $T_{cold} = 561.3^\circ\text{F}$ .

For hot leg mass and energy release rate transients to subcompartments:

[Figure 6-90](#) and [Figure 6-91](#)

1. A single ended split type break.
2. A break just outside the hot leg nozzle.
3. A break in the pressurizer loop.
4. A six node upper plenum model.
5. A 16 node broken hot leg pipe model.
6. A discharge coefficient ( $C_D$ ) equal to 1.0
7. A power condition of 3479 MWt (rated thermal power plus uncertainty) with  $T_{hot} = 623.9^\circ\text{F}$  and  $T_{cold} = 561.3^\circ\text{F}$ .

For the cold leg mass and energy release rate transient to subcompartments:

[Figure 6-92](#) and [Figure 6-93](#)

1. A single ended split type break.
2. A break just outside the cold leg nozzle.
3. A break located in the worst loop.
4. A six node upper plenum model.
5. A 16 node broken hot leg pipe model.
6. A discharge coefficient ( $C_D$ ) equal to 1.0
7. A power condition of 3479 MWt (rated thermal power plus uncertainty) with  $T_{hot} = 623.9^\circ\text{F}$  and  $T_{cold} = 561.3^\circ\text{F}$ .

For the mass and energy release rate transient to the pressurizer enclosure a 6 inch spray line pipe break was considered ([Table 6-49](#)).

1. A guillotine type break modeled as a  $0.147 \text{ ft}^2$  split in the cold leg at the pump discharge (area of the six inch pressurizer spray feed line) and a  $0.087 \text{ ft}^2$  split in the top of the pressurizer (area of 4 inch spray nozzle).
2. Valves in spray lines are assumed to be open.
3. No pipe resistance for the feed line considered.
4. A power condition of 3479 MWt (rated thermal power plus uncertainty) with  $T_{hot} = 623.9^\circ\text{F}$  and  $T_{cold} = 561.3^\circ\text{F}$ .
5. A discharge coefficient ( $C_D$ ) equal to 1.0.

#### 6.2.1.3.1.1 Energy Sources

The energy sources include:

1. Reactor coolant system
2. Accumulators
3. Pumped injection
4. Decay heat
5. Core stored energy
6. Primary metal energy
7. Secondary metal energy
8. Steam generator secondary energy
9. Secondary transfer of energy (feedwater into and steam out of the steam generator secondary)

The inventories are presented at the following times, as appropriate:

1. Time zero (initial conditions)
2. End of blowdown time (EOB)
3. End of refill time (EOE)
4. End of reflood time (EOF)
5. End of analysis. (EOFIL)

The methods and assumptions used to release the various energy sources are given in Reference [36](#) and [Table 6-21](#).

The following assumptions ensure that the core energy release is conservatively analyzed for maximum containment pressure.

1. Maximum expected operating temperature
2. Allowance in temperature for instrument error and dead band (+4°F)
3. Margin in volume (1.4 percent)
4. Allowance in volume for thermal expansion (1.6 percent)
5. Margin in core power associated with use of engineered safeguards design rating (ESDR). ESDR is 3579 MWt, and is a value used for the original design of the plant.
6. Allowance for calorimetric error (2 percent of ESDR). ESDR is 3579 MWt, and is a value used for the original design of the plant.
7. Conservatively modified coefficients of heat transfer
8. Allowance in core stored energy for effect of fuel densification
9. Margin in core stored energy (+20 percent)

#### 6.2.1.3.1.2 Description of Blowdown Model

Mass and energy release rate transients generated for the TMD pressure calculation are supported by an extensive investigation of short term blowdown phenomena (Reference [25](#)). The SATAN-V code was used to predict early blowdown transients. The study concerned then a verification of the conservatism of

the SATAN-V calculated transients. This verification was accomplished through two approaches: a review of the validity of the SATAN-V break model, and a parametric study of significant physical assumptions.

The SATAN-V code uses a control volume approach to model the behavior of the Reactor Coolant System resulting from a large break in a main coolant pipe.

Release rate transients are determined by the SATAN-V break model which includes a critical flow calculation and an implicit representation of pressure wave propagation.

The SATAN-V critical flow calculation employs appropriately defined critical flow correlations applied for fluid conditions at the break element. For the early portion of blowdown, subcooled, saturated and two phase critical flow regimes are encountered. SATAN-V uses the Moody (Reference 5) correlation for saturated and two phase fluid conditions and a slight modification of the Zaloudek (Reference 6) correlation for the subcooled blowdown regime.

Since most short term blowdown transients are characterized by a peak mass and energy release rate that occurs during a subcooled condition, the Zaloudek application is particularly significant. The Zaloudek correlation is modified to merge to Moody predicted mass velocities at saturation in the break element. This correlation appears in the critical flow routine of SATAN-V in the form:

$$G_{\text{crit}} = CK1 \sqrt{(5.553 \times 10^5)(P - C_1 P_{\text{sat}})}$$

where

$$G_{\text{crit}} = \text{critical flow in } \frac{\text{Lb}_M}{\text{sec ft}^2}$$

P = reservoir pressure psia

P<sub>sat</sub> = reservoir saturation pressure psia

C<sub>1</sub> = constant where 0.5 < C<sub>1</sub> < 1

$$CK1 = \frac{0.1037}{1 - C_1} = \text{constant adjusted such that when } P = P_{\text{sat}}, G_{\text{crit}} \text{ from Zaloudek matches the SATAN-V}$$

Moody critical flow calculated at zero quality. For the present analysis, C<sub>1</sub> equals 0.9 and CK1 equals 1.018.

The modification also more conservatively accounts for the phenomena of increasing mass velocity with increasing degrees of subcooling. The slope of the subcooled G versus P curve is steeper for the modified correlation.

The low quality portion of the SATAN-V critical flow model is presented in [Figure 6-94](#). The Moody saturation line corresponds to the condition upstream in the break element where quality equals zero and pressure equals saturation pressure. Thus when pressure equals saturation pressure in the break element the Zaloudek and Moody critical flow values are equal. When pressure exceeds saturation pressure in the break element, the modified Zaloudek is used for the critical flow calculation. The steep slope of the Zaloudek G versus P line indicates the conservative treatment of the subcooling effect.

#### Comparison to Other Critical Flow Models

The Henry-Fauske critical flow correlation was considered for comparison (References 2, 8 and 9). This correlation models flow nonequilibrium via an approach which includes an empirical parameter. This parameter describes the deviation from equilibrium mass transfer and depends on flow geometry. The value is selected for a particular configuration based on the range of throat equilibrium qualities. The

value for constant area ducts is used in the present analysis. This choice is based on the worst possible double ended break geometry described below.

For cold leg and hot leg breaks, the majority of the flow, about 65 percent, comes from the vessel side of the break. For this side, the geometry may be described as an entrance nozzle and a straight pipe of approximate 12 feet in length and with a diameter of 29 inches. This length of pipe represents the distance from the reactor vessel to the periphery of the biological shield. No double ended break can occur within the biological shield because of the restricted movement within the pipe annulus. Hence the constant area value is appropriate.

Like the SATAN-V model, the Henry-Fauske correlation yields a  $G_{crit}$  in terms of upstream conditions and like the SATAN-V model it also exhibits a steeper slope of the G versus P line for subcooled conditions. As can be seen in [Figure 6-94](#), the Henry-Fauske saturated liquid line is below the Moody saturated line (SATAN-V model) for pressures greater than about 1000 psia. For short term blowdown calculations, the significant pressure region is from 1000 psia to 1800 psia, with increased emphasis on subcooled conditions for the 1000 psia end. Subcooled mass velocity versus pressure is given for the two fluid temperatures corresponding to  $P_{sat} = 1000$  and  $P_{sat} = 1800$ . It is clear from the figure that the slope of the Zaloudek G versus P line is steeper in both cases. This increased sensitivity coupled with the higher value for Moody at saturation causes the SATAN-V model to predict higher mass velocities. Hence the SATAN-V model is a more conservative treatment of critical flow than the Henry-Fauske model.

In the original FLASH model (Reference [10](#)), the Moody correlation was extended to subcooled conditions. This treatment is employed in many blowdown codes and thus it is appropriate to compare the SATAN-V model to these values. This is illustrated in [Figure 6-95](#). Again the Zaloudek treatment yields higher mass velocities and the SATAN-V model is more conservative.

#### Comparison to Experimental Data

The margin included in the modified Zaloudek prediction of subcooled critical flow rates is demonstrated by a review of experimental subcooled critical flow data. [Figure 6-96](#) and [Figure 6-97](#) present a plot of measured versus predicted critical flow values for Zaloudek's own data (References [6](#) and [11](#)). The figures indicate that when the modified correlation is applied to Zaloudek's data, the predicted critical flow values are significantly higher than measured flow rates.

The margin associated with the SATAN-V critical flow calculation may also be demonstrated by a review of the low quality data presented by Henry (Reference [9](#)). Exit plane quality, in terms of the Moody model, is determined as a function of upstream conditions by assuming an isentropic expansion to exit plane (i.e., critical) pressure. The lowest exit plane qualities where the Moody model is applied in the SATAN-V code occur for expansion from saturated liquid conditions. A plot of these are shown in [Figure 6-98](#). For exit plane qualities above the line, the Moody model is used in the SATAN-V code. Below the line, the Modified Zaloudek model is used.

Henry's comparison between data and model shows that for the range of exit plane quality greater than 0.02, the Moody model overpredicts the data, hence is conservative.

For the region below 0.02, it is appropriate to compare Henry's results with the Modified Zaloudek model, as used in the SATAN-V code. This is done in [Figure 6-99](#) for all of Henry's data points. As can be seen, the Zaloudek model overpredicts the flow. A discharge coefficient of 0.6 would be more reasonable than the 1.0 value used in SATAN-V.

#### Application to Transient Conditions

The Zaloudek correlation was developed for stagnation (reservoir) pressure and quasi steady state critical flow conditions. It is extended to application in the SATAN-V break element and transient flow conditions. This extension is justified because of the following considerations.

The pressure in the break element differs from the value in a nearby large volume because of three effects:

1. Pressure drop due to friction
2. Pressure drop due to spatial acceleration (momentum flux)
3. Pressure drop due to the transient.

The friction term in the reactor application is quantifiable; this term is less important than the other two. The sensitivity of the break flow rate to fluid friction was evaluated via a parametric study. For the purposes of this study, an analysis was made wherein the frictional resistance between the vessel and the break was reduced from the design values by a factor of one hundred. Over the period from 0.0 to 60 milliseconds (which includes the peak break flow), the integrated mass flow differed by less than 18 lbs from the design friction case; the total release over this period was about 5000 lbs.

Spatial acceleration is the major source of pressure drop upstream of the break between the reservoir and the pipe, causing steep pressure gradients in the approach region to critical flow. This term is not calculated explicitly in the SATAN-V code. Spatial acceleration is accounted for by the use of critical flow correlations (Zaloudek or Moody) which contain this effect. No credit is taken for pressure drop due to spatial acceleration for elements other than the break element. Hence, the pressure calculated by SATAN-V may be interpreted as a stagnation pressure which is the appropriate pressure for the Zaloudek and Moody models.

Prior to the occurrence of the peak release rate, the break element and up-stream reservoir pressures differ as a result of the transient described by pressure wave propagation. The applicability of the SATAN-V break model to this situation is verified by the code's ability to match recorded Semiscale transients. SATAN simulations of LOFT transients support the SATAN-V transient calculation. [Figure 6-100](#) presents a comparison of LOFT pressure transient recorded near the break to the SATAN-V model of the LOFT break element transient. The graphs demonstrate the ability of the SATAN-V code to track pressure waves in the broken pipe.

Moreover, the critical flow correlation is implemented in the present analysis by combining the correlation with the appropriate momentum equation. This provides a model for predicting break flow acceleration vis-a-vis a quasi-steady simulation. This is found to have little effect on Containment pressure but is a more physical representation.

Thus the SATAN-V break model is supported by subcooled critical flow data, by comparison to other correlations, and ability to simulate short term transients.

#### Parametric Studies

With confirmation of the conservatism of the SATAN-V break model, a series of parametric studies were undertaken to identify the blowdown transient corresponding to the most severe TMD results. A series of basic sensitivities were first studied to set the scope of the more detailed investigations. The assumptions of break size, break type and break location were considered. The results of this analysis were evaluated using the TMD code.

#### Break Size, Type and Location

As part of the short term blowdown investigation, a parametric study was made to determine the effect of break size, type and location on short term mass and energy release rates. A range of break sizes from a break area corresponding to the main coolant pipe area to a break area of twice the pipe area was considered. Also considered were possible break locations in the hot leg, the pump suction leg, and the cold leg. From this study it was determined that the double ended break area yielded the highest release rate transients and that the pump suction leg break location resulted in much less severe mass and energy release rates. Thus short term blowdown transients and corresponding Containment pressure transients are presented for hot leg and cold leg double ended guillotine breaks.

A sensitivity study to determine the effect of break type on short term blowdown has been performed. The study consisted of a series of short term blowdowns for both guillotine and split type breaks. For a double ended break area, the split type break resulted in less severe mass and energy release transients than were observed for guillotine type breaks. The observed double ended sensitivity is reversed for single ended breaks. Release rate transients are less severe for single ended guillotine type breaks than for single ended split type breaks.

The sensitivities presented above are explainable in terms of the inherent differences between split and guillotine type breaks. The guillotine break models a complete separation of the ends of the broken pipe while the split break maintains the flow path through the broken pipe. Because physical separation of the ends exists for guillotine breaks throughout the blowdown transient, a significant difference is observed between pressures at the approach regions to the ends of the break. In particular for a double ended guillotine break the pressure at the vessel side of the break may exceed the loop side pressure by 300 psi. Communication allowed by the split break then, acts to bring the approach region pressure to an intermediate value between the two pressures observed at the ends of the guillotine break.

By bringing the approach region pressure to an intermediate value, the release rates are reduced for split type breaks of twice the coolant pipe area. Flow from the vessel end of the break is limited by a choked condition at the nozzle and thus is relatively unaffected by the lower pressure in the break element. The intermediate pressure for the split, however, is higher than occurs at the loop end of the guillotine break. As a result, the pressure gradient driving loop side flow is reduced.

For breaks of an area equal to the coolant pipe area, the split break acts to increase release rates. The sensitivity is reversed because a choked flow condition does not prevail at the vessel nozzle. The intermediate pressure again reduces the loop side pressure gradient and thus the loop side flow. However, the intermediate pressure results in a vessel side pressure gradient which is higher than occurs for the single guillotine type break. Because a choked flow condition does not exist at the nozzle, an increase in vessel side flow results from the higher pressure gradient. Since the vessel supplies at least 2/3 of the flow to the break, an overall increase in the total mass flow rate is observed for the single ended split type break.

The influence of break location on TMD peak pressure was considered by generating blowdown transients for possible worst break locations. The results indicated that a double ended break in the pump suction leg was clearly less severe for short term blowdown release rates and that no such clear decision could be made between hot and cold leg breaks.

More detailed parametric studies were continued for the cold leg and the hot leg double ended guillotine breaks. The two locations produce intrinsically different TMD pressure responses and therefore must be dealt with in separate parametric surveys.

#### Hot Leg Nodal Configuration

A study of the SATAN-V nodal configuration has been applied to the hot leg double ended guillotine break. It was found that for this break the nodal configuration of the broken hot leg and the upper plenum are significant to short term transients. Spatial convergence was achieved for the upper plenum after the addition of four nodes to the standard SATAN-V two node upper plenum model. These nodes are hemispherical shells arranged concentrically from the broken hot leg nozzle and approximate the propagation of the pressure wave in the upper plenum. They are significant in that they specify the inertial response of the upper plenum. Spatial convergence was demonstrated because doubling the number of nodes yielded less than one percent deviation in break flow at all times.

Sensitivity to nodal configuration in the broken hot leg pipe was also investigated. Models with from 4 to 16 nodes were used to generate transients. Increasing the number of nodes was found to give a better simulation of pressure wave propagation in the pipe.

### Cold Leg Studies

The cold leg break transient was also reviewed in terms of significant parameters.

The Reactor Coolant System behavior is different for cold leg breaks and the peak Containment pressure occurs later for cold leg breaks. The following studies were performed:

#### 1. Nodal Configuration

For the cold leg break the nodal configuration of the broken cold leg and the downcomer is significant to the transient. Spatial convergence was achieved with the addition of three additional nodes to the standard SATAN-V model. These are annular rings arranged concentrically from the broken cold leg nozzle and model propagation of the pressure wave in the downcomer.

As in the hot leg sensitivity, from 4 to 16 pipe node models were tried for the cold leg transient. Again, more nodes give a better simulation of the pressure wave propagation in the broken pipe.

#### 2. Pump Modeling

For the time period of interest, the variation in pump inlet density is small and the variation in pump speed is small. This model was found to have no effect.

### **6.2.1.3.2 Long-Term Mass and Energy Release Data**

Large break LOCA analyses have been performed to generate mass and energy release boundary conditions for determining the long term containment response to a rupture of the RCS piping. Reference [61](#) presented the long term mass and energy release analyses. Since the McGuire Nuclear Station containment has an ice condenser containment, the peak pressure following a rupture of the RCS piping will not occur during the blowdown phase. The peak pressure occurs after ice meltout during the post-reflood phase of the event. The RELAP5/MOD3.1DUKE computer code is used to generate boundary conditions for the containment pressure response analyses from the initiation of the piping break through the blowdown, refill, reflood, and post reflood phases of the long-term analysis. The RELAP5/MOD3.1DUKE code is derived from RELAP5/MOD3.1 (Reference [82](#)) which was developed by EG&G Idaho under NRC sponsorship.

Three double-ended guillotine pipe break locations are examined; hot leg, cold leg pump suction, and cold leg pump discharge. Split breaks and breaks of lesser flow area are not examined because it is well recognized that these breaks will not yield the limiting containment pressure. The mass and energy release boundary conditions generated from these break locations are used as input to the GOTHIC code (Reference [83](#)) to calculate the containment pressure response.

The analyses are performed for the NSSS with the Babcock and Wilcox Feeding Steam Generators (BWI FSG).

#### **6.2.1.3.2.1 Computer Code**

The RELAP5/MOD3.1DUKE code models the steady-state and transient behavior of a hydraulic system that may contain a mixture of steam, water, non-condensable gas or nonvolatile solute. The fluid system is modeled by discretizing the system into control volumes (nodes) joined by momentum cells (junctions). The hydraulic flow field treats the liquid and steam phases as separate fluids in a non-homogeneous, non-equilibrium manner, solving the mass, energy and momentum equations for each phase. Constitutive relationships are used to define flow regimes and to model interphase drag, vapor generation and interphase heat and mass transfer, and horizontal and vertical stratification. Empirical relationships are used to model convective heat transfer, energy partitioning between phases, choked flow and two-phase wall friction. The code supports simulation of the primary system, secondary system, feedwater train,

automatic control systems and core neutronics. Available component models include reactor point kinetics, pumps, valves, heat structures, heat exchangers, turbines, separators and accumulators.

6.2.1.3.2.2 LOCA Simulation Models

Reference 61 describes the RELAP5 nodalization used in the LOCA analyses. The vessel, piping and steam generator nodalization are of sufficient detail to assure that the requirements of ANS-56.4-1983 (Reference 84) are met (i.e., break flow quality is not overpredicted, and core-to-coolant, metal-to-coolant, and SG-to-coolant heat transfer will conservatively predict high containment peak pressures).

6.2.1.3.2.3 Critical Flow Model

The RELAP5 Ransom and Trapp critical flow model (Reference 82) is used as the break flow model. Flow discharge coefficients are applied so as to provide break flow results equivalent to that of the Moody/Henry-Fauske critical flow models.

6.2.1.3.2.4 Initial Conditions

The initial conditions for the RELAP5 LBLOCA mass and energy release analyses were chosen with consideration for the guidance presented in Reference 84. The intent is to select initial conditions that will maximize the stored energy in the primary and secondary coolant systems and thus contribute to a conservatively high peak pressure in the containment response analysis. The initial conditions in the RELAP5 mass and energy release analyses are listed below.

PARAMETER	ANS GUIDANCE	RELAP5
		Mass and Energy Analyses
Core power level	≥ licensed power level plus an uncertainty allowance	3479 MWt (rated thermal power plus measurement uncertainty)
Core inlet temperature	≥ normal operating temperature for the selected power level plus upward adjustment for uncertainties	Nominal + 4°F
RCS pressure	≥ normal operating pressure for the selected power level plus allowance for uncertainties	Nominal + 60 psi uncertainty allowance.
RCS flow	No guidance	High design flow rate plus 2.2% uncertainty.
S/G pressure	≥ normal operating pressure plus uncertainty allowance.	S/G pressure will be determined by RELAP5 initialization for power level and T <sub>AVG</sub> .
Pressurizer level	≥ maximum normal operating level plus uncertainty allowance.	Nominal + 9%.
S/G water level	≥ normal level associated with selected power level plus uncertainty allowance.	10% uncertainty allowances will be applied.

PARAMETER	ANS GUIDANCE	RELAP5
		Mass and Energy Analyses
Safety injection tank pressure and water level	Normal operating values with allowances for uncertainties biased to produce maximum containment pressure.	Low initial pressure and liquid volume.
Safety injection tank temperature	Normal operating value with allowance for uncertainties biased to produce maximum containment pressure.	High temperature.
Refueling water storage tank (RWST) liquid volume	Choose ECCS flows and delay times in accordance with single-failure criteria to produce highest peak containment pressure.	Low RWST inventory and early recirculation switchover are selected to minimize the heat sink effect of a large volume of cold water.
Main feedwater temperature	No guidance.	High MFW temperature is assumed in order to maximize the heat source effect of the SG.

#### 6.2.1.3.2.5 Boundary Conditions - Energy Sources

The energy released into containment by a pipe break is that energy that is (a) initially contained in the primary and secondary coolant systems fluids and the metal components of the system boundaries and the sensible heat stored in the core, plus (b) that additional energy that is produced and released subsequent to the break as a result of continued fission, fission product and actinide decay and metal-water reaction. This section describes how the energy sources are accounted-for in the analyses.

##### RCS and SG Inventory

The volume of the RCS piping system is increased by 1% to account for the increased inventory due to thermal expansion. Also, zero SG tube plugging is assumed.

##### RCS and SG Metal

Heat structures are assumed to be in thermal equilibrium with the coolant in which they are in contact.

##### Core Stored Energy

A core time-of-life is selected such that the combined effects of the core stored energy and decay heat release will provide a core stored energy release that bounds all core loadings for any point in the fuel cycle.

##### Fission Energy

The RELAP5 kinetics model, coupled with reactivity feedback from moderator density, Doppler, and boron, is used to determine the delayed neutron fission power as a function of time. Consistent with most standard LBLOCA modeling practices, all control rods are assumed to remain out of the core throughout the simulations. Therefore, the reactor is brought subcritical with the available reactivity feedback effects. The most dominant negative feedback during blowdown is moderator density, while boron is dominant during the refill phase. The positive feedback (Doppler feedback) introduced by decreasing fuel temperature during blowdown is also significant. All of these effects are modeled. The analyses performed to generate this function examine several combinations of burnup, enrichment, and

time-in-cycle. The combination which results in the least negative reactivity feedback function has been chosen for conservatism.

Because a point kinetics model is not capable of calculating spatial power distributions, nodal reactivities are flux-weighted to obtain a single reactivity value for use in the point kinetics model. A bounding beginning-of-cycle (BOC)  $\beta_{\text{eff}}$  is used for conservative moderator density feedback since end-of-cycle  $\beta_{\text{eff}}$  would provide a non-conservatively high Doppler effect greater than the increased density feedback effect of a BOC  $\beta_{\text{eff}}$ .

#### Fission Product and Actinides Decay

Radioactive decay of fission products and actinides is based on the ANSI/ANS-5.1-1979 standard with  $2\sigma$  uncertainty.

#### Metal-Water Reaction Rate

Heat resulting from exothermic metal-water reaction is considered. A simplified metal-water reaction is used to conservatively bound the expected reaction. The model assumes a total amount of clad reaction to be 1% of the amount that would be generated due to reaction of all of the cladding in the active region of all of the fuel rods. The metal-water reaction is assumed to begin when the PCT exceeds 1800°F and follows a parabolic rate. The hydrogen generated by the reaction is added to the containment atmosphere as a non-condensable gas.

### 6.2.1.3.2.6 Boundary Conditions - Assumptions

#### Limiting Single Failure

A loss of one train of Engineered Safeguards due to a diesel generator failure at the beginning of the accident is the limiting single-failure for LBLOCA. This assumption is based on the knowledge that peak containment pressure for a LBLOCA occurs in the post-reflood phase of the event when decay heat is the primary heat source and ECCS core cooling and containment spray are utilized for heat removal.

#### Break Location

The break is modeled to occur in the loop containing the pressurizer. However, since peak pressure occurs in the long-term post-reflood period, peak pressure results are not sensitive to the broken loop selection.

#### Emergency Core Cooling System Injection Flow

The initiation time for ECCS is assumed to be consistent with the Technical Specifications delay time. No direct spilling of injection flow to containment is assumed for the hot leg break and cold leg pump suction break case. ECCS injection flow spillage is accounted for in the cold leg pump discharge break case. To maximize break flow energy, a high value is selected for ECCS suction temperature during injection.

#### RWST Depletion and ECCS Switchover

The available RWST inventory is minimized. Net flow from the RWST is tracked and switchover (manual action) to recirculation initiated when the RWST level has decreased to a minimum volume corresponding to the low level alarm setpoint.

ND suction is switched first, then NV and NI pumps are switched following the low-low level alarm.

#### RCP Trip

RCPs are assumed to trip simultaneously with the main turbine and loss of offsite power (LOOP).

#### RCP Two-Phase Multipliers

The RELAP5 pump component model adds pump head to the mixture momentum equation. To account for degradation due to two-phase flow when void fractions are such that little head is developed, homologous difference curves are provided. Appropriate curves for the MNS RCPs, based on experimental data, are included in RELAP5 and used in the analyses. For two-phase flow with void fractions where the pumps are able to develop head, multipliers based on void fraction are applied.

#### SG Post-Trip Level Control

Main feedwater flow is assumed to continue until the feedwater isolation valves close. Post-trip SG level is then controlled by auxiliary feedwater flow (CA) under manual control.

#### Auxiliary Feedwater Flow Rates and Temperature

Auxiliary feedwater temperature is conservatively maximized for increased secondary to primary heat transfer. One of the motor-driven auxiliary feedwater pumps is unavailable due to loss of one ESF train. The Technical Specifications value for startup and loading of the available diesel generator is assumed for the delay in availability of the available diesel generator.

#### Post-Trip SG Pressure Control

The main steam isolation valves (MSIV) and main steam PORVs are assumed to close on the containment high-high pressure signal resulting from the LBLOCAs. Operator action is assumed for any subsequent main steam PORV operation to reduce SG pressure in accordance with procedural guidance.

#### Cold Leg Accumulator Nitrogen

Nitrogen used to pressurize the safety injection accumulators is assumed to be discharged into the RCS cold legs and subsequently into the containment.

#### Containment Backpressure

Containment backpressure affects mass and energy release rates during the reflood and post-reflood phases. However, the RELAP5 code used for the mass and energy release analysis is not coupled to the GOTHIC code used for the containment pressure analysis. GOTHIC output is input to RELAP5 in an iterative manner, until converged. Conservatively high back pressures are used.

#### Refill Assumption

Refilling of the reactor vessel is an integral part of the RELAP5 analysis. This modeling approach has a minor impact on long-term containment response.

#### 6.2.1.3.2.7 Cold Leg Recirculation Boundary Conditions

When the minimum water volume in the RWST is depleted, the lo-level alarm will actuate, and the operator must switch the ECCS pumps suction source over from the RWST to the containment sump. Containment sump level is verified via redundant, safety-powered level switches prior to swap to ensure adequate inventory is available to support sustained sump recirc.

#### Transfer to Cold Leg Recirculation Sequence Timing

According to the current station EOPs, the alignment of the ND system to the sump will be performed first, then the NI and NV systems follow. There is a time required to transfer the ND, NI, and NV pump suction and also operator action delay time. Therefore, for a portion of this time frame, the ECCS pumps will have the RWST as their suction source. The length of time required to complete each pump realignment has been conservatively minimized.

ND auxiliary spray operation is initiated manually when required by the operator only if 1) the Emergency Core Cooling System is operating in the recirculation mode, 2) more than 50 minutes have passed since the initiation of the accident, and 3) containment pressure exceeds a setpoint. Assuming a

large break LOCA with one train of Engineered Safeguards failed, the remaining ND Auxiliary Spray header is not required to maintain containment pressure within design values.

#### ECC Flow Rates During Cold Leg Recirculation

[Table 6-17](#) shows typical minimum ECC flow rates for MNS. The hot leg and pump suction break analyses utilize data shown for the no-spilling simulation, and the cold leg pump discharge break analyses utilize data shown for the with-spilling simulation.

#### ECC Temperature During Cold Leg Recirculation

ECCS temperature following switchover is dependent on several factors, one of which is the sump temperature. Since sump temperature is computed by GOTHIC and not by RELAP5, it must be determined through a GOTHIC/RELAP5 iterative process.

#### 6.2.1.3.2.8 Result of Mass and Energy Release Analyses

Various break locations are analyzed. The results show that the cold pump discharge break case generates the highest total integrated break vapor mass and energy release (Figures [6-201](#) to [6-204](#)).

Of the postulated RCS break locations, the hot leg break has the least vent path resistance. As a result, that break path results in the highest blowdown mass and energy release rates. However, following blowdown, the cold leg pump suction break case has a greater energy release rate due to the fact that the coolant picks up additional heat from an SG. Much later, during the cold leg recirculation phase, the mass and energy release rates of the cold leg pump discharge break case exceed those of the cold leg pump suction and the hot leg breaks due to ECCS spillage. As a result of these characteristics and of the heat removal capability of the containment cooling systems, the cold leg pump discharge break produces the limiting LBLOCA peak pressure.

### 6.2.1.4 Mass and Energy Release Analysis for Postulated Secondary System Pipe Ruptures Inside Containment

#### 6.2.1.4.1 Pipe Break Blowdowns Spectra and Assumptions

A series of steam line breaks were analyzed to determine the most severe break condition for containment temperature and pressure response. The following assumptions were used in these analyses:

1. Breaks ranging in size from 0.4 ft<sup>2</sup> to 2.4 ft<sup>2</sup> were analyzed. Due to the rapid steam line isolation, breaks larger than 2.4 ft<sup>2</sup> produce mass and energy releases that are similar to the 2.4 ft<sup>2</sup> break due to the presence of the steam generator outlet nozzle flow restriction.
2. Prior to tube bundle uncover, the blowdown from the broken steam line is assumed to be dry saturated steam; i.e., no water entrainment was assumed. Following tube bundle uncover, the blowdown from the broken steam line is assumed to be superheated steam.
3. Steam line isolation is completed 1 second after the isolation setpoint is reached. The isolation signal is generated by a high-high containment pressure signal. A conservatively fast closure time for the main steam isolation valves and no electronic delay are assumed in order to speed tube bundle uncover.
4. All breaks are initiated from 3479 MWt (rated thermal power plus measurement uncertainty). Since the amount of superheat that occurs is limited by the temperature of the primary fluid flowing through the tubes, maximizing hot leg temperature will result in higher enthalpy releases to the containment. The high initial power level, with the essentially constant cold leg temperature program, results in a higher steam generator inlet temperature in the primary system. For steam line breaks inside containment, reactor trip, safety injection, and steam line isolation signals are generated on high

containment pressure trips, which are not significantly influenced by the initial power level. Steam line breaks initiated from power levels less than full power are less limiting since a lower initial power level would result in lower steam generator inlet temperatures.

5. A total of six break sizes were analyzed. Prior to MSIV closure, these breaks model blowdown from one steam generator to the end of the break (forward flow) and from three steam generators to the other end of the break (reverse flow). Subsequent to MSIV closure, forward flow continues from the one steam generator through one side. Reverse flow is rapidly terminated since the isolated steam generators do not continue to blow down. The specific break sizes analyzed are 0.4 ft<sup>2</sup>, 0.6 ft<sup>2</sup>, 0.86 ft<sup>2</sup>, 1.1 ft<sup>2</sup>, 1.4 ft<sup>2</sup>, and 2.4 ft<sup>2</sup>.
6. The failure of one train of safety injection was assumed for all cases. In addition, a loss of offsite power was assumed for the containment analysis.
7. The mass and energy releases described in this section have been calculated to beyond the point at which the limiting parameter, containment temperature, has reached its peak value. Further releases will eventually be terminated by operator action, although no explicit assumption is made in the analysis about the time at which this occurs.
8. Main feedwater is assumed to be in manual control and thus is maintained at its initial flow rate until feedwater isolation occurs concurrent with reactor trip. No credit is taken for the rapid depressurization of the steam generator that would increase main feedwater flow and delay tube bundle uncover. A closure time of 1 second is assumed for the main feedwater isolation valves.
9. The Auxiliary Feedwater System is actuated by a safety injection signal due to high containment pressure. A delay of 60 seconds is assumed to speed tube bundle uncover in the faulted steam generator. The mass addition to the faulted steam generator is conservatively determined by assuming that the Auxiliary Feedwater System is instantaneously pumping at maximum capacity with the flow rate calculated from the feedwater system head curves and the system line resistance as a function of steam generator pressure.

#### 6.2.1.4.2 Break Flow Calculations

The following is a description of the break flow modeling of the blowdown of the steam generators and plant steam piping:

1. Break flows and enthalpies from the steam generators are calculated using RETRAN-02 (Reference [85](#)). Blowdown mass and energy releases determined using the RETRAN code include the effects of core power generation, main and auxiliary feedwater additions, engineered safeguards systems, reactor coolant system metal, and reverse steam generator heat transfer.
2. The contribution to the mass and energy releases from the secondary plant steam piping is included in the mass and energy release values in [Table 6-54](#) for the limiting break size of 2.4 ft<sup>2</sup>. For all ruptures, the steam piping volume blowdown begins at the time of the break and continues until the entire piping inventory is released. The flow rate is determined using the Moody correlation, the pipe cross-sectional area, and the steam pressure. Reverse flow from the intact steam generators continues until steam line isolation.

The blowdown model is discussed further in Section 4.0 of Reference [61](#).

#### 6.2.1.4.3 Single Failure Effects

The single failure of one train safety injection is assumed in order to minimize the injection of cold, borated water to the primary system. This single failure maximizes hot leg temperature which in turn maximizes the enthalpy of the steam released into the containment.

### 6.2.1.5 Minimum Containment Pressure Analysis for Performance Capability Studies of Emergency Core Cooling System

The Containment pressure analysis is performed with the LOTIC-2 code (Reference [24](#)). The transient pressure computed by the LOTIC-2 code can be input to the WCOBRA/TRAC code for the purpose of computing the reflood transient.

The Containment backpressure calculated for the ECCS analysis presented in Section [15.6.5](#) is presented in [Figure 6-205](#). The Containment backpressure is calculated using the methods and assumptions described in Reference [24](#). Input parameters, including the Containment initial conditions; Containment volume; passive heat sink materials, thicknesses, and surface areas; and starting time and number of Containment cooling systems used in the analysis, are described below.

For instrumentation details refer to Sections [6.2.2.15](#), [6.2.3.5](#) and Chapter [7.0](#).

#### 6.2.1.5.1 Mass and Energy Release Data

The mass/energy releases to the Containment during the blowdown and reflood portions of the best estimate LBLOCA reference transient are presented in [Table 6-62](#).

The mathematical models which calculate the mass and energy releases to the Containment are described below. The LOTIC code uses the control volume technique to represent the physical geometry of the system. Fundamental mass and energy equations are applied to the appropriate control volumes and solved by suitable numerical procedures. The initial conditions of the containment by compartment are specified before blowdown. Ice melt is calculated for the blowdown period based on the mass and energy released to the containment. After the RCS blowdown, the basic LOTIC code assumption made is that the total pressure in all compartments is uniform. This assumption is justified by the fact that after the initial blowdown of the RCS the remaining mass and energy released from this system into the containment are small and very slowly changing. The resulting flow rates between compartments will also be relatively small. These small flow rates are unable to maintain significant pressure differentials between the containment compartments.

#### 6.2.1.5.2 Initial Containment Internal Conditions

Containment data and initial conditions used in the analysis are presented in [Table 6-64](#). As detailed in Reference [79](#), it has been determined that containment parameters assumed in the minimum containment pressure analysis need not be the same as the Limiting Conditions for Operation (LCO) as defined in the Containment Technical Specifications. The LCOs in the Technical Specifications often represent extreme conditions that are not typically encountered during normal operation. In addition, the LCOs associated with the Containment Technical Specifications are based upon containment integrity and equipment operability considerations, not ECCS performance considerations. Consequently, some LBLOCA EM (evaluation model) values were chosen as being representative of limiting conditions during normal full power operation, and others were set at the Technical Specification LCO value. In all cases the combination of containment parameter values were chosen to assure that the overall calculation of containment pressure during a LBLOCA would be conservative.

#### 6.2.1.5.3 Containment Volume

The volume used in the analysis is 1,209,341 ft<sup>3</sup>.

#### 6.2.1.5.4 Active Heat Sinks

The Containment Spray System, the Ice Condenser and the Air Return Fan System operate to remove heat from the Containment. Containment spray operation is a conservative assumption following removal of automatic spray initiation.

Pertinent data for these systems, which were used in the analysis, are presented in [Table 6-65](#).

The sump temperature was not used in the analysis because the maximum peak cladding temperature occurs prior to initiation of the recirculation phase for the Containment Spray System.

#### 6.2.1.5.5 Steam-Water Mixing

Water spillage rates from the broken loop accumulator are determined as part of the core reflooding calculation and are included in the LOTIC-2 calculational model.

#### 6.2.1.5.6 Passive Heat Sinks

The passive heat sinks used in the analysis and their thermophysical properties are given in [Table 6-66](#).

#### 6.2.1.5.7 Heat Transfer to Passive Heat Sinks

The upper and lower compartment pressure response for the best estimate LBLOCA reference transient (DECLG,  $C_D = 1.0$ ) is presented in [Figure 6-205](#). The upper and lower compartment heat removal rates are given in [Figures 6-206](#) and [6-207](#) respectively. The heat transfer model used is described in Reference [24](#). [Figure 6-208](#) presents the temperature transient in both the upper and lower compartments. The heat removal from the ice bed, lower compartment drain, containment spray, and the sump are provided in [Figure 6-209](#), [Figure 6-210](#), and [Figure 6-211](#).

#### 6.2.1.5.8 Other Parameters

All parameters having a substantial effect on the minimum containment pressure analysis have been discussed or referenced in the preceding sections. The effect on the minimum containment pressure analysis of air lost through initially open Containment Purge (VP) System or Containment Air Release and Addition (VQ) System valves is insignificant. Therefore, neither the initial status nor the closure time of these valves has been modeled in this analysis. This position has been accepted as part of the McGuire Nuclear Station licensing basis as discussed in Reference [38](#).

### 6.2.1.6 Testing and Inspection

#### 6.2.1.6.1 Preoperational Testing

Prior to initial fuel loading certain tests were conducted to ensure the functional capability of the Containment and associated structures, systems, and components. The specific tests pertaining to the containment functional design are:

- Containment Spray System Functional Test
- Containment Structural Integrity Test
- Containment Initial Integrated Leak Rate Test
- Containment Air Return System Functional Test
- Ice Condenser System Functional Test
- Containment Divider Barrier Leakage Area Verification Test

Testing and environmental qualification of the air return and hydrogen skimmer fans have been performed in accordance with FSAR sections [3.10](#) and [3.11](#).

### 6.2.1.6.2 Periodic Inservice Surveillance

During plant operation certain tests and inspections are conducted to ensure the functional capability of the Containment and associated structures, systems, and components. Section 3.6 of Technical Specifications discusses the periodic inservice surveillance tests and inspections and gives, for each test or inspection, the acceptance criteria, the operational mode(s) in which these criteria are applicable, the actions(s) to be taken in the event the criteria are not satisfied, and the surveillance requirements necessary to demonstrate satisfaction of the criteria. The specific tests and inspection items pertaining to the Containment functional design are:

- Containment Integrity
- Containment Leakage
- Containment Air Locks
- Internal Pressure
- Air Temperature
- Containment Vessel Structural Integrity
- Reactor Building Structural Integrity
- Annulus Ventilation System
- Containment Ventilation System
- Containment Spray System
- Containment Isolation Valves
- Deleted Per 2009 Update
- Deleted Per 2008 Update
- Hydrogen Mitigation System
- Ice Condenser
- Ice Bed Temperature Monitoring System
- Ice Condenser Doors
- Inlet Door Position Monitoring System
- Divider Barrier Personnel Access Doors
- Divider Barrier Equipment Hatches
- Containment Air Return System and Hydrogen Skimmer System
- Ice Condenser Floor Drains
- Refueling Canal Drains
- Divider Barrier Seal

Bases for the periodic inservice surveillance tests and inspections are given in the Bases for Section 3.6 of Technical Specifications.

### 6.2.1.7 Instrumentation Requirements

Instrumentation is provided in the Containment to remotely monitor the following post-accident conditions:

1. Pressure
2. Sump Level
3. Radiation Level

These monitors, whose readout is located in the Control Room, are designed to remain functional and on scale for environmental conditions resulting from any postulated accident. Operational and testing requirements for the sump level and pressure monitors are presented in Section [3.11](#).

### 6.2.1.8 Materials

The original coating materials and coating systems were specified by Engineering and applied by the Duke Power Construction Department to all structures within the containment and to the Containment Vessel. The coating systems were qualified for radiation exposure, pressure, temperature, and water chemistry exposure during a DBA in accordance with ANSI N101.2.

Carboline coating materials are now used for maintenance of the existing coating systems and for any new applications. These coating systems are specified by Engineering and applied by the Duke Power Maintenance Department. The Carboline coating materials have been qualified over the existing Mobil/Valspar coatings as a mixed system and as a new coating system for radiation exposure, pressure, temperature, and water chemistry exposure during a DBA in accordance with ANSI N101.2.

The original, maintenance, and new coating systems defining temperature limitations, surface preparation, type of coating, and dry film thickness are tabulated on [Table 6-143](#).

The elements of the McGuire Coatings Program are documented in Nuclear fleet administrative procedures. The McGuire Coatings Program includes periodic condition assessments of Service Level I coatings used inside containment. As localized areas of degraded coatings are identified, those areas are evaluated for repair or replacement, as necessary.

A maximum of 16,500 square feet of unqualified coatings inside Containment is considered to be a negligible fraction of the Containment interior surfaces. The effect of non-qualified coating failure on the ECCS recirculation and Containment Spray functions is presented in Section [6.5](#).

## 6.2.2 Ice Condenser System

[Figure 6-113](#) shows the general layout of the Ice Condenser System and Subsection [6.2.2.14](#) has an overview of the Ice Condenser design bases and function.

### 6.2.2.1 Floor Structure and Cooling System

#### 6.2.2.1.1 Design Bases

The ice condenser floor is a concrete structure containing embedded Refrigeration System piping.

[Figure 6-114](#) shows the general layout of the floor structure. The functional requirements for both normal and accident conditions can be separated into five groups: wear slab, floor cooling, insulation section, subfloor and the floor drain. Each group is now described in detail.

#### Wear Slab and Floor Cooling System

##### 1. Function

The wear slab is a concrete structure whose function is to provide a cooled surface as well as to provide personnel access support for maintenance and/or inspection. The wear slab also serves to contain the floor cooling piping.

The Floor Cooling System intercepts approximately 90 percent of the heat flowing toward the ice condenser compartments from the lower crane wall and equipment room during normal operation. The Floor Cooling System is designed with defrost capability. During an accident the floor cooling is terminated by the Containment isolation valves which are closed automatically. The Refrigeration System interface and cooling function is described in Section [6.2.2.6.2](#). The cavity below the wear slab is filled with an insulation material to resist the flow of heat into the ice bed during all operating conditions.

##### 2. Design Criteria and Codes

Refer to Section [6.2.2.16](#). The following codes are also used in the design:

- a. ANSI B31.5-1974, Refrigeration Piping.
- b. American Welding Society Structural Welding Code - 1972, AWS Publication D1.1-72.
- c. ANSI Standard Code for Pressure Piping B31 including Refrigeration Piping ANSI B31.5.

### 3. Design Conditions

1. <u>Thermal Conditions</u>	
a. Initial Cooldown - top of Wear Slab	70F
b. Initial Cooldown - bottom of Wear Slab	12F
c. Defrost Cycle - top of Wear Slab	33F
d. Defrost Cycle - bottom of Wear Slab	70F
2. <u>Seismic Loading</u>	
a. 1/2 Safe Shutdown Earthquake (1/2 SSE) Vertical Acceleration	0.35 g
b. Vertical 1/2 SSE	0.13 g radial;
c. Horizontal 1/2 SSE	0.38 g tangential
d. Safe Shutdown Earthquake (SSE) Vertical Acceleration	0.55 g
e. Vertical SSE	0.28 g radial
f. Horizontal SSE	0.75 g tangential
3. <u>Design Basis Accident (DBA) Loads</u>	
a. Pressure load on floor	9 psi
b. Floor momentum load (due to deflectors)	36.4 kips
4. Ice Loading - assume 6 in. solid ice on floor	4300 lbs/bay
5. Live Loading	250 lbs/ft <sup>2</sup>
6. Dead Loads	
a. 1/4 inch plate	1410 lbs
b. 1/2 inch pipe	164 lbs
c. Concrete Wear Slab	9700 lbs
7. Wall Panel - 121 lbs/in. over back 8 in. of slab	
8. Volume of cavity in floor structure	7 yds <sup>3</sup> /bay
a. "Foam" concrete density	40 lbs/ft <sup>3</sup>

During seismic and/or accident conditions the insulation is designed to support loads transferred by the wear slab.

### Structural Subfloor

Refer to [Chapter 3](#).

### Floor Drain

#### 1. Function

The floor drain is a passive structural component during normal operation as its only function is to minimize heat/air inflow to the lower plenum. The section of floor drain pipe inserted vertically below the wear slab is designed to provide a high thermal resistance to minimize heat gain to the ice condenser. Under accident conditions the floor drains must not fall in a mode which prevents outflow of water.

#### 2. Design Criteria and Codes

Welding complies with American Welding Society, Structural Welding Code, AWS D1.1-1972, as specified in Section [6.2.2.18](#).

#### 3. Design Condition

##### Normal Operation

Design temperature, maximum	120°F
Nominal $\Delta P$ across valve	less than 1 psf

##### Accident Conditions

$\Delta P$ across check valve	12-14 psi
Temperature pipe and valve	250°F

### **6.2.2.1.2 System Design**

#### Wear Slab and Floor Cooling System

The wear slab is a 4 inch thick layer of high strength concrete (3000 psi) having an exposed top surface area of 139 ft<sup>2</sup>/bay. See [Figure 6-115](#) for top surface typical geometry. The concrete has a density of 150 lbs/ft<sup>3</sup> and is prepared with air entrainment admixtures to minimize spalling from freeze/thaw cycles. Steel reinforcing is used in the wear slab to assure adequate and uniform strength. A protective coating is applied to the top of the wear slab which provides an additional water barrier for the wear slab. The Floor Cooling System consists of 1/2 inch schedule 80 carbon-steel ASTM A-333 Grade 6 piping which is embedded in the wear slab of each bay in a serpentine fashion (See [Figure 6-115](#)) thereby providing ample cooling of the wear slab surface. The cooling pipes contained in each wear slab rest on a steel plate which extends across the full width of the floor for maximum effectiveness in intercepting heat passing up through the floor. Expansion joints are located at each bay and expansion material is located at the slab perimeter. The Floor Cooling System maximum coolant pressure is approximately 100 psi. The floor coolant flow rate per bay is adjusted by means of needle valves and is monitored by a temperature sensing element located at the downstream end of each of the bay floor piping. Should a leak develop each individual bay piping loop can be isolated by closing two valves. The coolant contained in the piping is a corrosion inhibited glycol/water solution.

The floor structure contains water vapor seals. The seals by design include: a protective surface coating on the wear slab top surface, a vapor barrier between the foam concrete and the structural subfloor, a leveling course of grout on the top surface of the foam concrete, and a steel plate (in the wear slab) with lapping material in the plate to plate joints. Additionally, by keeping the ice condenser floor cold with a protective layer of ice on it, the effects of water intrusion are minimized. Floor elevation monitoring prevents any movement from affecting the function of the lower inlet doors.

For defrosting purposes, electric heating of the glycol is provided. In general, components requiring periodic maintenance such as pumps, heaters and control valves are located outside of the ice condenser.

The original Westinghouse design of the Floor Cooling System includes electric heaters for defrosting the ice condenser floor so that water reaching the floor during wall panel defrosting would not form ice. The design assumed that the floor sealing and vapor barrier would provide ample water resistance to mitigate the effects of water on the ice condenser floor. Early in the operating life of the McGuire Nuclear Station maintenance and engineering personnel concluded that water should be minimized in the ice condenser because of its effects on flow channels, equipment and concrete. At that time no particular problems were envisioned but rather it was considered good practice. Therefore maintenance procedures were changed to replace floor defrosts with mechanical ice removal. Later the procedure was changed to leave approximately a 1/4" to 1/2" of ice on the floor of the ice condenser to protect the floor from tool damage, and also prevent any maintenance caused ice or frost melt from reaching the wear slab on the floor. The present practice is to leave the area between the lower turning vanes and the lower inlet doors and the area between the personnel walkway and the annulus wall clean. A layer of ice that ranges from 1/4 inch to over 2 inches thick is left on the floor in the area behind the lower turning vanes, under the glycol piping, and in the personnel walkway.

In 1992 Sequoyah Nuclear Station which is another ice condenser containment type power plant discovered their wear slab had pervasive cracking and had heaved upward causing interference with the lower inlet doors in both Units. This affected the function of the lower inlet doors. Root cause of the floor heave and cracking at Sequoyah was attributed to water intrusion coupled with floor freeze and thaw cycles. McGuire engineering concluded that the elimination of floor defrosting and leaving a protective coating of ice on the floor prevented and would continue to prevent this from occurring at McGuire Nuclear Station.

In 1997 McGuire Nuclear Station discovered localized cracking in the wear slab near the lower inlet door portal frame. Floor movement caused interference with the lower inlet doors in Unit 2. The same problem has not been experienced in Unit 1. Although the floor movement and door interference was much less than what occurred at Sequoyah the root cause was similar. Two water intrusion events had occurred in Unit 2. The steam generator drain valve steam leak (8/93) and the LOOP with PRT Rupture Disc Failure and loss of NF Glycol Cooling (12/93) cause actuation of the ice condenser which opened the lower inlet doors. This caused ice to melt and water to penetrate below the wear slab of the floor. The changes in heat load from going in and out of outages, and floor cooling system problems provided the cyclical thermal fluctuations which eventually caused the floor to move upward. The floor is still kept cold at all times with a protective layer of ice, however the mechanical interface between the ice condenser floor and the lower inlet doors has been removed and the gap between the two and/or the floor elevations is now monitored during outages to insure the problem does not re-occur.

The insulation cavity is filled with a low density, closed cell, foam concrete. The nominal density of the foam concrete is 35 lbs/ft<sup>3</sup>; the compressive strength is 110 psi. The thermal conductivity per inch thickness is nominally 1.0 Btu/hr-F-ft<sup>2</sup>. The insulation cavity for the foam concrete is sealed by a vapor barrier to provide additional assurance that the insulation section resists infusion of water vapor and thus retains a high thermal resistance. The top surface of the foam concrete is covered with a course of grouting which provides seating surface for the floor plate and cooling coil assemblies.

#### Floor Drain

Special consideration has been given in the design to prevent freezing of the floor drains and to minimize check valve leakage.

The floor drains employ a low thermal conductivity (transite) section of pipe 12 inches in diameter, inserted vertically below the wear slab to minimize heat gain to the ice bed. The horizontal run is a 12 inch diameter steel pipe embedded in the subfloor which is at a relatively warm temperature. The drain

check valve is a 12 inch diameter horizontal valve fabricated from 304 or 316 SS welded per AWS D1.1-1972. The valve is designed to remain closed against the cold air head in the ice condenser to minimize any heat inleakage and air outleakage during normal operation. The valve is designed to tolerate a 15 psi back pressure when closed. The check valve is in a warm environment and no freezing will occur. To minimize air currents induced by the temperature difference between the ice bed and the floor drain piping, the floor drain openings are covered with water soluble paper held in place with water soluble tape.

### **6.2.2.1.3 Design Evaluation**

#### Wear Slab

The wear slab, during normal operating conditions, is subject only to its dead weight consisting of concrete, steel reinforcing, steel plates and piping. Six inches of 100 percent density ice is assumed to be uniformly distributed over the entire floor. The dead weight amounts to 11,200 lbs per bay, the equivalent of 0.56 psi. The live load for maintenance purposes is assumed to be 250 lbs/ft<sup>2</sup>. The vertical seismic input is 0.35 g for 1/2 SSE and 0.55 g for SSE. The dead load plus seismic loads are insignificant because the highest load on the floor is contributed by blowdown pressure during design accident conditions. The blowdown pressure is 9 psi, and added to this value, for design purposes, is a 40 percent design margin, and a dynamic load factor of 1.53. This results in a minimum value for design of 19.28 psi.

The most severe loading condition is the combination of the dead load, the SSE seismic acceleration of 0.55 g, the 19.28 psi pressure load and 8.1 psi locally near the deflectors due to flow impulse loadings. The wear slab is designed to accommodate the heatup and cooldown cycles and 1/2 SSE without overstressing the concrete and coolant piping.

#### Floor Cooling System

The embedded piping for floor cooling is 1/2 inch schedule 80 pipe. The maximum coolant pressure in the pipe is approximately 100 psi. ANSI B31.5-68 data shows that the pipe can tolerate internal pressures of 4812 psi.

In addition, the piping is tested to 200 psi. The pipe is sized to allow for at least 38 mils of corrosion. Nevertheless, the glycol coolant contains corrosion inhibitors, and as a result pipe corrosion is negligible. The 1/4 inch floor plate is integrated with the concrete through 1/2 inch diameter anchors welded to the plate on 12 inch centers. These anchors prevent thermal loads from concentrating in the piping.

#### Insulation Section

The insulation section supports wear slab loads. For a conservative analysis the wear slab dead weight + seismic + DBA loads were assumed to be transferred to the foam concrete section. The compressive strength of the foam concrete is sufficient to accept these floor loads.

#### Floor Drain

Drains are provided at the bottom of the ice condenser compartment to allow the melt/condensate water to flow out of the compartment during a loss-of-coolant accident. These drains are provided with check valves that are designed to seal the ice condenser during normal plant operation to prevent loss of cold air from the ice condenser. These check valves remain closed against the cold air head (2 psf) of the ice condenser and open before the water head reaches a value of 18 inches of water, above center of the valve.

For a small pipe break, the water inventory in the ice condenser is produced in proportion to the energy added from the accident. The water collecting on the floor of the condenser compartment then flows out

through the drains. For intermediate and large pipe breaks the ice condenser doors are open and water drains through both the doors and the drains.

For a large pipe break, a short time of the order of seconds is required for the water to fall from the ice condenser to the floor of the compartment. Results of fullscale section tests performed at Waltz Mill show that, for the design blowdown accident, a major fraction of the water drained from the ice condenser, and no increase in Containment pressure was indicated even for the severe case with no drains.

A number of tests were performed with the reference flow proportional-type door installed at the inlet to the ice condenser and a representative hinged door installed at the top of the condenser. Tests were conducted with and without the reference water drain area, equivalent to 15 ft<sup>2</sup> for the plant, at the bottom of the condenser compartment.

These tests were performed with the maximum reference blowdown rate, with an initial low blowdown rate followed by the simulated core residual heat rate.

The results of all of these tests show satisfactory condenser performance with the reference type doors, vent, and drain for a wide range of blowdown rates. Also, these tests demonstrate the insensitivity of the final peak pressure to the water drain area. In particular, the results of these full-scale section tests indicate that, even for the reference blowdown rate, and with no drain area provided, the drain water did not exert a significant back pressure on the ice condenser lower doors. A major fraction of the water drained from the ice condenser compartment by the end of the initial blowdown. The effect of this test result is that Containment final peak pressure is not affected by drain performance.

Although drains are not necessary for the large break performance, 15 ft<sup>2</sup> of drain area was provided for small breaks.

For small breaks, water flows through the drains at the same rate that it is produced in the ice condenser. Therefore, the water on the floor of the compartment reaches a steady height which is dependent only on the energy input rate.

To determine that the 15 ft<sup>2</sup> drain area met these requirements, the water height is calculated for various small break sizes up to 30,000 gpm break. Above 30,000 gpm the ice condenser doors would be open to provide additional drainage. The maximum height of water required was calculated to be 2.2 ft above the drain check valve. Since this height resulted in a water level which is more than 1 ft below the bottom elevation of the inlet doors, it is concluded that water does not accumulate in the ice condenser for this condition and that a 15 ft<sup>2</sup> drain gives satisfactory performance.

During normal unit operation, the sole function of the valve is to remain in a closed position, minimizing air leakage across the seat. To avoid unnecessary unseating of the valve seat, a 1/2 inch drain line leading to a 2 inch drain header is connected to the 12 inch line immediately ahead of the valve. Any spillage or defrost water drains off without causing the valve to be opened.

The arrangement of the Drain System for the lower inlet region of the ice compartment is shown in [Figure 6-114](#).

Special consideration has been given in the design to prevent freezing of the check valves and minimize check valve leakage.

To minimize the potential for valve freezing, a low thermal conductivity (transite) section of pipe is inserted vertically below the wear slab, while the horizontal run of pipe (steel) is imbedded in a warm concrete wall before it reaches the valve. The valve itself is in the upper region of the lower compartment, where ambient temperature is above the freezing temperature.

The valve is held in a closed position by virtue of its design as an almost vertical flapper with a hinge at the top. The angle (10°) from the vertical holds the flap in place by gravity.

In order to reduce valve leakage to an acceptable value, a sealant is applied to the seating surface after installation of the valves. Tests show that this reduces leakage to practically zero. Maximum allowable leakage rate would be approached as a limit only if all the sealant were to disappear completely from all the valves, which is unlikely. Sealant is replaced as necessary.

#### Conclusion

On the basis of the structural analysis performed on the floor structure, it is concluded that the floor is adequate for all anticipated loading conditions.

### **6.2.2.2 Wall Panels**

#### **6.2.2.2.1 Design Basis**

##### Function

The wall panels are designed to thermally insulate the ice bed, under normal operating conditions, from the heat conducted through the crane wall, the Containment wall and the end walls. In addition, they are designed to provide a circulation path for cold air and a heat transfer surface next to the ice bed so that the ice is maintained at its design temperature range.

The supporting structure of the wall panel also provides for transfer of radial and tangential loads from the lattice frame columns to the crane wall anchor embedments.

##### Criteria and Codes

The structural parts of the wall panels are designed to meet the requirements given in Section [6.2.2.16](#).

##### Design Conditions

The service temperature range is 10°F to 20°F. The Design Basis Accident temperature is 250°F.

The design loads are presented in [Table 6-69](#). The loading combinations considered in the design are those given in Section [6.2.2.16](#). For the SSE plus DBA combination, ten (10) loading cases are considered.

#### **6.2.2.2.2 System Design**

The wall panel design incorporates provisions for installation on the crane wall, Containment wall, and end walls of the ice bed annulus. Containment and end wall panels are similar except for the omission of the lattice frame column attachments.

The crane wall panel design incorporates transverse beam sections which are fabricated from standard structural sections and to which the lattice frame column mounting lugs are attached. These sections are attached to the rear mounting angle assemblies by insulated bolts.

Wall panels are attached to the crane and end walls by studs welded to the anchor embedments and to the Containment by studs welded to the shell. The crane wall panels extend from the bottom of the upper plenum to the lower support structure where they are supported on the inner circumferential beams of the horizontal platform. The Containment wall panels extend from the bottom of the upper plenum to the top of the floor wear slab.

Cooling ducts are incorporated in the design to provide flow from the air handlers in the duct adjacent to the ice bed and return flow in the outer duct of the panel. This provides a flow path between the inner and outer duct to allow return flow through the outer duct.

The ducts are fabricated as sandwich panels utilizing corrugated sheet sections enclosed in sheet metal enclosures. This type of sandwich construction provides resistance to differential pressure loads and

results in minimal overall weight and flow restrictions. Flow sections of wall panels are seal welded to prevent air leakage.

Materials of construction of the wall panels conform to the Design Criteria of Section [6.2.2.18](#).

Areas between air ducts and walls are insulated and areas between adjacent air ducts are insulated and covered with a lap strip to provide a seal between wall surface and ice bed. Elastomers and sealants are insignificantly affected by exposure to a 5 r/hr gamma radiation field over a period of forty years.

### **6.2.2.2.3 Design Evaluation**

The wall panels have been analyzed for seismic and Design Basis Accident loading conditions as well as service loads.

#### Analysis for DBA Pressure Load

The wall panels are bolted to transverse beam sections with a maximum span of about 24 inches. In the analysis, the wall panels were taken as a 24 in. x 36 in. sandwich plate simply supported on all four sides.

The stress analysis was based on the general theory for sandwich plates presented in References [44](#) through [46](#). Elastic constants were determined by the method given in Reference [47](#).

A local stress analysis was also performed assuming an elastic foundation and the stability of the leg of the corrugated core was investigated, following Reference [48](#).

It is noted that a DBA pressure of 19 psig was used in these analyses. The duct internal pressure was neglected in the analyses because it is negligible in relation to the 19 psig (internal design pressure 0.5 psig).

#### Analysis for Seismic and DBA Transverse Beam Loads

A transverse beam section was investigated for its ability to transmit the imposed Seismic and DBA loads from the lattice frame column attachment to the crane wall. A two dimensional beam analysis utilizing the "STASYS" program was employed. Various loading modes were used with values as shown in [Table 6-69](#) Parts 2, 3, 4 and 5.

#### Overall Conclusion

Based on the analyses described in the foregoing, it is concluded that the wall panel assembly meets the design requirements given in Sections [6.2.2.16](#) and [6.2.2.18](#).

## **6.2.2.3 Lattice Frames and Support Columns**

### **6.2.2.3.1 Design Basis**

#### Function

The lattice frames and support columns assembly provide the following functions:

1. Positions the ice baskets in the ice bed and controls the hydraulic diameter.
2. Provides lateral support for the ice baskets under normal seismic and accident loads.
3. Allows passage of steam and air through the space around ice baskets.
4. Allows for basket installation and removal requirements.

#### Structural Requirements

Refer to Section [6.2.2.16](#).

### Design Criteria

1. The lattice frames are designed to be compatible with the periodic weighing procedure for the ice baskets.
2. The structure is designed to position the ice columns in the required array to maintain the performance of the ice condenser. In particular, the flow area around each ice column is maintained within the limits established by the general design criteria.
3. The lattice frame allows loading of the ice baskets in position, and permits lifting of complete basket columns for removal in sections.

### Materials Requirements

Refer to the listing of acceptable materials in Section [6.2.2.18](#). All accessible steel components are covered by protective coating.

### General Thermal and Hydraulic Performance

1. The lattice frames space the ice basket columns so that the hydraulic diameter around each ice column is maintained for all modes of operation.
2. Differential thermal expansion between crane wall and lattice frame structure, together with other applicable loads, does not stress the lattice frames or its associated supporting structure beyond the design limits, or adversely affect the spacing between lattice frames.
3. Forces across the lattice frames in the horizontal and vertical direction due to seismic and blowdown loads do not overstress the lattice frame and supporting structure beyond the design limits.

### Interface Requirements

#### 1. Lattice Frame to Ice Basket Columns

The lattice frame locates and aligns the ice basket array. Sufficient clearance shall be provided to assure ease of ice basket installation but shall limit radial basket motion to a nominal amount. The lattice frame structure is also capable of withstanding design and operating seismic and accidental loading.

#### 2. Lattice Frame to Lattice Frame Column

The lattice frame is attached to the lattice frame columns. The column bases is adjustable so that matching of columns to lower support structure can accommodate the range of manufacturing and installation tolerances.

#### 3. Lattice Frame Columns to Crane Wall Air Duct Panels

The lattice frame columns are bolted to the wall panel cradles. Lateral seismic loading from ice baskets and lattice frame is transmitted to the crane wall through the lattice frame columns and the wall panel cradles. The studs at the crane wall are capable of meeting the structural design criteria.

#### 4. Lattice Frame Columns to Lower Support Structure

Lattice frame columns interface with the lower support structures. The columns are designed to allow for accumulation of dimensional tolerances at interfaces.

#### 5. Lattice Frame Columns to Intermediate Deck

The top end of the lattice frame columns at each bay shall support the intermediate deck and related supports.

Allowance is made for mounting the Ice Condenser Temperature Sensing System onto the lattice frames.

Design Load

The lattice frames and support columns are designed to withstand dead loads, live loads, seismic loads including impact and accident loads and remain within the allowable limits established in Section [6.2.2.16](#). Differential thermal expansion loads due to normal and accident conditions are also considered. Structural loads are not transmitted through the lattice frames and columns to the containment structure.

[Figure 6-120](#) and [Figure 6-121](#) show the lattice frame loading orientation and distribution.

The lattice frame and column design loads are listed below.

1. Dead Loads

Lattice Frame Weight, lbs each	1200
Column Weight Crane Side, lbs each (2 1/4 in. x 4 inc. bar at 30.6 lbs/ft)	1500
Column Weight Containment Side, lbs each (3 in. x 5 inc. x 1/2 inc. x 48 ft @ 20.88 lbs/ft)	1000
Column Connector Bracket Weight, lbs/pari	50
Load on Columns from Intermediate Deck Doors, Framing and Grating, lbs per column	490

2. Seismic Loads

a. 1/2 Safe Shutdown Earthquake (1/2 SSE)

1) Horizontal 1/2 SSE

See [Table 6-70](#) for 1/2 SSE at 6 ft increments in elevation from 15 to 57 ft above floor. [Table 6-71](#) presents local load on lattice frame due to single ice basket.

2) Vertical 1/2 SSE

1/2 Safe Shutdown Earthquake to be applied to Dead Loads in Vertical Direction,  $g = 0.35$

b. Safe Shutdown Earthquake (SSE)

1) Horizontal SSE, Radial and Tangential

See [Table 6-72](#) for all safe shutdown earthquake loads for each of the eight levels of lattice frames.

2) Vertical SSE

Safe Shutdown Earthquake to be applied to Dead Loads in Vertical Direction,  $g = 0.55$

3. Design Basis Accident (DBA) Loads

a. Horizontal DBA, Radial and Tangential

See [Table 6-72](#) for all lattice frame design basis accident loads for each of the eight levels of lattice frames.

b. Vertical DBA on Lattice Frames

A design margin of 40 percent and a dynamic load factor of 1.1 should be used with the values in [Table 6-73](#).

Vertical DBA Loads from Intermediate Deck on Lattice Frame Columns

Column Position	DBA + 0.4 Margin (lbs)	1.2 DLF (lbs)	Drag Load at Max. Hinge Load DBA + 0.4 Margin (lbs)
A. Crane Wall Primary	18,800	22,600	1135
B. Crane Wall Intermediate	9,400	11,300	567
C. Crane Wall Intermediate	9,400	11,300	567
D. Crane Wall Primary	18,800	22,600	1135
E. Containment Primary	20,500	24,600	1135
F. Containment Intermediate	10,250	12,300	567
H. Containment Intermediate	10,250	12,300	567
I. Containment Primary	20,500	24,600	1135

Column loads are sequential and reflect adjacent bay loads. Primary columns are located at the bay ends and intermediates are between the primary.

#### Combined DBA + SSE Loads

Forces are transmitted to lattice frame and columns by the ice baskets when blowdown and vertical SSE occur simultaneously. Blowdown forces the baskets laterally against the lattice frame structural members while vertical SSE transmits the friction load vertically to lattice frames and columns.

[Table 6-72](#) lists the horizontal tangential and radial DBA and SSE force for each of the eight lattice frame levels. Using a friction coefficient of 0.50, the load for individual frames and columns are calculated. These friction forces are summarized in [Table 6-74](#).

The Specific Unit Parameters are as follows:

A. Minimum Service Temperature Inside Ice Condenser, °F	10
B. Maximum Service Temperature Outside Ice Condenser, °F	120
C. Operating Pressure, psig	0.3-0.5
D. Accident (DBA) Pressure (maximum), psig	9 + 40% = 12.6
E. Accident Temperature, °F	250

Column loads are sequential and reflect adjacent bay loads. Primary columns are located at the bay ends and intermediates are between the primary.

#### **6.2.2.3.2 System Design**

The lattice frames are structural steel grid work structures located in the ice condenser annulus and fitted between the lattice frame support columns and clearing the wall panel air ducts.

The lattice frames are mounted radially across the ice condenser annulus for the full 300 degrees of annulus circumference at each of eight levels between the lower support structure and the intermediate deck. The first level is located 15 ft above the wear slab or ice condenser floor and the next seven levels are vertically spaced at 6 ft intervals. A total of 576 lattice frames are required for the ice condenser assembly. Three lattice frames per level in each of the 24 bays and this configuration is repeated for the eight levels.

The lattice frames are mounted to rectangular steel columns which are placed at the crane wall side and at the Containment side of the condenser annulus. The column bases are attached to the lower support structures. Columns at the crane wall are attached along the length to the wall panel cradles and to the lower support structure, while those at the Containment side are free-standing, i.e., the bases are fastened to the lower support structure but there are no connections with the wall panels or the Containment vessel wall. This arrangement prevents transmission of loads from ice baskets, lattice frames and columns to the Containment vessel. The vertical columns and crane wall support and maintain the lattice frame geometry during normal and accident loading conditions.

The lattice frames are welded steel structures consisting of radial struts supported by welded cross bracing as shown in [Figure 6-118](#). Basically the lattice frame is about 125 in. long, 48 in. at its widest point and 7 1/2 in. deep. The entire welded structure weights about 1200 lbs. Individual free path penetrations are provided for each of twenty-seven ice baskets. The lattice frame struts that form the ice basket restraints are all double fillet welded to the stringers. This assures a consistent weld design and ensures the integrity of the entire structure in operation.

Flexible radial members on the lattice frame are located at the Containment side to accommodate differential thermal expansion in the tangential direction, and to allow for minor column misalignment at installation. The flexible radial members are attached to the vertical support columns.

The lattice frame attachment at the crane wall consists of horizontal earlike tabs that accommodates the bolting. One tab is slotted in the tangential direction to allow for differential thermal expansion between the concrete crane wall and the steel structures. Lattice frame tabs are fastened to brackets on the vertical support columns. The columns, in turn are bolted to the crane-side wall panel cradles. The wall panel cradles are fastened to the crane wall studs and transmit the lattice frame and ice basket horizontal loads to the crane wall, while the vertical loads are transmitted to the lower support structure.

The cross bracings and radial struts are arranged so that the ice baskets are positioned in the free path penetrations. The free path diameter controls the radial clearance between ice baskets and the lattice frames. The penetrations are spaced to assure the proper hydraulic diameter around each ice basket and to allow free passage of air and steam through the surrounding passages. Small pads on the radial struts control the tangential ice basket clearance.

All of the welding and inspection was done in accordance with the American Welding Standard Procedure, D1.1-72. The welds are inspected visually and then by magnetic particle inspection. The magnetic particle inspection is applied to selectively located welds throughout the structure. All accessible exposed steel components are covered by a protective coating.

### 6.2.2.3.3 Design Evaluation

The lattice frames are analyzed using the ICES-STRUDLE II System of computer programs for frame analysis. STRUDLE is a general program operating as a subsystem of the Integrated Civil Engineering (ICES) program. The lattice frames are treated as three dimensional structures composed of joints, support joints, and structural members connecting the joints. [Figure 6-119](#) illustrates the analytical model generated for the lattice frames. Each structural joint is assigned a circled number, and each structural member an uncircled number.

The lattice frame is treated as a cantilevered structure in the horizontal plane and restrained vertically at the four column connections. The model in [Figure 6-119](#) shows flexible connections at the crane wall and no connection at the Containment wall. Variations in flexibility of the crane wall connections are considered in the analysis to simulate the behavior of the slotted tab connection and the connections to lattice frame columns and air duct wall panels.

The analysis of the loads for the individual maximum of D + 1/2 SSE, D + SSE and D + DBA is determined. A survey is also conducted for the loading combinations of D + SSE + DBA for each lattice

frame level at reference seismic orientation, 45 degrees, and 90 degrees from reference (refer to [Figure 6-116](#)) to determine the maximum loading condition on the lattice frame. The survey shows that the highest loads occur on the lattice frame at the 33 ft level, and that the combination of D + SSE + DBA, horizontally and vertically produces the maximum stresses.

Maximum stresses are calculated at each structural member at the edge of the fillet weld for all loading conditions. These maximum stresses are summarized in [Table 6-75](#).

Fatigue stresses due to 1/2 SSE loading were calculated and are within the allowable limits defined in Section [6.2.2.16](#). [Table 6-76](#) summarizes the fatigue analysis.

The vertical support columns and brackets which support the lattice frames are structurally analyzed to determine structural integrity. The worst load combinations of D + 1/2 SSE, D + SSE, D + SSE + DBA are considered in the analysis. The resulting stress analysis indicates that the stresses in the supporting structure are within the allowable stress criteria limits defined in Section [6.2.2.16](#).

The vertical support members are also analyzed to determine buckling characteristics. Analysis using classical buckling methods indicates that this phenomena is not a concern.

## 6.2.2.4 Ice Baskets

### 6.2.2.4.1 Design Basis

#### Function

The function of the ice baskets is to contain borated ice in 12 inch diameter columns 48 feet high. The ice absorbs the thermal energy resulting from LOCA or steam line break in the Containment structure. The baskets are arranged to promote heat transfer from the steam to ice during and following these accidents. The function of the ice baskets is also to provide adequate structural support for the ice and maintain the geometry for heat transfer during or following the worst loading combinations.

#### Loading Modes

The following loading conditions are considered in the design of the ice baskets; dead weight, seismic loads, blowdown loads, and impact loads between the basket, ice and lattice frames. The baskets withstand these loads and remain within the allowable limits established in Section [6.2.2.16](#).

#### Design Consideration

1. The structural stability and deformation requirements are determined to ensure no loss of function under accident and safe shutdown earthquake loads.
2. The ice baskets are designed to facilitate maintenance and for a lifetime consistent with that of the unit.
3. The structure is designed to maintain the ice in the required array to maintain the integrity of performance of the ice condenser. In particular, the hydraulic diameter and heat transfer area are maintained within the limits established by test to be consistent with the containment design pressure.
4. Any section of the ice basket is capable of supporting the total weight of the ice above that section.

#### General Thermal and Hydraulic Performance Requirements

The ice baskets are fabricated from perforated sheet metal which has open area to provide sufficient ice heat transfer surface. The adequacy of the design and the performance were confirmed by test.

#### Interface Requirements

1. Lattice Frame

The lattice frames at every 6 ft act as horizontal restraints along the length. The design provides a nominal 1/4 in. radial clearance between the ice baskets and the lattice frames. Lattice frame and basket coupling elevations coincide to prevent damage to the basket during impact.

2. Lower Support Structure

Ice basket bottoms are designed to be supported by and held down by attachments to the lower support structure. The basket supports are designed for structural adequacy under accident and safe shutdown earthquake loads and permit weighing of selected ice baskets.

3. Basket Alignment

The ice condenser crane aligns with baskets to facilitate basket weighing and/or removal. The baskets are capable of accepting basket lifting and handling tools.

4. Basket Loading

The ice baskets are capable of being loaded by a pneumatic Ice Distribution System. The baskets contain a minimum of  $1.89 \times 10^6$  pounds of ice.

5. External Basket Design

The baskets are designed to minimize any external protrusions which would interfere with lifting, weighing, removal and insertion.

6. Basket Coupling

Baskets are capable of being coupled together in 48 foot columns.

7. Basket Couplings and Stiffening Rings

Couplings or rings are located at 6 ft intervals along the basket and shall have internal flanges (cruciforms) to prevent the ice from falling down to the bottom of the ice column during and after a DBA and/or SSE.

Design and Test Loads

The minimum test and basic design loads are given in Tables [6-77](#) and [6-78](#).

#### **6.2.2.4.2 System Design**

The ice condenser is an insulated cold storage room in which ice is maintained in an array of vertical cylindrical columns. The columns are formed by perforated metal baskets with the space between columns forming the flow channels for steam and air. The ice condenser is contained in the annulus formed by the Containment vessel wall and the crane wall circumferentially over a 300 degree arc.

The ice columns are composed of basket sections that total 48 feet long, filled with the flaked ice. The original basket sections were 12 feet long with four sections coupled together. Basket sections are now made in 2 foot, 3 foot, and 12 foot sections and any combination of these can be used to make the 48 foot columns. The perforations are 1.0 in. x 1.0 in. holes, spaced on a 1.25 inch center. The radius at the junction of the perforation is 1/16 inch. The ice basket material is made from ASTM A-569 which is a commercial quality, low carbon steel (A-622 and A-715 are acceptable alternate materials). The basket component parts are corrosion protected by a hot dip galvanized process. The perforated basket assembly has an open area of approximately 64 percent to provide the necessary surface area for heat transfer between the steam/air mixture and the ice to limit the Containment pressure within design limits. The basket heat transfer performance was confirmed by the autoclave test.

Cruciforms are installed in the ice baskets at 6 ft. intervals in all baskets except for row 8 and row 9 which are not required to have the bottom three cruciforms installed. These cruciforms prevent the ice in the

basket from displacing axially in the event of loss of ice caused by sublimation or partial melt down due to accident conditions. These cruciforms are not permanently fixed to the ice baskets.

Interconnection couplings and stiffening rings are located at the bottom and 6 ft. levels respectively of each basket section. The bottom coupling and stiffening ring are cylindrical in shape and approximately 3 inches high with a rolled internal lip. The lip provides stiffening to the basket. These couplings are attached to the ice basket by sheet metal screws and basket detents.

The baskets are assembled into the lattice frames to form a continuous column of ice 48 ft. high. The bottom grid assembly is designed to allow water to flow out of the basket and has attachments for mechanical connection to the lower support structure to prevent uplift of the ice baskets during SSE and DBA. The lattice frames provide only lateral ice basket support at intervals corresponding to the stiffened ice basket sections. The vertical loads of the ice and ice basket is transmitted by the basket to the lower support structure. The attachment between the ice basket and the lower support structure may be disengaged if required to permit weighing of the baskets. The columns of ice can be lifted and removed in sections, and provision is made for lifting and weighing the whole length of selected columns for surveillance purposes.

#### Fabrication

The fabrication steps are as follows:

1. The sheet metal is purchased in the hot-rolled and pickled condition.
2. The perforator oils and perforates the material and ships to the basket fabricator.
3. The basket fabricator rolls the perforated metal into a cylindrical shape 12 inches in diameter by 141.57 or 143.25 inches long (for bottom basket or upper basket respectively) and material is degreased.
4. The sides of the rolled cylinder are continuously welded using the gas metal arc process.
5. Following the welding the cylinder is pickled, washed, fluxed, hot dip galvanized, and dipped in a sodium dichromate bath.
6. The couplings and stiffening ring blanks are cut from sheets or coils or hot rolled, pickled and oiled material. These are formed by a rolling process and are 3 inches high with a roll-formed internal lip and are of a diameter to fit inside the perforated basket.
7. The cruciforms are die-formed from steel strip.
8. Following the forming operations, stiffeners and couplings with cruciforms in place are pickled, washed, fluxed, hot dip galvanized, and dipped in a sodium dichromate bath. Replacement cruciforms are made of stainless steel and will not be subjected to this treatment.
9. The column bottom is fabricated by a procedure similar to item (6) above. The appurtenances are welded in place and the piece is galvanized per item (8) above.
10. The remaining appurtenances are cut to size, machined, welded, where required followed by galvanizing as above, and plated where required.
11. The completed couplings, bottoms, appurtenances, stiffening rings and cylinders are next assembled. The stiffening rings are inserted inside the cylinder until the side is adjacent to the 2.5 or 2.75 inch (for bottom or upper basket, respectively) perforated area in the center of the cylinder and attached by a sheet metal screw and four basket detents.
12. For the column bottom, two U-bolts and nuts and washers fasten the mounting bracket assembly to the plate of the basket end. Swivel Bracket Assemblies may be substituted for the U-bolt assemblies.

13. The bottom is inserted into the cylinder until the cylinder rests against the step of the bottom and is attached mechanically by 12 sheet metal screws.
14. For the upper baskets, the couplings are inserted in the cylinders approximately 1-1/2 inches and attached with 12 screws as above.
15. All welding and inspection is performed in accordance with AWS publication D1.3, including latest revisions.

#### Installation

The completed baskets are placed in the lattice frames from the top deck by first lowering a bottom basket into the lattice frames and locking in place, extending approximately 2 inches above the top lattice frame. The second upper basket is lifted with the crane and gripper fixture and placed on top of the bottom basket inserting the coupling into the top of the bottom basket and attaching with sheet metal screws.

Next the locking or holding fixture is released and the two baskets lowered until the top is approximately 2 inches above the lattice frames as above. The third and fourth baskets are installed in the same manner as the second.

When the full column is assembled and ready to set on the lower support structure, the bolts and mounting bracket are loosened and the column lowered to facilitate alignment of the yoke with hole in the support structure. After alignment and insertion of the clevis pin, the 4 bolts are tightened. A hitch pin cotter is inserted to retain the clevis pin.

#### Materials

The discussion of acceptable materials for the ice basket is presented in Section [6.2.2.18](#).

### **6.2.2.4.3 Design Evaluation**

#### Basket Evaluation

The perforated metal baskets of A-622 low carbon steel of 14 gage sheet, with 1.0 in. by 1.0 in. holes on 1.25 in. centers, were evaluated by analyses and tests and found to be within the allowable limits defined in Section [6.2.2.16](#). Three different methods were used in determining the baskets' adequacy. The first method employed classical strength of materials techniques, the second used limit analysis and the third confirmed the basket integrity by tests.

#### Stress Analysis

This method considered the ice basket as being composed of a number of line (vertical basket element) and stay (circumferential basket element) elements and that the collapse of the ice basket may be precipitated by the local yielding and/or buckling of the individual line elements.

When the basket is loaded both axially and laterally as a beam, the line elements are subjected to an axial compression, a lateral shear and a bending load. This combined stress state can possibly lead to local yielding, plastic collapse, line element buckling and ultimately to structural failure. All these modes of possible failure were analyzed and the results were found to be well within the allowable criteria. Analysis indicates that the critical line element buckling load is about 303,000 lbs. The maximum vertical load, D + SSE is 2753 lbs. Therefore the possibility of elastic buckling is remote. For a case with only lateral load, the analysis indicates that a factor for safety of 3.15 exists between the allowable basket load and the maximum lateral load that exists. A summary of stresses are tabulated in [Table 6-79](#). For the various design cases considered, it is seen that the maximum stress is always below the allowable stress.

Analysis was also made of the case where the ice melts out so that it occupies only one half side of the basket. The eccentricity would be 3 inches but the ice mass would be halved giving a shear stress of 450 psi, for a combined maximum shear stress of 3850 psi, again well below the allowable.

#### Limit Analysis

Limit analysis is performed on the ice basket in order to determine by analysis the lower bound collapse load when the basket is simultaneously loaded in the axial and lateral directions. The following modes of failure are considered:

1. Plastic collapse of the compression side
2. Plastic yield of the compression side
3. Shear yield of the neutral plane
4. Plastic yield of the neutral surface line elements.

A summary of the combinations of concentric axial load and distributed load that causes basket failure is presented in [Figure 6-121](#). Also superimposed in this figure is the design and test load envelope. It can be seen that this envelope is well below the governing failure mechanism of plastic yielding of the neutral surface of the line elements.

#### Ice Basket Appurtenance Evaluation

The ice basket connections are analyzed to ensure structural integrity during all design load combinations of dead weight, 1/2 Safe Shutdown Earthquake, Safety Shutdown Earthquake and Design Bases Accident. The primary area of concern is the ice basket to lower support structure connection. This area is shown in [Figure 6-120](#). The item, material and minimum yield stress are presented in [Table 6-80](#). The allowable stress limits for D + 1/2 SSE, D + SSE, and D + SSE + DBA are tabulated in [Table 6-81](#) through [Table 6-83](#), respectively. The loads used in the analysis of these parts envelop minimum design loads plus load factors necessary for the Duke analysis.

#### Clevis Pin

The clevis pin transmits the ice basket loads to the lower support structure through a 1 x 2 inch bar welded to the top of the structure. A clearance of 1/32 inches is provided both vertically and horizontally to provide a pinned connection, thereby eliminating the transfer of any moment to the structure resulting from basket deflection because of horizontal loads.

The stresses on the 1/2 inch diameter pin are tabulated in [Table 6-84](#).

#### Column Bottom Mounting

The mounting bracket is attached to the basket bottom as shown in [Figure 6-120](#). The design loads are transmitted through the mountings and clevis pin from the ice basket bottom.

The stresses in the mounting bracket, assembly, plate and U-bolt are tabulated in [Table 6-85](#) through [Table 6-87](#), respectively.

#### Swivel Bracket Assemblies

A design change which replaces the U-bolt and mounting bracket assembly with a lug and two coupling halves (Swivel Brackets) has been implemented. This design consists of a lug which rests on the lower support structure, and two coupling halves which capture the plate spanning the ice basket bottom. The Swivel Bracket Assembly allows the ice basket to be rotated while the clevis is still secured, enabling the baskets to be freed of frost accumulation and weighed in place. Refer to [Figure 6-200](#) for details of the basket bottom modifications. All parts are stainless steel for corrosion resistance. The cast pieces are 15-5PH, while the bolting is grade BB.

The swivel bracket assembly increases the gap between the clevis pin and basket bottom, which increases the impact loads during combined SSE and DBA events. The revised basket loadings and swivel bracket stress analysis was evaluated (Reference [80](#)). Refer to [Table 6-142](#) for a stress summary.

#### Ice Basket End

The column bottom is shown in [Figure 6-120](#). The loads that are transmitted through the clevis pin assembly are distributed to the ice basket through the rigid plate and the cylindrical ice basket and section. Wire mesh is used to contain the ice and to provide drainage for water. The stress summary for the ice basket end is shown in [Table 6-88](#).

The intermediate ice basket coupling screws were also analyzed and the results of the analysis are given in [Table 6-89](#) through [Table 6-92](#) and indicate that the intermediate couplings are structurally adequate for maximum loading conditions defined in Section [6.2.2.16](#).

### **6.2.2.5 Crane and Rail Assembly**

#### **6.2.2.5.1 Design Basis**

##### Function

The crane and rail assembly is designed to carry components and tools into, out of, and within the ice condenser area during erection, maintenance, and inspection periods.

##### Criteria and Codes

The crane is designed in accordance with the requirements of the Electric Overhead Crane Institute Specification 61. It is designed so that under all loadings it is not derailed.

The rail is designed according to Section [6.2.2.16](#). These criteria provide assurance that the rail maintains its structural integrity.

##### Design Conditions

The service temperature range is 15°F to 100°F.

During unit erection, two cranes can be used in the ice condenser region, each carrying up to 6000 pounds. A separation of at least two bays is maintained between their centers. Prior to installation of air handling units, one crane is removed. The heaviest load actually expected after this time is less than 2,500 pounds. The crane remains normally parked (without load) outside the ice condenser while the reactor is at power. The crane and supporting structure are designed to withstand dynamic loading during operation modes specified above.

The design loads for the crane are presented in [Table 6-93](#).

#### **6.2.2.5.2 System Design**

The design of the 3 ton capacity crane is shown in [Figure 6-122](#). The bridge, boom and hoist of the crane are all motor operated. The bridge speeds are approximately 38 and 110 feet per minute. The boom member is capable of rotating 360 degrees in either direction at a speed of approximately 2 revolutions per minute. The electric hoist is mounted on the boom member with 2 stainless steel cables reeved over 2 sheaves mounted on the boom and around 2 sheaves on the hook block assembly. The hoist provides approximately 71 feet of lift at speeds of 7 and 20 feet per minute. It is equipped with an upper and lower limit switch to insure that the cables will not completely unwind from the hoist drum. The hoist automatically switches to low speed approximately 2 feet below the highest point of travel.

The total crane weight is approximately 7200 pounds.

The predominant material of construction is A36 steel. The main structural members are painted to prevent corrosion.

The crane travels on two circular rails that run through the ice condenser area as shown in [Figure 6-123](#). The circular diameters of the rails are 95 and 109 feet. The top flange plate and rail section are continuously welded to the web plate under controlled conditions. The top flange and web plates are A36 steel and the lower rail section is special analysis steel with a hard nonpeening rolling surface.

### 6.2.2.5.3 Design Evaluation

The crane rails and supporting structures are analyzed as a part of the top deck structure (see Section [6.2.2.10](#)). It is found that all stresses were maintained within limits prescribed in the design criteria, Section [6.2.2.16](#), for all design conditions defined in Section [6.2.2.5.1](#).

## 6.2.2.6 Refrigeration System

### 6.2.2.6.1 Design Basis

#### Function

The Refrigeration System serves to cool down the ice condenser from ambient conditions of the reactor containment and to maintain the desired equilibrium temperature in the ice compartment. It also provides the coolant supply for the ice machines during ice loading. The Refrigeration System additionally includes a defrost capability for critical surfaces within the ice compartment.

During a postulated loss-of-coolant accident the Refrigeration System is not required to provide any heat removal function. However, the Refrigeration System components which are physically located within the Containment must be structurally secured (not become missiles) and the component materials must be compatible with the post-LOCA environment.

#### Design Conditions

#### 1. Operating Conditions

See individual component sections:

- a. Floor cooling - Section [6.2.2.1](#)
- b. AHU - Section [6.2.2.7](#)

#### 2. Performance Requirements

- a. The mandatory design parameters that relate to refrigeration performance are:

Nominal initial total weight of ice in columns	$3.0 \times 10^6$ lbs
Minimum total weight of ice in columns	$1.89 \times 10^6$ lbs
Nominal ice condenser cooling air temperature	10°F - 15°F

- b. The design must also provide a sufficiently well insulated ice condenser annulus such that with a complete loss of all refrigeration capacity, sufficient time exists for an orderly reactor shutdown prior to ice melting. A design objective is that the insulation of the cavity is adequate to prevent ice melting for at least 7 days in the unlikely event of a complete loss of refrigeration capability.

- c. The non-directly safety related design objective parameters are:

- 1) Ice Sublimation

Ice sublimation and mass transfer is reduced to the lowest possible limits by maintaining essentially isothermal conditions within the ice bed and by minimizing local temperature gradients. A design objective is to limit the sublimation of the ice bed to less than 2 percent per year by weight. The normal steady state sublimation appearing on the wall panels as frost is calculated to be significantly less than the total design objective. Calculations incorporating both radiative and convective modes of heat transfer result in a sublimation rate of less than 0.3 percent per year to the wall panels.

- 2) An appropriate combination of refrigeration capacity and insulation capability is achieved to permit the following:
  - a) Maintain the average ice bed temperature in the range of 10°F to 15°F under the most adverse non-accident conditions.
  - b) Cool the ice condenser down to 15°F in 14 days (initial cooldown prior to ice loading).

The ice condenser is structurally designed to withstand the various extreme loading parameters including DBA + SSE. The ice condenser design and the reactor Containment supporting walls are analyzed for heat transfer through the boundaries of the ice condenser. The configuration and sizing of the cooling components is then determined to achieve the various design requirements.

One of the most important design criteria for the ice condenser is that the insulation shall maintain the ice condenser chamber below 31°F for a significant period of time given that a malfunction or failure of any refrigeration component has occurred. Most system anomalies can be remedied during this period. For any repair which would require more time, a scheduled reactor shutdown can be completed in a safe and orderly fashion. Eliminating the “emergency factor” from the operation of the Refrigeration System places the performance of the refrigeration components in an operational category without mandatory safety related design requirements.

#### **6.2.2.6.2 System Design**

The Refrigeration System serves as a central heat sink for the heat picked up in the ice condensers and in the ice machines. A Circulating System of ethylene glycol solution carries the heat from the various heat transfer surfaces to the chiller packages. Cooling of the ice condenser is achieved by a Three Stage System:

- First Stage - Refrigerant Loop
- Second Stage - Glycol Loop
- Third Stage - Air Cooling Loop

##### First Stage - Refrigerant Loop

Four 50 ton dual chiller packages and two 25 ton stand-alone chillers are installed in the plant. Each dual package consists of two separate 25 ton compressor units, individually operable. See [Figure 6-124](#) for refrigerant cycle diagram. Ethylene glycol solution is cooled during its passage through the evaporator, and heat is removed from the chiller unit by cooling water flowing through the condenser. The condenser cooling water is provided from the non-essential Recirculated Cooling Water System. The chiller units operate individually to maintain outlet temperature of ethylene glycol at -5°F.

Refer to [Table 6-94](#) for refrigeration system parameters such as operating temperatures, flow rates, pressure drops, rating basis, etc.

##### Second Stage - Glycol Loop

The second cycle ([Figure 6-125](#)) carries the heat removed from the ice condenser air handling units, the Floor Cooling System and the ice machines (when operating) to the refrigerant cycle evaporator/cooler units. The liquid circulating through this cycle is a corrosion inhibited 50 percent ethylene glycol solution. It is compatible with most common piping materials and standard gasket and packing materials. Piping and valve materials used in this loop are predominantly carbon steel with stainless or alloy trim. Diaphragm valves are provided with ethylene propylene diaphragms. Piping and equipment carrying chilled ethylene glycol solution are covered with low temperature thermal insulation.

Six glycol circulating pumps are designed to convey the cooled glycol from the ten refrigeration units to the air handling packages (30 per Containment) and to the ice compartment Floor Cooling System of each Containment. The design includes provisions for interconnecting the chiller packages and pumps, as required. The heated glycol is then returned to the refrigeration units thereby completing the glycol loop. The heat is extracted from the air in its passage through the air handlers and from the Floor Cooling System. Two rows of air handlers located along inner and outer walls are served by respective glycol supply and return headers. The return headers are connected to a vented expansion tank located above the upper deck in each unit. Pairs of Containment isolation valves are installed on supply and return lines on both sides of Containment penetration. Closure of these valves in response to a T-signal<sup>1</sup> isolates the ethylene glycol piping inside the containment vessel from the External Refrigeration System. In the event of a LOCA, the glycol heats up from approximately -5°F or 0°F to the Containment accident temperature and expands harmlessly into the expansion tank.

The ice condenser floor is kept cold by chilled glycol solution circulating through pipe coils embedded in the concrete wear slab. (See [Figure 6-115](#) for wear slab top surface area showing typical coolant piping layout.) During normal operation, one floor cooling pump feeds a circular header, which distributes the coolant to individual coils located in each bay. After passing through the floor coil, glycol flows through a panel coil located on the lower support structure radial beam, this aids in heat removal in the lower inlet door area. A second circular header returns the flow to pump suction.

The glycol solution is maintained at the proper temperature by continuously bleeding solution out of the system and feeding cold solution into it at the same rate. The cold solution is taken from the glycol stream returning from the air handling units to the External Refrigeration System. The bleed flow is sent back into the same line downstream of the feed connection. Feed and bleed flow is maintained by the same pump that drives solution through the coils. Bleed flow rate is regulated by a temperature control valve. A second pump is available for use while pump No. 1 is being serviced or during seasonal high demand periods. A manual throttling valve bypassing the temperature control valve can perform the latter's function during brief maintenance periods.

Components requiring periodic maintenance (pumps, heater, control valve) are located in the upper compartment. The cooling coils in the concrete wear slab rest on a steel plate to effectively intercept heat passing up through the floor. The coils are made of heavy steel pipe to minimize chances of developing a leak by gradual corrosion of pipe material. Should a leak develop, any individual loop can be isolated by closing two valves inside the lower region of the ice condenser.

[Table 6-94](#) has additional detailed parameters for the glycol cycle components.

### Third Stage - Air Cooling Loop

---

<sup>1</sup> Containment isolation signal, Phase A, derived from Safety Injection or manually.

The ice condenser compartment is designed to be kept below the freezing point throughout the life of the unit. During normal operation, it is cooled to approximately 15°F prior to ice loading and kept at that temperature indefinitely, barring occurrence of a loss-of-coolant accident, extensive failure of the Refrigeration System, or permissible excursion during ice loading. Ice bed temperature is maintained at the specified level by means of chilled air circulating through the boundary planes of the compartment. Starting in the upper plenum, which constitutes the top boundary, air enters one of 30 air handling packages located in the plenum. The air handler cools the air and blows it down through a series of insulated duct panels lining the inner, outer and end walls of the ice condenser. When the air reaches the lower support structure at the inner wall or end walls or the floor level at the outer wall, it turns back up to the plenum through a parallel path in the wall panels. See [Figure 6-126](#) for a schematic flow diagram of the air cooling cycle.

The air handling units are designed to provide a discharge or duct entrance air temperature of 10°F. A direct mounted thermometer in the AHU discharge duct provides local indication of air temperature.

Each AHU is sequenced to a defrost cycle by a time clock or by a manual pushbutton. Either signal completes a circuit which initiates the de-energizing of the fan motor, closing the glycol isolation valve and energizing the coil and drain pan heaters. The defrost cycle is completed by the time clock. Additionally, each unit contains a drain line heater to prevent coil defrost water from freezing in the drain line.

Provisions also exist for defrosting the wall panels by circulating heated air through the wall panels. The structural function and capabilities of the air cooling cycle components are discussed in the following sections:

1. AHU - Section [6.2.2.7](#)
2. Wall panels - Section [6.2.2.2](#)
3. Air distribution ducts - Section [6.2.2.12](#)

[Table 6-94](#) has additional parameters for the air handling units.

### 6.2.2.6.3 Design Evaluation

The Refrigeration System is sized to maintain the required ice inventory even under worst case operating conditions. The chiller package total capacity is sufficient to maintain both ice condensers.

- |   |       |
|---|-------|
| 1. Lower Containment, air temperature               | 120°F |
| 2. Upper Containment, air temperature               | 100°F |
| 3. Equipment room air temperature                   | 120°F |
| 4. Exterior Containment wall design air temperature | 110°F |

Items 1 through 3 are specified in the General Design Criteria. Item 4 is the design dry-bulb temperature in the region of North Carolina where the McGuire units are located for a 50 year hot summer, plus an additional margin of 9°F. The 1 percent factor is defined such that only 1 percent of the time the dry-bulb temperature during the summer months is above the specified temperature for a 50 year hot summer. Data was obtained from ASHRAE climatic guide for cooling and heating design conditions. For an average summer, the 1 percent design dry-bulb temperature for Charlotte is 96°F and for a 50 year hot summer, is 101°F. The average (4 quadrant) sol-air temperature for vertical walls corresponding to a maximum dry-bulb temperature of 95°F is about 107°F.

The major thermal boundaries of the ice condenser including the floor, cooled walls with ducts, lower inlet doors, and top deck support beams are analyzed using a Westinghouse developed computerized

technique, TAP-A, (or TAP-B). A program for Computing Transient or Steady-State Temperature Distributions, WANL-TME-1872, Dec. 1969. Subcontract NP-1.

The TAP-A program is applicable to both “transient and steady-state heat transfer in multi-dimensional systems having arbitrary geometric configurations, boundary conditions, initial conditions, and physical properties. The program can be utilized to consider internal conduction and radiation, free and forced convection, radiation at external surfaces, specified time dependent surface temperatures, and specified time dependent surface heat fluxes.”

The solution of the general heat conduction equation is determined with finite difference techniques. The program solves the equation as determined for the particular finite element or nodal model set up, either explicitly or implicitly. All cases studies for the ice condenser are solved implicitly.

The TAP-B program is a variation of TAP-A but includes fluid coupling to the finite element model. The TAP-B variation is used to analyze the cooled wall panels. Since the duct air temperature distribution is included in the model it is possible to evaluate the temperature distribution of the surface of the wall panel facing the ice condenser over the complete length of the duct.

The wall panel heat load comprises about 70 percent of the total heat load, through the thermal boundaries with the inner surface area of the wall panels covering just under 30,000 ft<sup>2</sup>.

The wall panel model for the crane wall is 48 ft long with 8 axial stations each 6 ft in length. The width of the model covers the region from the centerline of the duct region to the centerline of the lap strip region.

There are approximately 1,000 interior and surface nodes for the 48 foot length of the model which consists of 1/2 of a duct section.

Roughly 70 percent of the thermal load through the wall panels flows through the mounting brackets (or about 50 percent of the total thermal load of the ice condenser). The cold boundary temperature of the model was assumed to be 12°F in the ice bed with a 10°F duct entrance temperature.

The basic floor model utilizes TAP-B. The basic floor design is analyzed with fluid coupling. The results of the basic model justifies the design concept. Variations in the basic floor design are checked by hand calculations for overall thermal load. The basic floor model is comprised of approximately 1200 nodes in 5 layers and covers one quarter of a typical floor bay, of which there are 24 bays. The air temperature over the floor is assumed to be 14°F. The temperature of the glycol boundary is calculated for each fluid node. Over 90 percent of the heat entering the floor region is found to be removed by the Floor Cooling System. Use is made of the transient capabilities of the program to determine the defrost or warm-up time required when the glycol is heated. This is not performed at McGuire. See [6.2.2.1.2](#) for details. The heat transfer through the top surface of the floor is in two directions, both into and out of the wear slab. The new flow from the top surface to the ice condenser chamber is about 1000 Btu/hr. About 75,000 Btu/hr total is absorbed by the floor glycol coolant using the basic model.

The lower inlet door region while not contributing significantly to the overall thermal load on the Refrigeration System is extremely important when considering sublimation. Various models of portions of the door are postulated to determine effective means of limiting the heat flux through the lower inlet doors.

The total heat load through doors with appropriate insulation is maintained at less than 10,000 Btu/hr to the ice bed. The door assembly is analyzed in two segments, there are 24 complete 2 door assemblies in the ice condenser. The first door model covers the region from the centerline of one door panel to the central seal region. Hand calculations are used to determine the nature of the convection between the two door panels in the central seal region, and in the outer hinge region. The information on the type of convection present is necessary to locate insulation and to determine any advantage to be gained from positioning flaps or boots around the door perimeter. Flaps are not considered necessary in the door center because the convection is determined to be laminar with air conduction dominating. The central door

model contains about 150 internal nodes including insulation. The second region covered by a model is the hinge region. The hinge model is 15 inches deep (about 1/6 of) the door length and included effects of the reinforcement channels along the full width of the door. The extremities further away from the hinge region are only grossly modeled. There are a total of 168 internal nodes in the “hinge” model including a protective boot around the hinge. The hinge model also includes effects of the pillar in the crane wall upon which the door is mounted. The hinge region is of major importance in contributing to the internal thermal load with most of the heat input coming from the massive concrete pillar. It is necessary to protect the hinges with boots to limit the convective heat transfer which is quite effective in reducing the heat flow.

The top deck support beams are similarly modeled using TAP-A. The beams are a major source of thermal load in the plenum are thermal boundaries but only a small fraction of the total thermal load on the air handlers (not including air handler motor heat).

The modeling required for analysis of the components is extensive and detailed. The admittance of each node and connection; involving the determination of the length, volume, and area of each element was conservatively estimated where simplification of the model was required. The models are realistic since sufficient detail was considered and all significant modes of heat transfer were considered. Hand calculations back-up all major assumptions used to arrive at a model.

The summation of the thermal analysis gives a total nominal thermal load of 37 tons of 432,000 Btu/hr.

The breakdown is listed below. The values given are considered to be nominal expected loads. Design change required as a result of, e.g., change in air distribution duct configuration or other design re-evaluations would of course change the final summation. The final thermal load is still maintained at the same level consistent with stated refrigeration requirements.

	<u>x 10<sup>4</sup> Btu/hr</u>
Wall panels	29.2
Plenum and Top Deck	10.11
Leakage 50 cfm	1.1
Lower inlet doors	2.0 <sup>2 3</sup>
Floor	0.2
End walls	<u>1.17</u>
Total thermal load	43.78

The calculated heat loads show that a heat gain of 432,000 Btu/hr per containment may be expected from thermal boundaries of the ice condenser. Additionally each air handling unit fan motor generates less than 6,000 Btu/hr (Subtotal 30 AHU x 6,000 Btu/hr = 180,000 Btu/hr) based on 30 operating air handlers with a design allowance of 1.5 in. of H<sub>2</sub>O over the Air Delivery System. The Floor Cooling System, including pump heat, has a heat gain of 90,000 Btu/hr nominal.

---

<sup>2</sup> Calculated Load < 1 x 10<sup>4</sup> BTU/hr

<sup>3</sup> Design Allowance = 2 x 10<sup>4</sup> BTU/hr (includes miscellaneous items in addition to door load).

The circulating pumps (2 operating) add a total of 100,000 Btu/hr. The piping is estimated to pickup 7,000 Btu/hr. Therefore, a chiller package capacity of about 800,000 Btu/hr per Containment (base load) is required. Since this is a dual unit application and the chiller packages serve both units, the total chiller package capacity was chosen to be three (3) times the base load which is 2,400,000 Btu/hr. Since each chiller package is rated nominally at 600,000 Btu/hr depending on cooling water temperatures, four chiller packages are installed. Two additional 25 ton chillers were added prior to commercial operation to support maintenance activities and add cooling margin.

The Refrigeration System is designed for maximum flexibility. The six circulating pumps and ten chiller units have been provided with split sets of piping manifolds to conduct ethylene glycol solution into and out of any combination of these components. Consequently, the associated systems can be refrigerated from the central source with a minimum of interaction, and a high degree of redundancy is available for normal unit operation.

The three circulating pumps are conservatively sized to deliver the required coolant to each unit. One standby pump per unit is included in the design to assure adequate cooling solution flow even in the event of a pump failure. Similarly the air handling units are conservatively sized to handle the worst case cooling load. Thirty air handling packages are installed based on a 10/7 ratio of installed capacity to base load.

It should be noted that the ice bed is sufficiently subcooled and insulated so that even a complete breakdown of the Refrigeration System or of all air handlers should not initiate the melting of any ice for a period of one week. Anomalous conditions in the ice condenser are indicated by alarm annunciation from expansion tank level switches, the Temperature Monitoring System, or the Door Position Monitoring System. Refer to Section [6.2.2.15](#) for a discussion of the Ice Condenser Instrumentation System.

If one bay in the floor is not cooled because the glycol flow has to be isolated from that bay the heat load from that bay is about 3,000 Btu/hr. The additional sublimation rate would be under 0.25 percent per year per bay. It would be expected that one bay would not be permitted to go uncooled for extensive length of time. Once an operational sublimation rate is established it would not be unreasonable to assume that possibly 3 isolated uncooled floor bays could be permitted to be uncooled for about 1 year. If the Floor Cooling System is shut off completely, it should be put back in operation as soon as convenient. An annual sublimation rate of about 5 percent per year will result with no cooling in the floor, which would require ice bed replenishing in 3 years.

### **6.2.2.7 Air Handling Units**

#### **6.2.2.7.1 Design Basis**

##### Air Handling Units (AHU)

During normal operation the air handling units serve to cool the air and to circulate the cooled air through the ice condenser walls' panels to keep the ice subcooled in the ice beds. Normal structural loads expected are dead weight, seismic, SSE and thermal loads. During an accident the AHU's are designed to resist the normal structural loads plus SSE + DBA induced loads. Welding, welder qualification and weld procedures are in accordance with USASI B31.5 Refrigeration Piping and the ASME Boiler and Pressure Vessel Code, Section IX "Welding Qualification."

##### AHU Support Structure

###### 1. Function

The AHU support structure supports the air handling unit package under various design conditions which are detailed below:

## 2. Design Criteria and Codes

Refer to Section [6.2.2.16](#).

## 3. Design Conditions

### a. Normal Operation

Deadweight loads due to AHU, structure	2500 lbs
Design temperature, min.	15°F

### b. Accident Conditions

Post-accident Temperature (no uplift)

### 6.2.2.7.2 System Design

#### Air Handling Units

Each AHU is supported from its support structure, transmitting its major loads to top deck cross beams. See the AHU Support Structure Design Criteria for additional details.

The air is drawn by each AHU from the upper plenum, is cooled in the AHU and is discharged into the air distribution header. The gross cooling capacity of each AHU package is 30,000 Btu/hr with the plenum air entering at 19°F maximum and cooled by the AHU to 10°F nominal. Each package has a 3000 cfm nominal air delivery capacity. The entering glycol mixture is at -5°F nominal temp. and the discharge glycol temperature is 1.0°F nominal. Electrical power is provided for fan motor and defrost heaters as well as for control circuits.

In order to limit seismically induced loads the AHU and supports are designed to have a natural frequency in excess of 20 Hz. All materials used in the AHU's are compatible with both normal and post LOCA environments.

#### AHU Support Structure

The support structure supports the air handling unit vertically and tangentially from the cross beam of the top deck structure and is radially attached to the face of the crane or Containment wall. All parts are coated with a paint suitable for use inside Containment. [Figure 6-127](#) shows the design of the structure.

### 6.2.2.7.3 Design Evaluation

The pressure drop through the ducts and manifolds was estimated by using loss coefficients determined by using a standard reference (Reference [49](#)) as a guide. The pressure drop through the air handlers was determined by test. The overall system flow rate was established by superimposing the system flow versus  $\Delta P$  curve over the fan flow versus  $\Delta P$  curve.

With the flow rate established the capacity of the air handlers was determined. First the air handler capacity was theoretically determined for a set of design conditions approximating operating conditions. Next the air handler units were tested by the manufacturer to the set of specified design conditions. It was determined that the theoretical relationships adequately predicted air handler performance and these techniques were then used to adjust the test values to those of actual operation. The gross operating capacity of one air handler is just under 30,000 Btu/hr by test and calculation.

The nominal heat load of 432,000 Btu/hr is adjusted by a factor of 10/7 to insure adequate capacity under operating conditions for fouling, defrosting or isolated instances of one or several unit failures. Maintenance and inspection insures reliable mechanical operation and cooling performance.

An estimate of the number of air handlers required is made to initiate the calculation, the flow pressure and rates drops are then calculated and the fan motor heat and heat transfer rates of the air handler unit predicted. The predicted performance is compared with the required capability and the calculation is reiterated varying the number of AH units until the predicted performance just exceeds the required capability.

The final number of required air handlers was determined to be 30.

A modal frequency analysis was performed for the air handling unit housings and support structure. The results indicate that the design frequency is approximately 20 Hz, so that the fundamental mode is well out of the frequency range of peak amplification on the response spectra. In the process of designing the structure on the basis of stiffness, strength of members subjected various combinations exceeds specified limits by generous margins.

### **6.2.2.8 Lower Inlet Doors**

#### **6.2.2.8.1 Design Basis**

##### Function

The ice condenser inlet doors form the barrier to air flow through the inlet ports of the ice condenser for normal unit operation. They also provide the continuation of thermal insulation around the lower section of the crane wall to minimize heat input that would promote sublimation and mass transfer of ice in the ice condenser compartment. In the event of a loss-of-coolant accident, LOCA, causing a pressure increase in the lower compartment, the doors open, venting air and steam relatively evenly into all sections of the ice condenser.

The door panels are provided with tension spring mechanisms that produce a small closing torque on the door panels as they open. The zero load position of the spring mechanisms is set such that, with zero differential pressure across the door panels, the gasket holds the door slightly open.

The developed ice condenser cold head will then compress the gasket seals, and will also serve to re-close the doors should the panels briefly and inadvertently break away from the seal during normal operation.

For small incidents, initial inlet door opening (location and magnitude) is determined by local lower compartment pressure. As the developed ice condenser cold head is lost through open doors, the remainder of the doors will also tend to open, providing numerous pathways for steam to enter the ice condenser.

For larger incidents, the doors open fully and flow distribution is controlled by the flow area and pressure drops of inlet ports. The doors are provided with shock absorber assemblies to dissipate the larger door kinetic energies generated during large break incidents.

All high energy piping breaks postulated in accordance with draft standard ANSI N176 are reviewed individually as part of Duke's pipe rupture analysis to insure that pipe restraints, guard pipes, jet deflectors, etc.; are installed as necessary to prevent steam burnthrough of the ice condenser due to jet impingement upon the lower inlet doors.

As indicated in Section [3.5.4.1](#), Containment safety systems, operating deck and Containment shell within a potential path of a missile generated in the lower compartment can either withstand the effect of the missile or are protected by a shield wall able to contain the effects of such a postulated event. Design provisions require that potential missiles be oriented in such a manner so as to reduce the probability of striking critical targets.

##### Effect Of Steam Line Break On Lower Ice Condenser Inlet Doors

Postulated steam line breaks inside Containment cannot result in direct steam impingement of the lower ice condenser inlet doors due to the following design characteristics:

1. Piping arrangement with respect to the inlet doors was a major pipe routing consideration.
2. Guard piping of portions of the Main Steam System inside Containment is utilized to preclude:
  - a. steam burn-through of the ice condenser due to jet impingement on the lower inlet doors.
  - b. a LOCA caused by a postulated steam line break.
  - c. a subsequent pipe break of either the Main Steam or Feedwater System of unaffected steam generators.
  - d. local overpressurization caused by excessive flow rates.
3. Restraints and energy absorbers are utilized to restrict excessive movements from a postulated rupture and prevent direct steam impingement on the lower inlet doors.

#### Design Criteria

##### 1. Radiation Exposure

Maximum radiation at inlet door is 5 r/hr gamma during normal operations. No secondary radiation due to neutron exposure.

##### 2. Structural Requirements

Refer to Section [6.2.2.16](#).

##### 3. Loading Modes

- a. The door hinges and crane wall embedments, etc., must support the dead weight of the door assembly during all conditions of operation. Door hinges shall be designed and fabricated to preclude galling and self welding.
- b. Seismic Loads tend to open the door.
- c. During normal operations the outer surface of the door operates at a temperature approaching that of the lower compartment while the inner surface approaches that of the ice bed. During loss-of-coolant accidents, the outer surface is subjected to higher temperatures on a transient basis. Resultant thermal stresses are considered in the door design.
- d. During large break accidents, the doors are accelerated by pressure gradients then stopped by the Shock Absorber System. During small break accidents, doors open in proportion to the applied pressure with restoring force provided by springs. Upon removal of pressure, door closure results as a result of spring action.

##### 4. Design Criteria - Accident Conditions

- a. All doors open to allow venting of energy to the ice condenser for any leak rate which results in a divider deck differential pressure in excess of the ice condenser cold head.

The force required to open the doors of the ice condenser is sufficiently low such that the energy from an leakage of steam through the divider barrier can be readily absorbed by the Containment Spray System without exceeding Containment design pressure.

Deleted Per 2011 Update.

- b. The basic performance requirement for lower inlet doors for design basis accident conditions is to open rapidly and fully, to insure proper venting of released energy into the ice condenser. The opening rate of the inlet doors is important to insure minimizing the pressure buildup in the lower

compartment due to the rapid release of energy to that compartment. The rate of pressure rise and the magnitude of the peak pressure in any lower compartment region is related to the confinement of that compartment. The time period to reach peak lower compartment pressure due to the design basis accident is approximately 0.05 seconds.

- c. Doors are of simple mechanical design to minimize the possibility of malfunction.
- d. The inertia of the doors is low, consistent with producing a minimal effect on initial pressure.

5. Design Criteria - Normal Operation

- a. The doors restrict the leakage of air into and out of the ice condenser to the minimum practicable limit. The inlet door leakage has been confirmed by test to be within the 50 cfm total used for the ice condenser design.
- b. The doors restrict local heat input in the ice condenser to the minimum practicable limit. Heat leakage through the doors to the ice bed is a total of 20,000 Btu/hr or less (for 24 pairs of doors).
- c. The doors are instrumented to provide indication of their closed position. Under zero differential pressure conditions all doors remain 3/8 inch open.
- d. Provision made for adequate means of inspecting the doors during reactor shutdown.
- e. The doors are designed to withstand earthquake loadings without damage so as not to affect subsequent ice condenser operation for normal and accident conditions. These loads are derived from the seismic analysis of the Containment.

Deleted Per 2011 Update.

6. Interface Requirements

- a. Crane wall attachment of the door frame is via studs with a compressible seal. Attachment to the crane wall is critical for the safety function of the doors.
- b. Sufficient clearance is required for the doors to open into the ice condenser. Items to be considered in this interface are floor clearance, lower support structure clearance and floor drain operation and sufficient clearance (approximately six inches) to accommodate ice fallout in the event of a seismic disturbance occurring coincident with a loss-of-coolant accident. Original ice basket qualification testing (Topical Report WCAP-8110, Supplement 9-A), has shown freshly loaded ice is considered fused after five weeks. In the event of an earthquake (OBE or greater) which occurs within five weeks following the completion of ice basket replenishment, plant procedures require a visual inspection of applicable areas of the ice condenser within 24 hours to confirm that opening of the ice condenser lower inlet doors is not impeded by any ice fallout resulting from the seismic disturbance. This alternative method of compliance with the requirements of GDC 2 is credible based upon the reasonable assurance that the ice condenser doors will open following a seismic event during the 5 week period and the low probability of a seismic event occurring coincident with or subsequently followed by a Design Basis Accident.
- c. Door opening and stopping forces are transmitted to the crane wall and lower support structure, respectively.

Design Loads

Pressure loading during LOCA is provided by the Transient Mass Distribution (TMD) code from an analysis of a double-ended hot leg break in the corner formed by the refueling canal, with 100 percent entrainment of water in the flow. For conservatism, TMD results were increased by 40 percent in performing the design analysis for the lower inlet doors.

The lower inlet door design parameters and loads are presented in [Table 6-95](#).

### 6.2.2.8.2 System Design

Twenty-four pairs of inlet doors are located on the ice condenser side of ports in the crane wall at an elevation immediately above the ice condenser floor. General details of these doors are shown in [Figure 6-129](#) through [Figure 6-133](#). Each door panel is 92.5 in. high, 42 in. wide and 7.5 in. thick. Each pair is hinged vertically on a common frame.

Each door consists of a 0.5 in. thick Fiber Reinforced Polyester (FRP) plate stiffened by six steel ribs, bolted to the plate. The FRP plate is designed to take vertical bending moments resulting from pressures generated from a LOCA and from subsequent stopping forces on the door. The ribs are designed to take horizontal bending moments and reactions, as well as tensile loads resulting from the door angular velocity, and transmit them to the crane wall via the hinges and door frame.

Seven inches of urethane foam are bonded to the back of the FRP plate to provide thermal insulation. The front and back surfaces of the door are protected with 26 gauge stainless steel covers which provide a complete vapor barrier around the insulation. The urethane foam and stainless steel covers do not carry overall door moments and shearing forces.

Three hinge assemblies are provided for each door panel; each assembly is connected to two of the door ribs. Loads from each of the two ribs are transmitted to a single 1.572 inch diameter hinge shaft through brass bushings. These bushings have a spherical outer surface which prevents binding which might otherwise be caused by door rib and hinge bar flexure during accident loading conditions. The hinge shaft is supported by two self-aligning, spherical roller bearings in a cast steel housing. Vertical positioning of the door panel and shaft with respect to the bearing housing are provided by steel caps bolted to the ends of the shaft and brass spacer rings between the door ribs and bearings. Shims are provided between the shaft and caps to obtain final alignment. Each bearing housing is bolted to the door frame by four bolts, threaded into tapped holes in the housing. Again, shims are provided between the housings and door frame to maintain hinge alignment. Hinges are designed and fabricated to prevent galling and self welding.

The door frame is fabricated mainly from steel angle sections; 6 in. x 6 in. on the sides and 6 in. x 4 in. on the top and bottom. A 4 in. central I beam divides the frame into sections for each door. At each hinge bracket, extensions and gusset plates, fabricated from steel plate, are welded to the frame to carry loads to the crane wall.

The door panel is sealed to the frame by compliant bulb-type rubber seals which fit into channels welded to the door frame. During normal unit operations these seals are compressed by the cold air head of the ice bed acting on the door panels. As the seals operate at a much warmer temperature than the ice bed, frosting of the seal region is extremely unlikely.

Each door is provided with four return springs. One end of each spring is attached to the door panel and the other to a spring housing mounted on the door frame. The springs are adjusted during assembly such that, with no load on the doors, the doors are slightly open.

In order to dissipate the large kinetic energies resulting from pressures acting on the doors during a LOCA, each door is provided with a shock absorber assembly as shown in [Figure 6-133](#). The shock absorber element is a sheet metal air box 93 in. high, 46 in. wide, and 29.6 in. thick at its thickest section. The air box is attached to a back plate assembly which is bolted to the ice condenser lower support structure.

Two edges of the sheet metal box are fastened to the ends of back plate by clamping bars and bolts, making them air tight joints. The sheet metal is bent such that it has an impact face and a pre-folded side.

When the lower inlet doors open due to sudden pressure rise, they impact on the impact face of the air box. The impact face moves with the door. Because of a restraining straps within the box, the pre-folded side of the air box collapses inwards. The volume of the air trapped in the air box decreases as the impact

face moves towards the back plate, thereby increasing air pressure. Part of the kinetic energy of the door is used up in compressing air. To prevent excessive pressure rise, the air is allowed to escape through the clearance gap between the sheet metal and end plates. A portion of the energy of the doors is also used up in buckling of stiffeners.

#### Material

Door materials are consistent with the listing of acceptable materials as presented in Section 6.2.2.18. All exposed surfaces are made of stainless steel or coated with paint suitable for use inside the Containment. All insulation material is compatible with Containment chemistry requirements for normal and accident conditions.

#### **6.2.2.8.3 Design Evaluation**

The lower inlet doors are dynamically analyzed to determine the loads and structural integrity of the door for the design basis load conditions.

Using TMD results as input, the door dynamic analysis is performed using the “DØØR” Program. This computer program has been developed to predict door dynamic behavior under accident conditions. This program takes the door geometry and the pressures and calculates flow conditions in the door port. From the flow are derived the forces on the door due to static pressure, dynamic pressure and momentum. These forces, plus a door movement generated force, i.e., air friction, are used to find the moment on the door and from this are derived the hinge loads. Output from the program includes door opening angle, velocity and acceleration as functions of time as well as both radial and tangential hinge reactions.

#### Analysis Due to LOCA

The net load distributions on the door for both opening and stopping are determined by considering the applied pressures acting on the door and then solving the rigid body equations of motion such that the net forces and moments at the hinge point are zero. In the process, this produces expressions for the inertial forces in the door and the hinge reaction as functions of the applied pressure.

The expressions for net load distribution are integrated to determine door shear and moment as functions of distance from the hinge point. The resultant load, shear and moment distribution curves and the total hinge loads, calculated by the “DØØR” Program, provides the inputs for subsequent stress analysis.

Using this input, the door assembly is analyzed as a stiffened plate structure with vertical bending being taken by the FRP outer plate and horizontal bending plus radial tensile loads being resisted by the steel ribs. As inertial forces are directly accounted for in the analyses, no dynamic load factor was applied.

Hinge pin, hinge bracket, and frame stresses are analyzed under hinge reactions considering the effects of tension, shear bending, and torsion as appropriate. For these components, a dynamic load factor of 1.2 was calculated and applied.

Stresses in the door return springs are calculated considering dynamic effects as well as static ones. Welded and bolted connections are analyzed as part of the overall door, frame and hinge analysis.

All portions of the door and frame show factors of safety greater than one. The general acceptance criterion is that stresses be within the allowable limits of the AISC-69 Structural Code. This provides an additional margin of conservatism over the general ice condenser design criteria for D + DBA which permit stresses up to 1.33 times the AISC limits. For materials and components not covered by the Code, i.e., bearings, non-metallic materials, etc., conservative acceptance criteria are established on the basis of manufacturer's recommendations and/or engineering evaluations.

The effects of door closure were evaluated assuming the pressure is suddenly released from a fully opened door and the door allowed to shut under the effect of the door return springs. Stress levels in the door, gasket, and frame are found to be acceptable for this condition. In addition to the above analysis,

full scale simulated blowdown tests have been performed on prototype door and shock absorber assemblies. These tests confirm the adequacy of these components at test levels up to 140 percent of maximum loading conditions predicted by the TMD Code.

#### Analysis of Seismic Loading

Seismic analysis of the doors indicates that stresses are insignificant in comparison with those occurring during a LOCA. Under a SSE the doors could open several inches (actually, the crane wall will move away from the doors). At the termination of the earthquake, the doors immediately close and reseal under the effects of return spring tension and the ice bed cold air head. Thus, any loss of cold air during a 1/2 SSE or SSE is small and limited to a short period of time.

The dynamic testing of the air box shock absorber is discussed in Reference [54](#).

#### Surveillance Testing

To verify that the Lower Inlet Doors (LIDs) will function as intended, periodic testing is performed. Section 3.6.13 of Technical Specifications specifies tests and inspections performed to verify the functional capability of the LIDs. Bases for the surveillance tests and inspections are provided in the Bases for Section 3.6.13 of Technical Specifications.

Visual inspections of the LIDs are performed to verify that the doors are not impaired by ice, frost or debris. This provides assurance that the doors are free to open in the event of a Design Basis Accident (DBA). To provide assurance that the doors are not stuck in the closed position, a physical test is also performed on the closed LIDs to determine the torque required to pull the doors off of their seals.

In addition, a visual assessment of the door's motion through its swing arc (i.e., approximately 40° or to slight contact with the shock absorber) is performed to ensure the inlet door moves freely and return the door back toward the closed position, and also to monitor the performance of the hinges and spring closure mechanisms to ensure they are being properly maintained.

### **6.2.2.9 Lower Support Structure**

#### **6.2.2.9.1 Design Basis**

##### Function

The lower support structure is designed to support and hold down the ice baskets in the required array, to provide an adequate flow area into the ice bed for the air and steam mixture in the event of a Design Basis Accident, to direct and distribute the flow of air and steam through the ice bed, and to protect the Containment structure opposite the ice condenser inlet doors from direct jet impingement forces.

The last two functions are accomplished by turning vanes that are designed to turn the flow of the air and steam mixture up through the ice bed in event of a Design Basis Accident. For such an event, the vanes would serve to reduce the drag forces on the lower support structural members, reduce the impingement forces on the Containment across from the lower inlet doors and to distribute the flow more uniformly over the ice bed. In addition to the turning vanes, the lower support structure has a continuous impingement plate around the outer circumference of the lower support structure, designed to reduce the jet impingement forces on the Containment structure across from the lower inlet doors in the event of a Design Basis Accident.

##### Design Criteria and Codes

The loading combinations, stress limits and material specifications used in the design of the lower support structure are given in Sections [6.2.2.16](#) and [6.2.2.18](#).

##### Design Conditions

The normal operating temperature range is 10°F to 25°F. The normal operational temperature change, including maintenance operations is 10°F to 70°F. The maximum temperature during a Design Basis Accident is 250°F.

The loads used for the design of the lower support structure are given in [Table 6-96](#). The loads consist of dead weight (gravity), forces as a result of DBA, 1/2 SSE and SSE seismic loads and loads as a result of thermal changes.

The dead loads include the weight of the crane wall insulated duct panels, the weight of the intermediate deck doors and frames, the weight of the lattice frames and columns, and the weight of the turning vanes. The weight of the ice baskets filled with ice, the slotted jet impingement plate assemblies and the door shock absorber, also act on the lower support structure.

Forces and loadings that occur during LOCA were provided by the Transient Mass Distribution (TMD) Code from analysis of double-ended breaks in an end compartment near the refueling canal, with 100 percent entrainment of water in the flow. For conservatism, all forces and loads that are a result of TMD were increased by 40 percent in performing the detail design and analysis for the lower support structure. However, the loads as shown on [Table 6-96](#) are the basic forces and have not been increased by the 40 percent factor.

The lower support structure seismic design loads were developed using dynamic seismic analysis and the defined seismic response curves for the McGuire Nuclear Power Plant.

Thermal loading conditions, which result from two thermal excursions were specified for the lower support structure. One thermal excursion from 10°F to 70°F, is defined as a normal operating service load, and the other, defined as 70°F to 250°F, is the thermal excursion seen by the lower support structure following a LOCA.

The loading combinations considered in the design are given in Section [6.2.2.16](#).

### 6.2.2.9.2 System Design

The lower support structure is shown on [Figure 6-134](#) and [Figure 6-135](#). The lower support structure is contained in a 300 degree circular arc of the Containment. The three-pier lower support structure consists of 24 horizontal platform assemblies, 24 upper turning vane assemblies, 24 floor turning vane assemblies and 24 impingement plate assemblies. The aforementioned assemblies are supported by 25 radial portal frame assemblies with columns at radii of 45 feet 6 inches, 49 feet 11 3/4 inches, and 55 feet 8 1/2 inches. The 25 portal frame assemblies are spaced at approximately 12-1/2 degrees between adjacent portal frames. The total height of the structure is 9 feet 7 7/8 inches, measured from the top surface of the lower support structure to the pin. The design is such that the flow area at the ice basket interface for all 24 bays is at least 1088 square feet.

The horizontal platform consists of an inner and outer platform assembly for each bay. As assembled, the platform includes inner, middle and outer straight circumferential beams which span each portal frame. Nine radial beams formed by bar sections are welded to the inner, middle and outer circumferential beam. There is horizontal cross bracing between the inner and middle circumferential beams and the outer and middle circumferential beams.

The outer horizontal platform assembly consists of nine radial beams welded to the outer circumferential beam and welded to a channel which forms one half of the middle circumferential beam. The inner horizontal assembly is similar to the outer platform assembly. The channels of the inner and outer horizontal platform assemblies are field bolted to form a continuous middle circumferential beam.

For each bay, the platform inner and middle circumferential beams are connected to the portal frames with a shear connection, i.e., no moment is transmitted to the columns. The outer circumferential beam shear is connected to the portal column, but the connection is designed to transmit moment about a

vertical axis. Every alternate horizontal platform (per bay) is connected to the columns at one side by bolted connections, which are slotted along the axis of the circumferential beams to accommodate circumferential thermal expansion. The adjacent bay is not slotted in the circumferential direction and supplies the tangential shear resistance for the slotted bay.

There are nine radial beams in each portal bay and each radial beam supports nine ice basket columns. Provision is made for attaching, by bolting, each ice basket column to the radial beams.

The inner and outer circumferential beams of the platform assembly have the lattice frame column supports bolted to them. The insulated duct panels on the Containment wall interface the floor and the insulated duct panels on the crane wall are supported by the inner circumferential beams of the lower support structure. The inner, middle, and outer circumferential beams are straight beams.

Each radial portal frame is comprised of three columns. The primary radial shear resistance is provided by a 2 in. thick plate with attached welded channels forming the inner and middle columns thus forming a steel shear wall. The outer column (radius 55 feet 8 1/2 inches) is attached to the middle column assembly by a 2 in. thick plate. The 2 in. thick plate is pin-connected to the outer column by bars pinned at both ends and welded to the middle column. The column base plates are pin-connected to the ice condenser support floor. To accommodate thermal expansion, the middle pier column pin connections are designed to allow radial expansion, and every other outer column base plate pin connection is designed to allow circumferential expansion. The inner pier columns (near the crane wall) are designed to transmit all three force components. The base plate pin arrangement is shown on [Figure 6-134](#). The lower inlet door shock absorbers are mounted to the 2 in. thick portal frame plate.

Tangential or circumferential rigidity of the lower support structure is provided by a Cross Bracing System between the outer columns. The Cross Bracing System is provided in alternate bays, which coincide with the bays in which the circumferential platform beams are not slotted in their axial direction at the column attachment points.

To turn, direct and distribute the flow through the lower inlet doors during a LOCA, each portal bay has five turning vanes that span between the adjacent radial portal frames. The vanes are as indicated on [Figure 6-135](#). The vanes are slotted on one side in each bay to allow circumferential thermal growth.

In addition to the turning vanes, a beam gridwork spans between adjacent outer columns ([Figure 6-134](#)) and acts as a jet impingement shield for the fluid flow not turned by the vanes. The slotted plate assembly is provided in each bay of the lower support structure and is attached to the outer columns with a bolted connection. Similar to the turning vanes, the slotted plate assembly is bolted on one side with slotted holes to allow for circumferential thermal growth.

The material for the lower support structure is ASTM-A588 steel. Bolting materials are ASTM-A320 Grade L7 and nut material is ASTM-194 Grade 7. These materials conform to the Design Criteria (Section [6.2.2.18](#)). All welding meets the requirements of the American Welding Society Structural Welding Code-1972-AWS Publication D1.1-72.

The material used for the pins in the lower support structure is ASTM-A434 steel, AISI Grade 4340, Class BD. The material is normalized, then quenched and tempered. Chemical properties, physical test data and Charpy-V Notch test values at minus 20°F are required.

### 6.2.2.9.3 Design Evaluation

#### General

The lower support structure was analyzed using a finite element model. The ANSYS structural analysis program was used in the analysis. The seismic responses, in terms of equivalent acceleration and interface forces, in two horizontal directions (radial and tangential) and the vertical direction (z) were developed from a dynamic seismic response analysis performed for a combined lattice frame/ice basket/lower

support structure model. The seismic loads, as well as loads due to dead weight, thermal and the forces due to DBA, were applied to the lower support structure as static forces.

[Figure 6-136](#) and [Figure 6-137](#) show the finite element model used to represent the three pier lower support structure. The model is comprised of three dimensional beam elements having six degrees of freedom per node; flat triangular shell elements, each having six degrees of freedom per node such that both membrane and bending action of the plates is considered; and general six degrees-of-freedom lumped masses having a 6 x 6 diagonal mass matrix with three values,  $M_x$ ,  $M_y$ ,  $M_z$  and three moments of inertia,  $I_x$ ,  $I_y$ , and  $I_z$ . No horizontal ice mass is considered since this effect on the seismic response is accounted for in the results of the dynamic analysis of the combined lattice frames/ice baskets/lower support structure model. Rotary inertia terms are not used for the lumped masses.

### Structural Representation

#### 1. General

[Figure 6-136](#) shows an overall view of the one bay finite element model of the structural members. Each of the line members represents three dimensional beam elements. The loads generated from the model are used to design all the connecting joints, to the AISC-69 Code, Section 2.8. A separate finite element model is used to determine the maximum stresses in the beams. The impingement plate which spans the chord between the two outer columns is modeled using equivalent beam elements.

At beam connections where the beam centroidal axes do not intersect, either rigid links or specified offsets, which can be automatically accommodated for ANSYS beam elements, are used to preserve geometric compatibility between the elements. The connections of the horizontal platform to the portal frame are considered to be pin connections except at the outer column line where it is assumed that a moment around a vertical axis can be transmitted.

The impingement plate is attached to the outer columns assuming no moment can be transmitted from the plate to the columns. Similarly, the upper and floor turning vanes are idealized as beam elements which are pin connected to the portal assemblies. The remaining structural connections are considered to be moment connections.

#### 2. Mass Distribution

##### a. Structural Mass:

The structural mass of the lower support structure is represented automatically in the ANSYS program through the use of consistent mass matrices associated with each of the structural finite elements. Thus, only the material density is input to account for the structural mass.

##### b. Ice Mass:

The mass of the ice baskets is represented as lumped masses at node points along each radial beam. The mass is distributed based on the geometric placement of the ice baskets on the radial beams. Only mass in the vertical, Z direction, is assigned to the lumped masses representing the ice baskets, since the horizontal seismic effect of the ice basket mass is incorporated as loads on the radial beams. The horizontal seismic loads are determined from a dynamic analysis of a combined lattice frame/ice basket/lower support structure model.

#### 3. Displacement Boundary Conditions

Displacement boundary conditions are not specified for the tops of the columns nor for other nodes contained in the column radial plane. However, forces are applied to the columns which account for the adjacent bay loading.

To accommodate the thermally induced loads in the structural members, the base plates of the two middle columns are free to expand in a radial direction. Likewise, to accommodate the

circumferential thermal expansion, every other outer column base plate connection is free to expand circumferentially.

Referring to [Figure 6-138](#), the above boundary conditions imply that the outer column bases at odd numbered column lines are restrained against motion in the vertical, radial and circumferential directions, while the outer column bases at even numbered column lines are free to displace circumferentially.

The middle columns are free to move in the radial direction at all column lines and the inside columns (near the crane wall) are restrained for all three translations at all column lines. These boundary conditions minimize the thermally induced stresses and floor loads.

### Loading Conditions

#### 1. Seismic Loads

##### a. General

Analysis indicates that the frequency of the lower support structure is sufficiently high relative to the peaks of the response spectra and is one mode dominant in the vertical direction, so that a seismic modal response analysis is not required. Instead, an equivalent static analysis was performed for vertical accelerations based on the assumption of one mode dominance. For horizontal seismic loads, the largest forces in the radial and tangent directions as determined from a dynamic analysis of a combined ice basket/lattice frame/lower support structure model are applied as static concentrated forces to the lower support structure. The loads are summarized in [Table 6-96](#). A schematic of the applied loads is shown in [Figure 6-138](#).

##### b. Horizontal Radial Excitation

To account for the seismic loads transmitted from the ice baskets, lattice frames, and lattice columns, a dynamic analysis of the lattice frame and ice basket structures coupled to the lower support structure by means of flexibility coefficients which represent the lower support structure is performed. The loads transmitted to the lower support structure at the interface between the lower support structure and the ice baskets are applied as static concentrated forces. To account for the seismic loads transmitted from adjacent bays, radial forces are applied to the model at the required nodes.

##### c. Horizontal Tangential Excitation

The tangential loads transmitted from the lattice frames and ice baskets are determined in the same manner as the radial forces from the dynamic analysis performed.

The total tangential loads applied to the radial beams by the ice baskets are distributed in the same manner as the mass. Since the ice baskets are attached to the top surface of the radial beams, concentrated torques are applied at each of the nodes of the radial beams to account for the distance of approximately six inches from the top of the radial beam to the centroid of the cross section of the radial beam. The seismic loads from adjacent bays are considered by applying concentrated circumferential forces to the appropriate nodes.

#### 2. Blowdown Loads

##### a. General

The blowdown forces applied to the lower support structure are divided into four classifications:

- 1) Vertical Forces
- 2) Horizontal Radial Forces
- 3) Lower Inlet Door Impact Forces

#### 4) Horizontal Tangential Forces

The following sections discuss the loads for each of the classifications and the application of the loads to the finite element model of the three pier lower support structure.

#### b. Vertical Blowdown Loads

The vertical uplift loads acting on the lower support structure arise from the following phenomena:

- 1) Uplift on the ice baskets
- 2) Uplift on the radial beams
- 3) Uplift on the horizontal platform bracing
- 4) Uplift pressure across the intermediate deck
- 5) Uplift on lattice frames and lattice columns

#### c. Horizontal Radial Blowdown Forces

The horizontal blowdown forces acting on the structure arise from the following phenomena:

- 1) Momentum forces on the middle circumferential beam turning vane.
- 2) Momentum forces on the upper three turning vanes attached to the middle column.
- 3) Momentum forces on the floor turning vane attached to the middle column.
- 4) Momentum loading on the slotted impingement plate.
- 5) Forces on the outer circumferential beam.
- 6) Radial forces on the ice baskets.

The forces are transient in nature. However, only the basic static values with Dynamic Load Factors applied to account for the transient nature of the loading have been applied to the structural model, as concentrated forces on the appropriate nodes. To account for forces from adjacent bays, concentrated loads were applied to the portal frame connection points, as required.

### 3. Lower Inlet Door Impact Load

From results of studies performed to determine the force-time history transmitted through the shock absorber which arrests the inlet door motion, a total tangential load of 60 kips per door was applied to the lower support structure. The dynamic pulse characteristics of the force are accounted for by recommending a dynamic load factor of 2.0 for the pulse taken to represent the force versus time relationship for the shock absorber.

The door impact load is applied simultaneously in the same direction at both column lines 1 and 2 as a worst case. Thus, the loading considered is anti-symmetric tangential loading on the one bay model and creates an overturning moment about a radial axis through the lower support structure. In the design of the lower support structure, the bolt connections between the columns and the circumferential beams are designed to consider the possible loading from the door impact loads being applied in opposite tangential directions on the door arrester plates.

### 4. Horizontal Tangential Forces

The tangential force acting on the ice baskets due to cross flow in the ice condenser chamber was taken to be 23.8 lbs per linear foot. Similar to the radial forces, three feet of ice basket (one-half of the span between the top of the lower support structure and the attachment of the ice baskets to the

first lattice frame) was considered. The loads are applied to the finite element model as uniformly distributed loads on each of the beam elements comprising a radial beam.

### Dynamic Load Factors

#### 1. General

To account for the dynamic nature of the blowdown forces, dynamic load factors are applied to the DBA forces applied statically to the finite element representation of the lower support structure. The dynamic load factors (DLF) are as follows:

A. Vertical Uplift Forces	DLF - 0 or 1.8
B. Horizontal Radial Forces	DLF = 0 or 1.2
C. Lower Inlet Door Impact Forces	DLF = 0 or 2.0
D. Horizontal Tangential Forces	DLF = $\pm 1.2$

#### 2. Transient Analysis of Blowdown Loads

Following a LOCA, the inlet doors open admitting steam flow into the ice condenser chamber. The fluid flow through the lower support structure and upward through the ice bed cause time-dependent forces to be applied to the lower support structure. In general, there are four classifications of transient forces applied to the lower support structure: (a) vertical forces on the radial beams, ice baskets, lattice frames, lattice columns, and intermediate deck; (b) horizontal radial forces acting on the outer columns, the jet impingement plate, the outer circumferential beam, and turning vanes attached to the middle circumferential beam and middle column; (c) tangential forces, applied to the impact plates attached to the portal frames, resulting from arresting the motion of the inlet doors; and (d) tangential forces on the radial beams due to cross flow in the ice condenser compartment.

The dynamic load factors are determined by performing a transient response spectrum analysis for each force-time history, as described below.

#### 3. Single Degree of Freedom Representation

In general, the transient structural response of multi-degree of freedom system is given by the expression:

$$y_i(t) = \sum_{j=1}^N \Gamma_j \eta_j(t) \Psi_{ij}$$

where,

$y_i(t)$  is the structural response at any time (t).

$\Psi_{ij}$  is the jth mode shape of the structure.

$\Gamma_j$  is the participation factor of the jth mode shape for the transient load.

$\eta_j(t)$  is the generalized coordinate of the jth mode shape at any time (t).

The generalized coordinate  $\eta_j$  of the jth mode is given in terms of the forcing function  $f(t)$  by Duhamel's integral, or the convolution integral as:

$$\eta_j(t) = \omega \int_0^t f(\tau) \sin \omega(t - \tau) d\tau$$

Thus, the expression for the generalized coordinate for each mode,  $j$ , is the same as the amplification factor, or Dynamic Load Factor definition for a single degree of freedom system:

$$DLF(t) = \omega \int_0^t f(\tau) \sin \omega(t - \tau) d\tau$$

Assuming that  $\Gamma_j = 1$  for some  $j = k$  and  $\Gamma_j \sim 0$  for  $j \neq k$ , amounts to the assumption that only one mode dominates in the structural response to the transient. In this case, the structural response becomes:

$$y_i(t) = \eta_k(t) \Psi_{ik}$$

or,

$$y_i(t) \cong DLF(t) \Psi_{ik}$$

in which case the maximum structural response is given by:

$$y_{i\max} \cong DLF_{\max} \Psi_{ik}$$

Assuming that the dominant mode  $\Psi_{ik}$  can be approximated by the static deflection shape due to the loads applied to the structure, the maximum structural response can be approximated by:

$$y_{i\max} \cong DLF_{\max} y_{i\text{static}}$$

Thus, assuming that the response of the lower support structure to the transient blowdown forces may be represented by Equation 7, the dynamic effects of the transient may be investigated by evaluating the transient response spectra given by:

$$DLF_{\max}^{(\omega)} \text{ over } t = \max[\omega_0 \int_0^t f(\tau) \sin \omega(t - \tau) d\tau]$$

evaluated for  $\omega = \omega_n$  where  $\omega_n$  is the natural frequency estimate lower support structure.

A typical force transient for a hot leg break is shown in [Figure 6-139](#). The resulting dynamic load factor spectra hot leg break force transient is shown in [Figure 6-140](#).

#### 4. Discussion

The recommended dynamic load factors are the maximum values from the transient response spectra for zero damping and for a frequency greater than 10 Hz. When evaluating the Dynamic Load Factor to be used, the combined dynamic action of the lower support structure and the supporting floor must be considered. Preliminary estimates of the lowest frequency for the Coupled Floor-Structures System are in excess of 11 Hz.

As previously stated, transient response spectra used to determine the DLF are for zero damping, rather than, a damping of between 5 to 10 percent, which is more appropriate for the highly stressed, bolted lower support structure. Damping will reduce the dynamic response as indicated typically in [Figure 6-140](#) which shows the response for horizontal forces for 0, 5, 10 and 20 percent damping. Thus the DLF recommended are conservative from this standpoint.

In addition to the conservatism used to derive the DLF's used for design, additional conservatism has been incorporated into the design by specifying that the forces scaled by the DLF's be applied to the structure in the worst manner to determine the maximum member forces. Since the maximum DLF for each transient will not occur at the same time, combining the member forces derived for each transient in this manner is conservative. In particular, an RMS combination similar to that used in earthquake analysis could be justified because of the time separation of peak occurrence.

The recommended DLF's have been conservatively derived and applied in the design of the lower support structure. Therefore, the resultant member forces determined for the DBA, using the recommended DLF, result in a conservative prediction of the stresses induced in the structure.

### Design Load Case

It can be seen from the magnitude of forces shown in [Table 6-96](#) that the proportions of all members and structural elements of the lower support structure are sized by the load combinations which include DBA forces. The DBA forces are 2 to 5 times larger than other forces that are applied to the lower support structure. Therefore, only the load combinations which include DBA forces are presented, although six separate cases were analyzed.

For design of the lower support structure, the following design load condition was used:

$$DL + TN + EV + ER + ET + AV + AR + AT + LIDI$$

DL = Gravity

TN = Thermal 70°F to 250°F

EV = Safe Shutdown Earthquake Forces in the Vertical Direction

ER = Safe Shutdown Earthquake Forces in the Radial Direction

ET = Safe Shutdown Earthquake Forces in the Tangential Direction

AV = Vertical Forces Due to DBA

AR = Radial Horizontal Forces Due to DBA

AT = Tangential Horizontal Forces Due to DBA

LIDI = Lower Inlet Door Impact

Because of the oscillatory nature of the DBA forces, the above loading condition results in two maximum equivalent static design load cases which have different Dynamic Load Factors for DBA forces. The two load cases correspond to the maximum uplift condition on the lower support structure and a maximum down load on the lower support structure. For the maximum uplift case, the load equation including dynamic load factors (DLF) is:

$$DL + TN + EV(UP) + ER + ET + (1.8)(1.4) AV + (1.2)(1.4) AR + (1.2)(1.4) AT + 2 LIDI$$

The second load case, maximum down force is similar to the aforementioned load case, with the exception that the DLF for the vertical DBA is taken equal to zero and the vertical SSE forces (EV) are assumed to act downwards. The DBA forces used in the detailed analysis have been increased, as previously mentioned, by 40 percent for those listed in [Table 6-96](#).

### Results of Stress Analysis

#### 1. Members

The stress in the various structural members for all of the design load cases was found to be below the design criteria as specified in Section [6.2.2.16](#).

#### 2. Joints

The member forces at connections from the two load cases previously discussed that include DBA forces were used to proportion the connections. In the design of the connection for the load conditions including DBA, the recommendation of the AISC - 69 Code Section 2.8 were followed. In summary, the normal allowable AISC - 69 Code limits for bolted and welded connections were increased by 1.7 to determine an equivalent yield point stress condition. To be consistent with the conservative approach used in proportioning members, the allowable stresses were scaled by 1.7 and then multiplied by 0.9 to determine the joints stress limits used in the design.

### 6.2.2.10 Top Deck and Doors

The top deck, intermediate deck, Containment shell, crane wall and end walls form the boundaries of the ice condenser upper plenum. The upper plenum houses the air handling units and the distribution ducts to the wall panels and provides a working space for loading, weighing and maintaining the ice baskets.

#### 6.2.2.10.1 Design Basis

##### Function

An array of blanket panels forms a thermal and vapor barrier atop the upper plenum, allowing limited movement of air through vents during unit operation and free outflow of air during DBA. A grating deck supports the blanket panels and accommodates traffic by inspectors. The top deck structure supports the grating as well as the bridge crane and rail assembly and the air handling units.

##### Loading Modes

The following loading conditions are considered in the design of the top deck: deadweight, seismic loads, blowdown loads, and live loads. The top deck structure withstands these loads and remains within the allowable limits established in Section [6.2.2.16](#).

##### Design Considerations

1. The blanket panels are hinged on top of the crane wall. The major loads are applied directly into the crane wall.
2. A blanket panel must be flexible, i.e., be capable of deforming out of its plane in response to relatively low forces without disintegrating. Deformation of panels during DBA is permissible, but formation of missiles must be averted.
3. The deck forms an integral part of ice condenser performance during DBA. Structural loads are a function of air pressure and flow relationships, which in turn are affected by deck characteristics.
4. The top deck structures are subjected to loads from the air handling unit and bridge crane in addition to the deck design loads.

##### Material Consideration

1. Refer to Section [6.2.2.18](#) for steel structures.
2. Blanket material is fire resistant by its own composition or by means of a suitable cover sheet.
3. Blanket material is not a significant source of halides in gaseous form, either by gradual diffusion of inherent ingredients or by radiolysis of component materials following a DBA.
4. Blanket material is not a significant source of leachable halides during exposure to Containment spray following a DBA.

##### Thermal and Hydraulic Performance Requirements

1. Heat input to the plenum through the top deck assembly is limited to 13.5 Btu/hr-ft<sup>2</sup>.
2. Resistance to air flow during DBA is minimized, in terms of both inertia of panels and obstruction by grating. Panels may reclose or remain open following DBA. Vents open on low differential pressure for small flow rates.
3. A vapor barrier is established on the upper surface of the blanket panels.

##### Interface Requirements

1. In the process of opening, adjacent blanket panels interface with each other. This is acceptable in view of their flexibility.

2. Sealing strips are installed to connect panel vapor barrier to adjacent panels, to crane wall, to end walls and to Containment shell, without transmitting appreciable loads to the Containment shell.
3. The grating rests on, and is attached to, the cross beams between the top deck beams and transmits operating and drag loads to these structures. The structural members receive loads from bridge crane and air handling units as well as the deck itself.

#### Design Loads

Design loads used in the design of the top deck assembly are shown in [Table 6-97](#).

#### **6.2.2.10.2 System Design**

The design of the top deck is shown in [Figure 6-141](#) and [Figure 6-142](#).

The top deck doors consist of radially aligned flexible blanket panels resting on a grating deck and hinged on top of the crane wall.

A blanket pair covers one-half bay, extending from the radial centerline of a bay to the edge of the adjacent top deck beam. It consists of two blanket assemblies, one resting on the grating, the second one resting (mirror image) on the first one, with bands touching.

The parts of a blanket assembly and their respective functions are as follows:

1. Thermal insulation is provided by a flexible polyurethane foam blanket, 1 inch thick.
2. Approximately one-half of the centrifugal load is carried by bands of fully hardened stainless steel, 0.005 inch thick,
3. Stainless steel cover sheet (“skin”) or similar material serves as a vapor barrier (top surface), protects the blanket against wear and fire (top and bottom surfaces), and provides all of the lateral and about one-half of the centrifugal strength.
4. Parts 2 and 3 are bonded to the faces of the foam and extended along one edge to form a hinge.

The grating deck performs the structural functions of the top deck during non-accident conditions. It is supported from pairs of cross beams spanning the top deck beams, and its upper surface is flush with the top of the top deck beams. The bearing bars of the grating run parallel to the centerline of the particular bay. They are 2 inches high, 3/16 inch thick, and spaced on 2 3/8 inch centers. This design satisfies all requirements for open area and upward drag loads during DBA as well as for normal traffic loads. A clearance of no less than 3.5 inches is maintained between the grating and the containment.

The grating is fabricated from carbon steel, ASTM-A36, or A569 and provided with trim banding adjacent to top deck beams. Completed grating sections are galvanized for corrosion protection.

A hinge bar clamps one edge of each blanket assembly to the top surface of the crane wall. Anchor bolts transmit the hinge loads into the crane wall.

Static insulation pads are attached to the top of the radial beams.

Flexible seal membranes are attached between vapor barrier (top) surfaces of the blanket panels and against vent base, end walls, and static insulation.

A pressure equalization “curtain” suspended around the periphery of the top deck. The vent curtain minimizes diffusion of air under steady state conditions while permitting free movement of air in or out during momentary periods of pressure imbalance.

#### Fabrication

1. Grating sections are fabricated to specific shapes, complete with trim banding. The finished assemblies are cleaned and hot dip galvanized.

2. Structural members are cut and welded to suit.
3. Blanket assemblies are fabricated by an insulation contractor using specified bonding methods.
4. Hinge bars are machined from rectangular steel bars and painted or galvanized.

#### Installation

1. Radial and cross beams are installed.
2. The grating sections are placed and bolted down.
3. Static insulation pads and blankets are placed in position all around top deck.
4. Vent assemblies are installed.
5. Seals are installed.
6. Hinge bars are installed. Blankets are clamped. Static insulation is attached.

### **6.2.2.10.3 Design Evaluation**

#### Top Deck Blanket Doors

The top deck doors were dynamically analyzed to determine the loads and structural integrity of the door for the design basis load conditions.

Using TMD results as input, the door dynamic analysis was performed using a separate computer code named the "DØØR" Program. This computer program has been developed to predict door dynamic behavior under accident conditions. This program takes the door geometry and the pressures and calculates flow conditions in the door port. From the flow are derived the forces on the door due to static pressure, dynamic pressure and momentum. These forces, plus a door movement generated force, i.e., air friction, are used to find the moment on the door and from this are derived the hinge loads. Output from the program includes door opening angle, velocity and acceleration as functions of time as well as both radial and tangential hinge reactions.

#### Analysis Due to LOCA

The net load distributions on the door opening are determined by considering the applied pressures acting on the door and then solving the rigid body equations of motion such that the net forces and moments at the hinge point are zero. In the process, this produces expressions for the inertial forces in the door and the hinge bar reaction as functions of the applied pressure. The resultant horizontal and vertical hinge loads, calculated by the "DØØR" Program, provides the inputs for subsequent stress analysis.

Using this input, the blanket assembly is analyzed with horizontal and vertical forces being taken by direct stress in the skin and bands. As inertial forces are directly accounted for in the analysis, no dynamic load factor is applied.

The hinge bar and anchor bolt stresses are analyzed under hinge reactions considering the effects of the horizontal and vertical components of the tension band. For these components, no dynamic load factor is applied since the bars are very rigid themselves and are rigidly attached to the crane wall. Stresses in the blanket floor grating due to aerodynamic drag are also calculated. Loads used for stress calculations include 40 percent margin above computed TMD values. Certain aspects of the dynamic performance of a flexible door (e.g., tangential distortion, whipping, bowing) cannot be modeled with sufficient confidence.

A summary of the analysis performed and results are presented in [Table 6-98](#). All portions of the door show factors of safety equal to or greater than one. The general acceptance criterion was that stresses be within the allowable limits of the AISC-69 Structural Code. For materials and components not covered by the Code, i.e., spring temper stainless steel nonmetallic materials, floor grating, etc., conservative

acceptance criteria are established on the basis of manufacturer's recommendations or ASTM minimum tensile specifications.

#### Dynamic Test

A full scale test of a blanket pair (one-half bay) is performed for verification of analysis. Observed dynamic characteristics are found to correlate well with computed TMD values, and integrity of blankets is maintained within acceptable limits.

#### Top Deck Structure

The top deck structure is analyzed using the ANSYS finite element computer program, with three-dimensional beams representing the structural members, three-dimensional lumped masses representing the mass elements, and a stiffness matrix to represent the flexible connections in the system. Geometric compatibility is maintained using three-dimensional rigid elements.

Two bays considered representative of the system were isolated and modeled. Conservatively, four air handling units are assumed to be located in the two-bay region, two next to the crane wall and two next to the Containment wall.

Stresses are calculated for the various combinations of dead load, thermal, seismic and accident conditions. A modal analysis is performed to determine seismic amplification. Blowdown stresses are calculated using a computed dynamic load factor, and a 40 percent margin added to TMD loads. Maximum stresses produced in major members are all within the limits given in Section [6.2.2.16](#). The circumferential struts, AHU beams and crane rails have been analyzed and are structurally acceptable.

### **6.2.2.11 Intermediate Deck and Doors**

#### **6.2.2.11.1 Design Basis**

##### Function

The intermediate deck forms the ceiling of the ice bed region and the floor of the upper plenum. It serves as a thermal and vapor barrier, which allows limited air movement, through vents, between regions during normal plant operation and free out flow of air and steam following DBA.

##### Criteria

Refer to Section [6.2.2.16](#) for structural design criteria.

##### Loading Modes

The following loading conditions are considered in the design of the intermediate deck: deadweight, seismic loads, blowdown loads, and loads due to personnel traffic on deck. The intermediate deck structure withstands these loads and remain within the allowable limits established in Section [6.2.2.16](#).

#### 1. Design Criteria - Accident Conditions

- a. Resistance to air flow during DBA are minimized, in terms of both inertia of door panels and obstruction by the frames. Panels may reclose or remain open. Panels open on low pressure differential for small flow rates.
- b. At the end of their movement, pairs of doors collide. Distortion at the time is acceptable, provided doors do not become missiles.
- c. The doors are of simple mechanical design to minimize the possibility of malfunction.

#### 2. Design Criteria - Normal Conditions

- a. Heat conduction through the intermediate deck is limited to 0.6 Btu/°F-hr-Ft<sup>2</sup>.

- b. The design of the deck permits its use as a walking surface for maintenance of the air handling units and inspection of the ice bed.
  - c. The design of the deck provides a vapor barrier between the ice bed and upper plenum area.
  - d. The design of the upper deck provides convenient access to selected ice baskets for weighing and visual inspection.
3. Interface Requirements
- a. Sealing strips are installed to seal deck frames to wall panels as a continuation of the vapor barrier.
  - b. Hinge loads, drag loads, and live loads are transmitted from the deck through support beams to the lattice frame support columns.
  - c. Instrumentation cables from the Temperature Monitoring System penetrate the seal area of the deck.

#### Design Loads

Pressure loading during LOCA is provided by the Transient Mass Distribution (TMD) code from an analysis of a double-ended hot leg break in the corner formed by the refueling canal, with 100 percent entrainment of water in the flow. For conservatism, TMD results are increased by 40 percent in performing the design analysis.

The intermediate deck design parameters and loads are presented in [Table 6-99](#).

#### **6.2.2.11.2 System Design**

The intermediate deck is shown in [Figure 6-143](#). For ease of manufacture and installation, the deck is separated into 48 subsections. Each subsection covers an area extending over a length of three lattice frames and a width of approximately half the ice condenser annulus. Two types of subsections are used; the inner subsection have overall dimensions of 11 ft long by 5 ft 7 in. wide; and the outer subsection have dimensions of 12 ft by 4 ft 7 in. Except for dimensional differences, the designs of inner and outer subsections are identical.

Each subsection consists of four door panels mounted on a steel frame. The door panels are sandwich structures, consisting of 26 gauge galvanized steel sheets bonded to a 2.5 inch thick urethane foam core. Loads developed in the sandwich structures are transmitted to two panel hinge points by a 2.5 in. x 5 in. rectangular steel tube which forms a backbone for the panel. The panel is reinforced and sealed by a peripheral channel and two internal ribs, formed from 18 gauge steel sheet.

Plates, which are welded to the ends of the tubular backbone, are drilled to accommodate 1 in. diameter stainless steel hinge pins. These pins in turn are supported by welded steel support brackets which are bolted, through the door frame, to intermediate deck support beams. Thus, hinge loads are taken directly into the support beams and not into the frame itself.

The door frame is fabricated from steel angle and T-sections. A formed channel on the frame holds a compliant bulb-type rubber seal which is compressed by the door in its closed position. In addition to being clamped in place by the hinge support brackets as described above, additional bolts in the frame angles fasten the corners of the frame to the support beams and connect adjacent members of the inner and outer assemblies to each other.

The intermediate deck support beams are 8 in. wide flange steel members, which radially span the ice condenser annulus. They are bolted to the lattice frame support columns via welded plate bracket assemblies and compliant pads. The latter feature assures that beam end moments are not transmitted to the relatively flexible support columns.

Flexible membranes are installed between the intermediate deck frame and adjacent wall panels to provide a continuous vapor barrier.

Pressure equalization vents are installed at the Containment wall side of the intermediate deck. Vertical flaps minimize diffusion of air under steady state conditions while permitting free movement of air in or out during momentary periods of pressure imbalance.

### 6.2.2.11.3 Design Evaluation

The intermediate deck doors are dynamically analyzed to determine the loads and structural integrity of the door for the design basis load conditions.

Using TMD results as input, the door dynamic analysis is performed using a separate computer code named the “DØØR” Program. This computer program has been developed to predict door dynamic behavior under accident conditions. This program takes the door geometry and the pressures and calculates flow conditions in the door port. From the flow are derived the forces on the door due to static pressure, dynamic pressure and momentum. These forces, plus a door movement generated force, i.e., air friction, are used to find the moment on the door and from this are derived the hinge loads. Output from the program includes door opening angle, velocity and acceleration as functions of time as well as both radial and tangential hinge reactions.

#### Analysis Due to LOCA

The net load distributions on the door during opening are determined by considering the applied pressures acting on the door and then utilizing an analysis similar to that derived for the lower inlet door (Section [6.2.2.8](#)), to obtain shear, moment, and hinge reactions.

Using this input the door panel is analyzed as a sandwich panel; i.e., the outer steel skins are assumed to carry tensile and compressive membrane loads, while the urethane core carries transverse shear loads between the outer skins. The tubular backbone is analyzed as a beam with biaxial bending and torsion under the combined effects of panel shear loading, panel centrifugal loading and hinge reactions. Hinge pins and support brackets, including bolting, are analyzed by considering the effects of tension, shear, and bending as appropriate. No dynamic load factor is applied, as inertial forces are directly accounted for in the analysis.

The door frame and attachment bolting are analyzed under loadings created by the differential pressure acting on the frame members. The intermediate deck beams and attachments are analyzed under the effects of loads transmitted to them by the door hinges and frames. For these latter analyses, appropriate dynamic load factors are calculated and applied.

All results indicated positive margins of safety in comparison with the criteria contained in Section [6.2.2.16](#).

During a LOCA, stopping of the doors is accomplished by impacting adjacent door panels against each other. In the process, a significant portion of the door kinetic energy is absorbed through plastic deformation of the door panels. This is an acceptable mode of behavior as long as the doors do not break up and lose their insulation or otherwise generate missiles. During simulated blowdown tests on full-scale prototype doors at levels of up to 140 percent of maximum pressures predicted by TMD, the ability of the doors to withstand opening and stopping loads is confirmed. Only local deformation of the panels results and no missiles or insulation are released.

#### Seismic Analysis

A response spectra nodal analysis is performed on the intermediate deck structure to determine maximum seismic loadings during 1/2 SSE and SSE. Resultant loadings on the structure are found to be negligible

in comparison with LOCA loadings. Further, calculations indicates the doors will not open during either earthquake.

### 6.2.2.12 Air Distribution Ducts

#### 6.2.2.12.1 Design Basis

##### Function

The air distribution ducts distribute the cold air from all air handling units uniformly to the wall panels.

The loss of the air distribution function does not affect the safety of the unit as the ice bed is a passive component and can tolerate Refrigeration System failures.

##### Design Criteria

The air distribution ducts are permitted to deform during accident conditions but must not affect any safety related components located nearby.

##### 1. Normal Operation

Design temperature normal	10°F - 15°F
$\Delta P$ normal	2 inch WG

##### 2. Accident Conditions

Accident temperature maximum	190°F
(without $\Delta P$ )	

#### 6.2.2.12.2 System Design

The air distribution ducts are located in the upper plenum. The ducts are made of galvanized sheet steel. The design includes flexible connections separating each duct and each AHU. The flexible connections also serve as vibration breaks.

#### 6.2.2.12.3 Design Evaluation

The air distribution ducts are a part of the Refrigeration System and serve to distribute cold air to the wall panels thereby maintaining the readiness of the ice in the ice bed. The air distribution ducts are not required to function during an accident. The air distribution ducts are, therefore, non-safety related components. Refer to Section [6.2.2.6](#) for detailed discussions of the Refrigeration System performance during normal operating conditions and of its ability to tolerate refrigeration component failures.

During a LOCA the air distribution ducts are permitted to deform. Any deformation is outward toward the crane and liner wall insulation and therefore presents no problem to nearby safety related components.

### 6.2.2.13 Equipment Access Door

#### 6.2.2.13.1 Design Basis

##### Function

The equipment access door permits movement of crane, equipment and personnel into and out of the ice condenser plenum for ice loading and maintenance.

In closed position, the door constitutes a thermal and vapor barrier (normal unit operation) between ice condenser air and upper Containment atmosphere.

The basic functions of the equipment access door are non-safety related. It is important, however, to prevent failure of the door in any manner that may effect safety related components located nearby.

#### Design Criteria and Codes

The door is designed to comply with structural requirements of Section [6.2.2.16](#).

#### Design Conditions

##### 1. Normal Operation

Design temperature inside	15°F
Design temperature outside	100°F

##### 2. Accident Conditions

Maximum surface temperature	190°F
(without $\Delta P$ )	

#### **6.2.2.13.2 System Design**

An equipment access door is provided in each end wall thereby providing ample access to the upper plenum. The equipment access door includes: the insulated door panel, frame and hoist assembly, gasketing, and fasteners. The door frame slides from closed to open position within a fixed frame embedded in the concrete end wall. All exposed surfaces are protected against corrosion by appropriate coating.

Limit switches are provided to monitor movement of each door and to indicate position as a part of the Door Position Monitoring System.

#### **6.2.2.13.3 Design Evaluation**

The equipment access door is a non-safety related component. The door stresses during SSE + DBA loadings are below the allowable levels.

#### **6.2.2.14 Ice Technology, Ice Performance and Ice Chemistry**

##### **6.2.2.14.1 Design Basis**

The operational principle of the ice condenser is the condensation of steam by means of melting ice. Approximately three pounds of ice per pound of reactor coolant are required to absorb the coolant energy to prevent excessive Containment pressure and temperature buildup. The liquid resulting from the thawing process drains to the Containment sump where it is utilized during the recirculation phase of cooldown by the Emergency Core Cooling System. It is, therefore, necessary that the boron concentration of the recirculated primary coolant not be diminished through the action of the ice condenser. Hence, the ice condenser utilizes borated ice, which upon bulk melting delivers an aqueous solution containing approximately 2000 ppm boron to the Containment sump. The solution used in this case to produce the ice for the condenser is one containing approximately 2,000 ppm borax ( $\text{Na}_2\text{B}_4\text{O}_7 \cdot 10\text{H}_2\text{O}$ ).

The complete equilibrium freezing of this solution forms a eutectic composition with a melting point of  $-0.42^\circ\text{C}$  ( $31.2^\circ\text{F}$ ).

On a microscopic scale, the complete equilibrium freezing of a 2000 ppm aqueous solution of boron as sodium tetraborate, results in a solid consisting of crystals of pure ice (approximately 91 percent of the original water), surrounded by frozen eutectic. Microscopically this eutectic solid consists of individual crystals of pure ice and pure  $\text{Na}_2\text{B}_4\text{O}_7 \cdot 10\text{H}_2\text{O}$  (See Reference [50](#)).

#### 6.2.2.14.2 System Design

The ice for the ice condenser is produced in machines that yield ice in the form of a continuous ribbon, approximately 1/8 inch thick which is deposited in storage bins via gravity chutes.

The ice is kept at subcooled temperatures by chilled air flowing through the hollow walls and floor of the bin and over the exposed surface of the ice.

Ice is pushed out of the bin by a mechanized rake and carried to an ice chopper via two screw conveyor. The chopper reduces the size of the ice flakes to approximately 2 in. x 2 in. x 1/8 inch. The ice chopper discharges through a metering hopper into a pneumatic conveying valve.

The pneumatic conveying valve feeds ice at a measured rate into a stream of chilled compressed air, which carries the ice through temporarily erected piping to either one of the ice condenser units. The air/ice mixture is fed into a cyclone receiver atop of the ice baskets where the ice drops into the basket while the air is released into the Containment vessel. The air that is fed into the Containment vessel during this operation is removed by a vacuum receiver in order to maintain a stable Containment vessel pressure.

Deleted paragraph(s) per 2003 update.

The quantity and distribution of ice in the ice condenser must be verified to be maintained consistent with the design basis accident analyses. The operating characteristics of the ice condenser and methods for determining the quantity of ice mass in each ice basket have been considered in technical specifications which ensure the required quantity and distribution of the ice in the ice condenser. The basis for the methodologies used in establishing these technical specification requirements and acceptable methods for statistically verifying compliance with these requirements are described in Reference [60](#) and [61](#).

Deleted paragraphs per 2003 update.

#### 6.2.2.14.3 Design Evaluation

As the ice condenser is to be available to perform its engineered safety feature function for the life of the unit, ice storage characteristics are an important consideration. Two mechanisms influence the long term storage of the ice, the diffusion of sodium borate crystals through the ice crystals, and the sublimation of the ice.

##### Diffusion

For a discussion of the first mechanisms, it will be necessary to refer to the phase diagram presented in [Figure 6-145](#). When the temperature of an aqueous sodium tetraborate solution is continuously lowered, freezing begins with the formation of crystals of pure water surrounded by the salt solution. The temperature at which the first ice crystals form (assuming no supercooling) depends on the initial concentration of the solution. For example, a solution of  $\text{Na}_2\text{B}_4\text{O}_7 \cdot 10\text{H}_2\text{O}$  containing 2000 ppm boron begins to freeze at  $-0.41^\circ\text{C}$  ( $+31.27^\circ\text{F}$ ), under one atmosphere pressure (Point A in [Figure 6-145](#)). If the freezing process is allowed to continue reversibly, i.e., under conditions of the thermodynamic equilibrium, more ice crystallizes and the surrounding solution increases in concentration according to line AB in [Figure 6-145](#). Finally, when the system temperature is  $-0.42^\circ\text{C}$  ( $+31.24^\circ\text{F}$ ), the remaining liquid freezes to a solid with a boron concentration of 2220 ppm. The composition of this solid is known as the eutectic composition.

If the borated ice is made by the very slow freezing process just described, the pure water crystals first formed become the centers for further crystallization and therefore grow until the liquid reaches the eutectic composition. The total number of these relatively large pure ice crystals is determined by the number of nucleation sites available in the solution during the initial phase of the process. If the freezing rate is made extremely large, i.e., the process is carried out in an irreversible manner, the initial borate has crystallized. Such a path is represented by the line CD in [Figure 6-145](#). The solid obtained by this process is a uniform mixture of very small crystals of two kinds, ice and sodium tetraborate.

When a collection of various-sized crystals of a substance are maintained at constant temperature and pressure in contact with a solution saturated with respect to the substance, two processes tend to occur. The larger crystals tend to grow at the expense of the smaller ones, and the crystals or irregular form tend to become of regular form. Both of these phenomena are manifestations of systems tending toward thermodynamic equilibrium where the total free energy of the system (in this case the surface free energy) is at a minimum. The solution referred to above can also be a vapor and in the simplest case can be the pure saturated vapor of the crystalline substance. Note that kinetically the two processes are competitive and that both are subject to diffusional control. Therefore, diffusion of molecules, from one site to an adjacent one of the same crystal would be favored over migration to another larger crystal, in the case where rapid cooling of very dilute solutions causes many crystals to form that are small compared to the separation between them. Such is the case in practice with the ice condenser.

The driving force for diffusion between crystals of sodium borate through the pure ice matrix is a concentration gradient. If a large crystal is tending to grow, it causes depletion of sodium and borate ions in the immediately surrounding ice. If a small crystal tends to give up sodium and borate ions to feed the growth of the larger crystal then there is an increase in the concentrations of sodium borate surrounding the shrinking crystal. Since ice and sodium borate do not form as appreciable solid solution (note eutectic mixture of ice and sodium borate crystals), then the concentration of sodium borate around the shrinking crystal can not be large. For the sake of constructing an upper bound on diffusional effects in the borated ice, assume the maximum concentration to be approximately 10 percent of the eutectic solution concentration (i.e., 220 ppm).

Diffusion of sodium borate across a slab of pure ice can be estimated as follows:

Data for the diffusion of sodium borate in ice are not available, but the self-diffusion coefficients for deuterium, tritium and oxygen in ice have been reported by Franks (Reference [51](#)). At  $-11^{\circ}\text{C}$  ( $+12^{\circ}\text{F}$ ) the value for all species is approximately  $10^{-11}$   $\text{cm}^2/\text{sec}$ . Assuming that the coefficient for sodium and borate ions is of the same order of magnitude, the rate of diffusion of sodium borate through a 1/32 inch slab of pure ice is estimated to be approximately  $2 \times 10^{-13}$   $\text{g}/\text{cm}^2\text{-sec}$ . for an initial concentration of 220 ppm boron. If the concentration of boron in the ice phase on one face of the slab remained constant at 220 ppm while diffusion through the pure ice slab took place, it would take over 100 years for an amount of boron in a single piece of condenser ice to diffuse 1/32 inch, or halfway through the ice flake.

Since the quick frozen borated ice is of stable uniform composition, then upon bulk melting there should be formed a solution of borax of uniform concentration. If the entire borated ice-mass were to be uniformly warmed above  $-0.42^{\circ}\text{C}$  ( $+31.24^{\circ}\text{F}$ ) then melting would begin at the points of contact between water crystals and  $\text{Na}_2\text{B}_4\text{O}_7 \cdot 10\text{H}_2\text{O}$  crystals, and the ice-mass would lose structure. This is a phenomenon known as "rotting" and has been observed at times in sea-ice which has been subjected to slow (order of hours or days) temperature excursions to just above the melting point. If the melting process is rapid then the fact that the borated ice-mass is a mixture of crystals and not a homogeneous solid solution does not affect the performance of the ice condenser. Melting in the ice condenser occurs over a time span of the order of seconds, beginning at the contact between the steam and the ice-mass and progressing inwardly.

The above arguments are greatly simplified, but lead to conservative results. It can therefore be concluded from the above arguments that while some local changes undoubtedly occur in the quick-frozen borated ice, a maldistribution of the solute boron in the ice condenser, of such magnitude as to

affect the operation of the condenser as described in the first paragraph, is extremely remote. Furthermore, the microscopically heterogeneous composition of the borated ice-mass does not reflect itself in the ice condenser performance.

### Sublimation

The other mechanism that affects the long term storage of the ice is sublimation. Sublimation has several effects inside the ice condenser. The geometry of the ice mass changes where sublimation occurs, and the resulting vapor is deposited on a colder surface at another location inside the ice condenser.

In normal cold storage room application, the cooling coil is exposed to the air in the room, and moisture in the air freezes on the coil. If ice is stored in the room, all of the ice eventually migrates to the coil (which is defrosted periodically, draining the water outside the room) through a sublimation-mass transfer mechanism.

To avoid the mechanism, and maintain a constant mass of ice, the ice condenser is provided with double wall insulation. The annular gap between the insulated walls is provided with a heat sink in the form of a flow of cool, dry air that enters and leaves through the insulated panels.

However, a small amount of heat enters the system through the inlet doors, which are not double insulated, and also through the Double Layer Insulation System. The effect of this heat gain on the ice condenser has been examined analytically and experimentally through testing.

An analytical model of the sublimation process has been developed to provide an estimate of the expected sublimation rate as well as identify the significant parameters affecting the sublimation rate. The model develops a relationship identifying the fraction of total heat input which sublimates ice (the rest of the heat raises the temperature of the air, which transports the vapor to the cold surface where it freezes). The sublimation fraction depends on the difference in vapor pressure between warmest and coldest air temperatures within the ice condenser. The sublimation fraction decreases as the  $\Delta T$  decreases and also as the average ice condenser temperature decreases. For an average temperature of 15°F in the ice condenser compartment, the analytical model predicts a sublimation rate of about 1 percent of the ice mass sublimated per year per ton (12,000 Btu/hr) of heat gain to the ice storage compartment. The final heat gain calculations identified a heat gain into the ice storage compartment of 1 to 1.5 tons, most of which enters the compartment through the doors. For the purposes of this report, it is assumed that the reference heat gain for the unit is 1 ton, and therefore, the calculated reference sublimation rate would be 1 percent of the ice weight per year and provides a basis of comparison with test results.

Previous estimates of sublimation rates underestimated actual sublimation rates experienced during plant operation. To aid in predicting ice loss, a program has been implemented to track and trend sublimation rates for each ice basket. Weight data for each ice basket is maintained and average sublimation rates are calculated based on changes in ice basket weights. This information is used to predict future sublimation rates and determine the frequency and amount of ice to be added to the ice condenser.

Selected baskets are weighed periodically as indicated in Technical Specifications to verify that the actual sublimation rate has not excessively depleted the ice inventory.

### Chemical Additives

Sodium tetraborate is used as a chemical additive to the ice in the plant. The boron is needed for recirculation through the core and the tetraborate is used for iodine removal and Containment sump pH control. Boron or sodium tetraborate was also added to the ice used in the long-term storage tests. Chemical analyses were performed before and after certain storage tests to identify any change in boron concentration in the ice. These chemical tests showed that the boron concentration did not significantly change during long-term ice storage. Also, the tests proved that the boron is not transferred with the ice during the sublimation process. It remains as a residue at the original point of sublimation.

Samples of flake ice with sodium tetraborate additive were placed in the cold storage room at Waltz Mill on August 29, 1969, and chemical analyses were made of the ice used in the test samples. The samples were suitably isolated so that sublimation would be minimized or prevented. The tests were terminated on June 19, 1970, approximately 9-1/2 months after initiation, and chemical analyses were again made of several samples taken from different locations in the test section. These analyses indicated that there was essentially no change in the boron concentration from beginning to end of testing, confirming the diffusion theory discussed above.

### Testing

#### 1. General

The ice condenser design consists of 48 foot long columns of ice contained within perforated metal baskets.

In the long term storage of ice, the compression, shear, and creep characteristics are important considerations. Several years of testing at the Waltz Mill facility in these areas of interest has indicated that the ice bed maintains its geometry for its design life. While the construction of the ice baskets has changed since these tests were performed, the data is still applicable as the basic geometric configuration of the baskets has remained the same, and the same type of ice to be used in the unit was incorporated in the final series of tests. These Waltz Mill tests provide background on the testing that has been done to date, and presented in the next section is a discussion of planned tests that will provide additional information to further evaluate the mechanical performance of ice.

A number of mechanical loading test series have been performed at Waltz Mill to determine compaction, shear, or creep rates in the ice bed. The first series of tests initiated in 1966 used the tube ice (hollow cylinders, 1.50 inch o.d. by 0.5 inch i.d. by 2 inch length) produced in a commercial ice machine. The ice used in the above tests was made with no chemical additive, or with boron as a chemical additive to the ice. In some of these tests lead weights were placed on top of the ice samples to simulate the weight of various ice column heights.

The final series of tests initiated in 1969 used flake ice in the same type of baskets to determine the compaction and shear rates of the ice.

As the flake ice represents the basis for the configuration used in the ice condenser, only those test results applicable for this ice form are discussed.

#### 2. Compaction Tests

[Table 6-100](#) lists and describes the flake ice compaction tests performed, the duration of the tests, and the resulting compaction after one year of testing for these tests. The results of all of the tests showed that the greatest amount of compaction occurred during the first several months of testing. The amount of compaction varied with the equivalent height of the ice column, and depended on the type of ice employed. [Figure 6-146](#) presents the percent compaction versus time for flake ice test D'. Compaction of flake ice occurs much more rapidly than the other forms of ice due to the smaller and random size of the individual pieces of ice. After the initial year of compaction, the rate of compaction reduces significantly. The rate of compaction reduced almost to zero as the ice density approaches some value close to the density of solid ice. Inspection of the compaction tests indicated no evidence of ice being extruded out through the sides of the baskets. The use of water over the ice bed, as described in Section [6.2.2.14.2](#) is expected to reduce the compaction.

For these tests the compaction measured is for the bottom section of the ice bed only; the ice above this level (simulated by lead blocks) would be compacted to a lesser extent since it is loaded with less weight. Therefore, the test results were corrected for the effect of continuously reducing load from bottom to top of the ice column. When this correction was made, the results of the flake ice tests (D',E') suggest that the amount of compaction of an increment in the ice bed varies linearly with the

height of the ice bed above the increment. For flake ice the compaction rate must eventually change, as indicated by the dotted line, as the density of solid ice is approached. Application of this relationship would result in the estimated compaction relationship, shown in [Figure 6-147](#), for total compaction (in the first year) versus unsupported height of the ice bed. Since the baskets provide supports for the ice every 6 feet, the compaction of any 6 foot section of the ice bed would be limited to less than 4 inches. As mentioned, density enhancement via water addition is expected to reduce compaction.

### 3. Shear Tests

In these tests, ice was loaded into the basket on top of a temporary bottom support which was removed within one or two weeks after loading. The initial series of tests employed tube ice in expanded metal baskets with lead weights added to simulate additional weight of ice. All of the tests experienced an initial settlement within the first two months (after the temporary support was removed). Afterwards, the results show very low creep rates, which appear to be proportional to the weight added. Subsequently it was concluded that each increment of the ice in the basket would support its own weight by shear on the adjacent basket walls.

To evaluate this theory with flake ice, additional shear tests (G',H',I') were initiated. In these tests, unsupported ice bed heights of 1 foot, 3 feet and 5 feet were tested, with no lead weights added. In theory the shear rate should be the same, since each foot of ice column had the same shear support.

The results presented in [Table 6-100](#), confirmed that the shear rates for the three ice bed heights were of similar magnitude for a period of about 6 months. The rate measured was about 1 inch per year and was about 10 times the rate measured in the previous tests with tube ice in expanded metal baskets. From this information it is concluded that the shear capability of flake ice on the sides of the wire baskets is small. However, in the unit design the ice is supported by the horizontal supports at the bottom and center of each 12 foot section of ice column, so the stability of the ice bed does not depend on the shear forces existing between the ice and the baskets.

## 6.2.2.15 Ice Condenser Instrumentation

### 6.2.2.15.1 Design Basis

The ice condenser is a passive device requiring only the maintenance of the ice inventory in the ice bed. As such there are no actuation circuits, or equipment, which are required for the ice condenser to operate in the event of a LOCA. The instrumentation provided for the ice condenser serves only to monitor the ice bed status. Since the ice bed has a very large thermal capacity, postulated off normal conditions can be successfully tolerated for a week to two weeks. Therefore, the ice condenser instrumentation provides an early warning of any incipient ice condenser anomalies. In this way the operator can evaluate the anomaly and take the proper remedial action. Depending upon the anomaly, the operator typically may perform a local or system defrost, switch to a backup glycol circulation pump, start a backup chiller package, provide glycol makeup, isolate a glycol leak, or perform a safety and orderly shutdown. Since the ice condenser instrumentation can in no way actuate, nor prevent, a reactor trip or engineered safeguards action, there are no codes which apply to the design of the instrumentation systems. Any instrumentation failures or anomalies, however, are apparent in the Control Room where ice condenser temperature monitors, door position monitors, coolant liquid level monitors and valve position indications are displayed and alarmed. Ample time is available to investigate and alleviate or eliminate any off-normal condition without seriously degrading the ice inventory. The instrumentation is nevertheless designed for reliable operation which includes sufficient redundancy to insure that the operator can accurately monitor the ice condenser status. There are no special provisions for periodic testing of the instrumentation since normal testing and maintenance can be performed and is sufficient.

### 6.2.2.15.2 Design Description

Each equipment package (e.g., air handler, ice machine, chiller package) is provided with controls needed to regulate its normal operation. The ice condenser instrumentation serves to monitor the operation of the equipment packages and the ice bed status by providing to the operator the following Control Room information:

#### Ice Bed Temperature Monitoring

Forty-eight resistance thermometer bulbs are mounted on ice bed probes which are attached to lattice frames throughout the ice bed. The forty-eight resistance thermometer bulbs tie into one scanner unit suitably enclosed for mounting inside the Containment. A recorder is mounted in the Main Control Room, and an annunciator panel provides an alarm for a preset deviation from limits of ice bed equilibrium temperature.

#### Lower Inlet Door Position Indication

Limit switches are mounted on the lower inlet door frames with one limit switch per door panel, forty-eight door panels per Containment unit. The position and movement of the switches are such that the doors must be effectively sealed before the switches are actuated. A single annunciator window in the Control Room gives a common alarm signal when any door is open.

#### Equipment and Personnel Access Doors

Four limit switches are provided to monitor the position of the equipment access door and the personnel access door with two switches per door. These switches are fitted in a single series circuit providing Control Room indication of the position of the doors on a status light panel.

#### Expansion Tank Level

Annunciation and display are provided to warn the operator of coolant level excursions in the glycol expansion tank. Four indications are displayed corresponding to HI-HI, HI, LO, and LO-LO liquid levels. A loss of level would indicate a leak somewhere in the system or an erroneous valve operation. High level would result from malfunction or failure of the Refrigeration System. Two independent sensors are provided for each pair of level indications.

#### Isolation Valves

Two position lights (open and closed) located in the Control Room are provided for each of the glycol containment isolation valves. Individual annunciator windows in the Control Room alarm on isolation valve closure.

### 6.2.2.15.3 Design Evaluation

The ice condenser design provides adequate time for the proper evaluation of any adverse situations such that corrective action can be performed or an orderly unit shutdown can be scheduled and accomplished within the Technical Specification limits. The ice condenser monitoring instrumentation is tested and/or inspected on a periodic basis. Since the temperature recorders and alarms are active during the defrost periods, the performance of the monitoring instrumentation can be verified. Sufficient redundancy is provided in the ice condenser instrumentation to assure accurate monitoring of the ice condenser status.

## 6.2.2.16 Ice Condenser Structural Design

### 6.2.2.16.1 Applicable Codes, Standards, and Specifications

The ice condenser structural design analysis are based on the AISC specification (Reference [52](#)) where applicable. Material codes are discussed in Section [6.2.2.18](#).

**6.2.2.16.2 Loads and Loading Combinations**

1. Dead Load + 1/2 Safe Shutdown Earthquake loads (D + 1/2 SSE).<sup>4</sup>
2. Dead Load + Accident Induced loads (D + DBA).
3. Dead Load + Safe Shutdown Earthquake (D + SSE).
4. Dead Load + Safe Shutdown Earthquake + Accident induced loads (D + SSE + DBA).

The loads are defined as follows:

**Dead Load (D)**

Weight of structural steel and full ice bed at the maximum ice load specified.

**Live Load (L)**

Live load includes any erection and maintenance loads, and loads during the filling and weighing operation.

**Thermal Induced Load**

Includes those loads resulting from differential thermal expansion during operation plus any loads induced by the cooling of ice containment structure from an assumed ambient temperature at the time of installation.

**Accident Fluid Dynamic and Pressure Loads (DBA)**

Accident pressure load includes those loads induced by any pressure differential drag loads across the ice beds, and loads due to change in momentum.

**1/2 Safe Shutdown Earthquake (1/2 SSE)**

The 1/2 Safe Shutdown Earthquake loads are those induced loads determined from the response of the ice bed and supporting structure to the 1/2 SSE defined for the site.

**Safe Shutdown Earthquake (SSE)**

The Safe Shutdown Earthquake loads are those induced loads determined from the response of the ice bed and supporting structure to the SSE defined for the site.

**Note:** The Reactor Building Interior Concrete Structures and Steel Containment Vessel design calculations were revised/reviewed to address the effect of a 15% flow channel blockage in the ice bed and the TMD analysis due to changes in the steam flow path. It was concluded that all concerned compartments and sub-compartments will not be compromised nor invalidated by the assumed changes in the peak differential pressures.

**6.2.2.16.3 Design and Analytical Procedures**

Analysis, meeting the criteria presented in Section [6.2.2.16.4](#) is on the basis of elastic system and component analyses. Limited load analysis may be used as an alternate to the elastic analysis. Limit loads

---

<sup>4</sup> Also considered is D + L.

are defined using limit analysis by calculating the lower bound of the collapse load of the structure. Load factors are applied to the defined design basis loads and compared to the limit loads. The load factors determined for design basis load are used to provide margins of safety of the structure against collapse. A load factor of 1.43 is used when considering the mechanical loads due to dead weight and 1/2 SSE. A load factor of 1.3 is used for either D + SSE or D + DBA. A load factor of 1.18 is used for D + SSE + DBA. The material is assumed to behave in an elastic-perfectly-plastic manner. The minimum specified yield strength is used. Mechanical plus thermal induced load combination and fatigue is analyzed on an elastic basis and satisfy the limits of Section [6.2.2.16.4](#).

#### Experimental or Test Verification of Design

In lieu of analysis, experimental verification of design using actual or simulated load conditions may be used.

In testing, account is taken of size effect and dimensional tolerances (similitude relationships) which may exist between the actual component and the test models, to assure that the loads obtained from the test are a conservative representation of the load carrying capability of the actual component under postulate loading. The load factors associated with such verification are: 1.87 for D + 1/2 SSE, 1.43 for D + DBA or D + SSE, and 1.3 for D + SSE + DBA. If the load factor of 1.87 for D + SSE cannot be met, a load factor of 1.7 is used and these cases are presented to the AEC for their review.

A single test sample is permitted but in such cases test results are derated by 10 percent. Otherwise at least three samples are tested and the designs are based on the minimum load carrying capability.

#### **6.2.2.16.4 Structural Acceptance Criteria**

[Table 6-101](#) provides a summary of the allowable limits to be used in the design of the Ice Condenser Components.

For all cases the stress analysis is performed by considering the load combinations producing the largest possible stress values.

When limit analysis is performed on the ice condenser structure, or parts thereof, using the Alternate Analytical Criteria method, Section [6.2.2.16.3](#), justifications are provided to show that the results of the elastic systems analysis are valid.

#### Stress Criteria

The stress limits for elastic analysis are:

1. D + 1/2 SSE

Stress is limited to normal AISC, Part 1 Specification allowables (S). The members and their connections are designed to satisfy the requirements of Part 1, Sections 1.5, 1.6, 1.7, 1.8, 1.9, 1.10, 1.15, 1.16, 1.17, 1.20, 1.21 and 1.22 of the AISC Specification (stress increase in Sections 1.5 and 1.6 is disallowed for these loads). Where the requirements of Section 1.20 are not met, differential thermal expansion stresses are evaluated and the maximum range of the sum of mechanical and thermal induced stresses are limited to three times the appropriate allowable stresses provided in Sections 1.5 and 1.6 of AISC Specification.

2. D + SSE, D + DBA

Stresses are limited to normal AISC Specifications allowable given in Sections 1.5 and 1.6, increased by 33 percent (1.33 S). No evaluation of thermal induced stresses or fatigue is required. In a few areas, where the stresses exceed 1.33 S but are below 1.5 S, these cases are presented to the NRC for their review.

3. D + SSE + DBA

Stresses are limited to normal AISC Specification allowables given in Sections 1.5 and 1.6, increased by 65 percent (1.65 S). No evaluation of thermal induced stresses for fatigue is required.

For all cases, direct (membrane) mechanical stresses are not to exceed  $0.7 S_u$ , where  $S_u$  is the ultimate tensile strength of the material.

The summary of the ice condenser allowable limits is given in [Table 6-101](#).

## 6.2.2.17 Seismic Analysis

### 6.2.2.17.1 Seismic Analysis Methods

The lattice frames, ice baskets, wall panels on the crane wall side, and lower support of the ice condenser structure form a complex structural system. In order to perform a realistic seismic analysis of this structure, it is necessary to consider the gaps between the ice baskets and the lattice frame. It is not feasible to perform a response spectrum modal analysis when considering gaps because the structure is non-linear, thus requiring a dynamic time history analysis. Six different non-linear models are used to develop the design loads. Results are documented in Section [6.2.2.17.2](#).

#### Linear Seismic Analysis

Each level of lattice frames encompasses an approximate 300 degree horizontal arc and consists of 72 lattice frames. One level of eight levels of lattice frames is modeled so that the structural coupling between individual lattice frames could be evaluated.

The dynamic model used to determine the horizontal response characteristics of one level of lattice frames is shown in [Figure 6-148](#). It is a lumped-mass beam representation. Cantilever beam elements are used to represent the bending and shear stiffness of six interconnected lattice frames as shown in [Figure 6-149](#). For the model shown in [Figure 6-148](#), the mass associated with a set of six lattice frames is lumped at the end of the cantilever beam. The length used for the cantilever beam is representative of the distance to the center of gravity of the ice baskets associated with one lattice frame. The lumped masses are connected by tie members representing the combined coupling stiffness of six lattice frames.

The dynamic response characteristics of one level of lattice frames is obtained by computer program. It was determined that the structural coupling between individual lattice frames is negligible and that the fundamental response of the ice bed-lattice frame is essentially that of the individual lattice frames acting independently. Therefore, a lattice frame can be uncoupled from those in the same level for modeling purposes.

#### NonLinear Seismic Analysis

##### 1. Ice Condenser Seismic Load Study of the Effect of Gaps

A clearance or gap is required at the ice basket supports for installation and maintenance reasons. A schematic view of the ice basket gap is shown in [Figure 6-150](#). The design value for the gap is 1/4 inch radially or 1/2 inch on the diameter.

The effect of the gap during a seismic excitation is two-fold. First, impact loads are applied to the ice basket as it bounces within the clearance, which produce higher loads in the ice basket than would exist if there were no gap. Second, the repetitive impacting at the ice basket supports dissipate substantial amounts of energy. Stated differently, there is a higher damping within the structure than would exist if there were no gaps. This effect is illustrated with actual test results in [Figure 6-151](#).

##### 2. Description of Non-linear Models

Four non-linear models of lattice frames uncoupled from those in the same level were used to determine the effect of ice basket impact on the ice condenser loads. Two additional models with

adjacent lattice frame bays coupled by a phasing link were used to investigate lattice frame phasing. The six models are shown in [Figure 6-152](#) through [Figure 6-157](#) and are described as follows:

Shown in [Figure 6-152](#) is the two-mass model which is composed of two non-linear elements which represent the local impact stiffness existing between the lattice frame and ice basket, and a lattice frame spring between the lattice frame mass and the crane wall. The impacting mass represents twenty-seven ice baskets of six foot length.

Five other models were developed to assess the validity of the two mass model.

[Figure 6-153](#) shows the three mass tangential model whose purpose was to assess the effect of phasing between ice baskets in the tangential direction. There are three rows of ice baskets in the tangential direction across each lattice frame. Each lumped mass represents one ice basket. The lattice frame is modeled as truss members spanning each ice basket.

[Figure 6-154](#) shows the nine-mass radial model whose purpose is to assess phasing in the radial direction. Nine rows of ice baskets in the radial direction going out from the crane wall are represented in the model. Each basket has its associated impact elements on each side and the effective properties of the lattice frame spanning each ice basket.

[Figure 6-155](#) shows the 48 ft beam model which is a non-linear model containing twenty-seven ice baskets modeled as a continuous beam. The local effect of each lattice frame is represented by a pair of impact elements, one on each side of the ice basket. The lattice frame-wall panel stiffness is represented by a stiffness element. The lower support structure is modeled by a stiffness element at the bottom of the ice baskets. The purpose of this model is to investigate the influence of the full 48 ft ice basket column.

[Figure 6-156](#) shows the phasing mass model whose purpose is to evaluate the phasing link loads and crane wall reactions when adjacent bays of lattice frames respond out of phase with each other. The phasing mass model consists of a pair of two-mass models representing adjacent bays of the ice condenser. The lattice frames of the adjacent bays are coupled together with a phasing link. The design value for the phasing link gap is 1/16 inch between adjacent lattice frames.

[Figure 6-157](#) shows the non-linear 300 degrees phasing study model. The non-linear 300 degree phasing model is similar to the linear model shown in [Figure 6-152](#) except that it incorporates a phasing connector between lattice frames with a phasing gap of 1/16 inch between adjacent lattice frames. The purpose of this model was to demonstrate that the phasing link creates “phasing” within a specified tolerance and to demonstrate that it is still valid to model the basic ice condenser structure using only one lattice frame per level even though a phasing connector is used.

An extensive detailed seismic analytical study has been performed, presented in Reference [53](#), to substantiate the use of the two-mass model to develop seismic design loads for the Ice Condenser System. It was concluded from these studies that the seismic loads obtained from the two-mass model are in good agreement with the loads obtained from the more complex beam models. Therefore, the two mass model of [Figure 6-152](#) has been used to develop seismic design loads for the McGuire Ice Condenser System.

### Analytical Procedure and Typical Results

Using typical results obtained from the two-mass dynamic model, the procedure used in the non-linear analysis will now be discussed. First, the input acceleration-time histories are converted to displacement-time histories by double integration as shown in [Figure 6-158](#) through [Figure 6-164](#). The displacement-time histories were then input to the non-linear dynamic model. Results are shown in [Figure 6-160](#) through [Figure 6-161](#) for the case corresponding to a one-half inch gap between the ice basket and lattice frame, for tangential excitation.

[Figure 6-161](#) shows the output displacement-time history of the ice basket mass superimposed on the input displacement. It shows that the response generally follows the input displacements except for some amplification in the neighborhood of the peaks.

[Figure 6-162](#) shows the impact loads on the ice baskets for this particular case. Note the short duration time of the impact loads.

[Figure 6-163](#) shows the forces induced in the wall panels on the crane wall side as obtained from the two-mass dynamic model.

### 6.2.2.17.2 Seismic Load Development

#### Time History Dynamic Input

Crane wall seismic time histories for the 1/2 SSE and SSE, in the EW and NS directions, were developed using four synthesized earthquakes. These earthquakes are the same as used to develop the McGuire response spectra. These time histories were the actual earthquake records as modified by the building, i.e., as filtered through the building to the points of interest on the crane wall.

The structural response is computed for each earthquake and then averaged by computing the arithmetic mean of the four sets of response values. The seismic design loads are based on the seismic loads obtained by averaging.

#### Design Load Verification Analyses

As noted previously, it has been found that the seismic loads obtained from the two-mass dynamic model are in good agreement with the loads obtained from more complex beam models. For this reason the two-mass dynamic model has been used as the basic model to develop seismic design loads.

Non-linear seismic results obtained using the two-mass dynamic model are shown in [Table 6-102](#) and [Table 6-103](#) for the tangential and radial cases, respectively. The maximum wall panel loads and impact loads are shown for the 1/2 SSE and SSE north-south and east-west earthquakes with the respective design loads.

The lattice frame-wall panel stiffness used to obtain the analysis results shown were 24,000 lb/in for the tangential case and 50,000 lb/in for the radial case. These values are consistent with stiffness obtained from tests.

Analyses were made using the two-mass dynamic model and time histories associated with 825.22 ft elevation on the crane wall. The highest point on the crane wall is used since it has the highest seismic response characteristics. Therefore, the design loads developed are based on the most conservative seismic response.

[Table 6-104](#) gives a summary of the load results for the five non-linear dynamic models using seismic time histories for the east-west SSE. As stated previously, the highest loads are obtained using the two-mass model with the east-west time histories, as shown by [Table 6-102](#) and [Table 6-103](#). The loads obtained using the two-mass model agree satisfactorily with the loads obtained from the more complex models. These results verify the studies carried out in Reference [53](#) which showed good agreement between the models and resulted in the two-mass model being the basic model used to develop seismic design loads for the Ice Condenser System.

Seismic tangential and radial load distributions along the crane wall were found using the 48 ft beam model and are presented in [Figure 6-164](#) to [Figure 6-168](#). All loads are within the seismic load distribution design “envelope.” The time history used to analyze the 48 ft beam model is the Duke East-West Earthquake No. 4. This is the earthquake which produced the highest loads using the two-mass model.

Summarized below are applicable dynamic behavior characteristics which have been determined from previous studies reported in Reference [53](#).

The wall panel loads determined for a 1/2 inch nominal gap are found to be unaffected by large changes in impact damping. Loads are imperceptibly different using 10 percent and 50 percent impact damping.

The excitation function used in the non-linear analyses is crane wall displacement. In order to obtain the time-displacement record, the acceleration is integrated twice. The validity of double integration of accelerations to displacements has been checked by double differentiation of the displacement back to acceleration. It is found that the peak accelerations agree within about 5 percent.

As noted previously, the design loads are defined for a nominal 1/2 inch gap with all baskets in phase. In order to verify that misalignment of the baskets or partially stuck baskets do not produce higher seismic loads, verification analyses were performed. The conclusions reached are:

1. The effect of stuck baskets due to freeze-over is examined by varying the lattice frame and ice basket masses over a range of values. The non-linear dynamic model is used for these studies. It was found that the wall panel load decreases with increasing freeze-over.
2. The effect of vertical misalignment is examined with the 48 foot beam model. The load distributions defined by the cases with centered baskets are found to encompass the load distributions found for bent or cocked baskets.

The effect of sublimation as well as ice melt during and after DBA on the seismic loads, has been evaluated. These studies show that the seismic loads are smaller than those determined without sublimation or ice melt. This is due to the reduced ice mass, and an increased energy loss in the fracturing of the ice. Thus, the case of SSE during and after a DBA is not a limiting condition. It should be further noted that after a DBA the ice in the lower portion of the ice condenser has been used and no longer exists. Thus, the seismic loads in the lower portion of the ice condenser are significantly reduced.

A study was performed to investigate the amount which a lattice frame may be out of phase with an adjacent frame in the same level using the 300 degree phasing model. It is found that if no phasing connections are used, and all lattice frames in one level have similar mass-stiffness properties, then the amount that adjacent lattice frames are out of phase is insignificant, i.e., less than 1/32 inch. No impacts occur through the phasing links unless they are adjusted to a tolerance below 1/32 inch. If local out-of-phase occurs between two adjacent lattice frames due to their having different mass-stiffness relationships, the phasing links between the lattice frames force the load distribution around the crane wall to be similar to the in-phase load distribution. The fundamental response of the ice bed-lattice frame is essentially still that of an individual lattice frame acting independently.

The above studies lend substantial support to the conclusion that the basis for seismic design load calculations is in fact correct. The complexity of the non-linear analysis is such that it is quite important to be able to relate the results to physically intuitive behavior. The results from these verification analyses are relatable.

### Seismic Design Loads

Seismic design loads have been developed for the lattice frames, ice baskets, and the wall panels. They are shown in [Table 6-102](#) and [Table 6-103](#). The seismic design load distributions developed using the 48 ft beam model are shown in [Figure 6-164](#) to [Figure 6-167](#).

The non-linear analyses performed to develop seismic design loads uses 2 percent structural damping and 10 percent impact damping, and nominal gap size of 1/2 inch on the diameter between the baskets and the lattice frames. Note that a nominal gap size of 1/16 inch exists in the link between adjacent lattice frames.

[Table 6-105](#) gives a summary of parameters used in the seismic analyses. These parameters are based on analyses and tests of the Ice Condenser System.

### 6.2.2.17.3 Vertical Seismic Response

The combined floor and lower support structure are modeled in the vertical direction. The full weight of the baskets and ice were considered. It was found that the fundamental frequency, the dominant mode, of the combined structure in the vertical direction is above 14.7 Hz. There is no amplification of the crane wall in the vertical direction at the elevation of the lower support structure. Therefore, the vertical response spectra have the shape of the ground response spectra and are normalized to two-thirds of the seismic ground acceleration. The seismic response of the lower support-ice basket-supporting Floor Structural System is based on the one dominant mode. A participation factor of 1.5 was applied to this mode.

### 6.2.2.18 Materials

#### 6.2.2.18.1 Design Criteria

Structural steels for ice condenser components are selected from the various steels listed in the AISC Specification or Code (Reference [52](#)). When materials such as steel sheets, stainless steel or non-ferrous metals are required and are not obtainable in the AISC Code, these materials are chosen from ASTM specifications. Proprietary materials such as insulating materials, gaskets and adhesives are listed with the manufacturer's name on the component drawings.

Material certifications for chemical analysis and tensile properties will be required with testing procedure and acceptance standards meeting the AISC or ASTM requirements.

Because the concept of non-ductile fracture of ferritic steel is not a part of the AISC Code and Westinghouse recognizes its importance in certain ice condenser components where heavy plates and structurals are used such as the Lower Support Structure, Charpy V-notch (CVN) energy absorption requirements are stipulated as shown in [Table 6-106](#).

These criteria apply to the design of the following ice condenser components:

1. Ice basket and coupling
2. Lattice frame and columns including attachments and bolts
3. Structural steel supporting structures comprising the lower support structure, door frames and bolts
4. Wall panels and cooling duct support studs attached to the crane wall and end walls.
5. The supports of auxiliary components which are located within the ice condenser cavity but which have no safety function.

The various candidate materials, i.e., steel sheets, structural shapes, plates and bolting used in the Ice Condenser System are selected on the following bases:

1. Provide satisfactory service performance under design loading and environment and pressure or construction performance.
2. Assure adequate fracture toughness characteristics at ice condenser design conditions.
3. Be readily fabricated, welded, and erected.
4. Be readily coated for corrosion resistance, when required.

The candidate materials are of high quality and shall be made by steelmaking practices to be specified by Westinghouse. Principal candidate materials meeting the above bases are listed below. Other materials for specific applications are selected on a case by case basis.

### 6.2.2.18.2 Environmental Effects

The atmosphere in the ice bed environment is at 10°F - 15°F and the absolute humidity is very low. Therefore, corrosion of uncoated carbon steel is negligible.

To ensure that corrosion is minimized while the components of the ice condenser are in storage at the site or in operation in the Containment, components shall be galvanized, painted, or placed in a protective container. Galvanizing shall be in accordance with ASTM, A123, or A386.

Materials such as stainless steels with low corrosion rates shall be used without protective coatings.

Corrosion has been considered in the detailed design of the ice condenser components, and it has been determined that the performance characteristics of the ice condenser materials of construction are not impaired by long term exposure to the ice condenser environment.

Since metal corrosion rates are directly proportional to temperature and humidity, corrosion of ice condenser components at operating temperatures has been considered to be almost non-existent. Data available in the open literature do not reflect the exact temperature range and chemistry conditions that are expected to exist in the ice condenser, but do indicate that corrosion rates decreased with decreasing temperatures for the materials and conditions being considered. Although the data in the literature indicated that corrosion of components is not expected, several preventive measures in the construction of the Ice Condenser System will be used. To inhibit corrosion, the ice baskets will be galvanized. Tests have shown that galvanized material would not be expected to fail due to corrosion during a 40 year exposure to a 5°F - 15°F ice condenser refrigerated air environment. Other structural members will either be galvanized or protected by corrosion resistant paints that meet the requirements of ANSI 101.2-1972 (Protective Coatings (Paints) for Light Water Nuclear Reactor Containment Facilities) as a minimum, or will be constructed of stainless steel. Heavy plate and structural fabrications may be installed in the blasted and/or bare condition.

With due consideration of the non-corrosive environment, and judicious selection of component materials based upon sound engineering judgment, the structural integrity of the ice condenser components is not jeopardized, and the design criteria for the plant are met.

### 6.2.2.18.3 Compliance with 10CFR 50, Appendix B

The following sections of this report address themselves to demonstrating compliance with 10CFR 50, Appendix B. The Design Process Control Policy defines the criteria that must be considered when establishing design process control procedures. The design process procedures represent how Westinghouse controls its design processes relative to 10CFR 50, Appendix B requirements. The subject procedures are supplementary to the flow diagram and cross-reference is obtained through the use of activity numbers.

The products and scope of responsibility at Westinghouse are defined by the shop order description. From this base, the shop order flow diagrams were developed for the purpose of sub-dividing the job into its component activities and thereby creating generic categories of activities that require similar control systems. These categories are:

1. Interface Control
  - a. Interfaces are controlled by specifically identifying the relationship on the flow diagram and also by quantifying the information transmitted across the interface. There must be documentary evidence in the file of the vehicle used to cross the interface.
  - b. Document Control - a procedure employing a file log book is carefully maintained and provides control of document issue.
2. Analysis (includes review and comment, approval responsibilities)

These activities involved in providing or commenting on design information are controlled according to methods outlined in design process procedures. The nature of the product and its relative technical importance determine the level of controls applied.

### 3. Verification

These activities fulfill the requirement that design information must be validated by the originator prior to communication to a user. Techniques used vary due to the diverse nature of the products involved.

There is a design process control procedure for each shop order which consists of at least, a flow diagram, a shop order description, and Design Process Procedures.

The Design Process Procedures are related to the flow chart through the use of the activity numbers and the specific control methods.

Quality Assurance material; when required parts or welded fabrications will be inspected by visual, magnetic-particle (MT), liquid penetrant (PT) or ultrasonic (UT) methods according to ASTM Procedures, AWS D1.1., or Westinghouse Process Specifications. The method and extent of inspection will be designated on the component drawings.

## **6.2.2.18.4 Materials Specifications**

### Sheets

Carbon steel sheets are commercial quality (CQ), drawing quality (DQ), or drawing quality-special kilned (DQ-SK). The selection of the quality depends upon the part being formed. When higher strength, structural quality sheets are required, ASTM specification A607 is used. AISI Type 409 modified stainless steel is a potential alternate sheet material for the ice baskets.

The ice baskets will be made from perforated sheet material. The wall duct panels will be made from sheet material and the cradle supports from structural sections and plates.

### Structural Sections, Plates, and Bar Flats

Structural sections, plates, and bar flats are generally High-Strength Low-Alloy steels selected for suitable strength, toughness, formability and weldability.

The high strength low alloy steels are A441, A588, A572 or A633. These steels are readily oxygen cut and possess good weldability.

### Bolting

High strength alloy steel Type A320 L7 bolting for low temperature service is used for the lower support structure. Stocked bolting made from A325, A449 and ASTM A354 Grade BD (SAE J429 Grade 8) materials will be used for other parts. The above bolts must meet CVN 20 ft-lb at -20°F, for sizes greater than 1 inch in diameter.

### Non-metallic Materials

Non-metallic materials such as gaskets, insulation, adhesives and spacers are selected for specific uses. Freedom from detrimental radiation effects is required.

### Welding

All structural welding shall be in accordance with the AWS Structural Code for Welding, D1.1 (ASW Code). The AWS Code is an overall welding system for the design of welded connections, technique, workmanship, qualification and inspection for buildings, bridges, and tubular structures.

The quality of welds for the Ice Condenser System are based on paragraph 9.25 of the AWS Code.

Resistance welding is in accordance with AWS, Recommended Practices for Resistance Welding, C1.1.

Magnetic particle examination is performed on welds in each critical member of the lower support structure as indicated in design specifications and on drawings. Magnetic particle or liquid penetrant examinations, where applicable, are performed on critical members of the balance of the ice condenser structure as indicated in design specifications and design drawings. The nondestructive examination methods and acceptance standards are given in Section 6 and paragraph 9.25, Quality of Welds, of the AWS Code.

#### **6.2.2.19 Tests and Inspections**

The test and inspections are given in Section 3.6 Surveillance Requirements, of the Technical Specifications.

### **6.2.3 Annulus Ventilation System**

**Note:**

This section of the FSAR contains information on the design bases and design criteria of this system/structure. Additional information that may assist the reader in understanding the system is contained in the design basis document for this system/structure.

This section discusses the Annulus Ventilation System which serves the annular space between the Containment and Reactor Building. The Containment Ventilation System which serves the Containment interior is discussed in Section [9.4.5](#).

#### **6.2.3.1 Design Bases**

The Annulus Ventilation System is designed to accomplish the following:

1. Produce and maintain a negative pressure in the annulus following a LOCA.
2. Minimize the release of radioisotopes following a LOCA by recirculating a large volume of annulus air relative to the volume discharge for pressure maintenance.
3. Provide long-term fission product removal capability by decay and filtration.

#### **6.2.3.2 System Design**

##### Description

There are independent Annulus Ventilation Systems as shown on [Figure 6-169](#) for each unit. Each system has redundant trains consisting of an annulus ventilation fan, a filter package, associate piping, valves and controls as necessary to accomplish the design bases. Each filter package contains a moisture eliminator, electrical pre-heater, high temperature pre-filter bank, HEPA filter bank, electrical carbon bed pre-heater, deep bed carbon filter, and second HEPA filter bank. The HEPA filters are the bolted frame design with compression gasket type. The carbon bed filter is the deep bed type which is manually unloaded and reloaded in the field with bulk carbon. The response of the Annulus Ventilation System following a LOCA and the expected iodine removal efficiencies based on the composite filter efficiency are described

in the radiological accident dose analysis. Elevations of the exhaust and supply headers within the annulus are shown on [Figure 6-170](#) and [Figure 6-171](#).

#### Operation

The system functions to discharge sufficient air from the annulus to effect a negative pressure with respect to the containment and the atmosphere in approximately 120 seconds following a LOCA. Subsequent to attaining a negative pressure, additional air will be discharged as necessary to maintain the pressure at a maximum of -0.5 inches water gage. In order to mix the inleakage in as large a volume as possible, a large flow of air is displaced from the upper level of the annulus, passed through the filter, and returned to the annulus at a low level. The suction is accomplished using a ring distribution header. The return is a single point for Train A and a four point for Train B.

The design basis operation sequence is as follows:

1. Annulus Ventilation System activated by Containment high-high signal (3 psig).
2. Annulus ventilation fans are aligned to exhaust at 8000 CFM until annulus pressure is -3.5 inches of water gage. (This size fan accomplishes this task in approximately 180 seconds. A negative pressure is accomplished in approximately 120 seconds. These results assume an initial 34 second delay and partial flow for 34 to 39 seconds with full flow after 39 seconds. Pressures in the annulus assume an initial instantaneous enlargement of the Containment shell due to internal pressure and temperature.)
3. From the time the annulus pressure reaches its initial -3.5 inches water gage value to the end of the accident, the annulus ventilation fan discharges as necessary to maintain the annulus pressure within the bounds of -0.5 and -3.5 inches water gage. [Table 6-109](#) contains time, flow rate and quantity of discharge for the first 8 days after an accident. Thereafter the system is assumed to be in equilibrium and exhausts as necessary to account for inleakage into the annulus. There is expected to be no fouling of the filter due to the relatively short operating time. The computer code conservatively assumes a fouling factor which decreases the fan flow rate to 6800 CFM at 900 seconds.

#### Computer Code

The preceding results were obtained using the computer code ANVENT 2 which was developed by Duke Power Company to analyze the thermal effects of a loss-of-coolant accident (LOCA) in a Westinghouse "ice condenser" Containment.

ANVENT 2 is capable of evaluating the following factors:

1. Steady state (pre-LOCA) radial temperature distributions corresponding to fixed outside Reactor Building and inside Containment temperatures.
2. Radial temperature distributions in the steel Containment and concrete Reactor Building during post-LOCA transient.
3. Temperature and pressure in the annulus between the Containment and Reactor Building during the post-LOCA transient.
4. Capability of the annulus ventilation fans to quickly attain and maintain a vacuum in the annulus after a LOCA.

#### Components

All major components are located in the Auxiliary Building.

#### Annulus Ventilation Fans

Two full capacity annulus ventilation fans are provided for each unit. The fans are supplied with both normal and emergency power. Fan "A" of each unit is supplied emergency power from emergency diesel

generator “A” of that unit. Fan “B” of each unit is supplied emergency power from emergency diesel generator “B” of that unit.

#### Moisture Eliminator

The moisture eliminator consists of a mechanical demister and a heater which are designed to limit the relative humidity entering the filter train to below 70 percent assuming intake air at 100 percent RH.

#### Filter

Each carbon filter is sized to accommodate the fission products released into the annulus following any of the postulated accidents. Indications of filter train flow rate, pressure drop, and excessive carbon filter temperature are provided to detect excessive filter loading and temperature. The two fans and corresponding filter trains are completely separate and are 100% capacity.

Filter train design comparison to Regulatory Guide 1.52 is presented in [Table 6-110](#).

### 6.2.3.3 Safety Evaluation

A complete and independent Annulus Ventilation System is provided for each unit. System equipment is compatible with ANS Safety Class 3, where applicable, as delineated in [Table 3-4](#).

A failure analysis of the Annulus Ventilation System is presented in [Table 6-108](#). Occurrence of a filter failure is not considered credible during initial operation of the filter train during the first day following an accident as filter plugging and radioiodine deposition are cumulative and a function of operating time.

Through line leakage for process lines, hatches, and the fuel transfer tube is eliminated due to the design features of the Containment Isolation System as discussed in Section [6.2.4](#). The Containment Isolation System provides for double isolation by redundant valves or by combination of valve and closed system. The fact that penetration leakage and hatch seal leakage is into the annulus can be seen in Section [3.8.2.1](#) and [Figure 3-67](#) for the equipment and personnel hatches and [Figure 3-68](#) for mechanical and electrical penetrations. The Containment Purge System is the most critical isolation consideration. Normally both isolation valves in each inlet and discharge line are closed (the lower compartment purge is locked closed) so that only the inside valve sees the accident pressure differential. Notwithstanding the preceding comments, bypass leakage can occur assuming certain additional failures. [Table 6-112](#) classifies isolation valves into two categories “thru line leak class 1” and “thru line leak class 2”. Technical Specifications limit the total leakage acceptance criteria from those valves identified in [Table 6-112](#) as “thru line leakage class 2.”

The two secondary containment personnel access doors into the annulus area must be closed during operation of the Annulus Ventilation System. Should a LOCA occur, causing the Annulus Ventilation System to actuate, the proper operation of the system is insured as the personnel access doors are locked closed prior to exceeding 200°F Reactor Coolant System temperature. Verification that the doors are locked closed is accomplished by a sign off step in the normal startup operating procedure. The doors are under strict administrative control.

Additionally, modifications have been made to the containment personnel access hatches and to the main steam and feedwater piping penetrations in order to remove potential bypass leak paths. In the case of the personnel hatches, an enclosure has been added around the outside of the hatch such that any leakage past the door seals is directed back to the annulus. Similarly, for the main steam and feedwater penetrations, the test connections on the outer bellows of each penetration has been routed back to the annulus such that any leakage past the inner bellows is into the annulus. Passage through the access doors in the enclosures around the personnel hatches is controlled since these doors are required to be shut for proper operation of the Annulus Ventilation System.

Assumptions relating to the effectiveness of the Annulus Ventilation System in removing radioactive iodine following a design basis LOCA are presented in Section [15.6.5](#). The resulting offsite dose is presented in [Table 15-33](#).

A continuous guard pipe is utilized to prevent the pressurization of the annulus from postulated high energy process line breaks. Penetration details showing the guard pipe, primary containment and secondary containment are shown on [Figure 3-68](#).

#### **6.2.3.4 Tests and Inspections**

Tests and inspections were performed to assure and demonstrate the capability of components and the system to perform the assigned function.

##### Manufacturer Testing

The manufacturer was required to verify by appropriate tests the following: (Unit 1):

1. Carbon and High Efficiency Filters

The manufacturer provided in-place testing for both the carbon and high efficiency filters. He provides trained personnel and all equipment required to conduct such tests in general conformance with ORNL-NSIC-65 for the high efficiency filters and DP-1082 for the carbon filters and the latest state-of-the-art improvements.

2. Fan

Proper head and flow characteristics.

For Unit 2 the above testing was performed by station personnel using the same equipment and procedures used by the manufacturer.

##### System Testing and Inspection

Operational tests were performed prior to initial startup to demonstrate proper functioning of the system. Testing includes the following:

1. Leak tightness tests of components and system
2. System functional test

Each train of the Annulus Ventilation System was initially operated and monitored to verify system flow rates and damper operation. Each train was actuated individually and annulus pressure monitored as a function of time. Pressure response in the annulus was verified to be as described in Section [6.2.3.2](#). Operation of the system was continued and the pressure in the Annulus monitored for a sufficient period of time to demonstrate the capability of the system to maintain the pressure within the limits described in Section [6.2.3.2](#).

Thereafter, periodic tests and inspections are performed to demonstrate system readiness and operability:

1. Each Annulus Ventilation system is operated and alignment to emergency power sources verified.
2. Each charcoal and HEPA filter is tested and system flow rate verified.
3. Each system is given an automatic start signal and annulus pressure is monitored to insure that the required negative pressure is achieved within the required time.

Acceptance criteria for the functional tests are as follows:

1. Annulus pressure reaches -1.2 in wg within 22 seconds of a start signal.
2. Annulus pressure reaches -4.2 in wg within 48 seconds of a start signal.

3. The annulus pressure decay time from the beginning of a vacuum decay to -1.2 in wg is  $\geq 278$  seconds.

**Note:** The difference between the performance test acceptance criteria (-1.2 in wg to -4.2 in wg) and the Technical Specification requirements (-0.5 in wg to -3.5 in wg) for the annulus pressures are to compensate for the temperature induced variances between the pressure gradients inside the annulus and the outside atmosphere.

#### **6.2.3.5 Instrumentation Application**

This section describes the instrumentation employed for the actuation of the Annulus Ventilation System. This system is not operative during normal unit operation.

##### **6.2.3.5.1 Containment Pressure**

Two of the four Containment pressure transmitters through bistables are used to actuate the Annulus Ventilation System on Hi-Hi Containment pressure. High alarms and indications are located in the Control Room.

##### **6.2.3.5.2 Annulus Pressure**

Annulus pressure is controlled by recirculating to the annulus or exhausting to the station vent, as required. Pressure transmitters are provided to control the annulus pressure between -0.5 in. and -3.5 in. of water.

##### **6.2.3.5.3 Filter Train Differential Pressure**

Pressure transmitters are provided to measure the differential pressure across each filter bank. Indication is provided in the Control Room.

##### **6.2.3.5.4 Annulus Ventilation Fans Inlet Header Flow**

Flow transmitters are provided to measure the flow in the inlet header to the annulus ventilation fans. Indication and low alarm are also provided in the Control Room.

##### **6.2.3.5.5 Carbon Filter Temperature**

Temperature sensors, embedded in the carbon filter, are provided to indicate excessive filter temperature. Indication is provided in the Control Room. On a high temperature signal, a set of water sprays can be actuated to inhibit an uncontrolled fire.

##### **6.2.3.6 Materials**

Since the Annulus Ventilation System is entirely outside the Containment it is not subject to radiolytic or pyrolytic decomposition.

#### **6.2.4 Containment Isolation Systems**

The Containment Isolation Systems, shown schematically in [Figure 6-172](#), provide the means of isolating fluid systems that pass through Containment penetrations so as to confine to the Containment any radioactivity that may be released following a design basis event. The Containment Isolation Systems are required to function following a design basis event to isolate non-essential fluid systems penetrating the Containment.

### 6.2.4.1 Design Basis

The design bases for the Containment Isolation Systems are indicated below:

1. A double barrier is provided for all fluid penetrations to assure that no single failure or malfunction of an active component can result in loss of isolation or intolerable leakage, except as follows: (Penetration classifications are shown schematically on [Figure 6-172](#).)
  - a. Penetration Classification D5: This arrangement is used only for the residual heat removal heat exchanger line. With this system no single failure of an active or passive component can prevent the recirculation of core cooling water or adversely affect the integrity of the Containment; therefore, the intent of GDC 57 is met.
  - b. Penetration Classification C1: This arrangement is used only for the Containment sump suction lines. Passive failures are not postulated in this piping due to the low stress levels. For further details on pipe break analysis and assumptions refer to Section [3.6.2.2.1](#).
  - c. Process instrument impulse line penetrations: Impulse lines for process instrumentation located in the Annulus employ excess flow check valves outside Containment and appropriate orificing inside Containment to maintain Containment integrity in accordance with Regulatory Guide 1.11. Solenoid valves or motor operated valves must be used on lines connected to the containment atmosphere as insufficient differential pressure will exist to close the excess flow check valves in these applications.
  - d. Penetration Classification D3: This arrangement is used only for the main steam lines. This penetration type contains a drain valve which does not satisfy the requirements or meet the intent of GDC-57. Although this valve can be controlled from the control room, its controls are non-safety grade and may not work when called upon to mitigate an accident. See [Figure 6-172](#) for pictorial representation of this penetration.
2. Upon receipt of either a phase A(T) Containment isolation signal which is derived from the safety injection signal or a phase B(P) Containment isolation signal which is derived from the high-high Containment pressure signal, the Containment Isolation System closes fluid line penetrations not required for Engineered Safety Features operation. The valves which are used to isolate purge line penetrations opening directly to the Containment atmosphere close upon occurrence of a phase A Containment isolation signal or a high Containment activity (H) signal. [Table 6-113](#) lists the containment isolation valves and their associated isolation signal.

Isolation valves serving Engineered Safety Features do not automatically close with the Containment isolation signal or high-high Containment pressure signal, but have the ability to be closed by remote manual operation from the Control Room to isolate any Engineered Safety Features that may malfunction.

3. All Containment isolation valves are designed to assure leak tightness and reliability of operation.
4. Isolation valves outside the Containment are located as close to the Containment as practicable, and upon loss of actuating power, automatic isolation valves are designed to take the position that provides greater safety. That is, the selection of an isolation valve operator is predicated on safety considerations. Air operated valves are selected where fail closed is required. Piston operated valves are used in fail closed and in automatic mode applications. Spring operated valves are used for automatic mode operation. Hand wheel operated valves are used where no post-accident valve operation is anticipated. [Table 6-113](#) outlines the containment isolation valve normal, accident and failure positions.
5. Remote manually operated and automatic trip isolation valves are provided with control switches and position indicators in the Control Room.

6. Isolation valves are tested as part of the integrated leakage rate tests for the Containment system and as part of periodic valve operability tests.
7. The Containment isolation system is designed to satisfy the requirements of 10CFR50, Appendix A General Design Criterion 55, 56, and 57 and Regulatory Guide No. 1.11 except as noted in (a) and (d) above here.
8. Isolation valving systems from a seismic consideration are designed the same as the piping system and/or the penetration of which they are a part, whichever is the higher classification. Section [3.9.2.8](#) describes penetration design criteria, and Section [3.7.2.1](#) describes seismic design of valves including isolation valves.

The containment valve systems are designed such that resetting of the containment isolation signal will not cause any containment isolation valve to automatically reposition. Deliberate operator action is required to reposition isolation valves following a reset of the containment isolation signal.

[Table 6-111](#) lists the penetrations with pertinent isolation valve data with the exception of approximately 125 penetrations for process instrumentation impulse lines.

#### **6.2.4.2 System Design**

The Containment Isolation System's automatic isolation valves are required to function upon receiving an actuating signal following a design basis event. The two-barrier scheme used assures that in the event of failure of any component to function, a backup means exists to isolate the Containment.

A barrier is defined as a valve or a closed piping system.

The requirements for a closed system include the following:

1. Is neither part of the Reactor Coolant Pressure Boundary nor connected directly to the Containment atmosphere.
2. Safety classification is the same as for engineered safety system.
3. Does withstand external pressure and temperature equal to Containment design pressure and temperature.
4. Does withstand accident transient and environmental conditions.
5. Is missile protected.

Missile protection for isolation valves is the same as that provided for containment penetrations. Section [3.9.2.8](#) describes penetration design criteria. Penetrations and their isolation valves are located in areas which receive design considerations with respect to missiles. In addition to design criteria and physical considerations with respect to missiles, valve specifications speak directly to the requirement of post-accident and environmental operation which must be substantiated by the valve supplier by actual tests results.

Main steam line capability to withstand the dynamic forces of inadvertent isolation valve closure is described in Section [3.9.1.1](#).

Isolation valves and valve operators are selected with the same consideration for safety that accompanies the selection of all ANS Safety Class 2 equipment.

#### **6.2.4.3 Safety Evaluation**

Based on the criteria set forth in the design basis, leakage through all piping penetrations is minimized during accident conditions. By using double automatic barriers, isolation is assured upon actuation of the engineered safety systems or upon a high radiation signal. All postulated conditions of adverse

environment do not alter the proper operation of these valves. Selection of valves of the proper quality plus periodic testing of the valve operability and leak tightness assures a reliable isolation system under all conceivable conditions.

All manually operated isolation valves have permanent tags attached stating that the valve is to remain closed during unit operation. The operating procedure controlling unit startup includes requirements to verify that these valves are closed prior to unit operation.

Although the drain valves associated with penetration classification D3 do not meet GDC 57, they can be closed via local, manual operation within an acceptable time period if the non-safety controls have failed.

No system is provided to continuously monitor the leak-tightness of the Containment. However, the fact that redundant isolation is provided in all cases for valves required to operate following an incident, the administrative procedures concerning locked closed valves, and the testing procedures outlined in Technical Specifications provide confidence that the Containment Isolation System will perform its intended function.

#### 6.2.4.4 Tests and Inspections

Periodic testing of valves designed to effect containment isolation during accident conditions is performed to determine their leak-tightness. Test connections, test vents, drain connections and manual isolation valves are provided to permit pressurization from the containment side of the valves with the following exceptions:

1. Any globe or relief valve may be tested with pressure under the seat.
2. Butterfly valves are tested in the direction identified in [Table 6-112](#). The butterfly valves to be tested in the reverse direction have a seat construction designed for sealing against on either side as shown in [Figure 6-173](#). These butterfly valves are leak tested in both directions by the manufacturer to demonstrate equivalent leakage from either direction. Final certification provided by the manufacturer indicated that the valve seat leakage tests were performed with acceptable results when tested from either direction. Leak rate tests in the reverse direction are considered acceptable by the ASME Code, OMB - 1998 Subsection ISTC - 3630, since the test pressure is less than 15 psi.
3. Double disk gate valves may be tested by pressurizing between the seats.
4. Diaphragm valves may be tested by pressurizing from either direction. Equivalent leakage rates were verified by testing (See [Table 6-115](#)).

[Table 6-112](#) lists those valves subject to Type C leakrate testing per Appendix J to 10CFR 50. Also listed is the direction of test pressurization relative to post-accident containment pressure; however, this may be modified, consistent with the above exceptions.

[Table 6-112](#) also identifies the penetrations not subject to Type C leak rate testing. These penetrations are designed either as an open flow path through the containment vessel during post accident conditions or do not communicate with the containment and are therefore not required for leaktightness. Also, with the exception of the four main feedwater penetrations, these penetrations all connect to closed, seismic systems outside containment.

In addition to those identified in [Table 6-112](#), the following penetrations are not subject to Type C leakrate testing:

1. Main steam penetrations - main steam line isolation is provided for the purpose of preventing reverse steam flow following a steam line rupture. Containment atmosphere leak protection is provided by the seismic design of the steam generators and main steam piping within the containment.

2. Fuel transfer tube-A Type B test (pressurizing the volume between the two flange seals) is required for this penetration.
3. Residual heat removal normal letdown line - this penetration connects directly to an active ECCS subsystem.
4. Process instrument impulse line penetrations (except containment pressure).

Containment isolation valves located in lines where service can be interrupted are exercised as describe in Section [7.3.2.2](#). Containment isolation valves which cannot be exercised during normal operation are tested during shutdown periods.

In order that the Technical Specification surveillance requirement of determining the lower containment purge supply and exhaust valves are sealed closed every 31 days can be done without sending operators inside containment when the plant is up at power, five key locked switches (located on the HVAC main control board) are installed on the electric signal supplying the solenoid valves that open the lower containment purge isolation valves. These key switches prevent the valves from being opened by mistake and enable the operator to use the system without exposing personnel to a hostile environment.

Similarly, the upper containment purge supply and exhaust valves are sealed closed (power removed) by tagging open the containment purge supply and exhaust fan motor breakers. Maintaining the fan motor breaker open also removes control power to the solenoid valve, thus the valves are failed closed.

**6.2.4.5 Instrumentation Application**

Refer to Section [7.3](#) for a discussion of instrumentation employed for the actuation of the Containment Isolation System.

**6.2.4.6 Materials**

The Containment isolation valves are all stainless steel or carbon steel and as such are not subject to radiolytic or pyrolytic decomposition. The following materials are used in the Containment electrical penetrations.

<b>Equipment</b>	<b>Material</b>	<b>Estimated Qty (Wt.)</b>
Electrical Penetrations (100)	304 Type Stainless Steel Carbon Steel Jx Boxes Copper Conductor Material Silicone Rubber Sulfahexaflouride Gas Glass	It is estimated that the total weight of the penetrations with junction boxes will be approximately 10 tons with the 304 Type Stainless Steel comprising approximately 7 1/2 tons, the Carbon Steel Jx Boxes comprising 2 tons and the remaining components comprising less than 5% of the total weight.

## 6.2.5 Combustible Gas Control in Containment

### 6.2.5.1 Design Bases

The requirements for hydrogen recombiners have been eliminated per Tech Spec Amendments 227/209 dated April 4, 2005. The same amendments relaxed requirements for the containment hydrogen monitors. The containment hydrogen monitors are discussed in more detail in Section [1.8.26](#).

### 6.2.5.2 Deleted Per 2008 Update

### 6.2.5.3 Design Evaluation

The Hydrogen Purge System will be utilized only in the highly improbable event that the Hydrogen Mitigation System, described in Section [6.2.7](#), fail to control hydrogen concentration.

The system basically consists of a hydrogen purge blower and a configuration of valves to control the discharge from the Containment to the annulus. The blower is designed to purge at the rate of 100 SCFM.

The sampling system is Safety Class 2 inside the containment up to and including the manual isolation valves outside of the Containment. Separate and redundant Containment air sample valves are provided inside the Containment with a common header outside.

### 6.2.5.4 Deleted Per 2008 Update

### 6.2.5.5 Deleted Per 2008 Update

### 6.2.5.6 Deleted Per 2008 Update

## 6.2.6 Hydrogen Production and Accumulation

This section documents the Hydrogen generation analyses for the design basis LOCA, and is no longer part of the current licensing bases (Refer to Section [6.1.7](#)). The section verbiage, and associated tables are retained for “historical” documentation purposes.

Hydrogen accumulation in the Containment atmosphere following the Design Basis Accident can be the result of production from several sources. The potential sources of hydrogen are the zirconium-water reaction, dissolved hydrogen in the primary coolant, corrosion of construction materials, and radiolytic decomposition of the emergency core cooling solution. The latter source, solution radiolysis, includes both core solution radiolysis and sump solution radiolysis.

### 6.2.6.1 Method of Analysis

The quantity of zirconium which reacts with the core cooling solution depends on the performance of the Emergency Core Cooling System. The 10CFR 50.46 criteria for evaluation of the Emergency Core Cooling System requires that the zirconium-water reaction be limited to one percent of the hypothetical hydrogen generation from the reaction of all the metal in the cladding surrounding the fuel, excluding the cladding surrounding the plenum volume.

The use of aluminum inside the Containment is limited, and is not used in safety related components which are in contact with the recirculating core cooling fluid. Aluminum is more reactive with the Containment spray alkaline borate solution than other plant materials such as galvanized steel, copper, and copper nickel alloys. However, because of the relatively large amount of exposed galvanized and zinc-based painted surfaces in Containment, zinc corrosion must be considered as a contributing hydrogen source.

It should be noted that zirconium-water reaction and the aluminum and zinc corrosion with Containment spray are chemical reactions and thus essentially independent of the radiation field inside the Containment following a Loss-of-Coolant Accident. Radiolytic decomposition of water is dependent on the radiation field intensity. The radiation field inside the Containment is calculated for the maximum credible accident in which the fission product activities given in TID-14844 (Reference [67](#)) are used.

The hydrogen generation calculations are performed using Regulatory Guide 1.7 Methodology.

### 6.2.6.2 Typical Assumptions

The following discussion outlines the assumptions used in the calculations.

#### 6.2.6.2.1 Zirconium-Water Reaction

The zirconium-water reaction is described by the chemical equation:



Regulatory Guide 1.7 requires that the assumption for hydrogen produced from the zirconium-water reaction equal “5 times the extent of the maximum calculated reaction under 10CFR 50.46,” i.e., 5.0% for McGuire. For the Reactor Vessel and Pressurizer compartments it is assumed 2.5% reaction is more appropriate for small break LOCAs. The zirconium-water hydrogen source is assumed to be released over a 2-minute period from the start of the transient, and is distributed equally into all upper and lower compartments.

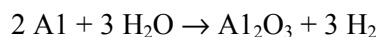
#### 6.2.6.2.2 Primary Coolant Hydrogen

The quantity of hydrogen assumed in the primary coolant is 483 scf. This value is expected to bound the total of the hydrogen dissolved in the coolant water and the corresponding equilibrium hydrogen in the pressurizer gas space. The volume of hydrogen is assumed to be released immediately into all upper and lower Containment compartments at the initiation of a LOCA.

#### 6.2.6.2.3 Corrosion of Plant Materials

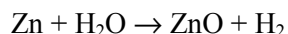
Oxidation of metals in aqueous solution results in the generation of hydrogen gas as one of the corrosion products. Extensive corrosion testing has been conducted to determine the behavior of the various metals used in the Containment in the emergency core cooling solution at Design Basis Accident conditions. Metals tested include Zircaloy, Inconel, aluminum alloys, cupronickel alloys, carbon steel, galvanized carbon steel, and copper. Tests conducted at ORNL (References [69](#) & [70](#)) have also verified the compatibility of the various materials (exclusive of aluminum) with alkaline borate solution.

The corrosion of aluminum may be described by the overall reaction:



Therefore, three moles of H<sub>2</sub> are produced for every two moles of Aluminum that is oxidized. This corresponds to approximately 20 standard cubic feet of hydrogen for each pound of aluminum corroded.

The corrosion of zinc may be described by the overall reaction:



Therefore, one mole of hydrogen is produced for each mole of zinc that is oxidized. This corresponds to approximately 5.5 standard cubic feet of hydrogen for each pound of zinc corroded.

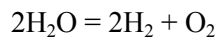
The time-temperature curve considered in the calculation of aluminum and zinc corrosion is based on a conservative representation of the postulated post accident Containment transient. The corrosion rates at

the various temperatures are determined from the aluminum and zinc corrosion rate design curves shown in [Figure 6-174](#) and [Figure 6-198](#). The calculation assumes an increase in the aluminium corrosion rate during the final setup of the post accident Containment temperature transient corresponding to 200 mils/yr as specified in Regulatory Guide 1.7. The corrosion data points include the effects of temperature, alloy, and spray solution conditions.

Based on the corrodable metal inventory limits given in [Table 6-117](#), the contribution of aluminum and zinc corrosion to hydrogen accumulation in the Containment following the Design Basis LOCA has been calculated. For conservative estimation, no credit is taken for protective shield effects of insulation or enclosures from the spray, and complete and continuous immersion is assumed.

#### 6.2.6.2.4 Radiolysis of Core and Sump Water

Water radiolysis is a complex process involving reactions of numerous intermediates. However, the overall radiolytic process may be described by the reaction:



Of interest here is the quantitative definition of the rates and extent of radiolytic hydrogen production following the Design Basis Accident.

An extensive program has been conducted by Westinghouse to investigate the radiolytic decomposition of the core cooling solution following the Design Basis Accident. In the course of this investigation, it became apparent that two separate radiolytic environments exist in the containment at design basis accident conditions. In one case, radiolysis of the core cooling solution occurs as a result of the decay energy of fission products in the fuel. In the other case, the decay of dissolved fission products, which have escaped from the core, results in the radiolysis of the sump solution. The results of these investigations are discussed in Reference [71](#).

#### 6.2.6.3 Core Solution Radiolysis

As the emergency core cooling solution flows through the core, it is subjected to gamma radiation by decay of fission products in the fuel. This energy deposition results in solution radiolysis and the production of molecular hydrogen and oxygen. The initial production rate of these species will depend on the rate of energy absorption and the specific radiolytic yields.

The energy absorption rate in solution can be assessed from knowledge of the fission products contained in the core, and a detailed analysis of the dissipation of the decay energy between core materials and the solution. The results of Westinghouse studies show essentially all of the beta energy is absorbed within the fuel and cladding and that this represents approximately 50 percent of the total beta-gamma decay energy. This study shows further that of the gamma energy, a maximum of 7.4 percent will be absorbed by the solution in core. Thus, an overall absorption factor of 3.7 percent of the total core decay energy ( $\beta + \gamma$ ) is used to compute solution radiation dose rates and the time-integrated dose. For the maximum credible accident case, the contained decay energy in the core accounts for the assumed TID 14844 release of 50 percent halogens and 1 percent other fission products. To be conservative, the noble gases are assumed by the TID 14844 model to escape to the containment vapor space where little or no water radiolysis would result from decay of these nuclides.

The radiolysis yield of hydrogen in solution has been studied extensively by Westinghouse and ORNL. The results of static capsule tests conducted by Westinghouse indicate that hydrogen yields much lower than the maximum of 0.44 molecules per 100 ev would be the case in-core. With little gas space to which the hydrogen formed in solution can escape, the rapid back reactions of molecular radiolytic products in solution to reform water is sufficient to result in very low net hydrogen yields.

However, it is recognized that there are differences between the static capsule tests and the dynamic condition in core, where the core cooling fluid is continuously flowing. Such flow is reasoned to disturb the steady state conditions which are observed in static capsule tests, and while the occurrence of back reactions would still be significant, the overall net yield of hydrogen would be somewhat higher in the flowing system.

The study of radiolysis in dynamic systems was initiated by Westinghouse, which formed the basis for experimental work performed at ORNL. Both studies clearly illustrate the reduced yields in hydrogen from core radiolysis; i.e., reduced from the maximum yield of 0.44 molecules per 100 ev. These results were published (References [71](#) and [72](#)).

For the purposes of this analysis, the calculations of hydrogen yield from core radiolysis are performed with the very conservative value of 0.44 molecules per 100 ev. That this value is conservative and a maximum for this type of aqueous solution and gamma radiation is confirmed by many published works. The Westinghouse results from the dynamic studies show 0.44 to be a maximum at very high solution flow rates through the gamma radiation field. The referenced ORNL work (Reference [72](#)) also confirms this value as a maximum at high flow rates. A. O. Allen (Reference [73](#)) presents a very comprehensive review of work performed to confirm the primary hydrogen yield to be a maximum of 0.45 molecules per 100 ev.

On the foregoing basis, the production rate and total hydrogen produced from core radiolysis, as a function of time, has been conservatively estimated for the Design Basis Accident case.

#### 6.2.6.4 Sump Solution Radiolysis

Another potential source of hydrogen assumed for the post accident period arises from water contained in the reactor containment sump being subjected to radiolytic decomposition by fission products. In this consideration, an assessment must be made as to the decay energy deposited in the solution and the radiolytic hydrogen yield, much in the same manner as given above for core radiolysis.

The energy deposited in solution is computed using the following basis:

1. For the Design Basis Accident, a TID-14844 release model (Reference [67](#)) is assumed where 50 percent of the total core halogens and 1 percent of all other fission products, excluding noble gases, are released from the core to the sump solution.
2. The quantity of fission product release is equal to that from a reactor operating at full power for 980 days prior to the accident.
3. The total decay energy from the released fission products, both beta and gamma, is assumed to be fully absorbed in the solution.

The yield of hydrogen from sump solution radiolysis is most nearly represented by the static capsule tests performed by Westinghouse and ORNL with the alkaline sodium borate solution. The differences between these tests and the actual conditions for the sump solution, however, are important and render the capsule tests conservative in their predictions of radiolytic hydrogen yields.

In this assessment, the sump solution will have considerable depth, which inhibits the ready diffusion of hydrogen from solution. This retention of hydrogen in solution will have a significant effect in reducing the hydrogen yields to the containment atmosphere. The build-up of hydrogen concentration in solution will enhance the back reaction to formation of water and lower the net hydrogen yield, in the same manner as a reduction in gas to liquid volume ratio will reduce the yield. This is illustrated by the data presented in [Figure 6-175](#) for capsule tests with various gas to liquid volume ratios. The data show a significant reduction in the apparent or net hydrogen yield from the published primary maximum yield of 0.44 molecules per 100 ev. Even at the very highest ratios, where capsule solution depths are very low, the yield is less than 0.30, with the highest scatter data point at 0.39 molecules per 100 ev.

With these considerations taken into account, a reduced hydrogen yield is a reasonable assumption to make for the case of sump radiolysis. While it can be expected that the yield will be on the order of 0.1 molecules per 100 ev or less, a conservative value of 0.30 molecules per 100 ev has been used in the maximum credible accident case.

[Table 6-118](#) shows the results of the calculation for hydrogen production and accumulation from the following sources: (1) zirconium-water reaction, (2) primary system hydrogen, (3) aluminum and zinc corrosion, and (4) radiolytic decomposition of core and sump solution. [Table 6-118](#) gives the total hydrogen production rate as a function of time following the design basis LOCA, as well as the total quantity of hydrogen accumulated in the Containment as a function of time up to 30 days.

## 6.2.7 Supplemental Hydrogen Control System/Hydrogen Mitigation System

(REF. [74](#) & [75](#))

The licensing requirements relative to the provisions for hydrogen control prescribed in 10CFR 50.44 have evolved from numerous deliberations among the Nuclear Regulatory Commission (NRC), the Advisory Committee on Reactor Safeguards (ACRS), and utilities. The NRC's requirement for ice condenser containments is that a supplemental hydrogen control system be provided so that the consequences of the hydrogen release generated during the more probable degraded core accident sequences do not involve a breach of containment nor adversely affect the functioning of essential equipment.

Based on a determination that a Hydrogen Mitigation System would provide additional assurance of safety in the event of excessive hydrogen generation resulting from an accident beyond the design bases for McGuire Nuclear Station, an Interim Distributed Hydrogen Ignition System was installed in McGuire Units 1 and 2.

As a part of research activities, Duke Power in cooperation with Tennessee Valley Authority (TVA) and American Electric Power (AEP) continued to investigate alternative measures of hydrogen control. As a result of continued studies, a deliberate ignition system, similar to the interim system, provides adequate safety margins in controlling the consequences of degraded core accidents. The permanent Hydrogen Mitigation System (EHM) is identical in concept to the interim system but provides some system design improvements. The Hydrogen Mitigation System is non safety-related because the requirements of 10 CFR 50.44 to mitigate hydrogen generated as a result of a 75% metal-water reaction address beyond design-basis combustible gas control.

### SYSTEM DESCRIPTION

The Hydrogen Mitigation System is a system of thermal igniters and ancillary equipment installed within the containment of McGuire Units 1 and 2. The igniters are designed to ensure a controlled burning of hydrogen in the unlikely event that excessive quantities of hydrogen are generated as a result of a postulated degraded core accident. The Hydrogen Mitigation System is designed to promote the combustion of hydrogen in a manner such that containment integrity is maintained. The Hydrogen Mitigation System is virtually identical to the interim system evaluated by the staff in early 1981 except for slight modifications in the number and location of igniters. The permanent igniter system utilizes glow coil type igniters. The igniter is powered directly from a 120V ac source. Each igniter assembly consists of a 1/8-in. thick stainless steel box (6 in. H x 10 in. W x 8 in D), which contains all electrical connections and partially encloses the igniter. This enclosure meets National Electrical Manufacturers Association (NEMA) Type 4X specifications for watertight integrity under various environmental conditions, including exposure to water jets and protection against corrosion.

Deleted Per 2015 Update.

The enclosures incorporate a spray shield to reduce water impingement on the igniter from above. In addition, the Hydrogen Mitigation System is seismically mounted.

#### Igniter Power Supply

The igniters in the Hydrogen Mitigation System are equally divided into two redundant groups, with separate circuits and circuit breakers per group. The number of igniters on each circuit ranges from 1 to 10. Igniters located at elevations near the flood level (those in the pipe chase) are on dedicated circuits. Each group has independent and separate control, power, and igniter locations to ensure adequate coverage even in the event of a single failure. The system is manually actuated from the Control Room.

The igniters are powered from the Class 1E 600 VAC power system that has normal and alternate power supply from emergency power. In the event of a loss of offsite power, the igniters would be powered from the emergency diesel generators. Group A igniters receive power from the train A diesels and Group B igniters from the train B diesels. In addition, Train A igniters receive power from a motor control center in the Class 1E 600VAC power system that can be aligned to the Standby Shutdown Facility (SSF) diesel generator as well as the emergency diesel generators.

Considering the plant's electrical design features, the NRC staff concluded that qualitatively the reliability of the McGuire ac power supply system should be better than average and should reduce the likelihood of station blackout at McGuire.

#### Igniter Coverage

The Hydrogen Mitigation System consists of 70 igniter assemblies distributed throughout the upper, lower, dead-ended, and ice condenser compartments. Following the onset of a degraded core accident, any hydrogen that is produced would be released into the lower compartment. To cover this region, igniters (equally divided between the power trains) have been provided. 2 located by the PR Tank, 2 located above each RC Pump, 2 located above the Pressurizer, 2 located above the Reactor Vessel, 2 located above each Steam Generator.

Any hydrogen not burned in the lower compartment would be carried up through the ice condenser and into its upper plenum. Because steam would be removed from the mixture as it passes through the ice bed, thus concentrating the hydrogen, mixtures that were nonflammable in the lower compartment would tend to become flammable in the ice condenser upper plenum. Controlled burning in the upper plenum is preferable to burning in the upper compartment because upper plenum burns involve smaller quantities of hydrogen per burn. Duke has taken advantage of the beneficial characteristics of combustion in the upper plenum and has distributed 12 igniters around it. These igniters are located in a staggered fashion alternately between the crane wall and the containment shell wall sides of the upper plenum, at 12 almost equally spaced azimuthal locations.

To handle any accumulation of hydrogen in the upper compartment, 8 igniters are located in the Upper Compartment dome and one additional igniter located above each Steam Generator. The air return fans provide recirculation flow from the upper compartment through the dead-ended volume and back into the lower compartment. To cover the dead-ended region, 2 igniters are located in each of the 2 Fan Rooms, 2 igniters are located in Accumulator Rooms A - B - C - D and 2 igniters in the area adjacent to Accumulator Room C through which the recirculation flow passes. In addition, 6 igniters are provided in the Pipe Chase, 2 igniters at the Incore Instrument Tunnel Area (PC Duck Walk), and 2 igniters near the Seal Table in the Incore Instrumentation Area.

#### System Actuation

The emergency operating procedure for responding to loss-of-coolant accidents (LOCAs) includes instructions for actuating and securing the hydrogen mitigation system. The hydrogen igniters are turned on after diagnosing a LOCA inside containment during a design basis event. As recommended in the

interim evaluation, the air handling units used for normal refrigeration in the ice condenser will be tripped for both units for accidents in which the Hydrogen Mitigation System is actuated.

The LOCA procedure calls for the Hydrogen Mitigation System to remain actuated (1) for 24 hours after the establishment of adequate core cooling if any indication of inadequate core cooling exists or has existed or (2) until the containment pressure drops below 0.25 psig if adequate core cooling has always existed for the duration of the transient. The procedure instructs the operator to reactuate the Hydrogen Mitigation System if there is indication of return to inadequate core cooling.

#### Surveillance Testing

To ensure that the Hydrogen Mitigation System will function as intended, a surveillance testing program was established for the system. Preoperational testing, performed before startup, verified the electric current drawn by each group of igniters was within tolerance, and that the temperature of each igniter was at least 1700°F. The current measured in each circuit during preoperational tests provided the baseline for the surveillance tests.

The Hydrogen Mitigation System is subjected to surveillance testing on a quarterly basis. This testing consists of energizing the Hydrogen Mitigation System and taking current and voltage readings of the igniter circuits at the emergency lighting panelboards. If the power consumption does not compare favorably with that measured during preoperational testing, the igniters on the affected circuits will be individually inspected to ensure their operability. In addition to power consumption measurements, the igniter temperatures are measured at specified intervals.

### **6.2.8 References**

1. "Ice Condenser Containment Pressure Transient Analysis Method," *WCAP-8077* (Proprietary) and *WCAP-8078* (Non-Proprietary) March, 1973.
2. Henry, R. E., and Fauske, H. K., "The Two-Phase Critical Flow of One-Component Mixtures in Nozzles, Orifices and Short Tubes," *Journal of Heat Transfer*, May, 1971.
3. Isbin, H. S., Fauske, H. K., Petrick, M., Robbins, C. H., Smith, R. W., Szawlequcz, S. A., and Zaloudek, F. R., *Proc. of the Third Intl. Conf. for the Peaceful Uses of Atomic Energy, Geneva, Switzerland, Aug.-Sept., 1964*
4. Carofano, G. C., and McManus, H. N., "An Analytical and Experimental Study of the Flow of Air-Water and Steam-Water Mixtures In a Coverging-Diverging Nozzle," *Progress in Heat & Mass Transfer*, Volume 2.
5. F. J. Moody "Maximum Flow Rate of Single Component, Two-Phase Mixture," *ASME publication, Paper No. 64-HT-35*.
6. F. R. Zaloudek, "Steam-Water Critical Flow From High Pressure Systems," *Interim Report HW-68936*, Hanford Works, 1964.
7. Bordelon, F.M., Massie, H.W., Jr., and Zordan, T.A., "Westinghouse Emergency Core Cooling System Evaluation Model - Summary", *WCAP-8339*, June, 1974.
8. R. E. Henry, "A Study of One-and Two-Component, Two-Phase Critical Flows at Low Qualities," *ANL-7430*.
9. R. E. Henry, "An Experimental Study of Low-Quality, Steam-Water Critical Flow at Moderate Pressures," *ANL-7740*.
10. F. W. Kramer, "FLASH - A Digital Computer Code for the Loss of Coolant Accident Analyses," *WCAP-1678*, January, 1961.

11. F. R. Zaloudek, "The Critical Flow of Hot Water Through Short Tubes," *HW-77594*, Hanford Works, 1963.
12. Dittus, F. W., and L. M. K. Boelter, University of California (Berkeley), *Publs. Eng.*, 2, 433 (1930).
13. Jens, W. H., and P. A. Lottes, "Analysis of Heat Transfer, Burnout, Pressure Drop, and Density Data for High Pressure Water," USAEC Report *ANL-4627*, 1951.
14. Bergles, A. E., and W. M. Rohsenow, "The Determination of Forced-Convection Surface-Boiling Heat Transfer," *ASME Paper No. 63-HT-22*, 1963.
15. Macbeth, R. V., "Burnout Analysis, Pt. 2, The Basis Burn-out Curve", U. K. Report *AEW-R 167*, Winfrith (1963). Also Pt. 3, "The Low-Velocity Burnout Regimes," *AEW-R 222* (1963); Pt. 4, "Application of Local Conditions Hypothesis to World Data for Uniformly Heated Round Tubes and Rectangular Channels", *AEW-R 267* (1963).
16. D. M. McEligot, L. W. Ormand and H. C. Perkins, Jr., "Internal Low Reynolds - Number Turbulent and Transitional Gas Flow with Heat Transfer", *Journal of Heat Transfer*, 88, 239-2465 (May 1966).
17. W. H. McAdam, *Heat Transmission*, McGraw-Hill 3rd edition, 1954, p. 172.
18. Dougall, R. S., and W. M. Rohsenow, Film Boiling on the Inside of Vertical Tubes with Upward Flow of Fluid at Low Quantities, *MIT Report 9079-26*.
19. Cunningham, W. P., and H. C. Yeh, "Experiments and Void Correlation for PWR Small-Break LOCA Conditions", *Transactions of American Nuclear Society*, Vol. 17, Nov. 1973, pp. 369-370.
20. Grim, N. P., and Colenbrander, H. G. C., "Long Term Ice Condenser Containment Code - LOTIC Code," *WCAP-8354* (Proprietary) and *WCAP-8355* (Non-Proprietary), July, 1974.
21. Idel'Chik, I. E., *Handbook of Hydraulic Resistance*, Translated from Russian, Published by the USAEC, 1966.
22. "Final Report Ice Condenser Full-Scale Section Tests at the Waltz Mill Facility", *WCAP-8282*, February, 1974.
23. Wallace, G. B., et al., "Two Phase Flow and Boiling Heat Transfer," *Quarterly Progress Report (July-September, 1974) NYD-3114-4*.
24. Hseih, T. and Raymund, M., "Long Term Ice Condenser Containment Code - LOTIC Code," *WCAP-8354, Supplement 1* (Proprietary) and *WCAP-8355, Supplement 1* (Non-Proprietary), June 1975.
25. Shepard, R. M., Massie, H.W., Mark, R. H. and Docherty, P. J., "Westinghouse Mass and Energy Release Data for Containment Design", *WCAP-8264-P-A* (Proprietary) and *WCAP-8312-A, Revision 1* June, 1975 (Non-Proprietary).
26. Letter from T. M. Novak (NRC) to H. B. Tucker (DPC) dated October 14, 1982. Enclosure: Safety Evaluation Report On Response To I.E. Bulletin 80-04.
27. Deleted Per 1998 Update
28. C. Eicheldinger, Letter of 10/27/76, No. NS-CE-1250.
29. C. Eicheldinger, Letter of 6/14/77, No. NS-CE-1453.
30. C. Eicheldinger, Letter of 12/7/77, No. NS-CE-1626.
31. Deleted Per 1998 Update.
32. Deleted Per 1998 Update.
33. Deleted Per 1998 Update.

34. Deleted Per 1998 Update.
35. Deleted Per 1998 Update.
36. "Westinghouse LOCA Mass and Energy Release Model for Containment Design" - March 1979 Version, *WCAP 10325*, April, 1979.
37. Letter from S. S. Kilborn (Westinghouse) to T. F. Wyke (Duke), DAP-88-530, March 21, 1988.
38. NUREG-0954, "Safety Evaluation Report related to the operation of Catawba Nuclear Station, Units 1 and 2", Supplement No. 2, June, 1984, p.6-1.
39. Test Plans and Results for the Ice Condenser System, *WCAP-8110*, April 16, 1973.
40. Test Plans and Results for the Ice Condenser System, *WCAP-8110*, Supplement 1, April 30, 1973.
41. Test Plans and Results for the Ice Condenser System, *WCAP-8110*, Supplement 2, June 19, 1973.
42. Test Plans and Results for the Ice Condenser System, *WCAP-8110*, Supplement 3, July 18, 1973.
43. Test Plans and Results for the Ice Condenser System, *WCAP-8110*, Supplement 4, November 15, 1973.
44. Allen, H. G., *Analysis and Design of Structural Sandwich Panels*, Pergamon Press, London, 1969.
45. Plantema, F. F., *Sandwich Construction*, John Wiley, New York, 1966.
46. Raville, M. E., Deflection and Stress in a Uniformly Loaded Simply Supported Rectangular Sandwich Plate, *FPL Report No. 1948*, September, 1962.
47. Libove, C. and Huboka, R. E., Elastic Constants for Corrugated-Core Sandwich Plates, *NACA Report No. TN-2289*.
48. Timoshenko, S. P., *Theory of Elastic Stability*, McGraw-Hill, 1961.
49. Idel'chik, Handbook of Hydraulic Resistance, *AECTR 6630*, NTIS, Springfield, Va.
50. Nies, N. P. and Hulbert, R. W., *Journal of Chemical and Engineering Data*, Vol. 12, No. 3, pp. 303-313, 1967.
51. Franks, F., *Water*, V. 1, Plenum (1972), Ch. 4.
52. *Specification for the Design, Fabrication and Erection of Structural Steel for Buildings*, American Institute of Steel Construction, 1969 Edition.
53. *Donald C. Cook Nuclear Plant, FSAR*, American Electric Power Service Corporation, Docket Numbers 50-315 and 50-316.
54. Ice Condenser System Lower Inlet Door Shock Absorber Test Plans and Results, *WCAP-8336*, May 1974 (Westinghouse NES Proprietary) and *WCAP-8110*, Supplement 5, May 1974.
55. Final Report-Ice Condenser Full-Scale Tests at the Waltz Mill Facility, *WCAP-8282*, February 1974 (Westinghouse NES Proprietary), and *WCAP-8110*, Supplement 6, May 1974.
56. Final Report-Ice Condenser Full-Scale Tests at the Waltz Mill Facility, *WCAP-8282*, Addendum 1, May 1974, (Westinghouse NES Proprietary) and *WCAP-8110*, Supplement 7, May 1974.
57. Stress and Structural Analysis and Testing of Ice Baskets, *WCAP-8304* (Westinghouse NES Proprietary) and *WCAP-8110*, Supplement 8, May 1974.
58. Ice Fallout from Seismic Testing of Fused Ice Basket, *WCAP-8110*, Supplement 9-A, May, 1974.
59. Static Testing of Production Ice Baskets, *WCAP-8110*, Supplement 10, September 1974.

60. Application of the Active Ice Mass Management Concept to the Ice Condenser Ice Mass Technical Specification, *ICUG-001*, Ice Condenser Utility Group, Revision 2, June 2003.
61. "Mass & Energy Release and Containment Response Methodology," DPC-NE-3004-PA, Rev. 1, Duke Power Co., SER dated February 29, 2000.
62. Deleted Per 2008 Update.
63. Deleted Per 2008 Update.
64. Deleted Per 2008 Update.
65. Deleted Per 2008 Update.
66. Deleted Per 2008 Update.
67. J. J. DiNunno, F. D. Anderson, R. E. Baker, and R. L. Waterfield, "Calculation of Distance Factors for Power and Test Reactor Sites," TID-14844, March 1962.
68. Safety Guides for Water Cooled Nuclear Power Plants, Safety Guide 7, "The Control of Combustible Gas Concentrations in Containment Following a Loss of Coolant Accident," Division of Reactor Standards, U.S. Atomic Energy Commission.
69. W. B. Cottrell, "ORNL Nuclear Safety Research and Development Program Bi-Monthly Report for July August 1968," ORNL-TM-2368, November 1968.
70. W. B. Cottrell, "ORNL Nuclear Safety Research and Development Program Bi-Monthly Report for September - October 1968," ORNL-TM-2425, p. 48, January 1969.
71. W. D. Fletcher, et. al., "Post-LOCA Hydrogen Generation in PWR Containments," *Nucl. Technol.* 10, 420-427, (1971).
72. H. E. Zittel, and T. H. Row, "Radiation and Thermal Stability of Spray Solutions," *Nucl. Technol.* 10, 436-443, (1971).
73. A. O. Allen, "The Radiation Chemistry of Water and Aqueous Solutions," Princeton, N. J., Van Nostrand, 1961.
74. Safety Evaluation Report NUREG-0422 Supp. No. 7 Operation of McGuire Nuclear Station Units 1 & 2, May, 1983.
75. Duke Power Company, An Analysis of Hydrogen Control Measures at McGuire Nuclear Station, February 17, 1981.
76. Parker, W. O., Duke, letter to H. R. Denton, NRC, "An Analysis of Hydrogen Control Measures at McGuire Nuclear Station," October 30, 1982; Revision 1, December 31, 1981; Revision 2, January 22, 1982; Revision 3, March 11, 1982; Revision 4, May 4, 1982; Revision 5, November 5, 1982; Revision 6, February 15, 1983; Revision 7, March 16, 1983; Revision 8, April 22, 1983.
77. U. S. Nuclear Regulatory Commission, "NRC Staff Analysis of Hydrogen Control Measures for McGuire Nuclear Station, Units 1 and 2," Docket No.s 50-369 and 50-370, February 17, 1981.
78. Deleted Per 1998 Update.
79. W Letter, DAP-92-034, DCP-92-026 to DPC, June 9, 1992.
80. Stress Evaluation for revised Ice Basket Lower Supports, McGuire Nuclear Station Units 1 and 2, Westinghouse Calculation No. MED-PCE-10522, June 1991, M.F. Hankinson.
81. Deleted Per 2011 Update.
82. RELAP5/MOD3 Code Manual, Volumes 1 to 5, NUREG/CR-5535, EGG-2596 (Draft), June 1990.

83. GOTHIC Containment Analysis Package, Version 4.0, RP3048-1, Prepared for Electric Power Research Institute, Numerical Applications, Inc., September, 1993.
84. ANSI/ANS-56.4 - 1983, "American National Standard Pressure and Temperature Transient Analysis for Light Water Reactor Containments", American Nuclear Society, December 23, 1983.
85. "RETRAN-02: A Program for Transient Thermal-Hydraulic Analysis of Complex Fluid Flow Systems," EPRI-NP-1850-CCM, Revision 6.1, EPRI, June, 2007.
86. M.S. Tuckman (Duke) letter dated November 11, 1998 to Document Control Desk (NRC), "Response to Generic Letter 98-04: Potential Degradation of the Emergency Core Cooling System and the Containment Spray System After a Loss-of-Coolant Accident Because of Construction and Protective Coating Deficiencies and Foreign Material in Containment," McGuire Nuclear Station, Units 1 and 2, Docket Nos. 50-359, 370.
87. Deleted Per 2011 Update.
88. D.H. Warren (Westinghouse) letter DPC-10-13 dated April 7, 2010 to K. Rice (Duke), "Transmittal of McGuire and Catawba Reactor Cavity Sub-Compartment Analysis Evaluation Report."

**THIS PAGE LEFT BLANK INTENTIONALLY.**

## 6.3 Emergency Core Cooling System

The Emergency Core Cooling System (ECCS) is discussed in detail in this section. For additional information on the ECCS see the following sections:

1. Components which are necessary following a postulated loss-of-coolant accident (LOCA) over the entire range of break sizes are discussed in Section [15.6.5](#).
2. External forces and their effect on the operation of the ECCS are treated in Sections [3.7](#) and [3.9](#).
3. Pre-operational system testing is discussed in [Chapter 14](#).
4. The actuation of the ECCS is discussed in detail in Section [7.3](#).
5. Instrumentation available to the operator to monitor conditions after an ECCS actuation is found in Section [7.5](#).
6. Testing intervals are discussed in the Technical Specifications, Section 5.5.8.

### 6.3.1 Design Basis

#### 6.3.1.1 Range Of Coolant Ruptures And Leaks

The Emergency Core Cooling System is designed to cool the reactor core as well as to provide additional shutdown capability following initiation of the following accident conditions:

1. A pipe break or spurious valve lifting in the Reactor Coolant System which causes a discharge larger than that which can be made up by the normal makeup system, up to and including the instantaneous circumferential rupture of the largest pipe in the Reactor Coolant System.
2. Rupture of a control rod drive mechanism causing a rod cluster control assembly ejection accident.
3. A pipe break or spurious valve lifting in the steam system, up to and including the instantaneous circumferential rupture of the largest pipe in the steam system.
4. A steam generator tube rupture.

The acceptance criteria for the consequences of each of these accidents is described in [Chapter 15](#) in the respective accident analyses sections.

#### 6.3.1.2 Fission Product Decay Heat

The primary function of the Emergency Core Cooling System following a loss of coolant accident is to remove the stored and fission product decay heat from the reactor core such that fuel rod damage, to the extent that it would impair effective cooling of the core, is prevented. The acceptance criteria for the accidents, as well as analyses of the accidents are provided in [Chapter 15](#).

#### 6.3.1.3 Reactivity Required For Cold Shutdown

The Emergency Core Cooling System provides shutdown capability for the accidents listed above by means of chemical poison (boron) injection. The most critical accident for shutdown capability is the steam line break, and for this accident the Emergency Core Cooling system meets the criteria defined in [Chapter 15](#).

#### 6.3.1.4 Capability To Meet Functional Requirements

In order to ensure that the Emergency Core Cooling System performs its desired function during the accidents listed above, it is designed to tolerate a single active failure during the short term immediately following an accident, or to tolerate a single active or passive failure during the long term following an accident. This subject is detailed in Section [3.1](#).

The Emergency Core Cooling System is designed to meet its minimum required level of functional performance with onsite emergency diesel power system operation (assuming offsite power is not available) or with offsite electrical power system operation (assuming onsite power is not available) for any of the above abnormal occurrences assuming a single failure as defined above.

The Emergency Core Cooling System is designed to perform its function of insuring core cooling and shutdown capability following an accident under simultaneous safe shutdown earthquake loading. The seismic requirements are defined in [Chapter 3](#).

### 6.3.2 SYSTEM DESIGN

#### 6.3.2.1 Schematic Piping And Instrumentation Diagrams

Flow diagrams of the Emergency Core Cooling System are shown in [Figure 6-176](#) and [Figure 6-177](#). Process parameters for the various phases of ECCS operation, assuming minimum safeguards available, are provided in [Figure 6-183](#).

#### 6.3.2.2 Equipment and Component Design

Pertinent design and operating parameters for the components of the Emergency Core Cooling System are given in [Table 6-123](#). The codes and standards to which the individual components of the Emergency Core Cooling System are designed are listed in [Table 3-4](#).

The component design and operating conditions are specified as the most severe conditions to which each respective component is exposed during either normal operation, or during operation of the Emergency Core Cooling System. For each component, these conditions are considered in relation to the code to which it is designed. By designing the components in accordance with applicable codes, and with due consideration for the design and operating conditions, the fundamental assurance of structural integrity of the Emergency Core Cooling System components is maintained. Components of the Emergency Core Cooling System are designed to withstand the appropriate seismic loadings in accordance with their safety class as given in [Table 3-4](#).

The emergency core cooling system is designed to permit maintenance during the recirculation mode following a loss of coolant accident. Among the features provided are flushing connections at the discharge of the RHR pumps, drain connections at the suction of the RHR pumps, drain connections on the RHR heat exchanger water boxes, and drain connections in piping low points. The RHR pumps, the centrifugal charging pumps, and the safety injection pumps are all arranged and shielded so that maintenance can be performed on a faulted pump while the other pumps are operating. The piping and valves associated with the pumps are arranged so that they can be drained and flushed prior to maintaining the pumps. Connections are provided for washing down compartment floors and walls to reduce contamination following a spill. The pump compartments are ventilated to allow access for all maintenance while the other pumps are operating.

As part of the FLEX mitigation strategy in response to NRC Order EA-12-049, the ability to provide makeup from the RWST to the Reactor Coolant System is required following a postulated beyond design basis event. Safety Injection System piping connections are provided for this capability on the 733' and 750' Elevations of the Auxiliary Building.

### 6.3.2.2.1 Components Description

The major mechanical components of the Emergency Core Cooling System are:

#### Cold Leg Injection Accumulators

These accumulators are pressure vessels filled with borated water and pressurized with nitrogen gas. During normal operation each accumulator is isolated from the Reactor Coolant System by two check valves in series. Should the Reactor Coolant System pressure fall below the accumulator pressure, the check valves open and borated water is forced into the Reactor Coolant System. One accumulator is attached to each of the cold legs of the Reactor Coolant System. Mechanical operation of the swing-disc check valves is the only action required to open the injection path from the accumulators to the core via the cold leg.

Connections are provided for remotely adjusting the level and boron concentration of the borated water in each accumulator during normal operation as required. Accumulator water level may be adjusted either by draining to the reactor coolant drain tank, or by pumping borated water from the refueling water storage tank to the accumulator using the safety injection pumps.

Accumulator nitrogen pressure over-pressure can be adjusted as required during normal operation; however, the accumulators are normally isolated from the source of this nitrogen supply. Gas relief valves on the accumulators protect them from pressures in excess of design pressure.

The accumulators are located within the Containment but outside of the secondary shield wall which protects them from missiles. Since the accumulators are located within the Containment, a release of the nitrogen gas in the accumulators would cause an increase in normal Containment pressure. Containment pressure increase following release of the gas from all accumulators has been calculated and is well below the Containment pressure setpoint for Emergency Core Cooling System actuation.

Release of accumulator gas would be detected by the accumulator pressure indicators and alarms. Thus the operator could take action promptly as required to maintain operation within the requirements of the Technical Specification covering accumulator operability.

The complete listing of the design parameters for the cold leg injection accumulator is presented in [Table 6-123](#).

#### Pumps

##### Residual Heat Removal Pumps

Each residual heat removal pump is a single stage, vertical position, centrifugal pump. It has an integral motor-pump shaft, driven by an induction motor. The unit has a self-contained mechanical seal cooling system. Component cooling water is the heat exchange medium.

A minimum flow bypass line is provided for the pumps to recirculate through the residual exchangers and return the cooled fluid to the pump suction should these pumps be started with their normal flow paths blocked. Once flow is established to the Reactor Coolant System, the bypass line is automatically closed. This line prevents deadheading the pumps and permits pump testing during normal operation.

To respond to NRC IE Bulletin 88-04, an additional mini-flow line was added to each pump. The additional mini-flow path prevents dead-heading the weaker RHR pump, in-the-event of a single failure of the stronger RHR pump mini-flow valve. The McGuire response to NRC Bulletin 88-04 was provided to the NRC by letters dated January 15, 1990 and January 10, 1991 (References [18](#) and [19](#)). In a followup letter dated June 16, 1992, Duke notified the NRC of completion of the mini-flow line modifications (Reference [20](#)).

Based on analysis of the limiting ECCS alignments, RHR pump flow is less than the pump design runout flow of 5300 gpm.

The residual heat removal pumps are also discussed in Section [5.5.7](#).

#### Centrifugal Charging Pumps (CCP)

Each centrifugal charging pump is a multistage diffuser design, barrel type casing with vertical suction and discharge nozzles. The pump is driven through a speed increaser connected to an induction motor. The unit has a self-contained lubrication system.

The CCP Suction is aligned to the Volume Control Tank during normal operation to provide adequate minimum flow under all conditions. The minflow direct return path is locked closed (Ref. [3](#) Section [6.3.6](#)). The minimum flow bypass line contains two valves in series which are closed by operator action per the emergency operating procedures when actual RCS pressure drops to the manual reactor coolant pump trip setpoint. The charging pumps may be tested through the use of the minimum flow bypass line. The centrifugal charging pumps are also discussed in Section [9.3.4](#).

#### Safety Injection Pumps

Each high head safety injection pump is a multistage, centrifugal pump. The pump is driven directly by an induction motor. The unit has a self-contained lubrication system.

A minimum flow bypass line is provided for each pump with a common discharge header to recirculate flow to the refueling water storage tank in the event the pumps are started with the normal flow paths blocked. This line also permits pump testing during normal operation. The minimum flow bypass line is isolated by operator action during transition to the recirculation mode.

#### Residual Heat Exchangers

The residual heat exchangers are conventional shell and U-tube type units. During normal operation of the Residual Heat Removal System, reactor coolant flows through the tube side while component cooling water flows through the shell side. During emergency core cooling recirculation operation, water from the Containment sump flows through the tube side. The tubes are seal welded to the tubesheet.

A further discussion of the residual heat exchangers is found in Section [5.5.7](#).

#### Valves

Design parameters for all types of valves used in the Emergency Core Cooling System are given in [Table 6-123](#).

[Table 6-135](#) lists the type, size, actuation device and environmental design criteria for valves required to ensure safe shutdown of the reactor.

1. Where practical, packless valves are used.
2. Where globe valves are installed, recirculation fluid pressure is under the seat to prevent stem leakage of recirculated (radioactive) water when the valves are closed.
3. Relief valves are enclosed, i.e., they are provided with a closed bonnet.
4. All control valves, motor operated valves, and manually operated globe and gate valves (larger than 2 inches) exposed to recirculation flow have double packed stuffing boxes and stem leakoff connections to the Liquid Waste Recycle System and the Boron Recycle System.

#### Motor Operated Valves

Where possible the seating design of motor operated gate valves are of the parallel disc design or the flexible wedge design. These designs release the mechanical holding force during the first increment of travel so that the motor operator works only against the frictional component of the hydraulic unbalance on the disc and the packing box friction. The discs are guided throughout the full disc travel to prevent

chattering and to provide ease of gate movement. The seating surfaces are hard faced to prevent galling and to reduce wear.

Where a gasket is employed for the body to bonnet joint, it is in accordance with material limits from the Power Chemistry Guide (no asbestos allowed) with provisions for seal welding, or it is of the pressure seal design with provisions for seal welding. The valve stuffing boxes are designed with a lantern ring leakoff connection with at least a three-ring set of packing above the lantern ring and at least a five-ring set of packing below the lantern ring. Packing is pure graphite (chlorine-free) configured as braided end rings and die-formed filler rings. The three-ring set consists of two braided and one filler ring; the five-ring set consists of two braided and three filler rings.

The motor operators are specifically designed for optimum valve actuation, combining low inertia with high starting and stalling torque. This provides a substantial reserve of power above that required for mainseating or backseating valves. This power reserve combined with a starting, lost motion, "hammerblow" features allows the motor to impact the valve away from mainseat or backseat, thereby assuring unseating and proper operation.

All motor operators are equipped with mechanically independent handwheel drives for manual operation. In all cases, the handwheel drive is automatically disengaged when the motor starts and powered operation is immediately restored to the valve/operator assembly.

Motor operators are designed to produce sufficient torque to actuate the valves with a pressure drop across the valve disc as high as the maximum system pressure. This assures valve actuation under all system operating pressure conditions.

#### Manual Globe, Gate and Check Valves

Gate valves are either solid wedge design or flexible disc and are straight through. All gate valves have backseat and outside screw and yoke.

Globe valves, "T" and "Y" style, are full ported with outside screw and yoke construction with the exception of packless valves.

Check valves are either tilting disc or swing disc type. Stainless steel check valves have no body penetrations other than the inlet, outlet and bonnet. The check hinge is serviced through the bonnet.

The stem packing and gasket of the stainless steel manual globe and gate valves are similar to those described above for motor operated valves. Carbon steel manual valves are employed to pass non-radioactive fluids only and therefore are not required to contain the double packing and seal weld provisions.

#### Diaphragm Valves

The diaphragm valves are of the Saunders patent type which uses the diaphragm member for shut off with even weir bodies. These valves are used in systems not exceeding 189°F and 220 psig design temperature and pressure.

#### Accumulator Check Valves

The accumulator check valve is designed with a low pressure drop configuration with all operating parts contained within the body. The pressure containing parts are designed in accordance with ASME Boiler and Pressure Vessel Code, Section III.

Design considerations and analyses which assure that leakage across the check valves located in each accumulator injection line do not impair accumulator availability are as follows:

1. During normal operation the check valves are in the closed position with accumulator pressure equalized across the disc. Since the valves remain in this position except for testing or when called upon to function, and are not, therefore, subject to the abuse of flow operation or impact loads caused

by sudden flow reversal and seating, they do not experience significant wear of the moving parts, and hence are expected to function with minimal leakage.

2. When the Reactor Coolant System is being pressurized during the normal heatup operation, the check valves are tested for leakage when there is a stable differential pressure of about 100 psi or more across the valve. This test confirms the seating of the disc and whether or not there has been an increase in the leakage since the last test. When this test is completed, the discharge line motor operated isolation valves are opened and the Reactor Coolant System pressure increase is continued. There should be no increase in leakage from this point on since increasing reactor coolant pressure increases the seating force and decreases the probability of leakage.
3. The experience derived from the check valves employed in the emergency injection system indicate that the system is reliable and workable; check valve leakage has not been a problem. This is substantiated by the satisfactory experience obtained from operation of the Ginna and subsequent plants where the usage of check valves is identical to this application.
4. The accumulators can accept some in-leakage from the Reactor Coolant System without affecting availability. In-leakage would require, however, that the accumulator water volume be adjusted according to Technical Specification requirements. An alarm is also provided as an added safeguard against excessive accumulator in-leakages.

#### Butterfly Valves

Each main residual heat removal line has an air-operated butterfly valve which is normally open and is designed to fail in the open position. These valves are left in the full open position during normal operation to maximize flow from this system to the Reactor Coolant system during the injection mode of the Emergency Core Cooling System operation.

#### Piping

The piping layouts for the ECCS are shown in [Figure 6-182](#). All piping joints and most component connections are welded; others are bolted flanges.

Weld connections for pipes sized 2-1/2 inches and larger are butt welded. Reducing tees are used where the branch size exceeds one-half of the header size. Branch connections of sizes that are equal to or less than one-half of the header size conform to the ANSI code. Branch connections 1/2 inch through 2 inches are attached to the header by means of full penetration welds, using pre-engineered integrally reinforced branch connections.

Minimum piping and fitting wall thicknesses as determined by ANSI B31.1.0-1967 edition formula are increased to account for the manufacturer's permissible tolerance of minus 12-1/2 percent on the nominal wall and an appropriate allowance for wall thinning on the external radius during any pipe bending operations in the shop fabrication of the subassemblies.

The ECCS water boron concentration is maintained sufficiently low enough ([Table 6-124](#)), that boron crystallization is not expected to occur so long as the water is maintained at a temperature above freezing.

#### **6.3.2.2 System Operation**

The operation of the Emergency Core Cooling System, following a loss of coolant accident, can be divided into two distinct modes:

1. The injection mode in which any reactivity increase following the postulated accidents is terminated, initial cooling of the core is accomplished, and coolant lost from the primary system in the case of a loss of coolant accident is replenished, and

2. The recirculation mode in which long term core cooling is provided during the accident recovery period.

Discussion of these modes follows.

#### Break Spectrum Coverage

The principal mechanical components of the Emergency Core Cooling System which provide core cooling immediately following a loss of coolant accident are the accumulators, the safety injection pumps, the centrifugal charging pumps, the residual heat removal pumps, refueling water storage tank, and the associated valves, and piping.

For large pipe ruptures, the Reactor Coolant System would be depressurized and voided of coolant rapidly, and a high flow rate of emergency coolant is required to quickly cover the exposed fuel rods and limit possible core damage. This high flow is provided by the passive cold leg accumulators, the charging pumps, safety injection pumps, and the residual heat removal pumps discharging into the cold legs of the Reactor Coolant System. The residual heat removal and safety injection pumps deliver into the accumulator injection lines, between the two check valves, during the injection mode. The charging pumps deliver directly into cold legs.

Emergency cooling is provided for small ruptures primarily by the high head injection pumps<sup>1</sup>. Small ruptures are those, with an equivalent diameter of 6 inches or less, which do not immediately depressurize the Reactor Coolant System below the cold leg accumulator discharge pressure. The centrifugal charging pumps deliver borated water at the prevailing Reactor Coolant System pressure to the cold legs of the Reactor Coolant System. During the injection mode, the charging pumps take suction from the refueling water storage tank. The pumps discharge directly into the Reactor Coolant System.

The safety injection pumps also take suction from the refueling water storage tank and deliver borated water to the cold legs of the Reactor Coolant System. The safety injection pumps begin to deliver water to the Reactor Coolant System after the pressure has fallen below the pump shutoff head.

The residual heat removal pumps take suction from the refueling water storage tank and deliver borated water to the Reactor Coolant System. These pumps begin to deliver water to the Reactor Coolant System only after the pressure has fallen below the pump shutoff head.

Core protection is afforded with the minimum Engineered Safety Feature equipment. The minimum Engineered Safety Feature equipment is defined by consideration of the single failure criteria as discussed in Section [3.1](#). The minimum design case ensure the entire break spectrum is accounted for and core cooling design bases of Section [6.3.1](#) are met. The analyses for these cases are presented in Section [15.6.5](#).

For large Reactor Coolant System ruptures, the accumulators and the active high head and low head pumping components serve to complete the core refill. One residual heat removal pump is required for long term recirculation.

If the break is small (6 inch equivalent diameter or less) the accumulators with one charging pump and one safety injection pump ensure adequate cooling during the injection mode. Long term recirculation requires one residual heat removal pump and components of the auxiliary heat removal systems which are required to transfer heat from the Emergency Core Cooling System (e.g., Component Cooling System and Nuclear Service Water System). The loss of coolant analyses are presented in Section [15.6.5](#).

---

<sup>1</sup> The charging pumps and safety injection pumps are commonly referred to as “high head pumps” and the residual heat removal pumps as “low head pumps.” Likewise, the term “high head injection” is used to denote charging pump and safety injection pump injection and “low head injection” refers to residual heat removal pump injection.

Certain modifications (i.e., reduced component availability) to the normal operating status as given in [Table 6-124](#) the Emergency Core Cooling System are permissible without impairing the ability of the Emergency Core Cooling System to provide adequate core cooling capability. Accordingly, Technical Specifications have been established to cover these modifications.

A discussion of allowable delays in actuation of components is presented in Section [6.3.3.6](#).

Accumulator injection occurs when the RCS is depressurized below accumulator operating pressure.

The cold leg injection accumulators can be isolated from the RCS by closure of their motor operated isolation valves.

#### Injection Mode After Loss Of Primary Coolant

The injection mode of emergency core cooling is initiated by the safety injection signal ("S" signal). This signal is actuated by any of the following:

1. Low pressurizer pressure
2. High Containment pressure
3. Manual actuation

Operation of the Emergency Core Cooling System during the injection mode is completely automatic except for the CCP minimum flow bypass line valves (see Section [6.3.2.17](#)). Refer to [Figure 7-1](#) for complete safety injection logic and control diagrams. The safety injection signal automatically initiates the following actions:

1. Starts the diesel generators and, if all other sources of power are lost, aligns them to the shutdown boards.
2. Starts the charging pumps, the safety injection pumps, and the residual heat removal pumps.
3. Aligns the charging pumps for injection by:
  - a. Opening the valves in the charging pump discharge line to the four RCS cold legs.
  - b. Closing the valves in the charging pump discharge line to the normal charging line.
  - c. Opening the valves in the charging pumps suction line from the refueling water storage tank.
  - d. Closing the valves in the charging pump normal suction line from the volume control tank.

Remotely operated valves for the injection mode which are under manual control (i.e., valves which normally are in their ready position and do not require a safety injection signal) have their positions indicated on a common portion of the control board. If a component is out of its proper position, its monitor light indicates this on the control panel. At any time during operation when one of these valves is not in the ready position for injection, this condition is shown visually on the board, and an audible alarm is sounded in the Control Room.

Upon receipt of the RWST pre-low level alarm, the operator verifies adequate sump level is available for RHR pump operation. If the minimum required level is not available, the RHR pumps will be secured and restarted when adequate containment sump level is indicated if required by procedure.

The injection mode continues until the low level is reached in the refueling water storage tank at which time the recirculation mode is initiated.

#### Recirculation Mode

Water level indication, in the sump and in the RWST, and alarms on the RWST provide ample warning to terminate the injection mode while the operating pumps still have adequate net positive suction head. Since the injection mode of operation following a loss of coolant accident is terminated before the RWST

is completely emptied, all pipes are kept filled with water and suction will not be lost for any of the ECCS pumps.

Automatic opening of the isolation valves in the containment sump suction lines to the RHR pumps (NI184B and NI185A), and automatic closure of the isolation valves in the suction lines from the RWST to the RHR pumps (ND19A and ND4B), initiate the changeover from injection to recirculation. Manual actions by the operators complete the switchover.

The switchover sequence (as delineated in [Table 6-125](#)) is followed regardless of which power supply is available (offsite or emergency onsite). The control room operator is assumed to require a maximum of 195 seconds to accomplish steps M1 through M5.b=, and 240 seconds for steps M21 through M30.

A scenario in which one of the isolation valves in the suction lines from the RWST to the RHR pumps fails to close is limiting since the RWST outflow is maximized for this case. The time required to complete the operation is the time required for an operator to perform manual operations, switchgear to operate and equipment to respond. Controls for Emergency Core Cooling System components are grouped together on the main control board. The component position lights verify when the function of a given switch has been completed.

A failure analysis which reviews the most critical operator errors is delineated in [Table 6-127](#).

The RWST level alarms and setpoints are designed to meet single failures, including spurious valve movement. The signal for initiating the switchover is derived from RWST level instrumentation which is actuated at a water level corresponding to 74,284 gallons above the lower level instrument tap for the wide range instrumentation. This is the low level setpoint. This signal in turn automatically opens the isolation valves in the containment sump suction lines to the RHR pumps (NI184B and NI185A). The RHR pump/RWST isolation valves (ND4B and ND19A) in each pump suction line automatically close when the corresponding containment sump valve reaches its full open position.

A control room alarm will alert the operator that the RHR pumps have been switched over automatically and the remaining ECCS pumps must be switched over manually using the procedure in [Table 6-125](#). The RWST low low level alarm is actuated at 15,639 gallons above the lower level instrument tap for the wide range instrumentation.

If containment pressure is above 3.0 psig, one spray pump will be manually started after switchover, taking suction from the containment sump upon verification of adequate sump level.

After the injection phase, water collected in the containment sump is cooled and returned to the Reactor Coolant System by the low head/high head recirculation flow path. The Reactor Coolant System can be supplied simultaneously from the RHR pumps discharge to the RCS cold legs and/or from a portion of this discharge taken after the residual heat exchangers. This portion is then directed to the charging pumps and safety injection pumps, which return the water to the Reactor Coolant System. The latter mode of operation assures flow in the event of a small rupture where the depressurization proceeds more slowly such that the Reactor Coolant System is still in excess of the shutoff head of the residual heat removal pumps at the onset of recirculation.

The design of the Emergency Core Cooling System includes the provision for diversion of a portion of the RHR pump flow from the low head injection path to auxiliary spray headers in the upper containment volume. For this mode, the RHR pumps continue to supply recirculation flow from the containment sump to the core via the safety injection and centrifugal charging pumps.

The diversion of the RHR flow from the low head injection path to the auxiliary spray headers occurs only after the switchover to the recirculation mode greater than 50 min from event initiation and only in the event that containment pressure exceeds a certain pressure.

This procedure requires that low head safety injection flow to the core be terminated prior to initiating RHR spray flow. If RHR flow were allowed to be directed simultaneously to the low head injection path,

the auxiliary spray header, and the suction of the high head (centrifugal charging and safety injection) pumps, the resulting flow would not exceed design and no pump damage would result. Section [6.3.3.9](#) provides additional discussion regarding RHR spray.

In accordance with emergency operating instructions, and several hours after the switchover to recirculation, hot leg recirculation is initiated to ensure termination of boiling and preclude excessive boron concentration in the reactor vessel. To begin the manual changeover, the electrical power to the hot leg recirculation valves must be returned. The operator then performs the operations as delineated in [Table 6-129](#). Note that if residual containment spray is required from an operating RHR train, that train would not be aligned to RHR hot leg injection (back-up to safety injection pump hot leg recirculation) in order to preserve the residual containment spray flow. During and upon completion of switchover, the operator can quickly access proper system alignment by scanning the monitor light panel.

The RWST is protected from inadvertent pressurization from the Reactor Coolant System. All connections to the RWST are provided with valves that prevent inadvertent flow to the tank. When the Reactor Coolant System is hot and pressurized, there is no direct flow path to the RWST. When the Reactor Coolant System is being cooled and the RHR System is in service, the RHR System is isolated from the RWST by a manual valve, and a motor operated valve in series with a check valve.

Redundancy in the external recirculation loop is provided for by the inclusion of duplicate charging, safety injection, and RHR pumps and residual heat exchangers. Inside the containment, the charging pump and safety injection pump discharge are piped separately into all four cold legs. The safety injection pumps further provide flow to all four hot legs, two of which are common to RHR.

The RHR pumps take suction through redundant lines from the containment sump and discharge through the four cold legs (common injection point with cold leg accumulators and Safety Injection Pumps) to the Reactor Coolant System. This design provides adequate NPSH for the RHR pumps to operate in the recirculation mode.

The design of the containment ECCS sump strainer is discussed further in Section [6.5.2](#).

Each recirculation line from the sump is run outside the Containment to a sump isolation valve. Any excessive leakage or passive failure downstream of the sump valves can be contained and isolated from the sump by closure of the sump valve in the affected train. Passive failures are not required to be postulated upstream of the sump valves due to the low stress levels.

Pressure relieving devices, from portions of the Emergency Core Cooling System located outside Containment which might contain radioactivity, discharge to the pressurizer relief tank.

During recirculation, significant margin exists between the design and operating conditions (in terms of pressure and temperature) of the Emergency Core Cooling System components.

Since redundant flow paths are provided during recirculation, a leaking component in one of the flow paths may be isolated. This action curtails any further leakage and renders the component available for corrective maintenance. Maximum potential leakage from components during normal operation is given in [Table 6-130](#).

### **6.3.2.3 Applicable Codes and Classifications**

The codes and standards to which the individual components of the ECCS are designed are listed in [Table 3-4](#).

### **6.3.2.4 Materials Specifications and Compatibility**

Materials employed for components of the ECCS are given in [Table 6-131](#). Materials are selected to meet the applicable material requirements of the codes in [Table 3-4](#) and the following additional requirements:

1. All parts of components in contact with sump solution during recirculation are fabricated of austenitic stainless steel or equivalent corrosion resistant material.
2. All parts of all components in contact with borated water are fabricated or clad with, austenitic stainless or equivalent corrosion resistant material, with the exception of pump seals and valve packing.
3. Valve seating surfaces are hardfaced with Stellite No. 6 or equivalent to prevent galling and reduce wear.
4. Valve stem materials are selected for their corrosion resistance, high tensile properties, and resistance to surface scoring by the packing.

The elevated temperature of the sump solution is well within the design temperature of all the Emergency Core Cooling System components. In addition, consideration has been given to the potential for corrosion of various types of metals exposed to the fluid conditions prevalent immediately after the accident or during the long term recirculation operations.

Environmental testing of the Emergency Core Cooling System equipment inside the Containment, which is required to operate following a loss-of-coolant accident is discussed in reference (1). The chemistry used in the test program was obtained by using a spray solution similar to that of a post accident environment resulting from the release of sodium-tetraborate following the ice-melt. The ice-melt is discussed in greater detail in Section 6.2. The results of the test program indicate that the safety features operate satisfactorily during and following exposure to the combined Containment post-accident environments of temperature, pressure, chemistry, and radiation.

Deleted paragraph(s) per 2002 revision.

#### **6.3.2.5 Design Pressures and Temperatures**

The component design pressures and temperatures are presented in [Table 6-123](#).

#### **6.3.2.6 Coolant Quantity**

The minimum storage volume for the accumulators and the refueling water storage tank is given in [Table 6-124](#). The minimum storage volume in the RWST and the accumulators is sufficient to ensure that, after a Reactor Coolant System break, sufficient water is injected and is available within the Containment to permit recirculation cooling flow to the core, and to meet the net positive suction head requirements of the residual heat removal pumps. A further discussion of coolant requirements is contained in [Chapter 15](#).

Credible NC System break locations have been identified that may cause a diversion of coolant inventory to the Incore Instrument Room, where it would not be recoverable for ECCS Sump operation. UFSAR Section 6.3 describes the ECCS system design and expected system LOCA response, but the LOCA sequence for ECCS injection and transfer to cold-leg recirculation was based on the limiting large break LOCA. The UFSAR Section 15.6.5 accident analysis addresses SBLOCA break sizes of 3", 4" and 6" diameter, which were intended to be the bounding cases with respect to fuel clad considerations.

For a postulated range of less limiting breaks within the incore room, the containment sump level may be less than the normal swapper minimum level of approximately 3 feet at the time of RWST low level. Sump inventory would be limited due to the combination of inventory diversion and diminished ice melt. Emergency Procedures (EPs) ensure the RHR pumps are secured if adequate sump level cannot be verified at the FWST Pre-Low level alarm. The RHR pumps are manually restarted (if required) when adequate sump level is indicated. Adequate sump level is assured prior to reaching the RWST low-low level.

### 6.3.2.7 Pump Characteristics

Performance curves for the residual heat removal pumps are given in [Figure 6-179](#). Performance curves for the centrifugal charging pumps are given in [Figure 6-181](#). Power requirements for these pumps are given in Section [8.3](#).

### 6.3.2.8 Heat Exchanger Characteristics

Residual heat exchanger characteristics are found in Section [5.5.7](#).

### 6.3.2.9 ECCS Flow Diagrams

ECCS diagrams are given as [Figure 6-182](#) through [Figure 6-183](#).

### 6.3.2.10 Relief Valves

The ECCS relief valves, their capacities and settings are given in [Table 6-132](#).

The accumulator relief valves are sized to pass nitrogen gas at a rate in excess of the accumulator gas fill line delivery rate. The relief valves also pass water in excess of the expected accumulator in-leakage rate, but this is not considered to be necessary, because the time required to fill the gas space gives the operator ample opportunity to correct the situation. Other relief valves are installed in various sections of the Emergency Core Cooling System to protect lines which have a lower design pressure than the Reactor Coolant System. The valves are of the enclosed bonnet type which provides an additional barrier for isolating system fluids.

### 6.3.2.11 System Reliability

#### Definitions Of Terms

Definitions of terms used in this section are located in Section [3.1](#).

#### Active Failure Criteria

The Emergency Core Cooling System is designed to accept any single failure at any time following the incident without loss of its protective function. The system design tolerates the failure of any single active component in the Emergency Core Cooling System itself or in the necessary associated service systems at any time during the period of required system operations following the incident.

A single active failure analysis is presented in [Table 6-133](#), and demonstrates that the ECCS can sustain the failure of any single active component in either the short or long term or any passive component failure in the long term (see [Table 6-134](#)) and still meet the level of performance for core cooling.

Since the operation of the active components of the Emergency Core Cooling System following a steam line rupture is identical to that following a loss-of-coolant accident, the same analysis is applicable, and the Emergency Core Cooling System can sustain the failure of any single active component and still meet the level of performance for the addition of shutdown reactivity. Passive failure is not considered for the short term.

In response to Generic Letter 2008-01 "Managing Gas Accumulation in ECCS, Decay Heat Removal, and Containment Spray Systems", an evaluation concluded that system procedures and design are adequate to maintain the ECCS sufficiently full of water to ensure operability. Inadequate system fill and vent can result in pump cavitation, pump gas binding, or water hammer. The complete Duke response can be viewed via Reference [17](#).

#### Passive Failure Criteria

The following philosophy provides for necessary redundancy in component and system arrangement to meet the intent of the NRC General Design Criteria on single failure as it specifically applies to failure of passive components in the ECCS. Thus, for the long term, the system design is based on accepting either a passive or an active failure.

#### Redundancy of Flow Paths And Components For Long-Term Emergency Core Cooling

In design of the Emergency Core Cooling System, Westinghouse utilized the following criteria:

1. During the long-term cooling period following a loss-of-coolant, the emergency core cooling flow paths are separable into two subsystems, either of which can provide minimum core cooling functions and return spilled water from the floor of the Containment back to the Reactor Coolant System.
2. Either of the two subsystems can be isolated and removed from service in the event of a leak outside the Containment.
3. Adequate redundancy of check valves is provided to tolerate failure of a check valve during the long-term as a passive component.
4. Should one of these two subsystems be isolated in this long-term period, the other subsystem remains operable.
5. Provisions are also made in the design to detect leakage from components outside the Containment, collect this leakage and to provide for maintenance of the affected equipment.

Thus, for the long-term emergency core cooling function, adequate core cooling capacity exists with one flow path removed from service whether isolated due to a leak, because of blocking of one flow path, or because failure in the Containment results in a spill of the delivery of one injection flow path.

#### Subsequent Leakage from Components in Safeguards Systems

With respect to piping and mechanical equipment outside the Containment, considering the provisions for visual inspection and leak detection, leaks are detected before they propagate to major proportions. A review of the equipment in the system indicates that the largest sudden leak potential would be the sudden failure of a pump shaft seal. Evaluation of leak rate assuming only the presence of a seal retention ring around the pump shaft showed flows less than 50 gpm would result. Shaft leak rates have been calculated for bushings (assuming only the presence of a seal retention ring) of the design used in the residual heat removal pumps. The leak rates shown in [Figure 6-185](#) were determined using the following equation:

$$Q = \frac{VA}{0.321}$$

where

Q = leakage (gpm)

A = bushing clearance area (in<sup>2</sup>)

V = velocity (fps), defined by

$$V^2 = \frac{2h_L g}{F(L/d) + 1.5}$$

**Note:** The above equation was revised in 1999 update.

where

$h_L$  = head loss-ft. (related to pressure differential across the bushing)

$g$  = acceleration of gravity

$F$  = friction factor = 0.15

$L$  = bushing length = 5/16 in.

$d$  = diametrical bushing clearance (in.)

Actual pump shaft leak rates have been determined in tests performed on bushings similar in design and construction to those used in the residual heat removal pumps. The test program was performed to determine the performance characteristics of the bushing under simulated normal operating conditions, as well as under simulated extreme conditions.

The testing included in excess of 1000 hours of operation under various conditions. The final phase of testing to simulate extreme conditions consisted of operation at 3600 rpm with 2 percent boric acid solution at 160°F - 180°F fluid temperature over a pressure range of 0-60 psig. The leakage rate (as a function of pressure) after severe operation is shown in [Figure 6-186](#).

The tested bushing showed no signs of distress or degradation at the conclusion of the test program.

Both the calculated and experimentally determined bushing leak rates demonstrate that, in the event of a sudden pump shaft seal failure, the leak rate would be significantly less than 50 gpm.

Piping leaks, valve packing leaks, or flange gasket leaks have been of a nature to build up slowly with time and are considered less severe than the pump seal failure.

Larger leaks in the Emergency Core Cooling System are prevented by the following:

1. The piping is classified in accordance with ANS Safety Class 2 and receives the ASME Code 2 quality assurance program associated with this safety class.
2. The piping, equipment and supports are designed to insure no loss of function for the safe shutdown earthquake.
3. The system piping is located within a controlled area on the site.
4. The piping system receives periodic pressure tests and is accessible for periodic visual inspection.
5. The piping is austenitic stainless steel which, due to its ductility, can withstand severe distortion without failure.

Based on this review, the Auxiliary Building and related equipment is designed for handling leaks up to a maximum of 50 gpm. The use of instruments to identify the location and the safeguards train that sustained the failure is not feasible. Pressure and flow instrumentation would not indicate the change in pressure or flow if a passive failure occurred due to the minor effects on the flow characteristics. However indications are available to detect abnormal inputs into the sumps in the lowest level of the Auxiliary Building. Additional, a control room annunciator is actuated when sump levels exceed normal levels and a control room gage monitors water level above floor level at 695'. Any indication of abnormal conditions would prompt operator action. The ND/NS sump pumps transfer water to the Waste Evaporator Feed Tank (WEFT) or the Floor Drain Tank (FDT). These tanks are maintained at a level such that under abnormal input conditions into the ND/NS sump, an alarm or Control Room annunciator will be actuated before either tank would overflow. If leakage was not isolated and tank contents not processed, the WEFT and/or FDT would overflow and eventually begin flooding the Auxiliary Building lowest level. There is sufficient hold-up capacity in the lowest level to prevent adverse affect on safety-related Residual Heat Removal equipment with a 50 gpm leak sustained for approximately 45 hours. If leakage were to occur in areas that do not drain to the ND/NS sump, water would be directed to the FDT via the floor drain system. Unanticipated FDT levels of 80% or more would prompt investigation by Chemistry personnel.

The containment sump isolation valves are conservatively designed to 600 psig and 400°F. During and subsequent to a LOCA, the maximum pressure at this valve will be only 25 psig. With the valves 15 packing rings intact, the shaft leakage would be negligible. In addition to the packing rings, the valve has a backseat which would prevent shaft leakage when the valve is open. Leakage past the shaft (through the packing) would not exceed 17.5 gpm, assuming a single failure. This is well below the maximum assumed leak rate for any single failure of 50 gpm. With this relatively small leak rate, adequate time is available for the operator to detect and isolate the leak by closing the valve which in turn isolates the bonnet area from the process pipe.

The sump valve operators are designed to operate in an environment of 100 percent relative humidity at 148°F per IEEE 382-1980. The actuator enclosures are sealed by water tight o-rings per NEMA 6, IEC 529-1P67. [Figure 6-187](#) presents a cutaway view of a similar actuator and shows the locations of all the o-rings. These valve actuators have been qualified to withstand the effects of containment spray, even though they would not be exposed to this condition. Thus, due to the design of the operators, there will be no deleterious effects due to stem leakage.

#### Submerged Valves

All motor operated valves located below the maximum LOCA water level are categorized as to their operation in relation to flooding. These three cases are:

- Case #1 The valve is not required to post-LOCA operation of any of the safeguard systems. Therefore, operation subsequent to flooding is unnecessary.
- Case #2 The valve is normally in the post-LOCA position. Therefore, it is not required to reposition before or after flooding.
- Case #3 The valve receives a safety signal to close upon the occurrence of a LOCA and is not required to reposition subsequent to flooding.

Motor operated valves which are located below the maximum LOCA water level above elevation 725' + 0" fall into the above categories as listed below:

Case #1	Valve No.	Elevation	Description
	1KC394A	730'+0"	Reactor coolant pump 1A thermal barrier cooling water isolation valve. It is not required for post-LOCA operation.
	1KC345A	727'+6"	Reactor coolant pump 1C thermal barrier cooling water isolation valve. It is not required for post-LOCA operation.
	1KC364B	727'+6"	Same as for 1KC345A except valve is an isolation for pump 1B.
	1KC413B	727'+6"	Same as for 1KC345A except valve is an isolation for pump 1D.
Case #2	Valve No.	Elevation	Description
	1ND1B	737'+2-7/8"	Isolation valves between the Reactor Coolant and Residual Heat Removal System. They are normally closed (LOCA position) and receive no engineered safeguards signal.
	1ND2AC	740'+4-3/16"	

Case #2	Valve No.	Elevation	Description
	1NI54A	733'+0"	Cold leg accumulator isolation valves. These valves are normally open and deenergized. However, if a valve is closed, it receives a S <sub>s</sub> signal to open and is thus open prior to flooding.
	1NI65B	733'+0"	
	1NI76A	733'+0"	
	1NI88B	733'+0"	
Case #3	Valve No.	Elevation	Description
	1BB5A	734'+1"	Containment isolation valves which receive an S <sub>t</sub> signal.
	1BB6A	730'+3"	
	1BB7A	734'+1"	
	1BB8A	730'+3"	
	1KC332B	739'+9"	Containment isolation valves which receive an S <sub>t</sub> signal.
	1KC429B	730'+3"	
	1NC54A	730'+3"	Containment isolation valve which receives an S <sub>t</sub> signal.
	1NI95A	728'+9"	Containment isolation valve which receives an S <sub>t</sub> signal.
	1NM22A	740'+2 1/2"	Containment isolation valves which receive an S <sub>t</sub> signal.
	1NM25A	740'+11 1/4"	
	1NM72B	734'+5"	
	1NM75B	733'+6"	
	1NM78B	734'+0"	
	1NM81B	733'+6"	
	1NM190A	732'+6"	
	1NM200B	731'+9"	
	1NM210A	731'+9"	
	1NM220B	731'+9"	
	1NV94A	732'+6 1/2"	Containment isolation valve which receives an S <sub>t</sub> signal.
	1RN253A	732'+10"	Reactor coolant pump motor air handling unit cooling water isolation valves. Receive S <sub>p</sub> signal to close on Hi-Hi Containment pressure signal.
	1RN276A	734'+1"	
	1RV33B	734'+1"	Containment isolation valves. Receive S <sub>p</sub> signal to close on Hi-Hi Containment pressure signal.
	1RV76A	734'+1"	
	1WL2A	732'+6"	Containment isolation valve which receives an S <sub>t</sub> signal.
	1WL39A	730'+0"	
	1WL64A	726'+10"	
	1WL321A	734'+1"	

### 6.3.2.12 Protection Provisions

The provisions taken to protect the system from damage that might result from dynamic effects are discussed in Section 3.6. The provisions taken to protect the system from missiles are discussed in Section 3.5. The provisions to protect the system from seismic damage are discussed in Sections 3.7, 3.9 and 3.10. Thermal stresses on the Reactor Coolant System are discussed in Section 5.2.

#### Emergency Core Cooling System Piping Failures

The rupture of the portion of an injection line from the last check valve to the connection of the line to the Reactor Coolant System can cause not only a loss of coolant, but impair the injection as well. To reduce the probability of an emergency core cooling line rupture causing a loss of coolant accident, the check valves which isolate the Emergency Core Cooling System from the Reactor Coolant system are installed as close as possible to the reactor coolant piping.

For a small break, the reactor pressure maintains a relatively uniform back pressure in all injection lines so that a significant flow imbalance does not occur. A rupture in the cold leg accumulator injection line is accounted for in the analyses by assuming that for cold leg breaks the entire contents of the associated accumulator is discharged from the break.

The consequences of the accident described above would be a 10" break which is equivalent to a .5 ft<sup>2</sup> break in the cold leg. The effect of the loss of one Safety Injection train (1 RHR pump, 1 safety injection pump and 1 charging pump) would be to shorten core uncovering time. Flows from the intact and broken injection lines are shown in [Figure 6-199](#). The fluid characteristics are based on the assumption of one train failed and the lowest resistance line spilling to the Containment.

### 6.3.2.13 Provisions for Performance Testing

The provisions incorporated to facilitate performance testing of components are discussed in Section [6.3.4](#).

### 6.3.2.14 Net Positive Suction Head

The Emergency Core Cooling System is designed so that adequate net positive suction head is provided to system pumps in accordance with Regulatory Guide 1.1. To demonstrate that adequate NPSH is provided for the ECCS pumps, it is not necessary to provide a graph of NPSH as a function of time; it is only necessary to demonstrate that the NPSH is adequate under the worst limiting conditions. Adequate net positive suction head is shown to be available for all pumps as follows:

#### 1. Residual Heat Removal Pumps

The net positive suction head of the residual heat removal pumps is evaluated for both the injection and recirculation modes of operation for the design basis accident. The recirculation mode of operation gives the limiting NPSH requirement for the residual heat removal pumps, and the NPSH available is determined from the following equation:

$$\text{NPSH}_{\text{actual}} = \frac{(\text{h}) \text{ containment pressure}}{\text{pressure}} - \frac{(\text{h}) \text{ vapor pressure}}{\text{pressure}} + \frac{(\text{h}) \text{ static head}}{\text{head}} - (\text{h}) \text{ loss}$$

Head loss developed across the ECCS Sump Strainer will tend to be offset over time by increasing sump pool level and decreasing pool vapor pressure (decreasing temperature).

To evaluate the adequacy of the available NPSH, several conservatisms are applied:

- a. No increase in Containment pressure from that present prior to the accident is assumed.
- b. The Containment sump fluid temperature is assumed to be 200°F which envelops the expected sump temperature at the time of sump recirculation initiation.
- c. The static elevation head is calculated from the floor elevation of the sump (elevation 725' + 0") and credits minimum sump level of 3 feet. The elevation of the RHR pump is 699' + 6" (Centerline of discharge pipe).
- d. The head loss is evaluated based on all pumps running at the maximum calculated flow with representative friction factors.

- e. The required NPSH is based on one pump running at a flowrate above its maximum calculated flow rate.
- f. The limiting NPSH available is calculated early in the event at the time of realignment of the pump suction to the ECCS Sump pool from the RWST, and conservatively assumes that most of the debris in the pool that can transport to the strainer has already done so. In actuality the transport paths for a significant portion of this debris are long and circuitous, which would delay arrival at the strainer surface.

Using all of these conservative inputs, the NPSH available is calculated to be >23 feet and the NPSH required is 19 feet. This provides an NPSH margin of > 4 feet. The actual available NPSH will always be greater than the calculated value. The residual heat removal head-capacity and NPSH curves are given in [Figure 6-179](#). Related details of ECCS sump strainer design and performance are given in Section [6.5.2](#), “Generic Letter 2004-02.”

## 2. Safety Injection and Centrifugal Charging Pumps

The net positive suction head for the safety injection pumps and the centrifugal charging pumps is evaluated for both the injection and recirculation modes of operation for the design basis accident. The end of the injection mode gives the limiting NPSH requirement for the safety injection pumps and the centrifugal charging pumps, and the NPSH available is determined from the following equation:

$$\text{NPSH}_{\text{actual}} = \frac{(\text{h}) \text{atmospheric}}{\text{pressure}} - \frac{(\text{h}) \text{vapor}}{\text{pressure}} + \frac{(\text{h}) \text{static}}{\text{head}} - (\text{h}) \text{loss}$$

To evaluate the adequacy of the available NPSH, several conservatisms are applied:

- a. The RWST fluid temperature is assumed to be 100°F.
- b. The static elevation head is calculated taking no credit for water level above the bottom of the RWST (elevation 761' + 2"). Elevations of the ECCS components are given in [Figure 6-182](#).
- c. The head loss is evaluated based on all pumps running at the maximum calculated flow with representative friction factors.
- d. The required NPSH is based on one pump running at its maximum runout flow.

For this limiting case condition, the net positive suction head available is > 55 feet for the safety injection pumps and > 50 feet for the centrifugal charging pumps. The net positive suction head required is 35 feet to the safety injection pumps and 23 feet for the centrifugal charging pumps. The actual available NPSH will always be greater than the calculated value. The head-capacity, and net positive suction head curves for the safety injection pumps are given in [Figure 6-180](#). The head-capacity and net positive suction head curves for the charging pumps are given in [Figure 6-181](#).

### 6.3.2.15 Control of Motor-Operated Isolation Valves

The design of the control circuit for a motor operated isolation valve in a line connecting a cold leg accumulator to the Reactor Coolant System provides protection against inadvertent closure of that valve. Additional discussion regarding alignment and control of the accumulator discharge isolation valves is provided in Sections [6.3.2.16](#) and [7.4.1.6](#). No testing is required during operation. A further discussion of these valves is found in Section [6.3.5.5](#).

### 6.3.2.16 Motor Operated Valves and Controls

Remotely operated valves for the injection mode which are under manual control (i.e., valves normally in the ready position not requiring an SIS signal) have their position indicated on a common portion of the control board. If a component is out of its proper position, its monitor light indicates this on the control panel. At any time during operation when one of these valves is not in the ready position for injection, this condition is shown visually on the board, and an audible alarm is sounded in the Control Room.

The motor operated isolation valves located between the high pressure RCS and the relatively low pressure RHRs are discussed in Sections [5.5.7](#) and [7.4.1.5.1.4](#).

The ECCS is designed to meet the single failure criteria as defined in Section [3.1](#).

To provide additional assurance against the possibility of a spurious movement, power is removed from the following valves.

Cold Leg/Hot Leg Isolation Valves	Accumulator Disch. Valves	RHR Pump Disch. Valves
1NI162A	1NI54A	1NI173A
1NI121A	1NI65B	1NI178B
1NI152B	1NI76A	
1NI183B	1NI88B	

Of the above ten valves, it should be noted that four of the valves, i.e., the accumulator discharge valves, are not required to move during power operation and are only realigned during plant startup and shutdown operations, and when reactor coolant temperature falls below an Emergency Procedure temperature setpoint following a LOCA. The accumulator discharge valves are open during normal operation and above 1000 Psig RCS pressure. Below 1000 Psig, the accumulator discharge valve is closed to prevent inadvertent injection of the accumulator contents into the RCS. Accordingly, these valves normally have power disconnected and are only energized as required. In addition, these valves are equipped with a pressure interlock to assure positive opening during startup and a confirmatory “S” signal to assure positive opening following a LOCA. The remaining six valves are required to realign the ECCS from the cold leg to the hot leg recirculation mode.

The spurious action of 1NI334B has been determined to be acceptable based on minimum safeguards.

The valves listed below are required to function during the ECCS realignment from injection to recirculation:

- 1NI100B SI Pump RWST suction valve
- 1NI185A Containment sump valve
- 1NI184B Containment sump valve
- 1FW27A RHR pump/RWST suction valve
- 1NI147A SI pump miniflow

Power disconnects and/or circuitry logic are employed to eliminate the possibility of spurious valve movement for the above mentioned valves resulting in loss of adequate core cooling.

While the safety injection pumps are running with the normal injection flow paths unavailable, spurious closure of 1NI147A could possibly cause damage to both safety injection pumps. Thus, power is normally disconnected to valve 1NI147A. During switchover, power may be realigned from the Control Room in order to close 1NI147A as delineated in step 16 of [Table 6-125](#).

When the safety injection pumps are running during the injection mode of the postulated LOCA, spurious closure of 1NI100B would cause a loss of injection from both safety injection pumps. To alleviate this problem, power is disconnected to valve 1NI100B. During switchover power may be realigned from the Control Room in order to close 1NI100B as delineated in step 24 of [Table 6-125](#).

Spurious opening of either 1NI184B or 1NI185A during the injection mode of the postulated LOCA would cause the RWST to drain to the sump, thus minimizing the time available to complete switchover. To alleviate this problem a limit switch on 1NI184B will close 1ND4B when 1NI184B reaches its full open position. Correspondingly, as 1NI185A reaches its full-open position, a limit switch on 1NI185A will close 1ND19A. The low design pressure for the McGuire Containment, the piping configuration and the elevation of the RWST ensures that upon spurious opening of either 1NI185 or 1NI184 during the injection phase, check valve 1FW28 would remain open and water would continue to flow from the RWST.

Spurious closure of 1FW27A during the injection mode of the postulated LOCA would cause a loss of injection from both RHR pumps. To alleviate this problem, power is normally disconnected to valve 1FW27A. During switchover, power may be realigned from the Control Room in order to close 1FW27A as delineated in step 11 of [Table 6-125](#).

The above design meets the single failure criteria as delineated in [Table 6-127](#).

In regard to the choice of motor operated valves over manual valves, it is felt that motor operated valves are more reliable and provide added flexibility with respect to system operation following an accident. It should be noted that motor operated valves are sequenced from the control room and thereby provide additional protection to the operator. In the event of a passive failure or leak in the ECCS piping, remote-controlled motor operated valves facilitate rapid isolation, whereas a locally-operated valve might be inaccessible. Moreover, a number of valves must be sequenced shortly after the accident to terminate injection and establish the recirculation mode. The use of motor operated valves provides a means for performing the realignment procedure entirely from the control room and assures that adequate time will be available in which to perform it. Locally operated valves do not provide such assurance.

#### **6.3.2.17 Manual Actions**

The only manual action required by the operator for proper ECCS operation during the injection mode is the isolation of the CCP minimum flow bypass line when RCS pressure drops to the manual reactor coolant pump trip setpoint. Operator action is also required to open the CCP minimum flow bypass line if RCS pressure increases to greater than 2000 psia. The only actions required by the operator for proper ECCS operation following injection mode are those required to realign the system for the cold leg and hot leg recirculation modes of operation.

#### **6.3.2.18 Process Instrumentation**

Process instrumentation available to the operator in the Control Room to assist in assessing post-loss-of-coolant accident conditions are tabulated in Section [7.5](#).

#### **6.3.2.19 Materials**

The ECCS components inside containment are primarily austenitic stainless steels (refer to [Table 6-131](#)). There are some limited exceptions (e.g. CLA block valve actuators and containment sump level instrumentation) in which ECCS components contain some non-stainless steel subcomponents; however, the components are qualified for operation in a post-accident environment (refer to Section [6.3.2.4](#)), as required. The ECCS components are not prone to radiolytic and pyrolytic decomposition. Thus, the total material volumes and chemical compositions are deemed inconsequential.

### 6.3.2.20 General Letter 2004-02

This topic is discussed in Section [6.5.2](#).

## 6.3.3 Performance Evaluation

### 6.3.3.1 Evaluation Model

The following analyses are performed to ensure that the limits on core behavior following a Reactor Coolant System pipe rupture are met by the Emergency Core Cooling System operating with minimum design equipment:

1. Large Pipe Break Analysis
2. Small Line Break Analysis
3. Recirculating Cooling

The flow delivered to the Reactor Coolant System by the Emergency Core Cooling System as a function of reactor coolant pressure with the operation of minimum design equipment is analyzed in [Chapter 15](#).

The design basis performance characteristic is derived from the specified performance characteristic for each pump with a conservative estimate of system piping resistance, based upon piping layouts illustrated in [Figure 6-182](#).

The performance characteristic utilized in the accident analyses includes a decrease in the design head of the pumps for margin. When the initiating incident is assumed to be the severance of an injection line, the injection curve utilized in the analysis accounts for the loss of injection water through the broken line.

### 6.3.3.2 ECCS Performance

#### Large Break LOCA

The large pipe break analysis is used to evaluate the initial core thermal transient for a spectrum of pipe ruptures from a break size of 1.0 ft<sup>2</sup> up to the double ended rupture of the largest pipe in the Reactor Coolant System.

The injection flow from active components is required to control the cladding temperature subsequent to accumulator injection, complete reactor vessel refill, and eventually return the core to a subcooled state. The results indicate that the maximum cladding temperature attained at any point in the core is such that the limits on core behavior as specified in Section [15.6.5](#) are met.

#### Large Break LOCA During Shutdown

The occurrence of a large break LOCA during the plant shutdown process, i.e., from a lower temperature and pressure than full power conditions, has been evaluated on a generic basis for plants with Westinghouse-designed NSS systems (Reference [16](#)). A LOCA from 1000 psig and 425°F was analyzed assuming that core shutdown had occurred at least 2.5 hours previously. This evaluation assumed that the cold leg accumulator isolation valves had just been closed upon reaching this temperature and pressure condition. The evaluation concluded that the peak clad temperature reached would be less than 2200°F acceptance criterion in 10CFR 50.46. McGuire operating procedures for a normal shutdown contain an instruction to cool down to no hotter than 425°F before isolating the cold leg accumulators at 1000 psig.

#### Small Break LOCA

The small pipe break analysis is used to evaluate the initial core thermal transient for a spectrum of pipe ruptures from 3/8 inch diameter up to 1.0 ft<sup>2</sup>. For breaks 3/8 inch or smaller, the charging system can

maintain the pressurizer level at the Reactor Coolant System operating pressure and the Emergency Core Cooling System would not be actuated.

The results of the small pipe break analysis indicate that the limits on core behavior are adequately met, as shown in Section [15.6.5](#).

#### Inadvertent Steam Line Valve Opening

Analyses of reactor behavior following any single active failure in the main steam system which results in an uncontrolled release of steam are included in Section [15.1.4](#). The analyses assume that a single valve (largest of the safety, relief, or bypass valves) opens and fails to close, which results in an uncontrolled cooldown of the Reactor Coolant System.

Results indicate that if the incident is initiated at the hot standby condition, which results in the worst reactivity transient, reactor power may return to as high as 14% RTP. DNB analysis concludes that the ECCS provides sufficient negative reactivity to prevent fuel damage. Thus, the Emergency Core Cooling System provides adequate protection for this incident.

#### Steam Line Rupture

Following a steam line rupture ECCS is automatically actuated to deliver borated water to the Reactor Coolant System from the RWST.

This accident is discussed in detail in Section [15.1.5](#). The limiting steam line rupture is a complete line severance.

When offsite power is not assumed lost, credit is taken for the uninterrupted availability of power for the Emergency Core Cooling System components.

The results of the analysis in Section [15.1.5](#) indicate that the design basis criteria are met. Thus, the Emergency Core Cooling System adequately fulfills its shutdown reactivity addition function.

The safety injection actuation signal initiates identical actions as described for the injection mode of the loss-of-coolant accident, even though not all of these actions are required following a steam line rupture, e.g., the residual heat removal pumps are not required since the Reactor Coolant System pressure remains above their shutoff head.

The charging pumps deliver borated water from the refueling water storage tank, until enough water has been added to the Reactor Coolant System to make up for the shrinkage due to cooldown. The safety injection pumps also deliver borated water from the refueling water storage tank for the interval when the Reactor Coolant System pressure is less than their shutoff pressure. After pressurizer water level has been restored, the injection is manually terminated. A high pressurizer water level alarm in the Control Room would warn the operator to terminate injection flow if this were not done previously.

The sequence of events following a postulated steam line break is described in Section [15.1.5](#).

### **6.3.3.3 Fuel Rod Perforations**

Discussions of peak clad temperature and metal-water reactions appear in Section [15.6.5](#). Analyses of the radiological consequences of RCS pipe ruptures also are presented in Section [15.6.5](#).

### **6.3.3.4 Effects of ECCS Operation on the Core**

The effects of the ECCS on the reactor core are discussed in [Chapter 15](#).

### 6.3.3.5 Use Of Dual Function Components

The Emergency Core Cooling System contains components which have no other cooperation function as well as components which are shared with other systems and perform normal operating functions. Components in each category are as follows:

1. Components of the Emergency Core Cooling System which perform no other function are:
  - a. One accumulator for each loop which discharges borated water into its respective cold leg of the reactor coolant loop piping.
  - b. Two safety injection pumps which supply borated water for core cooling to the Reactor Coolant System with the exception of periodic cold leg accumulator make-up.
  - c. Associated piping, valves and instrumentation.
2. Components which also have a normal operating function are as follows:
  - a. The residual heat removal pumps and the residual heat exchangers: These components are normally used during the latter stages of normal reactor cooldown and when the reactor is held at cold shutdown for core decay heat removal, as described in Section [5.5.7](#). However, during all other operating periods, they are aligned to perform the low head injection function.
  - b. The centrifugal charging pumps: These pumps are normally aligned for charging service. As a part of the Chemical and Volume Control System, the normal operation of these pumps is discussed in Section [9.3.4](#).
  - c. The refueling water storage tank: This tank is used to fill the refueling canal for refueling operations, as described in Section [9.2.5](#). However, during all other operating periods it is aligned to the suction of the safety injection pumps and the residual heat removal pumps. The charging pumps are aligned to the suction of the refueling water storage tank upon receipt of the safety injection signal.

An evaluation of all components required for operation of the Emergency Core Cooling System demonstrates that either:

1. The component is not shared with other systems, or
2. If the component is shared with other systems, it is aligned during normal operation to perform its accident function; or if not aligned to its accident function, two valves in parallel are provided to align the system for injection, and two valves in series are provided to isolate portions of the system not utilized for injection. These valves are automatically actuated by the safety injection signal.

[Table 6-136](#) indicates the alignment of components during normal operation, and the realignment required to perform the accident function.

#### Dependence on Other Systems

Other systems which operate in conjunction with the Emergency Core Cooling System are as follows:

1. The Component Cooling System cools the residual heat exchangers during the recirculation mode of operation. It also supplies cooling water to the residual heat removal pumps during the injection and recirculation modes of operation.
2. The Nuclear Service Water System provides cooling water to the component cooling heat exchangers, charging pumps, the safety injection pumps, and the ESF equipment room coolers.
3. The electrical systems provide normal and emergency power sources for the Emergency Core Cooling System.

4. The Engineered Safety Features Actuation System generates the initiation signal for emergency core cooling.

#### Limiting Conditions for Maintenance During Operation

Maintenance on an active component is permitted if the remaining components meet the minimum conditions for operation and the following conditions are also met:

1. The remaining equipment has been demonstrated to be in operable condition, within its prescribed surveillance interval.
2. A suitable time limit is placed on the total time span of successful maintenance which returns the components to an operable condition, ready to function.

The design philosophy with respect to active components in the high head/low head safety injection system is to provide backup equipment so that maintenance is possible during operation without impairment of the safety function of the system. Routine servicing and maintenance of equipment of this type would generally be scheduled for periods of refueling and maintenance outages.

#### 6.3.3.6 Lag Times

The minimum active components are capable of delivering full rated flow within a specified time interval after process parameters reach the setpoints for the safety injection signal. Response of the system is automatic, with appropriate allowances for delays in actuation of circuitry and active components. The active portions of the system are actuated by the safety injection signal. In analyses of system performance, delays in reaching the programmed trip setpoints and in actuation of components are established on the basis that only emergency onsite power is available. A further discussion of the starting sequence is given in Section [8.3](#).

In the loss-of-coolant accident analysis presented in [Chapter 15](#), safety injection flow to the RCS as a function of system pressure is used as part of the input, and no credit is assumed for the availability of offsite power sources.

For smaller loss-of-coolant accidents, there are some additional delays before the process variables reach their respective programmed trip setpoints since this is a function of the severity of the accident. Allowances are made for this in the analyses of the spectrum of reactor coolant pipe breaks.

#### 6.3.3.7 Thermal Shock Considerations

Thermal shock considerations are discussed in Section [5.2](#).

#### 6.3.3.8 Limits on System Parameters

A comprehensive testing program has been undertaken to demonstrate that the Emergency Core Cooling System components and associated instrumentation and electrical equipment which are located inside the Containment operate for the time period required in the combined post-loss-of-coolant accident conditions of temperature, pressure, humidity, radiation, and chemistry (Reference [1](#)).

Components such as remote motor operated valves and flow and pressure transmitters have been shown capable of operating for the required post-accident periods, when exposed to post-loss-of-coolant environmental conditions. All other Emergency Core Cooling System components are located outside of the Containment.

The specification of individual parameters as given in [Table 6-123](#) and [Table 6-124](#) includes due consideration of allowances for margins over and above the required performance value (e.g., pump flow

and net positive suction head), and the most severe conditions to which the component could be subjected (e.g., pressure, temperature, and flow).

This consideration ensures that the Emergency Core Cooling System is capable of meeting its minimum required level of functional performance.

#### 6.3.3.9 Use of RHR Spray

After switchover to sump recirculation mode greater than 50 min from event initiation, a portion of the low head RHR flow may be diverted from the core low head injection path to the auxiliary spray headers, in lower containment, in the event that containment pressure exceeds the pressure specified in the emergency procedures. This auxiliary containment spray could be aligned during design basis events based on emergency procedure setpoint and potential instrument uncertainty, although it is not credited by the safety analysis to perform a spray function.

If RHR spray is aligned with minimum safeguards, one high head safety injection pump and one centrifugal charging pump would supply the coolant to the core after realignment of a portion of the RHR pump discharge to the auxiliary spray headers. The amount of water which should be supplied to the core at a reactor coolant system pressure of 10 psig (which is approximately the peak containment pressure) is approximately 100 lbm/sec. At 50 minutes after hypothetical LOCA the core has been quenched so that effluent carryover has been terminated. The time that effluent carryover or entrainment from the core ends is conservatively assumed to occur when the core mixture height reaches the 10 foot elevation.

At 50 minutes, the thin and thick metal sensible heat has been removed and temperatures reduced to the saturation temperature for the containment pressure. The only heat generation at saturation time is decay heat.

The decay heat mass boiloff at 50 minutes, which is the time specified in the operating procedures that the RHR low head flow can be diverted to the RHR spray is 61.5 lbm/sec based on the following assumptions:

1. 102 percent of engineered safeguards design rating of 3579 MWt. The engineered safeguards design rating of 3579 MWt is a value used for the original design of the plant.
2. ANS infinite decay heat with 20 percent margin (10CFR 50.46 Appendix K).
3. Coolant entering the core is subcooled by 60 Btu/lbm.

Therefore, the coolant entering the Reactor Coolant System piping is about 200 percent of that required by the decay heat mass boiloff, calculated with conservative assumptions.

#### 6.3.3.10 Boron Precipitation Evaluation

An analysis has been performed to determine the maximum boron concentration in the reactor vessel following a hypothetical LOCA. This analysis used the method and assumptions described in Reference 5 with the principal input parameters given in [Table 6-137](#). The analysis considers the increase in boric acid concentration in the reactor vessel during the long term cooling phase of a LOCA, assuming a conservatively small effective vessel volume including only the free volumes of the reactor core and the upper plenum below the bottom of the hot leg nozzles. This assumption conservatively neglects the mixing of the boric acid solution with directly connected volumes, such as the reactor vessel lower plenum. The calculation of boric acid concentration in the reactor vessel considers a cold leg break of the Reactor Coolant System in which steam is generated in the core from decay heat while the boron associated with the boric acid solution is completely separated from the steam and remains in the effective vessel volume.

The results of the analysis show that the maximum allowable boric acid concentration established by the NRC, which is the boric acid solubility limit minus 4 weight percent, will not be exceeded in the vessel if hot leg injection is initiated approximately 6 hours after the LOCA occurs.

The safety injection flow to the Reactor Coolant System hot legs will exceed (assuming failure of one ECCS train) the decay heat mass boil off (of approximately 35 lbm/sec) at this time. The recommended flow rate should be at least 46 lbm/sec. This hot leg flow will dilute the reactor vessel boron concentration by passing relatively dilute boron solution from the hot leg through the vessel to the cold leg break location. Centrifugal charging pump flow will continue to be provided to the Reactor Coolant System cold legs and will preclude any boron concentration buildup in the vessel for breaks in the hot leg.

A single active failure analysis is presented in [Table 6-133](#). A passive failure analysis is presented in [Table 6-134](#).

Since the ECCS is designed to meet the single failure criterion, no back up means is required to be provided to prevent the buildup of boron concentration. All components of the ECCS are ANS Safety Class 2 and Seismic Category 1.

ECCS testing is discussed in Section [6.3.4](#).

### 6.3.4 Tests and Inspections

In order to demonstrate the readiness and operability of the Emergency Core Cooling System, the components are subjected to periodic tests and inspections. Performance tests of the components were performed in the manufacturer's shop. An initial pre-operational system flow test was performed to demonstrate the proper functioning of all of the components.

Prototype testing was performed to determine the acceptability of the ECCS sump strainer design. The main objective of this test was to determine the head loss across the debris bed under various debris and flow conditions. In addition, testing was performed to ensure that vortices and air ingestion would not occur.

Deleted per 2008 Update.

#### Quality Control

Tests and inspections were carried out during fabrication of each of the Emergency Core Cooling System components. These tests were conducted and documented in accordance with the Quality Assurance program discussed in [Chapter 17](#).

These tests were intended to evaluate the hydraulic and mechanical performance of the passive and active components involved in the injection mode by demonstrating that they had been installed and adjusted so they would operate in accordance with the design intent. These tests were divided into several individual sections that were performed as conditions allowed without compromising the integrity of the tests.

One of these individual sections consisted of system actuation tests to verify the operability of all Emergency Core Cooling System valves initiated by the safety injection "S" signal, the phase A Containment isolation "T" signal, the operability of all safeguard pump circuitry down through the pump breaker control circuits; and the proper operation of all valve interlocks.

Another of the individual sections was the accumulator injection test. The objective of this section was to check the accumulator injection line to verify that the lines are free from obstructions and that the accumulator check valves would operate correctly. The test objectives were met by a low pressure blowdown of each accumulator. The cold leg accumulator test was performed with the reactor head and internals removed.

Another of the individual sections consisted of operational tests of all of the major pumps - i.e., the charging pumps, the residual heat removal pumps, and the safety injection pumps. The purpose of these tests was to evaluate the hydraulic and mechanical performance of the pumps delivering through the flow paths required for emergency core cooling. These tests were divided into two parts: pump operation under miniflow conditions and pump operation at full flow conditions.

The predicted system resistance was verified by measuring the flow in each piping branch, as each pump delivered from the refueling water storage tank to the open reactor vessel, and adjustments were made where necessary to assure that no one branch had an unacceptably low or high resistance. During this flow test, the system was also checked to assure there was sufficient total line resistance to prevent excessive runout of the pump. At the completion of the flow test, the total pump flow and the total flows of the three highest resistance branch lines were compared with the minimum acceptable flows as given in Technical Specifications.

Preoperational testing of the Emergency Core Cooling System conformed to the guidelines of Regulatory Guide 1.79 (Rev. 1) with the following exceptions:

1. The recirculation test was not performed since this mode of operation is checked by analyses and operation of individual components. As described in Section 3.9.1 in-shop tests were performed on ECCS pumps to qualify the pumps for minimum available NPSH. In addition the ECCS was tested as described in Section 6.3.4 to verify proper pump and valve operation using the refueling water storage tank as the suction source. As stated in Sections 6.3.2.14 and 6.5.2, there was more than adequate margin in NPSH requirements to account for any differences in test loop and installed conditions.

Prototype testing has determined that vortex suppression grating and enclosure solid top plate prevent the strainer modules from ingesting air via vortex.

A replacement intake strainer of approximately 1700 square feet is installed. To verify acceptability of this replacement strainer, testing was performed on a prototype strainer section. This testing, in addition to analysis of the entire strainer assembly, verified that the greatly increased surface area of the replacement strainer was acceptable for ECCS flowrates and filtration with acceptable head loss.

Based on the above tests and analyses, it was Duke's position that a recirculation test was not required.

2. Core flooding accumulator isolation valves were tested under maximum differential pressure conditions of zero RCS pressure and maximum expected accumulator precharge pressure utilizing both normal and emergency power to the isolation valves. This is acceptable since the isolation valve operators are supplied from motor control centers that receive power from either a normal or emergency power source.
3. Flow test, hot operating conditions, were done with RCS temperature at greater than 500°F versus normal operating temperature.

Deleted paragraph(s) per 2002 revision.

#### Periodic Component Testing

Routine periodic testing of the Emergency Core Cooling System components and all necessary support systems is performed. Valves which operate after a loss of coolant accident are operated through a complete cycle, and pumps are operated individually on their miniflow lines. If such testing indicates a need for corrective maintenance, the redundancy of equipment in these systems permits such maintenance to be performed without shutting down or reducing load under certain conditions. These conditions include considerations such as the period within which the component should be restored to service and capability of the remaining equipment to provide the minimum required level of performance during such a period.

The operation of the remote stop valve and the check valve in each accumulator tank discharge line may be tested by opening the remote test line valves just downstream of the stop valve and check valve respectively. Flow through the test line can be observed on instruments and the opening and closing of the discharge line stop valve can be sensed on this instrumentation.

Test lines are provided for periodic checks of the leakage of reactor coolant back through the accumulator discharge line check valves and to ascertain that these valves seat whenever the Reactor Coolant System pressure is raised. Normally, this test is routinely performed when the reactor is being returned to power after an outage and the reactor pressure is raised above the accumulator pressure. To implement the periodic component testing requirements, Technical Specifications have been established. During periodic system testing, a visual inspection of pump seals, valve packings, flanged connections, and relief valves is made to detect leakage. Inservice inspection provides further confirmation that no significant deterioration is occurring in the Emergency Core Cooling System fluid boundary.

1. Active components may be tested periodically for operability (e.g., pumps on miniflow, certain valves, etc.).
2. An integrated system actuation test<sup>2</sup> can be performed when the unit is cooled down and the Residual Heat Removal System is in operation. The Emergency Core Cooling System is arranged so that no flow is introduced into the Reactor Coolant System for this test.
3. An initial flow test of the full operational sequence can be performed.

The design features which assure this test capability are specifically:

1. Power sources are provided to permit individual actuation of each active component of the Emergency Core Cooling System.
2. The safety injection pumps can be tested periodically during operation using the minimum flow recirculation lines provided.
3. The residual heat removal pumps are used every time the Residual Heat Removal System is put into operation. They can also be tested periodically when the unit is at power using the miniflow recirculation lines.
4. The centrifugal charging pumps are either normally in use for charging service or can be tested periodically on miniflow.
5. Remote operated valves can be exercised during routine maintenance.
6. Level and pressure instrumentation are provided for each accumulator tank, for continuous monitoring of these parameters during operation.
7. Flow from each accumulator tank can be directed at any time through a test line to determine check valve leakage and to demonstrate operation of the accumulator motor operated valves.
8. A flow indicator is provided in the safety injection pump header, and in the residual heat removal pump headers. Pressure instrumentation is also provided in these lines.
9. An integrated system test can be performed when the unit is cooled down and the Residual Heat Removal System is in operation. This test does not introduce flow into the Reactor Coolant System but does demonstrate the operation of the valves, pump circuit breakers, and automatic circuitry

---

<sup>2</sup> Details of the testing of the sensors and logic circuits associated with the generation of a safety injection signal together with the application of this signal to the operation of each active component are given in [Section 7.2](#).

including diesel starting and the automatic loading of Emergency Core Cooling System components on the diesels (by simultaneously simulating a loss of offsite power to the vital electrical buses).

The Emergency Core Cooling System components are designed and fabricated to permit inspection and in-service tests in accordance with ASME Code Section XI.

Deleted paragraph(s) per 2002 revision.

### **6.3.5 INSTRUMENTATION APPLICATION**

Instrumentation and associated analog and logic channels employed for initiation of Emergency Core Cooling System operation are discussed in Section 7.3. This section describes the instrumentation employed for monitoring Emergency Core Cooling System components during normal operation and also Emergency Core Cooling System post accident operation. All alarms are annunciated in the Control Room.

#### **6.3.5.1 Temperature Indication**

##### Residual Heat Exchanger Inlet and Outlet Temperature

The fluid temperature at the inlet and outlet of each residual heat exchanger is recorded in the Control Room.

##### Refueling Water Storage Tank (RWST) Temperature

Three temperature channels are provided to monitor the RWST temperature. One channel ties to a receiver gauge on the main control board. A 2/3 channel circuit actuates a computer and annunciator alarm and controls the tank heaters.

#### **6.3.5.2 Pressure Indication**

##### Safety Injection Header Pressure

Safety injection pump discharge header pressure is indicated in the Control Room.

##### Accumulator Pressure

Duplicate pressure channels are installed on each cold leg accumulator. Pressure indication in the Control Room and high and low pressure alarms are provided by each channel.

##### Test Line Pressure

A local pressure indicator used to check for proper seating of the accumulator check valves between the injection lines and the Reactor Coolant System is installed on the leakage test line.

##### Residual Heat Removal Pump Discharge Pressure

Residual heat removal discharge pressure for each pump is indicated in the Control Room. A high pressure alarm is actuated by each channel.

#### **6.3.5.3 Flow Indication**

##### Charging Pump Injection Flow

Injection flow to the reactor cold legs injection header is indicated in the Control Room.

##### Residual Heat Removal Pump Injection Flow

Flow through each residual removal injection and recirculation header leading to the reactor cold or hot legs is indicated in the Control Room.

### Test Line Flow

Local indication of the leakage test line flow is provided to check for proper seating of the accumulator check valves between the injection lines and the Reactor Coolant System.

### Residual Heat Removal Pump Minimum Flow

A local flow meter installed in each residual heat removal pump discharge header provides control for the valve located in the pump minimum flow line.

## **6.3.5.4 Level Indication**

### Refueling Water Storage Tank Level

The water level in the RWST is measured by three separate channels of instrumentation each with readouts on the main control board.

Two out-of-three logic from the three channels provides an alarm when the pre-low level is reached in the RWST which allows time to verify containment sump level prior to automatic switching of the RHR pump suction from the RWST to the containment sump and secure the pump if adequate level is not available.

Two-out-of-three logic from the three channels provides an alarm when the low level is reached in the RWST, and automatically switches the RHR pump suction from the RWST to the Containment sump during post LOCA operation. Additional two-out-of-three logic provides a low-low level alarm when 15,639 gallons remain in the RWST above the lower level instrument tap for the wide range RWST level instrumentation.

One channel of instrumentation is also provided to alarm when the RWST level is below that required by the Technical Specifications. This level is referred to as the makeup level setpoint. An additional alarm is provided to preclude overflow. This level is referred to as the overflow level setpoint, which is called "HI" for the annunciator alarm and computer alarm.

### Accumulator Water Level

Duplicate water level channels are provided for each accumulator. Both channels provide indication, for each accumulator, in the Control Room and actuate high and low water level alarms.

### Containment Sump Water Level

Two Containment sump water level indicator channels provide the Control Room with water level indication. Also, two level switches are provided to annunciate when swap to sump is allowable for ECCS and NS.

### RHR And Containment Spray Pump Room Sump Level

A level transmitter is installed in the Containment Spray and RHR Pump room sump which is located in the lowest level of the Auxiliary Building to monitor the post LOCA leakage. The level transmitter is supplied with a level indication in the Control Room. The operating range of this equipment is sufficient to detect water levels above the sump i.e., above the floor level. The level alarms and level indication provide a reliable means for detecting and isolating any postulated post LOCA leakage.

## **6.3.5.5 Valve Position Indication**

Valve positions which are indicated on the control board are done so by a "normal off" system; that is, should the valve not be in its proper position, a bright white light is illuminated and thereby gives high visible indication to the operator.

Valve position is also indicated by a second system employing a “red-green” light system on the control board. Thus should any bulb fail in service, the true position of the valve is still indicated.

#### Accumulator Isolation Valve Position Indication

The accumulator isolation valves are provided with red (open) and green (closed) position indication lights located at the control switch for each valve. These lights are powered by valve control power and actuated by valve motor operator limit switches.

A monitor light that is on when the valve is not fully open is provided in an array of monitor lights that are all off when their respective valves are in proper position enabling safeguards operation. This light is energized from a separate monitor light supply and actuated by a valve motor operated limit switch.

An alarm annunciator point is activated by both a valve motor operator limit switch and by a valve position limit switch activated by stem travel whenever an accumulator valve is not fully open for any reason with the system at pressure (the pressure at which the safety injection block is unblocked). A separate annunciator point is used for each accumulator valve. This alarm is recycled at approximately one hour intervals to remind the operator of the improper valve lineup.

#### Refueling Water Storage Tank Isolation Valve

The control and indications provided for these valves are identical to those provided for the cold leg accumulator isolation valves, with the exception that a safety injection signal is not applied to the valves between the safety injection pumps, and residual heat removal pumps, and the refueling water storage tank.

### **6.3.5.6 ECCS Leakage Detection**

#### Inter-System Leak Detection

Leakage past the check valves in an injection line downstream of either the safety injection pumps or the residual heat removal pumps will result in the lifting of a safety valve which discharges to the pressurizer relief tank inside containment. This tank is provided with high level, low level and high pressure alarms. The high pressure alarm will be actuated in the Control Room within approximately 18 hours following initial safety valve actuation, assuming a one gpm leak and minimum water level in the PRT (Ref. 4).

#### Post-LOCA Leakage Detection

A level transmitter is installed in the Containment Spray and RHR Pump Room sump which is located in the lowest level of the Auxiliary Building. This level transmitter is supplied with a level indicator in the Control Room. The operating range of this equipment is sufficient to detect water levels above the top of the sump, i.e., above floor level. The level transmitter meets the requirements of IEEE 323-1971 and IEEE 344-1971. This level indication along with the level alarms provide a reliable means for detecting and isolating any postulated post-LOCA leakage.

### **6.3.6 References**

1. Igne, E. G., and Locante, J., Environmental Testing of Engineered Safety Features Related Equipment (NSSS-Standard Scope), WCAP-7744, Volume 1, August, 1971.
2. Deleted Per 2008 Update.
3. Letter from W. O. Parker, Jr. (Duke) to J. P. O'Reilly (NRC) dated September 29, 1980. Subject: Response to I. E. Bulletin 80-18. Letter from T. M. Anderson (Westinghouse) to V. Stello (NRC) dated May 8, 1980. Subject: Centrifugal Charging Pump Operation Following Secondary Side High Energy Line Rupture.
4. Letter from W. O. Parker, Jr. (Duke) to Edson G. Case (NRC) dated April 4, 1978.

5. Letter from C. L. Caso (W) to T. M. Novak (NRC), April 1, 1975.
6. Deleted Per 2002 Update.
7. Deleted Per 2002 Update.
8. Deleted Per 2002 Update.
9. Deleted Per 2002 Update.
10. Deleted Per 2002 Update.
11. Deleted Per 2002 Update.
12. Deleted Per 2002 Update.
13. Deleted Per 2002 Update.
14. Deleted Per 2002 Update.
15. Deleted Per 2002 Update.
16. Ivey, J.S., et. al., Evaluation of LOCA during Mode 3 and Mode 4 Operation for Westinghouse NSSS, WCAP-12476, November 1991.
17. Letter to the U.S. Nuclear Regulatory Commission from T.P. Harrall dated October 13, 2008, titled "Duke Energy Carolinas, LLC (Duke) Oconee Nuclear Station, Units 1, 2 & 3, Docket Nos. 50-269, 50-270, 50-287, McGuire Nuclear Station, Units 1 & 2, Docket Nos. 50-369, 50-370, Catawba Nuclear Station, Units 1 & 2, Docket Nos. 50-413, 50-414, Generic Letter 2008-01, 9-Month Response."
18. Letter from Hal B. Tucker (Duke to U. S. NRC dated January 15, 1990. Subject: NRC Bulletin No. 88-04, Potential Safety-Related Pump Loss, Action 4 Final Report.
19. Letter from M.S. Tuckman (Duke) to U. S. NRC dated January 10, 1991. Subject: NRC Bulletin No. 88-04, Potential Safety-Related Pump Loss, Description of Actions Completed or in Progress.
20. Letter from Ted C. McMeekin (Duke) to U. S. NRC dated June 16, 1992. Subject: NRC Bulletin 88-04, Potential Safety-Related Pump Loss.

THIS IS THE LAST PAGE OF THE TEXT SECTION 6.3.

## 6.4 Control Area (Habitability) Ventilation System

**Note:**

This section of the FSAR contains information on the design bases and design criteria of this system/structure. Additional information that may assist the reader in understanding the system is contained in the design basis document for this system/structure.

### 6.4.1 Design Bases

The Control Area Ventilation and Air Conditioning Systems are designed to maintain the environment in the Control Room, Control Room Area and Switchgear Rooms, as indicated on [Figure 6-191](#), within acceptable limits for the operation of unit controls, for maintenance and testing of the controls as required, and for uninterrupted safe occupancy of the control room during post-accident shutdown. (See Section [7.6.10](#)). Because of these criteria, systems are designed as Engineered Safety Feature Systems with absolute and carbon filtration in the outside air intakes and equipment redundancies for use as conditions require.

Two 100 percent Safety Class 3 redundant air handling systems are provided for the Control Room, two 100 percent Safety Class 3 redundant air handling systems are provided for the switchgear rooms, and two 100 percent Safety Class 3 redundant air handling systems are provided for the Control Room Area (Equipment Rooms, Cable Room, Battery Room, MCC Room, etc.).

The Safety Class 3 air handling units for the Control Room, Control Room Area and Switchgear Rooms are supplied with chilled water by two 100 percent Safety Class 3 redundant chilled water systems, each with one 100 percent capacity chiller and one 100 percent chilled water pump (See [Figure 6-188](#) and [Figure 6-189](#)).

If only one air handling unit in each area and one chilled water system remain operable (see Section [7.6.10](#) for details) the Control Area ventilation retains the capacity to remove the heat generated under design conditions, and the safety function is unaffected by a single failure in either train.

Makeup air for the Control Room Area is provided by two 100% capacity fans.

General Design Criteria (GDC) 5 applies to this system. This design meets the requirements of GDC 5.

Essential electrical apparatus involved with the cooling, heating and pressurizing of the Control Room during accident conditions is connected to emergency standby power.

Air filtration is accomplished by use of prefilters on all air handling units.

The control room air handling units are aligned to filter units upon receipt of the ESF signal. The resetting of the system requires deliberate manual action by the operator.

Instrumentation is provided for the air conditioning systems to control and indicate the temperature, and to indicate radioactivity levels. Early warning ionization type smoke detectors are located near the return air inlets in the duct work serving the Control Area Ventilation System.

The MNS Emergency Plan contains information on food and sanitary facilities to be provided for habitability in coping with site emergencies. Accordingly, Commodities and Facilities is responsible for obtaining food and drinking water for site personnel. Radiation Protection is responsible for monitoring the site for radiological conditions and wind data in order to direct emergency workers to the appropriate response facility.

### 6.4.2 System Description

The Control Room, Control Room Area and Switchgear Rooms, Ventilation and Air Conditioning Systems are shown on [Figure 6-191](#). The areas serviced by the Control Room Ventilation System are located between column lines AA and EE and Rows 53 and 59 as shown on [Figure 1-6](#).

Separate air supply systems, each with fan, cooling coils and heating coils are provided to serve the Control Room and other groups of electrical equipment rooms for flexibility of control. The Control Room, Control Room Area and Switchgear Rooms have 100 percent standby air handling equipment.

During normal plant operation, the control room area is provided some fresh air through outside air intakes. The two redundant Outside Air Pressure Filter Trains (OAPFT) are OFF and ISOLATED from the air stream by dampers CR-OAD-1,3,5, and 7 and the Control Room is provided 100% recirculated air during normal plant operation.

During a LOOP or LOCA the Emergency Safety Features Actuation System (ESFAS) will automatically start both Outside Air Pressure Filter Trains. The Control Room is pressurized to prevent entry of contamination by two redundant 100% capacity Filter Trains each served by a single 100% capacity fan.

Following a Fuel Handling Accident in Containment or the Spent Fuel Storage Building, a CRAVS filter train is started by manual operator action.

The control complex is analyzed to be capable of withstanding a loss of chilled water cooling following a Station Blackout (SBO) event for up to 1.25 hours and remain within established temperature limits (see Section [8.4.9](#)).

Air conditioning maintains the Control Room and Control Room Area at approximately 75°F and the Switchgear Rooms at approximately 85°F. Should the Control Room temperature exceed the equipment design temperature of 90°F, the Action Statement for Tech. Spec 3.7.10 shall apply. The OAPFT fans supply about 2000 CFM each. The Control Room AHU fans supply about 25,000 CFM each. The Control Room Area outside air fans supply about 1000 CFM each. The Control Room Area ventilation fans supply about 57,500 CFM each. Cooling capacity is approximately 60 tons for the Control Rooms, 140 tons for the Control Room Area and 23 tons for each Switchgear Room. The Control Room volume is 116,000 cubic feet.

The outdoor air pressure filter train provides approximately  $2,000 \pm 10\%$  CFM of filtered outside air used for pressurization of the Control Room. Each of the two filter packages contains a 2-stage heater, a demister/pre-filter, a HEPA filter, a gasketless carbon adsorber, and a 100% capacity fan. The HEPA filters are the bolted frame with compression gasket type. The carbon bed filter is the deep bed type which is manually unloaded and reloaded in place with bulk carbon.

The response of the control room ventilation system following a LOCA and the expected iodine removal efficiencies based on the composite filter efficiency are described in the radiological accident dose analysis.

Outdoor air is taken from two locations such that a source of uncontaminated air is assumed regardless of wind direction following an event which releases radioactivity to the atmosphere. The fresh air intake is at elevation 767 + 0 at the intersection of column line CC and column lines 46 and 66 located such that each is placed on the outside of Reactor Building diametrically opposed to that unit's vent (see [Figure 1-6](#)). Upon receipt of a safety features actuation signal, air is taken from both intake locations.

The Control Room and all ventilation and air conditioning equipment is located within a shielded area and is readily accessible at all times. Sections [7.8.5](#) and [12.1.2](#) provide additional discussion of Control Room shielding.

### 6.4.3 Safety Evaluation

The Control Area Ventilation Systems serve the Control Room, Control Room Area and Switchgear Rooms. The Control Room Ventilation System is independent of the other ventilation systems. This assures the integrity and availability of the Control Room in the event of any postulated fire or contamination generated in the other areas.

The design of the Control Area Ventilation System is such that the maximum radiation dose received by the Control Room personnel under accident conditions is within the limits of General Design Criterion 19 of Appendix A to 10CFR 50. The dose evaluation is presented in Section [15.6.5.3](#).

There is potential for CO<sub>2</sub> buildup in the Control Room when it is isolated. Self-Contained Breathing Apparatus (SCBA) are available for respiratory protection against such noxious gases. SCBA are also available should the outside air pressure filter train intake chlorine monitors alarm. However even the worst case postulated chlorine ruptures would not approach the toxicity limits.

The following hazardous gaseous chemicals have been identified as potential hazards because of their toxicity, quantity, and the location relative to the Control Room and Control Area Ventilation System outside air intakes.

- Chlorine
- Nitrogen
- Propane

There are no permanently installed chlorine gas cylinders at the McGuire Site. Chlorine gas temporarily brought on site would be stored in standard 150 lb. cylinders at either the gas cylinder storage yard, located west of the Unit 1 Turbine Building, or the gas cylinder storage shed, located on the east side of the Service Building. To remain exempt from the requirements of 29CFR1910.119, the quantity of chlorine at a single location must not exceed 1500 lbs.

Chlorine gas causes discomfort in mild concentrations and death from breathing heavy concentrations.

It is assumed that only one cylinder of chlorine would rupture. The cylinders are independent vessels and not connected in any way. The accidental breakage of the cylinder valve would be the most likely failure. Analysis of the failure of the cylinders has addressed both a leak from the vessel and a burst release due to a rupture. The gas is visible as a yellow color, is heavier than air, and is readily detected as a disagreeable odor. Any chlorine leakage event would be responded to by the Site Hazmat (Hazardous Material) Team which is trained and equipped for this event.

A large amount of chlorine is stored outside the McGuire Station facility at the North Mecklenburg Water Treatment Facility located about 3 miles south east of McGuire. Chlorine can be transported to the facility via highway, and could pass within 0.4 mile of the Control Room via NC State Highway 73. The evaluation of the water treatment facility and the chlorine tanker transport demonstrates that the Control Room environment does not approach the toxicity limits given significant releases of chlorine.

The location of the Control Area Ventilation System outside air intakes are elevated, thus decreasing the possibility of drawing in any released gas. If this system were to draw in chlorine, Self-Contained Breathing Apparatus (SCBA) are provided in the Control Room and there is a significant period of time available to put on the equipment.

Nitrogen is stored on the McGuire site in both gaseous and liquid refrigerated forms. The burst and leak accident scenarios for the bounding nitrogen tank do not approach the toxicity limit for the Control Room.

Propane is stored at various locations on the McGuire site. The bounding propane event addresses the burst and leak accident of a propane delivery transport. Neither of these scenarios approach the toxicity limit for the Control Room.

The Control Area Ventilation Systems are designed to maintain the proper temperatures and cleanliness in the Control Room, the Control Room Area and the Switchgear Rooms during plant operation, shutdown, post accident conditions and all feasible weather conditions. Ventilation provided to battery rooms by the Control Area Ventilation System is designed to maintain proper temperatures as specified in Section 16.9.23 and to maintain hydrogen concentrations below the lower flammability limit. The Control Room outside air pressure filter trains are designed to maintain the proper post accident pressurization of the Control Room. A failure analysis is presented in [Table 6-138](#). Pressuring filter train design comparison to Regulatory Guide 1.52 is presented in [Table 6-110](#).

Failure of any active component does not result in loss of function due to 100 percent redundancy of components.

Analysis has shown that if both outside air intake locations are closed, assuming a 1/32" crack around all duct openings, cable openings, and door openings due to aging of the sealant, a 1/8" watergauge pressure differential would cause a 950 CFM leak rate. A pressure differential of 0.05" watergauge, which would be a more realistic figure, would cause a 600 CFM leak rate.

#### **6.4.4 Tests and Inspections**

Tests and inspections were performed to ensure the functional and operational capability of components and the system.

##### Manufacturer Shop Testing

The manufacturer was required to verify by appropriate tests the following:

1. Carbon filter:
  - a. Carbon filter capabilities for removal of molecular iodine - 131 and methyl iodide
  - b. Carbon filter iodine collection capability
  - c. Carbon filter cell leak-tightness integrity
  - d. Carbon filter flow resistance
2. Fan:
  - a. Proper head and flow characteristics
3. Heating and Cooling Coils
  - a. Proper heating and cooling capabilities

##### System Testing and Inspection

Operational testing was performed prior to initial startup to demonstrate proper functioning of the system. Testing includes the following:

1. Leak tightness tests of components and system
2. Functional verification of system controls and interlocks
3. Demonstration of proper system alignment and actuation upon receipt of an Engineered Safety Features Actuation System signal.

Periodic tests are performed to provide assurance of continued filter unit capabilities in accordance with Technical Specifications. Tests for HEPA filter and charcoal filter penetration and bypass, filter unit air flow quantity, filter bank differential pressures, and heater function are performed. Also in accordance with Technical Specifications, charcoal samples are removed and tested periodically for methyl iodide penetration.

The system filter testing is described in Technical Specification 5.5.11 Ventilation Filter Testing Program (VFTP).

The Control Room Area Ventilation System (CRAVS) testing is described in Technical Specification 5.5.16 Control Room Envelope Habitability Program.

#### **6.4.5 Instrument Application**

Temperature control of the Control Room is by room thermostats located in the Control Room by zones. There are four (4) temperature zones. Room thermostats are of the reverse-acting type to insure failure to cooling. The thermostats act to modulate chilled water flow in the central apparatus cooling coils by use of a three-way control valve and are arranged in such a manner that the zone requiring the greatest cooling determines the temperature of the air leaving the cooling coils. Remaining zone thermostats act to apply re-heat to maintain temperature. Reheaters are actuated by fail open devices to insure cooling if a failure in the controlling mechanism should occur, i.e., the system is totally designed toward the concept of "fail-safe-to-cooling."

Control Room outside air intakes are monitored for radiation and chlorine concentrations. High radiation is sensed by a radiation monitor located at each location. High chlorine concentration is sensed by a chlorine monitor located at each intake. A high radiation or high chlorine condition is annunciated in the Control Room and isolated manually. In the event one of these conditions is sensed at both outside air intake locations, the least contaminated intake is selected.

Control Room outside air intakes are also monitored for smoke concentration in the duct of each Control Room AHU and the Control Room Area AHU. Smoke detector instrumentation is provided in the air ducts of the above AHUs by the Fire Detection System, (EFA). A detected high smoke level stops the AHU with the high smoke level. A smoke purge fan with manual controls is provided to clear the Control Room of smoke.

The Control, Equipment and Cable Rooms Heating, Ventilation and Air Conditioning System design is described in Section [7.6.10](#).

**THIS PAGE LEFT BLANK INTENTIONALLY.**

THIS IS THE LAST PAGE OF THE TEXT SECTION 6.4.

## 6.5 Containment Spray System

### 6.5.1 Design Bases

#### Heat Removal Capability

Adequate heat removal capability for the Containment is provided by the Containment Spray System whose components operate in the sequential modes described in Subdivision [6.5.2](#). Redundant trains of the system are independently capable of delivering the necessary flow.

The primary purpose of the spray system is to spray cool water into the Containment atmosphere, when appropriate, in the event of a loss-of-coolant accident (LOCA) and thereby assure the Containment pressure cannot exceed containment design pressure of 15 psig. This protection is afforded for all pipe break sizes up to and including the double-ended rupture of the largest pipe in the Reactor Coolant System. The Containment Spray System design is based on the conservative assumption that the core residual heat is continuously released to the Containment as steam, eventually melting all ice in the Ice Condenser. The heat removal capability of each spray system is sized to keep the Containment pressure below design pressure after all the ice has melted and steam generated in the core continues to enter the Containment. The residual heat generated from the time of the accident through the time that the ice melts is absorbed by the ice condenser. In addition to energy from the Reactor Coolant System blowdown, the ice condenser accommodates the release of 50 million BTU of undefined energy.

The Containment Spray System is also evaluated assuming the energy release from a metal-water reaction of 33 percent of the Zircaloy fuel cladding, with hydrogen burned as it is produced, in addition to the energy input to the Containment assumed for the design bases described above. The spray system is designed to limit the Containment internal pressure for these cases to below the containment design pressure of 15 psig.

The secondary design basis for the Containment Spray System is the suppression of steam partial pressure in the upper volume due to operating deck leakage from a small break. The requirement is that the Containment Spray System be able to absorb steam leakage through the operating deck at the maximum possible long-term deck differential pressure of one pound per square foot, equivalent to the ice condenser door opening differential pressure.

The Containment Spray system piping and spray rings are used as a means to flood containment in Emergency Management Guidelines as part of the Duke commitment in response to EA-02-026 (B.5.b requirements).

#### Operability

The Containment Spray System is designed to operate over an extended period of time and under environmental conditions existing following a Reactor Coolant System failure.

Detection of leakage from the Containment Spray System involves the use of sump level instrumentation and floor drain tank level instrumentation, and Waste Evaporator Feed Tank level instrumentation. The spray pumps are in separate rooms and drain to a common sump.

Indications are available to detect abnormal inputs into the sumps in the lowest level of the Auxiliary Building. Additionally, a control room annunciator is actuated when sump levels exceed normal levels and a control room gage monitors water level above floor level at 695'. Any indication of abnormal conditions would prompt operator action. The ND/NS sump pumps transfer water to the Waste Evaporator Feed Tank (WEFT) or the Floor Drain Tank (FDT). These tanks are maintained at a level such that under abnormal input conditions into the ND/NS sump, an alarm or Control Room annunciator will be actuated before either tank would overflow. If leakage was not isolated and tank contents not processed, the WEFT and/or FDT would overflow and eventually begin flooding the Auxiliary Building

lowest level. There is sufficient hold-up capacity in the lowest level to prevent adverse affect on safety-related Residual Heat Removal equipment with a 50 gpm leak sustained for approximately 45 hours. If leakage were to occur in areas that do not drain to the ND/NS sump, water would be directed to the FDT via the floor drain system. Unanticipated FDT levels of 80% or more would prompt investigation by Chemistry personnel.

### Reliability

The Containment Spray System, including required auxiliary systems, is designed such that it will tolerate a single active or passive failure during the recirculation phase following a Reactor Coolant System failure, without loss of protective function.

System active components are redundant. System piping located within the Containment is redundant and separated in arrangement unless fully protected from consequential damage which may follow any Reactor Coolant System pipe failure.

In response to Generic Letter 2008-01 "Managing Gas Accumulation in ECCS, Decay Heat Removal, and Containment Spray Systems", an evaluation concluded that system procedures and design are adequate to maintain the NS system sufficiently full of water to ensure operability. Inadequate system fill and vent can result in pump cavitation, pump gas binding, or water hammer. The complete Duke response can be viewed via Reference [3](#).

### Seismic Criteria

The Containment Spray System is designed to accommodate the operating basis earthquake within applicable codes stress limits. The spray system will withstand the safe shutdown earthquake without rupture or loss of protective function.

## **6.5.2 System Design**

The Containment Spray System is shown on [Figure 6-194](#). The spray system consists of two spray pumps and spray heat exchangers in parallel, with associated piping, valves and spray headers in the upper Containment volume. This system can be supplemented with two Residual Heat Removal System pumps and two residual heat exchangers in parallel, with associated piping, valves and individual spray headers in the upper Containment volume.

One train of the Containment Spray System is defined as one spray pump with its associated spray heat exchanger. Each train provides complete backup for the other. Partial flow from an ND system pump through its associated heat exchanger can be used to supplement each train.

Adequate Containment cooling is provided by one spray system train operating in the following sequential modes:

1. Recirculation of water from the Containment sump by the Containment spray pumps through the Containment Spray heat exchangers and back to the Containment after the refueling water storage tank has been drained to the low level alarm and adequate containment sump level has been confirmed.
2. Diversion of a portion of the recirculation flow from the residual heat removal system to auxiliary spray headers if required by procedure.

One train of the Containment Spray will be aligned and manually initiated from the control room. The Containment Spray System provides two redundant heat removal trains. The operator manually actuates the system controls for positioning all valves to their operating positions and starting the pumps, as required. The realignment procedure for the spray pumps is detained in [Table 6-125](#).

The passive portions of the spray systems located within the Containment are designed to withstand, without loss of functional performance, the post-accident Containment environment conditions and to operate without benefit of maintenance. All of the active components of the Containment Spray System are located outside the Containment and are not required to operate in the steam-air environment produced by the accident.

The spray headers which are located in the upper Containment volume are separated from the reactor and reactor coolant loops by the operating deck and inner wall of the ice bed. These spray headers are therefore protected from missiles originating in the lower compartment of the Containment.

### Refueling Water Storage Tank

This tank serves as a source of emergency borated cooling water for injection. It is normally used to fill the refueling canal for refueling operations. However, during all other operating periods it is aligned to the suction of the Safety Injection System pumps, the Residual Heat Removal System pumps and the Containment Spray System pumps.

### Pumps

The two containment spray pumps are of the vertical single stage, end-suction side discharge centrifugal type driven by electric motors. These motors can be powered from either normal or emergency power.

The design head of the pumps is sufficient to provide adequate flow at limiting conditions.

Pump motors are direct-coupled and large enough for the maximum power requirement of the pump. Materials of construction suitable for use in mild boric acid solutions (such as stainless steel or equivalent corrosion resistance material) are used. The Containment Spray System is designed so that adequate net positive suction head (NPSH) is provided to the Containment Spray pumps in accordance with Regulatory Guide 1.1.

To demonstrate that adequate NPSH is provided for the Containment spray pumps, it is not necessary to provide a graph of NPSH as a function of time. It is only necessary to demonstrate that the NPSH is adequate under the worst limiting conditions. NPSH for the Containment spray pumps is evaluated for both the injection and recirculation modes of operation for the design basis accident. The recirculation mode of operation gives the limiting NPSH requirement for the Containment spray pumps, and the NPSH available is determined from the following operation:

$$\text{NPSH}_{\text{actual}} = \frac{(\text{h}) \text{ containment pressure}}{\text{pressure}} - \frac{(\text{h}) \text{ vapor pressure}}{\text{pressure}} + \frac{(\text{h}) \text{ static head}}{\text{head}} - (\text{h}) \text{ loss}$$

Head loss developed across the ECCS Sump Strainer will tend to be offset over time by increasing sump pool level and decreasing pool vapor pressure (decreasing temperature).

To evaluate the adequacy of the available NPSH, several conservatisms are applied:

1. No increase in Containment pressure from that present prior to the accident is assumed.
2. The Containment sump fluid temperature is assumed to be 200°F which envelops the expected sump temperature at the time of sump recirculation initiation.
3. The static elevation head is calculated from the floor elevation of the sump (elevation 725' + 0")= and credits minimum sump level of 3 feet. The elevation of the spray pump is 701' + 1" (centerline of discharge pipe).
4. The head loss is evaluated based on all pumps running at the maximum calculated flow with representative friction factors.
5. The required NPSH is based on one pump running at a flowrate above its maximum calculated flow.

Deleted Per 2014 Update.

6. The limiting NPSH available is calculated early in the event at the time of realignment of the pump suction to the ECCS Sump pool from the RWST, and conservatively assumes that most of the debris in the pool that can transport to the strainer has already done so. In actuality the transport paths for a significant portion of this debris are long and circuitous, which would delay arrival at the strainer surface. Related details of ECCS sump strainer design and performance are given in Section [6.5.2](#), "Generic Letter 2004-02."

Using all these conservative assumptions, the NPSH available is calculated to be > 19.5 feet and the NPSH required is 17.5 feet. This provides an NPSH margin of > 2 feet. The actual available NPSH will always be greater than the calculated value.

Preoperational tests are performed to further demonstrate adequate NPSH.

Design parameters for these pumps are presented in [Table 6-139](#).

The Residual Heat Removal System pumps, which can be used to provide auxiliary spray, are described in Section [6.3](#).

#### Heat Exchangers

The Containment Spray heat exchangers are of the shell and tube type with the tubes welded (HX 2B is rolled) to the tube sheet. Except for the 2B heat exchanger, borated water from either the refueling water storage tank or the Containment sump circulates through the tubes (shell for HX 2B) while nuclear service water circulates through the shell (tubes for HX 2B) side. For the 2B heat exchanger, the borated water flows through the shell side while the nuclear service water circulates through the tubes. The spray heat exchangers are designed to assure adequate heat removal capacity from the spray water during the recirculation mode. Design parameters are presented in [Table 6-139](#).

#### Spray Nozzles

The stainless steel spray nozzles are of the hollow cone ramp bottom design. Each nozzle sprays at a rate of 15.2 gpm and produce a drop size spectrum with a mean diameter of less than 700 microns at a 40 psi differential pressure. These nozzles have an approximately 3/8 inch spray orifice and are not subject to clogging by particles less than 3/32 inch in maximum dimension. During the recirculation phase of operation, fluid is screened through perforated plate with 3/32 inch openings and pumped to the nozzles. The nozzles and headers are positioned to maximize coverage of the Containment volume from each set of spray headers. Design parameters are presented in [Table 6-139](#). [Figure 6-195](#) shows the mass distribution of the spray nozzles.

#### Valves

##### Pump Discharge Line

There are normally closed, motor-operated eight-inch gate valves in each pump discharge line which are manually aligned to permit spraying into the Containment.

Check valves close when the respective containment Spray Pump is stopped. This prevents formation of a vacuum in the risers.

Check valves are located in the pump discharge piping to prevent water hammer effects during pump restart.

#### Test Lines

There are two pump test lines sized at 4 inches and 8 inches. Each test line can be aligned to either Containment Spray Pump for flow testing. There is one 4-inch globe valve and one 8-inch butterfly valve on each branch of the test lines. These valves are manually operated during testing; otherwise, they are

locked closed. A globe valve on the main 4-inch test line and the butterfly isolation valves on the 8-inch line may be used to throttle the total flow. The test lines allow for pump testing without spraying in the Containment.

A spectacle blind plate is installed in the 8-inch line. The orifice side of the spectacle plate provides Containment Spray pump run-out protection. The blind side of the spectacle plate is used during hot shutdown through power operations to ensure isolation. The 8-inch line is required to be isolated due to Refueling Water System isolation valves, 1(2)FW-1 and 1(2)FW-32, not being qualified to automatically close when subjected to the discharge pressure of an operating Containment Spray pump. Also, the blind plate isolates the 8-inch test line to prevent leakage back to the FWST (considering a post-LOCA environment).

### Piping

The Containment Spray System piping is austenitic stainless steel. This is required because the piping contains reactor coolant during recirculation operation.

### Instrumentation and Control

The Containment Spray System is normally aligned to the refueling water storage tank with the appropriate isolation valves open.

After initiation of the ECCS recirculation phase, in conjunction with an enable permissive from the Containment Pressure Control System, Containment Spray pump suction is manually aligned to the Containment sump and one train of Containment Spray is manually initiated. Position indication is provided in the Control Room for all remotely operated valves.

### Material Compatibility

Parts of the system in contact with borated water are stainless steel or an equivalent corrosion resistant material. The amount of unqualified coatings within containment is limited to 16,500 square feet. The remaining surfaces within the Containment have qualified coatings which are not subject to breakdown under exposure to containment spray and can withstand the steam, pressure and temperature associated with the LOCA (without spalling or flaking). Insulation within the Containment does not contain materials which could potentially enter the pump and cause plugging of ECCS and Containment spray strainers and equipment. An analysis of the affects of failed coatings and insulation is provided in the following section, Containment Sump. Electrical circuitry and equipment within the Containment which are required for accident and post-accident conditions are water tight or submersible and suitable for accident pressure and temperature conditions.

For the hypothetical double-ended rupture of a Reactor Coolant System pipe, the pH of the sump solution (and, consequently, the spray solution) is raised to at least 8.0 within one hour of the onset of the LOCA. It is possible to adjust the pH of the sump solution using the chemical mixing tank and the charging pumps, should it become necessary.

### Containment Sump

The design of McGuire does not provide for a Containment sump as such. The lower compartment of the Containment collects sufficient volume of water following the injection phase of safety injection to allow the initiation of recirculation. Water collected in the lower Containment compartments reaches the sump strainer by flowing through a series of spare penetrations in the polar crane wall located near the Containment floor level. Refer to [Figure 1-10](#) and [Figure 1-16](#) for plan and elevation drawings of the Containment sump. The design of the Containment sump strainers are shown on [Figure 6-196](#).

The Containment sump structure and strainer assemblies are located in the pipe chase area outside the crane wall and inside the crane wall. The sump strainer assemblies have a strainer gross surface area of approximately 1700 ft<sup>2</sup>. The strainer components outside the crane wall are installed within the original

recirculation sump screen footprint at the 180° azimuth. The strainer assemblies located inside the crane wall (lower containment) extend out from the 180° azimuth in both directions. Additional strainer assemblies extend towards the primary shield wall at the 180° azimuth. The strainer modules (Tophats) are made of stainless steel perforated plate for straining debris from the water. The openings in the perforated plate are nominally 3/32 inch in diameter and the modules also contain a fine wire mesh (debris bypass eliminator) installed between the perforated plates. The ECCS recirculation lines are connected to the main waterboxes of the strainer assembly outside the crane wall using 18" piping. The strainer assembly inside the crane wall is connected to the strainer assembly outside the crane wall using 18" piping installed through two 30" penetrations in the crane wall. Vortex suppression, constructed of stainless steel floor grating, is installed directly over the top-hat strainer assemblies located outside the crane wall (in the pipechase). The strainer assemblies located inside the crane wall are completely enclosed with a stainless steel enclosure to maintain a 'remote' pipe chase strainer. The enclosure has perforated steel plate sides, and a solid top deck which also provides vortex suppression. The strainer assemblies located in the pipe chase do not have a solid top deck because there are no pipe whip, water/steam jet loads, or missiles projected to affect the containment sump structure and strainer assembly area within this area.

In the case of a LOCA that progresses to the point that sump recirculation is required, greater than twenty minutes will pass between the initial break and the swapon to sump recirculation. This time will allow some of the large debris (damaged insulation, etc.) generated by the blowdown phase to settle to the containment floor. This time also allows water level to rise above the enclosure solid top deck (inside the crane wall) and the vortex suppression grating (in the pipechase). Prototype testing has demonstrated that the vortex suppression grating and enclosure solid top deck prevent the strainer modules from ingesting air.

Some of the LOCA generated debris will remain suspended in the water, and will transport along with the water thru the crane wall and to the sump strainer. The resultant debris bed that forms upon the strainer surface (comprised of perforated plate with 3/32" diameter holes) will not impede the functions of the ECCS or Containment Spray systems. The containment spray nozzles, which have 3/8" spray orifices, are not subject to clogging by particles less than 3/32" in maximum dimension. All other valves, pumps and heat exchangers have sufficient clearance to pass particles of less than 3/32".

Equipment insulation is designed so as not to become a source of sump blockage. The types of insulation used in the Containment are reflective or mass insulation as listed on [Table 6-140](#).

The reflective insulation or mass (encapsulated/blanket) insulation, which is utilized on high energy piping, is expected to be stripped off during a postulated rupture in the vicinity of the rupture. All insulation in the vicinity of postulated pipe breaks is in the lower Containment area and would pose no problems in clogging drains. However, in the event that a break occurred, and reflective insulation, mass (encapsulated/blanket) insulation or parts thereof were thrown into the ice condenser via the lower inlet door, there is a possibility of clogging a bay drain. Under these circumstances, water would run over to the next bay after exceeding a level of 1 inch in the affected bay.

Non-safety related equipment in the Containment is also designed so as not to become a source of sump blockage.

The containment sump structure design is in conformance with Regulatory Guide 1.82 Rev 0 except that Section C is revised as follows:

- C.1: A configuration utilizing the containment side structure and floor as the intake structure boundary is considered acceptable for those plants in which the post LOCA water level in the containment is sufficiently high, thus making additional sump depressions in the floor non-productive. Redundance is provided by two separate suction pipes protected by guard pipes.

- C.2: The containment recirculation intake structure and suction piping are protected from high energy piping systems to the extent practical to preclude damage by whipping pipes or high-velocity jets of water or steam. ECCS/CSS train separation within the common sump strainer is not required due to the absence of any credible loads which could fail the sump strainer.
- C.3: The sump is located on the lowest floor elevation in the containment exclusive of the reactor vessel cavity. A substantial strainer is provided to filter debris from recirculated coolant. The crane wall and containment strainer enclosure act as a primary filter to prevent large debris from reaching the sump strainer.
- C.6: The location of the sump strainer assembly provides protection from missiles and large debris. The crane wall and containment strainer enclosure act as a primary filter to prevent large debris from reaching the sump strainer.
- C.7: A sump strainer with complex geometry, crediting all effective strainer surface area, is provided that precludes loss of NPSH for ECCS and CSS pumps during the period these components are required to operate.
- C.8: Vortex suppression is provided to preclude air entrainment in the recirculated coolant.
- C.9: Sump strainers are designed to withstand the vibratory motion of seismic events without loss of structural integrity.
- C.10: The size of openings in the sump strainer is based on the minimum restrictions found in systems served by the sump. The minimum restriction takes into account the overall operability of the system served. Strainer perforations are less than 1/10 inch in diameter.
- C.12: Materials for the sump strainer assembly and associated enclosure are selected to avoid degradation during periods of inactivity and operation and have low sensitivity to adverse effects such as stress assisted corrosion that may be induced by chemically reactive spray during LOCA conditions.
- C.13: The sump strainer assembly and associated enclosure include access openings to facilitate inspection.
- C.14: Inservice inspection requirements for ECCS containment sump components (strainer assembly and enclosure) include the following:
- a. ECCS containment sump components are inspected during every refueling downtime, and
  - b. The inspection consists of a visual examination of the components for evidence of structural distress or corrosion.

Water is available, for recirculation, from the following sources:

1. Refueling water storage tank
2. Reactor Coolant System
3. Safety Injection System - accumulators
4. Ice Condenser - ice melt

After the usable volume of the refueling water storage tank is transferred to containment during the injection phase of operating, at least 350,000 gallons of water are in the lower compartment of the Containment prior to the start of recirculation. After all the ice has melted, there is an additional 225,000 gallons (minimum) available for recirculation. Water is collected in the refueling cavity during the initial

transfer of water and during recirculation. Depletion of the recirculation supply is prevented by terminating the six refueling cavity drains in the lower compartment of the Containment.

#### Codes and Classifications

Safety class and code class for major components of the system are given in [Table 3-4](#).

#### Generic Letter 2004-02

The NRC initiated Generic Safety Issue (GSI)-191, "Assessment of Debris Accumulation on PWR Sump Performance," in 1996 based upon the findings that the amount of debris generated from a high energy line break and resulting head loss across the ECCS Sump Strainer could be greater than previously anticipated. This precursor to Generic Letter 2004-02 focuses on reasonable assurance that the provisions of Title 10 of the Code of Federal Regulations (10 CFR) Section 50.46(b)(5) are met. This rule requires maintaining long-term core cooling after initiation of the Emergency Core Cooling Systems. The objective of GSI-191 and the subsequent Generic Letter 2004-02 is to ensure that post accident debris blockage will not impede or prevent the operation of the Emergency Core Cooling Systems (ECCS) and Containment Spray System (CSS) in recirculation mode during LOCAs.

The McGuire Unit 1 and Unit 2 ECCS Sump Strainers were designed to meet the requirements of USNRC Generic Letter 2004-02, "Potential Impact of Debris Blockage on Emergency Recirculation During Design Basis Accidents at Pressurized-Water Reactors", including the guidance outlined in NEI 04-07, "Pressurized Water Reactor Sump Performance Evaluation Methodology", and its companion Safety Evaluation Report (SER).

In response to the NRC staff SER conclusions on NEI 04-07, the Pressurized Water Reactor Owners Group (PWROG) sponsored the development of the following Topical Reports (TRs):

- TR-WCAP-16406-P-A, "Evaluation of Downstream Sump Debris Effects in support of GSI-191," to address the effects of debris on piping systems and components
- TR-WCAP-16530-NP-A, "Evaluation of Post-Accident Chemical Effects in Containment Sump Fluids to Support GSI-191," to evaluate the chemical effects which may occur post-accident in containment sump fluids.
- TR-WCAP-16793-NP-A, "Evaluation of Long Term Cooling Considering Particulate, Fibrous and Chemical Debris in the Recirculating Fluid," to address the effects of debris on the reactor core.

The NRC staff reviewed the TRs and found them acceptable to use (as qualified by the Limits and Conditions stated in the respective SERs).

ECCS Sump Strainer design considerations and exceptions to these documents are identified and justified in McGuire letters to NRC of February 28, 2008, April 30, 2008, July 2, 2012 and July 31, 2013. The NRC documented their acceptance of the McGuire responses and closeout of Generic Letter 2004-02 in a letter dated April 24, 2014 and accompanying Staff Review document.

Significant aspects of the McGuire Unit 1 and Unit 2 ECCS Sump Strainer design related to GL 2004-02 are described following:

#### Design Considerations:

A fundamental function of the ECCS is to provide long term post-accident cooling of the core. This is accomplished by recirculating water that has collected at the bottom of the containment building (sump pool) through the reactor core following a break in the reactor coolant system piping. If a

LOCA occurs, thermal insulation and other materials may be dislodged by the two-phase jet emanating from the broken RCS pipe. The debris may transport via flows coming from the RCS break or from the containment spray system to the sump pool following a LOCA. Once transported to the sump pool, the debris could be drawn towards the ECCS Sump Strainer which is designed to prevent debris from entering the Emergency Core Cooling Systems and the reactor core. If this debris were to clog the strainers, long term core cooling as well as containment cooling could be degraded and the potential for core damage and containment failure would increase.

It is also possible that some fine debris could bypass the ECCS Sump Strainer and lodge in the reactor core. This could result in reduced core cooling and potential core damage.

Resolution of GSI-191 and subsequently Generic Letter 2004-02 involves two distinct but related safety concerns:

1. Potential clogging of the sump strainers that results in ECCS and/or Containment Spray pump failure (due to inadequate NPSH available) or gross structural failure of the ECCS Sump Strainer; and
2. Potential clogging of flow channels within the reactor vessel because of debris bypass of the ECCS Sump Strainer (in-vessel effects).

Clogging at any point (the strainer, the downstream piping components or in the reactor vessel) can result in the loss of the long-term cooling safety function.

#### Design Description

The Containment Recirculation Sump Strainer Assembly is located on Elevation 725' of the Containment Reactor Building. The strainer assembly is both outside the crane wall in the pipe chase at the 180° azimuth, and inside the crane wall, shielded and surrounded by an enclosure. The overall strainer assembly height above the containment building floor is lower than the predicted minimum containment water level for a small break LOCA. The strainer assembly is designed to withstand a safe shutdown earthquake.

The strainer modules ("Top-Hats") are made of two concentric cylinders formed from perforated plates for straining debris from the water. Each Top-Hat module has an outer diameter of 8 inches and an inner diameter of 6 inches with a length varying from approximately 24 to 45 inches. The strainer openings are 3/32 inch in diameter. Water will enter the Top-Hats through the perforated plates and flow horizontally within the annulus of each Top-Hat. Within the annulus of each Top-Hat is knitted wire mesh material which provides additional filtration for any debris that may enter. Upon exiting the Top-Hats, water will flow through a cruciform support plate and into the plenum boxes. Connected plenum boxes direct flow to the two 18" ECCS recirculation suction lines. Each 18" ECCS recirculation suction line ties into its own strainer assembly main plenum water box, and these plenum boxes are connected via cross-over plenum boxes. The plenum boxes for the strainer modules inside the crane wall also tie in to the cross-over plenum (reference [Figure 6-196](#)).

For strainer modules located in the pipechase, the strainer design includes vortex suppressors above the Top-Hat strainer modules. The vortex suppressors are constructed of floor grating and install directly over the Top-Hats. For strainer modules located inside the crane wall, the solid top deck of the sump strainer enclosure provides the function of vortex suppression.

#### Break Selection:

The McGuire ECCS Sump Strainers were designed to accommodate the debris generation from a double-ended guillotine break of a primary loop. Break locations throughout the RCS were analyzed based on their debris generation and transport potential and the break selected is the limiting case for debris generation. This limiting break generates the highest quantity of fibrous debris and also transports the highest portion of that fibrous debris to the strainer. The bounding break location is on

the Unit 2 Bloop hot leg, adjacent to the steam generator [Reference [11](#)]. Breaks on the hot leg are generally more limiting than breaks on the crossover and cold legs due to their proximity to the adjacent loop hot leg piping.

Secondary line breaks were not considered in the evaluation of debris generation. For debris generation, the smaller secondary side breaks inside the crane wall are bounded by the primary side breaks. Further, for a secondary system break inside containment, the steam release will terminate following isolation of feedwater to the faulted steam generator. For a design basis steam line break, the RCS remains intact and long term operation with the ECC Sump Strainer is not required.

#### Debris Generation:

There are three kinds of conventional debris assumed to be generated from the limiting break: failed insulation, failed coatings, and latent debris (i.e., placards, tags, labels, dust/dirt and lint). The insulation debris, coating debris and dust/dirt and lint debris generated during blowdown and transported to the ECCS Sump Pool can vary in size and texture, from pieces/clumps, to individual strands, to particulates. Additionally, large fiber clumps that do not transport to the strainer are conservatively assumed to partially erode over time into individual fiber strands, which do transport.

Several types of insulation systems are used inside containment within the Zone of Influence (ZOI) of high energy breaks: Reflective Metal Insulation (RMI), Nukon® Low Density Fiberglass (LDFG) fiber insulation, and Thermal-Wrap® LDFG fiber insulation. Both jacketed and unjacketed LDFG fiber insulation systems are used. A spherical zone of influence is measured as a function of the pipe diameter and centered at the break location used for the debris generation analysis. The ZOI used for evaluation of RMI is 28.6D and the ZOI for Nukon® and Thermal-Wrap® LDFG is 17D regardless of the jacketing. These ZOIs are consistent with the recommendations of NEI 04-07 and the associated NRC Safety Evaluation.

The destroyed RMI is not buoyant and therefore does not pose a threat to the operation of the ECCS sump strainer. Therefore, the quantity of RMI either within containment or destroyed due to a high energy line break is not considered a critical parameter with respect to ECCS Sump Strainer performance.

The maximum amount of LDFG fibrous debris generated in the limiting break was documented in Reference [11](#). NEI 04-07 and the associated NRC Safety Evaluation were used to determine this overall debris quantity. In addition, the predicted debris generated due to the LOCA jet is characterized by debris size (fines, small pieces, large pieces, and intact blankets). The amount of LDFG debris generated as well as the size distribution of the debris is based on the proximity of the insulation to the break. This characterization of debris is critical to the sump strainer analysis as the transportability and thus debris load on the ECCS Sump Strainer is dependent on debris size.

Coatings inside the Containment are classified as either qualified or unqualified for the purposes of debris generation analysis, which encompasses all of the coating systems used within Containment. Unqualified coatings in Containment are assumed to fail as particulates, in accordance with NEI 04-07 guidance. Qualified coatings are assumed to fail as particulates within a 50 ZOI based on the methodology outlined in WCAP-16568-P. The amount of qualified coatings is documented in Reference [10](#). For unqualified coatings, NEI 04-07 guidance directs utilities to assume 100% failure of unqualified coatings into transportable particulate. McGuire performed an alternative analysis utilizing EPRI OEM coatings failure data to refine the quantity of unqualified coatings assumed to fail. Utilizing this data, an overall volume of failed unqualified coatings was documented in Reference [13](#). All of the failed coatings are assumed to transport to the ECCS Sump Strainer as particulate debris. In order to allow margins for emergent coatings failures, ECCS sump strainer testing used a debris load corresponding to an unqualified coatings value of 16,500 sq ft, in addition to the other particulate sources.

Walkdowns were performed on each Unit to assess the quantity of dust, dirt, and lint per NEI 02-01 guidance and a bounding value of 200 lb was used in the debris generation evaluation. The actual results of the walkdowns indicated significantly less than 200 lb however, the use of this bounding value is consistent with guidance provided in NEI 04-07. The characterization of dust, dirt, and lint is also addressed in NEI 04-07. 15% of the overall quantity of dust, dirt, and lint on a mass basis is assumed to be lint with fibrous like behavior (301b or 12.5 ft<sup>3</sup>). The remainder of the debris (170 lb) is assumed to be dust/dirt which can be represented by particulate debris.

Placards, tags, labels and other miscellaneous latent materials in containment were included in the debris generation analysis consistent with NEI 04-07 guidance. Refinements to the tag and label analysis were performed to account for the torturous path labels in some locations would be required to traverse to transport to the ECCS Sump Strainer. The total surface area of tags and labels assumed to dislodge and transport to the ECCS Sump Strainer is documented in Reference [14](#). When determining actual strainer surface area blockage, this total is reduced by 25% to account for overlap and compression of the debris consistent with the NEI 04-07 guidance.

In response to NRC Bulletin 2003-01, McGuire committed to the following actions to minimize the potential for debris build-up on the ECCS Sump Strainers:

- Containment cleaning and inspection during each refueling outage
- Establishment of controls for the procurement, application and maintenance of Service Level 1 coatings inside containment
- Enhancements to administrative controls programs and equipment labeling processes

In addition to the conventional debris, chemical precipitates can form in the post-LOCA environment inside containment. The quantity of chemical precipitates that could form was estimated using the models and methodologies from WCAP-16530-NP-A. By executing this model using plant specific containment material inventories and environmental conditions, a bounding mass of chemical precipitates as well as a temperature at which the precipitates form was determined and included in the scope for ECCS Sump Strainer head loss testing. The key material for this analysis is aluminum inventory as documented in Reference [15](#).

#### Debris Transport to ECCS Sump:

The methodology used in the debris transport analysis was based on the NEI 04-07 guidance report for refined analyses, as modified by the NRC SER, as well as the refined methodologies suggested by the SER in Appendices III, IV, and VI. Assumptions used in the debris transport analysis are listed in McGuire's Letter to NRC of February 29, 2008; deviations from the NEI 04-07 guidance and their justification are also listed in that letter. The Computational Fluid Dynamics (CFD) calculation for recirculation flow in the ECCS Sump Pool was performed using Flow-3D® version 9.0. The assumptions used in the CFD model are also listed in the response to question 3(e)(2) of the February 28, 2008 letter. The transport fraction of each type of debris was determined using the velocity and Turbulent Kinetic Energy (TKE) profiles from the CFD model output, along with the initial distribution of debris. The quantity of debris that could experience erosion due to the break flow, spray flow, or ice melt drainage was determined. McGuire assumes (based on industry testing) that 10 percent of all LDFG that is destroyed but is too large to transport to the ECCS Sump Strainer erodes to individual fiber strands that are transportable. The overall transport fraction for each type of debris was calculated by combining each of the previous steps in a logic tree.

The design, placement and sheltering of the ECCS Sump Strainer also provides for the filtration of large debris (i.e., fiber insulation clumps and pieces of RMI) entrained in the sump pool prior to reaching the strainer via passage of water through openings in the crane wall.

For the postulated limiting break, all fine debris (i.e., dust/dirt, lint, failed coatings particulates, and failed LDFG insulation constituent fibers) was assumed to transport to the ECCS sump pool, and to the strainer itself. Upstream fine debris settling was not credited.

#### ECCS Sump Strainer Head Loss:

The ECCS Sump Strainer head loss is determined by combining the calculated clean strainer head Loss (hydraulic losses through a clean top-hat module, plenums and waterboxes) with debris head losses obtained from prototype array testing that was performed to determine the cumulative head loss under fiber, particulate and chemical effects loading. The WCAP-16530-NP-A analysis described above predicts that chemical effects will not occur until the sump pool temperature cools to 165°F. As a result, for sump pool temperatures above 165°F, the conventional debris head loss is used while at temperatures below 165°F, the conventional debris combined with the chemical effects head loss is used. Both the conventional debris and chemical effects head losses were determined based on data obtained during prototype array head loss testing.

At the initiation of sump recirculation, the ECCS Sump Strainer is completely submerged and it is assumed a full conventional debris bed has formed on the strainer. No credit is taken for the time-dependent building of a debris bed as the ECCS Sump Strainer is placed in service. In addition, no credit is taken for the static head of water above the minimum height at which the ECCS Sump Strainer can be placed into service. These assumptions as well as additional conservative inputs for the RHR and Containment Spray pump calculation of NPSH margin are assumed as described in Sections [6.3.2.14](#) and [6.5.2](#).

Considering NPSH, as the ECCS sump pool cools during the ECCS Sump Strainer mission time, the decrease in sump pool temperature (and thus vapor pressure) will largely offset the effect of head loss across the ECCS Sump Strainer, particularly in the SBLOCA case (considerably less debris would be generated and ECCS flow would be lower). However, as the pool cools and chemical precipitates form, the head loss across the strainer will increase. Thus, the design structural limit of the ECCS Sump Strainer also defines the acceptable head loss across the strainer and debris load. The ECCS Sump Strainer head loss throughout the required 30 day required mission time was determined via combination of testing and analytical methods and was found to be acceptable from both an NPSH and structural integrity perspective.

In addition to ECCS Sump Strainer head loss testing, additional tests were successfully performed to demonstrate the effectiveness of the ECCS Sump Strainers ability to resist air entrainment due to vortex formation, quantification of debris that bypasses the ECCS sump strainer, and the ability of the McGuire ECCS Sump Strainer to accommodate various conventional debris load combinations without forming a thin, high-density debris bed that can result in high head losses.

#### Strainer Bypass and Downstream Effects

Testing and analyses have been performed to quantify the amount of fibrous debris that could pass through the Top Hat perforated plates, the Debris Bypass Eliminators, and the gaps/openings in the strainer plenums. The results of the analyses show that the maximum total amount of fiber bypass during the ECCS mission time is significantly less than 15g/fuel assembly for the limiting McGuire unit. This limit is used as a criterion for implementing Closure Option 1 outlined in SECY-12-0093, "Closure Options for Generic Safety Issue 191, Assessment of Debris Accumulation on Pressurized-Water Reactor Sump Performance". Since McGuire is classified as an "Option 1" or "clean plant", WCAP 16793-NP, Revision 2 can be utilized to address in-vessel downstream effects.

This evaluation addressed blockage due to the physical debris that is assumed to bypass the ECCS Sump Strainer as well as chemical precipitants that can form. The methodology and models described in WCAP-16793-NP as well as the Limits and Conditions imposed in the Staff's SER were utilized and addressed to perform this in-vessel evaluation. The results of the evaluation conclude the

accumulation and deposition of conventional debris and chemical precipitate debris at the reactor core will not challenge the ability to maintain post-accident Long Term Core Cooling (LTCC) at McGuire.

The effects of debris that bypasses the ECCS Sump Strainer was also evaluated on downstream ECCS components such as pumps, valves, orifices and heat exchangers. By utilizing testing performed by Duke Energy as well as the industry, it was determined the quantity and characteristics of debris that bypasses the McGuire ECCS Sump Strainer is below the expected concentration of debris found within the guidance of WCAP-1604-P, Revision 1. Utilizing the methodologies of WCAP-1604-P as well as addressing the Limits and Conditions contained within the Staff's SER, McGuire demonstrated that downstream ECCS components will not fail due to post-LOCA debris that passes through ECCS Sump Strainer components.

### 6.5.3 Safety Evaluation

The Containment Spray System provides two full capacity heat removal trains for the Containment, sized as described in [Table 6-139](#) to preclude an increase of the Containment pressure above design limits.

The spray system design is based on the spray water being raised to the temperature of the Containment in falling through the steam-air mixture within the building. The minimum fall path of the droplets is approximately 75 feet from the spray headers to the operating deck. The actual path is longer due to the trajectory of the droplets sprayed from the header. Heat transfer calculations, based upon 700 micron droplets, show that essentially 100 percent of thermal equilibrium is reached in a distance of a few feet. Thus the spray water reaches essentially the saturation temperature.

The containment spray system operates independently of other engineered safety features. One Containment spray system train provides adequate heat removal capability to limit Containment pressure and temperature below design limits (see Section [6.2.1.3](#)). For extended operation in the recirculation mode, water can be supplied to the containment Auxiliary spray headers through the residual heat removal pumps and heat exchangers. Auxiliary spray may be initiated manually, only after switchover to the recirculation mode and no earlier than 50 minutes after initiation of the LOCA, if required by procedure. At this time one ND pump can provide sufficient Auxiliary spray as well as adequate core flow via the high lead (one centrifugal charging and one safety injection) pumps. The Auxiliary spray may be required due to high containment pressure. High containment pressure would be indicated to the operator via safety-related redundant pressure indication in the control room. (See Section [6.3.3](#) for the performance evaluation of the ND pumps in their core cooling function.)

Normal and emergency power supply requirements are discussed in [Chapter 8](#).

A failure analysis has been made on all active and passive components of the system to show that the failure of any single active component does not prevent fulfilling the design function. This analysis is summarized in [Table 6-141](#).

### 6.5.4 Tests and Inspections

All active components in the Containment Spray Systems are adequately tested both in preoperational performance tests in the manufacturer's shop and in-place testing after installation. An initial system flow test demonstrates proper dynamic functioning of the system. Thereafter, periodic tests are performed in accordance with Technical Specifications and the Pump and Valve Inservice Testing Program.

The Component Cooling System pumps and heat exchangers which supply the cooling water to the residual heat exchangers and the nuclear service water pumps which supply cooling water to the Component Cooling System heat exchangers are in operation on a relatively continuous schedule during operation and no additional periodic tests are required.

Permanent test lines for the containment spray loops are located so that all components up to the isolation valves upstream from the spray nozzles may be tested. These isolation valves are checked separately. The air test lines, for checking that spray nozzles are not obstructed, connect downstream of the isolation valve.

An initial test of the containment spray header is made to check the free flow out of the spray nozzles. An air supply is used to provide a large quantity of relatively low pressure air. It is connected to an appropriate test valve after the corresponding spray ring has been isolated.

The spray nozzles can be periodically tested with the blower using the same method as in the initial test. The spray nozzles can also be periodically tested using a vacuum blower to induce air flow through each nozzle to verify unobstructed flow.

### 6.5.5 Instrumentation Application

This section describes the instrumentation employed for the monitoring and actuation of the Containment Spray System. This instrumentation includes that which is used during normal and post-accident operation for measurement of temperature, pressure, and flow.

#### Temperature

##### Containment Spray Heat Exchanger Inlet

Local indication is provided for each heat exchanger to measure fluid temperature in the containment spray heat exchanger inlet.

##### Containment Spray Heat Exchanger Outlet

A temperature sensor is provided for each heat exchanger to measure fluid temperature in the containment spray heat exchanger outlet. The temperature is indicated in the Control Room.

#### Pressure

##### Containment Pressure Control System

These pressure sensors are part of the Containment Pressure Control System which is designed to maintain the containment pressure within design limits.

Under accident conditions, the Containment Air Return System is automatically actuated when the internal pressure in the containment reaches 3 psig. The Containment Spray System is manually activated if containment pressure exceeds 3 psig and ECCS operation in the recirculation mode has successfully initiated.

The system's fans and pumps continue operating until they are shut off, either manually or automatically by this Pressure Control System. The Pressure Control System is activated when the internal pressure is greater than .35 psig. The Containment Pressure Control System consists of eight (8) independent pressure sensors (i.e., four (4) on each train) which provide interlocks to prevent the system's fans and pumps from starting if the containment pressure is below .35 psig, thus eliminating the possibility of inadvertent operation of these pressure reducing systems. (Refer to Section [7.6](#)).

##### Containment Pressure

Two out of three hi pressure signals (1 psig) produce an Ss signal or safety injection signal. Two out of four hi-hi pressure signals produce an Sp signal or Phase B Isolation signal.

##### Containment Spray Pump Suction Pressure

These pressure indicators are mounted near each pump inlet line and are designed to measure the inlet or suction pressure for each pump.

### Containment Spray Pump Discharge Pressure

These pressure indicators are mounted locally, measuring the discharge pressure for each pump.

### Containment Spray Pump Inlet Strainer $\Delta P$

Pressure test points are provided to measure the pressure drop across the temporary strainer during the initial system flushing operations.

### Flow Instrumentation

#### Containment Spray Pump Discharge Flow

A flow orifice is located in the discharge line of each pump with control room indication.

#### Containment Spray Pump Test Line Flow

A local flow indicator is provided to measure the flow in the 4-inch test line from the pumps to the refueling water storage tank.

### Humidity Instrumentation

Containment humidity indication is provided in the control room.

## 6.5.6 References

1. Letter, B.H. Hamilton (Duke) to USNRC Document Control Desk, Subject: NRC Generic Letter 2004-02, "Potential Impact of Debris Blockage on Emergency Recirculation During Design Basis Accidents at Pressurized-Water Reactors," dated February 28, 2008.
2. Letter, B.H. Hamilton (Duke) to USNRC Document Control Desk, Subject: Response to NRC Generic Letter 2004-02, "Potential Impact of Debris Blockage on Emergency Recirculation During Design Basis Accidents at Pressurized-Water Reactors," dated April 30, 2008.
3. Letter to the U.S. Nuclear Regulatory Commission from T.P. Harrall dated October 13, 2008, titled "Duke Energy Carolinas, LLC (Duke) Oconee Nuclear Station, Units 1, 2 & 3, Docket Nos. 50-269, 50-270, 50-287, McGuire Nuclear Station, Units 1 & 2, Docket Nos. 50-369, 50-370, Catawba Nuclear Station, Units 1 & 2, Docket Nos. 50-413, 50-414, Generic Letter 2008-01, 9-Month Response."
4. Letter to the U.S. Nuclear Regulatory Commission from Regis Repko dated September 30, 2010, McGuire Nuclear Station Units 1 and 2 and Catawba Nuclear Station Units 1 and 2, "Draft Responses to NRC Request for Additional Information (RAI) related to Generic Letter (GL) 2004-02 - Potential Impact of Debris Blockage on Emergency Recirculation During Design Basis Accidents at Pressurized Water Reactors".
5. Letter to the U.S. Nuclear Regulatory Commission from Regis Repko dated July 2, 2012, McGuire Nuclear Station Units 1 and 2, "Final Responses to NRC Request for Additional Information (RAI) related to Generic Letter (GL) 2004-02-Potential Impact of Debris Blockage on Emergency Recirculation During Design Basis Accidents at Pressurized Water Reactors".
6. Letter to the U.S. Nuclear Regulatory Commission from Steven Capps dated May 8, 2013, McGuire Nuclear Station Units 1 and 2, "Closure Options for Generic Safety Issue (GSI)-191- Assessment of Debris Accumulation on Pressurized-Water Reactor Sump Performance in resolution of final issues related to Generic Letter (GL) 2004-02- Potential Impact of Debris Blockage on Emergency Recirculation During Design Basis Accidents at Pressurized Water Reactors".

7. Letter to the U.S. Nuclear Regulatory Commission from Steven Capps dated July 31, 2013, McGuire Nuclear Station Units 1 and 2, "Response to In-Vessel Downstream Effects Request for Additional Information for Generic Safety Issue (GSI)-191- Assessment of Debris Accumulation on Pressurized-Water Reactor Sump Performance in resolution of final issues related to Generic Letter (GL) 2004-02-Potential Impact of Debris Blockage on Emergency Recirculation During Design Basis Accidents at Pressurized Water Reactors".
8. Letter from NRC to Steven Capps dated April 24, 2014, McGuire Nuclear Station Units 1 and 2, "Closeout of Generic Letter, 2004-02-Potential Impact of Debris Blockage on Emergency Recirculation During Design Basis Accidents at Pressurized Water Reactors".
9. NEI 04-07, Pressurized Water Reactor Sump Performance Evaluation Methodology.
10. MCC-1552.08-00-0387, GSI-191 Debris Generation Calculation.
11. MCC-1552.08-00-0388, McGuire Units 1 And 2 GSI-191 Debris Transport Calculation.
12. MCC-1552.08-00-0389, McGuire Units 1 And 2 GSI-191 Debris Head Loss Calculation.
13. MCC-1552.08-00-0401, Refinement of Unqualified Coating Failure Assumptions for Contributions to ECCS Sump Strainer Particulate Loads.
14. MCC-1552.08-00-0386, McGuire Unit 1 And 2 Containment Buildings Tag and Label Reductions.
15. MCC-1223.02-00-0013, Aluminum Inventory Inside Containment.
16. MCC-1552.08-00-0390, Containment Recirculation Sump Top-Hat Strainer Performance Calculation.

THIS IS THE LAST PAGE OF THE TEXT SECTION 6.5.